Biogeochemical Conversion of Nitrogen in Enclosed Pelagic Coastal Ecosystems of the German Bight:

Mesocosm and Modelling Studies

Dissertation zur Erlangung des
Doktorgrades der Naturwissenschaften im Fachbereich
Geowissenschaften der Universität Hamburg

Vorgelegt von
Ling Ren
aus Zhejiang, China

Hamburg

im Sept. 2002

Als Dissertation angenommen vom Fachbereich Geowissenschaften
der Universität Hamburg

auf Grund der Gutachten von Herrn Dr. U.H. Brockmann
und Herrn Prof. Dr. V. Ittekkot

Hamburg, den 26. Juni 2002

Prof. Dr. U. Bismayer
Dekan
des Fachbereichs Geowissenschaften

Contents

Glossary

CEPEX	Controlled Ecosystem Population EXperiment, U.S. program in collaboration with Canadian scientists (1974-1979). Enclosure experiments on the response of plankton communities and on trophodynamics.
chl*a*	Chlorophyll *a*
DFAA	Dissolved free amino acids
DIN	Dissolved inorganic nitrogen (NO_3^-+NO_2^-+NH_4^+)
DOC	Dissolved organic carbon
DOM	Dissolved organic matter
DON	Dissolved organic nitrogen
MM3	ModelMaker 3, software for numerical simulation
N	Nitrogen
NH_4	Ammonium
NO_2^-	Nitrite
NO_3^-	Nitrate
Pa	Pascal, air pressure
PN	Particulate nitrogen
PO_4^{3-}	Phosphate
POC	Particulate organic carbon
POM	Particulate organic matter
POSER	Plankton Observation with Simulataneous Enclosures in Rosfjorden. Mesocosm experiments, carried out in in Norway, started from spring, 1979.
PP	Particulate phosphorus
PSU	Practical salinity units
series 1	Mesocosm experiment in Büsum in spring 1999, 15/03-09/04/1999
series 2	Mesocosm experiment in Büsum in summer 1999, 01/06-14/06/1999
Si	Silicate
SUR	Specific uptake rates
T1, T3, T5	Number of bags of the control system in spring experiment (series 1)
T2, T4, T6	Number of bags of the experimental system in spring experiment (series 1)
T7	Number of the harbour water (as reference) in spring experiment (series 1)
T8, T9, T10	Number of bags of the control system in summer experiment (series 2)
T11, T12, T13	Number of bags of the experimental system in summer experiment (series 2)
T14	Number the harbour water (as reference) in summer experiment (series 2)
TN	Total nitrogen (DIN+DON+PN)
TU	Turner units
w/v	Weight per volume
v/v	Volume per volume
Whatman GF/C	Glass-fiber filter
µM	µmol L^{-1}

ABSTRACT

The German Bight is characterised by high nutrient concentrations mainly due to N-rich discharges of the rivers Elbe and Weser. However, strong gradients and permanent tidal advection complicate quantification of biogeochemical processes. For this reason, mesocosm experiments, eliminating the frequent tidal shifts of gradients and tidal advection were carried out to study the development of phytoplankton community and nutrient cycling under seasonal physical and chemical conditions. In this paper, mainly nitrogen cycling in the enclosed pelagic ecosystem was studied based on the data analyses of the mesocosms. A box model was meanwhile developed and applied as complementary tool to quantify transformation of main N phases in the pelagic ecosystem within the low trophic level.

Two series of mesocosm experiments with natural (controls) and nutrient-enriched (experimental) plankton populations were carried out in Büsum in spring and summer, 1999. During both the spring and summer experiments, physical parameters (irradiance, temperature and turbidity), chemical parameters (nutrients, DOM, POM and DFAA) and biological parameters (primary production, chlorophyll *a* and phytoplankton species, bacteria) were frequently monitored, up to every two hours. Significant correlations of the parameters measured in the parallel bags reveal excellent reproducibility. The comparison of forcing parameters in the enclosures with those in the harbour surrounding and at offshore station indicates the representativity of the mesocosm experiments which were for the starting conditions given for the surrounding area, influenced by the spreading Elbe river plume.

The spring experiment was successful in tracing the start of a typical diatom spring bloom, dominated by *Thalassiosira* species with a long slow-growing phase prior to the exponential growth.

The light climate is the most essential factor to trigger phytoplankton spring bloom. In the enclosures, the compensation depth was lifted to the upper 2 – 3 m by keeping the planktonic community at the surface (2 to 3 m) of the turbid water. In the open water of the same turbidity, frequent vertical mixing which was including 20 m deep tidal channels, inhibited net primary production and prevented the formation of phytoplankton bloom in the adjacent area. Accordingly, both in spring and summer, no significant phytoplankton bloom was detected in the surrounding turbid inshore waters.

The development of phytoplankton growth within the mesocosms was controlled by the available nutrient concentrations. In spring, high DIN/DIP ratio in the water column indicated possible P limitation. P addition prolonged phytoplankton exponential growth and consequently caused an increase of the final phytoplankton standing stock. Nitrate, phosphate and silicate were taken up in relations close to Redfield ratios during the exponential growth phase.

In summer experiment, phytoplankton started exponential growth immediately after enclosure. The exponential growth phase lasted only for 3 days and was followed by a stationary and decay

phase caused by complete exhaustion of nutrients. Diatoms were succeeded by flagellates due to longer lasting Si regeneration. By daily addition of nutrients (NO3, PO4 and Si) to some mesocosms phytoplankton was kept in exponential growth. In spite of deviating ratios from Redfield relations of added NO_3^-: PO_4^{3-}: Si, the ratios of particulate matter synthesis (ΔPOC:ΔPN:ΔPP) were close to Redfield ratios.

Significant negative correlations of nutrients with chlorophyll *a* indicated the dominance of phytoplankton biomass synthesis in nutrient conversion both in spring and summer. The succession of NH_4^+ and NO_3^- utilisation was observed during spring and summer when ammonium concentrations dropped below 3 µM. Co-uptake occurred when NH_4^+ was in the range of 1.0 to 3.0 µM. NO_2^- release was observed during luxury NO_3^- uptake in both spring and summer, reaching about 1% of NO_3^- uptake. NO_2^- uptake followed NO_3^- depletion (< 1 µM). Results from model runs show during spring exponential growth phase nitrate uptake of 8 – 10 µM/d which were in the same order for control and nutrient enriched systems. During summer only 2 µM/d nitrate were utilised but 5 µM/d ammonium, reaching in total the same range as during spring. Following addition of nitrate, its uptake rate increased to 13 – 14 µM/d.

In the enclosures, DON remained at steady state concentrations around 20 µM, controlled by the processes of production and losses by bacteria utilisation during most of the experiments. During spring, a slight increase of DON was related to phytoplankton cell release during the exponential growth phase. During summer, DON increases were mostly attributed to the detritus decomposition related to bacterial activity. Modelled fluxes generating the fraction of dissolved organic nitrogen were in spring calculated between 0.06 and 0.22 µM/d, balanced by decomposition rates of 0.14 – 0.18 µM/d. These fluxes were during summer significantly increased: 0.96 – 2.49 µM/d increase and 0.69 – 0.9 µM/d decomposition, indicating the temperature effect on bacterial turnover.

Mass balances of nitrogen revealed significant N loss during both spring and summer experiments, which were attributed to denitrification by particle-attached bacteria. Calculated denitrification rates were 1.5 mmol m^{-2} d^{-1} in spring and 2.5 mmol m^{-2} d^{-1} in summer.

By frequent sampling, diurnal changes of phytoplankton turnover such as nitrate uptake and nitrite release could be followed. Phytoplankton photosynthesis rates were higher in later morning of 5 to 8 µg POC (µg chl*a*)$^{-1}$ h^{-1} and showed a decrease during nights and reached to the low rates of –1 to –2 µg POC (µg chl*a*)$^{-1}$ h^{-1}. Diurnal NO_3^- uptake estimated from spring varied from 0.001 to 0.025 µM (µg chl*a*)$^{-1}$ h^{-1} at night and 0.004 to 0.052 µM (µg chl*a*)$^{-1}$ h^{-1} at daytime.

A box model mainly focusing on nitrogen cycling in the pelagic system was applied to study the biogeochemical conversion of the main phases of nitrogen within the lower trophic level, including two groups of phytoplankton (diatoms and flagellates), herbivorous zooplankton, nutrients (nitrate, nitrite, ammonium, phosphate and silicate), dissolved organic matter (DON, DOP) and detritus. It was driven by the forcing variables of irradiance and temperature. After

calibrated with the measurements in the spring control system, the model was validated with data from the summer control system. It was then applied to 'hindcast' the development of the spring and summer experimental systems with nutrient enrichments with the purpose of verification.

Comparing the simulations with the measurements, the model simulated successfully the development of the main N compartments in control bags in spring and summer, and was able to simulate the experimental systems as well. Based on the good consistency between the simulations and measurements, N fluxes of the main processes were calculated. Phytoplankton biomass formation was the dominant process both in spring and summer, accounting for 75% and 60% of DIN uptake, respectively. 5% of DIN utilised in spring and 22% in summer were remineralised to ammonium which was taken up again by the phytoplankton nearly completely.

Limitations of the model were given by the ability of phytoplankton cells to store P and modifications of nutrient utilisation due to the different nutrient status within the cells, which could not be considered by the applied Michaelis-Menten-Monod equation. This resulted in unsatisfactory simulations of PO_4^{3-} and Si uptake during the period of nutrient addition in the summer experimental bags. In the current model, bacteria were only implicitly included in degradation, nitrification and denitrification, causing higher deviations between model results and measurements during summer due to higher bacterial activity compared to spring.

The combination of mesocosm experiments with the box model allowed a detailed analysis of the biogeochemical fluxes within the dynamic nutrient-rich coastal waters, as shown by nitrogen compounds. The knowledge of the reaction potential of river plume water is of importance for future management measures.

1 INTRODUCTION

1.1 Nitrogen cycling in coastal water

Since a long time, nitrogen is regarded as the limiting nutrient element in the marine environment (Dugdale and Georing 1967, Carpenter and Capone 1983, Vitousek and Howarth 1991, Oviatt et al. 1995). Compared to the other macro nutrient elements, phosphorus and silicate, the cycling of nitrogen is much more complex, because nitrogen occurs in several oxidised and reduced forms in seawater. Additionally, it can be fixed, or lost as gaseous nitrogen. Different forms of nitrogen can be utilised by both phytoplankton and bacteria (Parsons et al. 1984). For these reasons, nitrogen has got more attention from marine scientists especially during the past three or four decades with the improvement of measurement techniques of various forms of nitrogen. The results have been compiled in several monographs (e.g. Carpenter and Capone 1983, Blackburn and Sϕrensen 1988, Wada and Hattori 1991, Howarth 1996).

In coastal ecosystems, cycling of nutrient elements is always affected by physical processes such as: tides, wave forces, residual or wind driven advection, as well as river discharges which influence the chemical gradients (nutrients, organic matter) and hydrodynamic conditions (salinity, temperature gradients and stratification). River discharges are mostly affected by human activities, increasing e.g. the loads of nutrients. Results from several recent analyses of the global N cycle (Mackenzie et al. 1993, Ayres et al. 1994, Galloway et al. 1995) generally agree that anthropogenic activities mobilise about 10 Tmol $N \cdot yr^{-1}$ (Tmol = 10^{12} moles) and that human activities mobilise N at rates equal to natural terrestrial processes (Galloway et al. 1996). Since most of these river loads are discharged to the sea, the coastal ecosystems are effected as well. Also atmospheric deposition of anthropogenic NO_x became important at least in coastal waters (Beddig et al. 1997). A conceptual scheme of nitrogen cycling in coastal ecosystem is shown in Fig. 1-1.

1.2 Mesocosm experiments as a tool for biogeochemical process studies

Mesocosms, enclosing water masses of several cubic meters, have been developed for many different purposes (Parsons 1991). The first enclosure experiment with floating bags has been conducted at Nanaimo, BC, Canada (Strickland and Terhune 1961) to study chemical and biological changes occurring during a phytoplankton bloom excluding advective interference. Since then, enclosure experiments have been developed as an important tool in ecosystem research and served as a bridge between laboratory experiments and field investigations (Strickland 1967). Several experiments have been realised with different designs for specific purposes (Grice and Reeve 1982, Parsons 1991).

Floating mesocosms have been proved to be a valuable tool for investigating interactions within the plankton ecosystem, including the effects of dissolved pollutants. Many pelagic processes have been studied including primary production, phytoplankton succession, nutrient uptake and DOM release (Brockmann 1990), remineralisation, effects of pollutants. In some experiments, processes in

sediments have been involved: element cycling, the interaction of benthos with pelagic systems (De Wilde 1990).

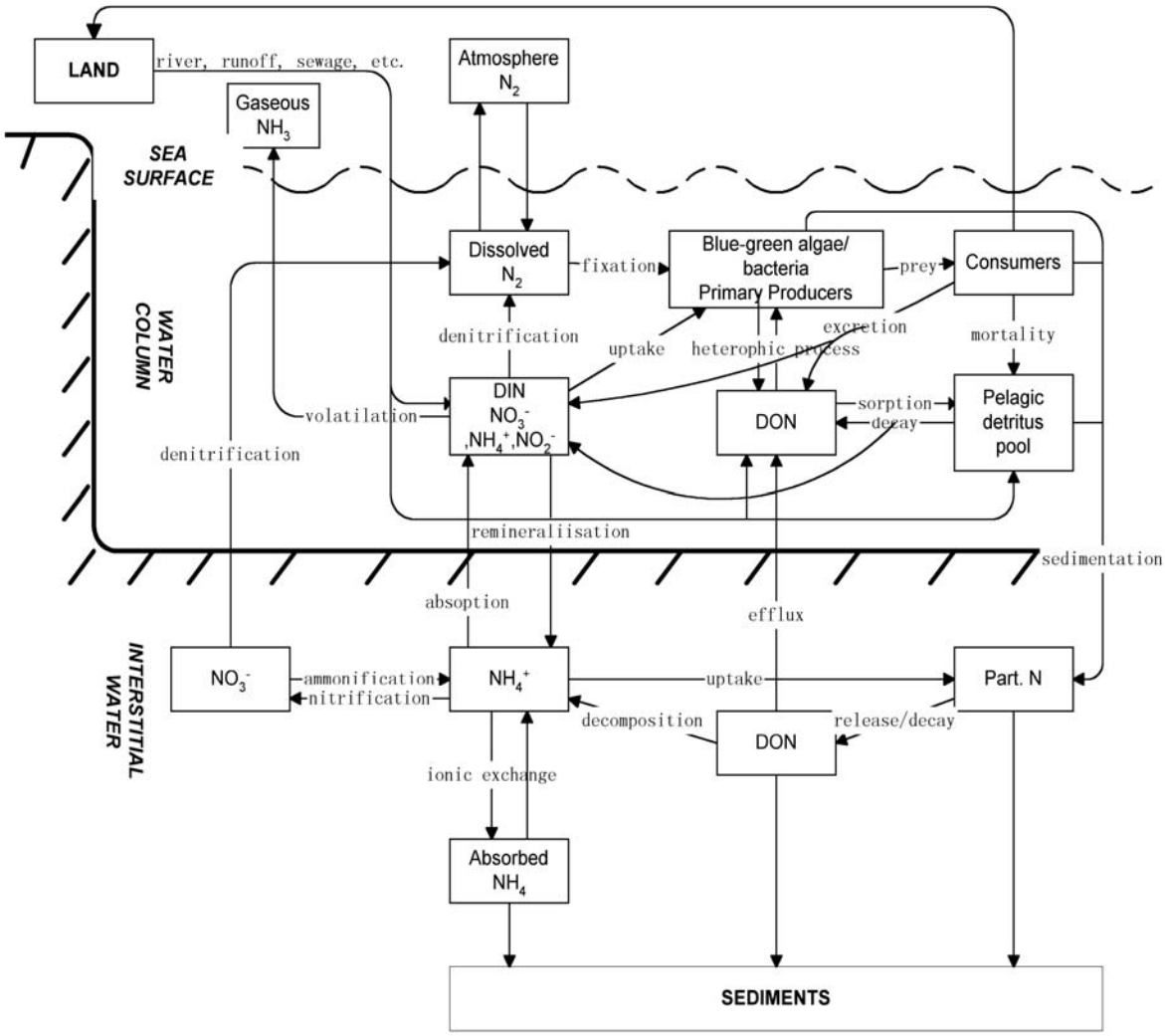

Fig. 1-1 Simplified scheme of major transformations and transport of nitrogen in marine environments (redrawn from Valiela 1992)

The advantages of utilising enclosure experiments to marine ecosystem studies were summarized by Banse (1982) and Lalli (1990). Mesocosm experiments allow e.g. to trace the diurnal variation of phytoplankton activity and their effects on chemical constituents under semi-natural conditions (Brockmann 1990), which is difficult to do during field investigation due to the influence of tides and mixing processes (Brockmann 1999b), as well as in lab experiments due to artificial conditions and limited volume for longer lasting experiments and frequent sampling.

Among the limitations of mesocosm experiments, the main problems are their representativity (which is much more critical for laboratory experiments) and reproducibility of the relatively large,

open and exposed systems. The representativity or field validation of mesocosm experiments can be demonstrated via (i) comparing the mesocosm results with the key parameter concentrations and changes in the natural system during the experiment, considering the variability of the open system; (ii) comparing the experimental results with process data from laboratory and field studies to prove causal relationships and predictive capability, as was shown for some mesocosm experiments (Takahashi et al. 1975, Oviatt 1984). The reproducibility of enclosure experiments has been proved for several systems (Takahashi et al. 1975, Brockmann et al. 1977, Kuiper 1977, 1981, Smith et al. 1982). But large mesocosms cannot be controlled completely nor precisely repeated like laboratory experiments because of the formation of horizontal gradients, losing by this the advantage of enclosed, defined systems (Reeve et al. 1982).

In recent mesocosm experiments, the changes of phytoplankton biomass and the shifts of species caused by nutrient manipulations have been studied in detail. In most cases effects of nutrient enrichments have been investigated (Taylor et al. 1995, Jacobsen et al. 1995, Schlüter 1998, Egge and Jacobsen 1997). On the other hand, the influences of reduction of nutrient inputs have also been tested (Escaravage et al. 1996) in relation to the reduction of anthropogenic phosphorus discharges in the North Sea during the past 20 years (Zevenboom 1994).

1.3 Numerical modelling as a tool for ecological research

Data from mesocosm experiments are ideal for testing and validating mathematical ecosystem models prior to the field data due to its continuous time-series and exclusion of advection interference. Data from these experiments could also provide databases for further model developments especially concerning the biological and chemical processes, which could be simulated and followed by frequent sampling and parallel analyses of many of the interacting parameters. At the same time, a model is a complementary tool for quantifying linked processes in complex ecosystems. The conjunction of mathematical models with mesocosm research was critically reviewed by Parsons (1990). Model research, tested with mesocosm data avoiding advection interference is regarded as an assistant tool in interdisciplinary understanding of ecosystem processes.

During the past decades, several models have been developed derived from mesocosm experiments. During the POSER experiments (Brockmann 1983a), a predator-prey model was developed to study the role of heterotrophic nano-flagellates in the marine planktonic microbial loop (Laake et al. 1983). Andersen and Nival (1987, 1989) set up a model mainly concerning the planktonic system from CEPEX mesocosm experiments.

A series of mesocosm experiments have been conducted in the Netherlands to analyse the effects of temperature, light climate and nutrients loading (N and P) on species composition and productivity in marine coastal environments. A model was also developed to simulate the variation of phytoplankton community (van der Rol and Joordens 1993).

With the increasing problem of eutrophication in the coastal areas, effects of nutrients disturbance on

primary production and phytoplankton composition as well as effects on zooplankton and higher trophic levels have also been tested using mesocosm experiments combined with simulation modelling.

Most models were good in reproducing the results from mesocosm results, and assisted in explaining the results, but were short in prediction. Quite recently, some models have been developed to predict the changes of phytoplankton and zooplankton with nutrients manipulation, using mesocosm data to calibrate and validate the models (Suzuki et al. 2000, Holz et al. 2000).

1.4 Purpose and questions of this investigation

River discharges intensify eutrophication effects in the German Bight, especially during summer. It was estimated that 36% of annual Elbe-Weser discharged N corresponded to the biomass accumulated in the bottom layer of the German Bight causing oxygen depletion to less than 4 mg/L (Brockmann and Eberlein 1986). From the 60s to the 80s, anthropogenic inputs of N and P into the North Sea have increased by factors of 4 and 6 respectively, which led to frequent eutrophication effects in coastal areas in the North Sea (Von Westernhagen et al. 1986, Hickel et al. 1994, Zevenboom 1994). Moreover, a shift in nutrient inputs in relation to silicate changed the nutrient ratios, which may favor a certain kind of flagellates. It was observed that changes in phytoplankton stock at Helgoland roads resulted from an increase of flagellates since the end of the 1970s (Radach and Bohle-Carbonell 1990).

A series of measures have been taken to reduce the input of N and P to the North Sea during the last two decades. P-discharges had been reduced by 50%, but N-discharges, controlled mainly by diffusive sources only by 25% (Quality Status Report 2000, p62). Observations showed that during summer periods average chlorophyll *a* has not been reduced as could have been expected in correspondence to P reduction (Cadèe and Hegeman 1993, Lenhart et al. 1996, De Jonge 1996, Philippart and Cadèe 2000). The increase of N:P ratio (Hickel et al. 1995) and relative shifts in species of phytoplankton led to further problems, such as increased toxicity of harmful algae (Riegman et al. 1992, Nehring et al. 1995). To study the effects of changing nutrients on eutrophication in the ecosystem of coastal zones, it is of importance to focus on N cycling and conversion in coastal areas, influenced by nitrogen-rich river plumes of the Weser and Elbe, such as the German Bight.

In order to study the development of coastal phytoplankton species composition and nutrient cycling under various physical and chemical conditions, three series of mesocosm experiments were conducted in the German Bight in spring and summer 1999. These allowed: (i) the investigation of the high nutrient discharges during spring and its effects on the start of the phytoplankton spring bloom; (ii) the analyses of lower discharge during summer time when eutrophication effects occurred; and (iii) the study of enrichment of limiting nutrients on phytoplankton development during summer as well. Büsum was chosen as location of the experiments because it is the type of coastal area which is affected by the river plume of the river Elbe mostly, stretching northward by the coastal current,

passing the tidal flats off Büsum. Tidal action frequently exchanges large amounts (>50%) of harbour water, passing the sluice which is only closed at high storm tide.

Based on the experiments, a box model on nitrogen cycling in the pelagic system was applied. It is focussed on the biogeochemical conversion of the main phases of nitrogen and phosphorus within the low trophic level. The model is based on the N cycling model of Fasham et al. (1990), which has also been used to simulate nitrogen cycling in the water column of Jiaozhou Bay, China (Ren et al. 2002a). Different data sets from the mesocosm experiments were used for adaptation, calibration and validation of the model. And the model was finally used to 'hindcast' the effects of nutrient enrichments on N cycling in the enclosed system.

2 MATERIALS AND METHODS

2.1 Mesocosm setup and techniques

Three series of enclosure experiments on planktonic processes have been conducted in the harbour of Büsum (Fig. 2-1), at the German Bight in spring and summer 1999. The water from the harbour was pumped into plastic bags through a 1 mm net to remove larger zooplankton. Every bag with 1 m diameter and 3 m depth was filled with about 2.3 m^3 water and fixed to a floating framework with about 6 m diameter and about 2 m height or in aluminium rings supported by 3 buoys (Fig 2-2). The bags, performed of a combined plastic foil consisting of two layers: 100 µm of polyethylene inside and 30 µm of polyamide outside, allowing experiments at nearly natural conditions (Brockmann et al. 1974, 1992). All bags were kept vertically by weights of several kilograms fixed to the bottom. The bags were covered with the same plastic foil to avoid any contamination from the atmosphere. Air bubbles were pumped through tubes, fixed at the bottom of the bags, mixing the water column in the bags every minute to keep the whole water column homogeneous.

This design of enclosure experiments had been utilised in several investigations and proven to be a good tool to study various processes within the lower trophic level (Brockmann et al. 1974, Brockmann et al. 1983a). Compared to some other enclosure systems such as: Loch Ewe, Den Helder Enclosures and CEPEX (Grice and Reeve 1982), this kind of design has many advantages (Brockmann et al. 1983a) such as: easy launching, simple mounting system, low costs. The seamless plastic tubes are physiologically inert and impermeable to gases and trace metals but is light permeable and allows transfer of turbulence. The small diameter ensures the horizontal homogeneousness of the water column and by this the representativity of samples.

2.2 Sampling strategy and sampling

For every experiment, there were two identical sets of mesocosms, one for control and one for experimental manipulation. In order to monitor the reproducibility of the system, every set consists of three parallel bags, one main bag and two additional bags. Sampling in all bags was started simultaneously. The main bags were sampled every 2 hrs so that it was possible to follow the diurnal variation of the main biological and chemical parameters. The additional bags were sampled every 6 hrs as references.

In order to detect the representativity of the development within the enclosed water, harbour water was also monitored every 6 hours. Off shore water samples from outside the harbour were taken every day to trace the development of temperature, salinity, phytoplankton, and nutrients in the coastal water during the experimental period.

Samples were divided into subsamples for direct measurements such as: pH, salinity, turbidity, oxygen, chlorophyll *a*, etc. and were filtrated for different purposes. Filtrates were used for analyses of nutrients, DOC, DON, DOP etc. and filters for the measurements of suspend and particulate matter (POC, PN, PP). The experiment strategy and sampling periods are listed in the table 2-1.

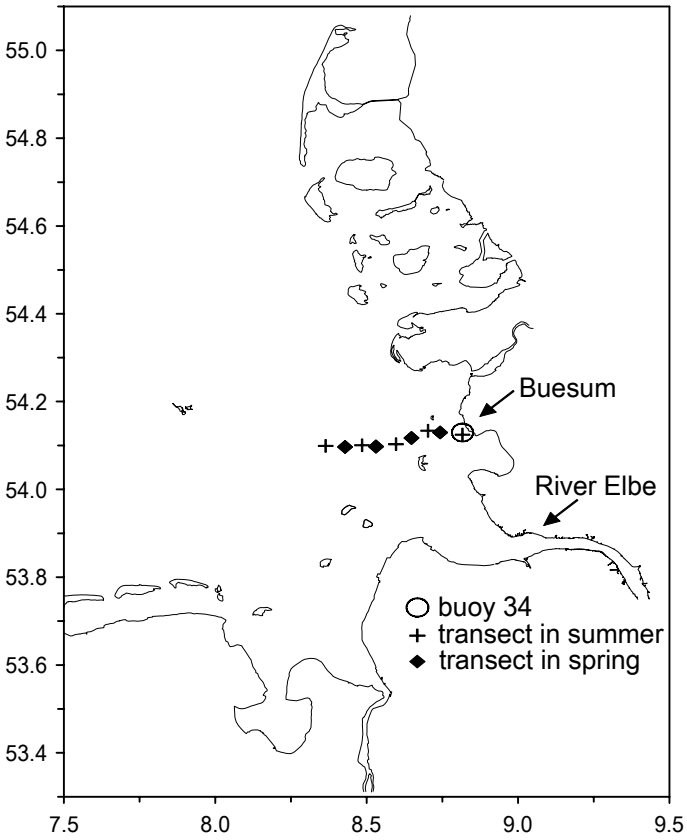

Fig. 2-1 Location of Büsum where the mesocosm experiments were carried out in spring and summer 1999 (X-axis: longitude, °E; Y-axis: latitude, °N).

Fig. 2-2 Mesocosm setup in the harbour in Büsum, 1999

2.3 Analytical methods

2.3.1 Physical parameters

Irradiance was measured by a pyranometer (constructed by the Institute of Physics, University Oldenburg) during the whole experimental period. The data were recorded automatically by a data logger averaged for every minute.

Temperature and salinity were measured every 2 hours directly in plastic bags by a combined portable probe (switch gear probe model F/14372, Kent Industrial Measurements Ltd., England/LF 191 salinometer, WTW. Weilheim, Germany). pH was measured by pH electrodes (pH meter 330, WTW, Weilheim, Germany) and turbidity by a nephelometer (TD40 Turner Design, USA) from the water samples taken for nutrient analyses. Transmission was measured by 1 Hz fluorometer (BBE, Kiel, Germany) from the water samples taken specifically for chl*a* and phytoplankton measurements.

2.3.2 Chemical parameters

Nutrients and dissolved organic matter: water samples for measuring nutrients and other chemical parameters were taken from the bags at a depth of 0.5 m through silicon tubes by vacuum pumping into 2 litres polyethylene bottles, and were immediately filtered through pre-combusted glass fibre filters (Whatman GF/C) at constant vacuum (<0.2 Pa). The filtrates were measured with a Technicon AutoAnalyzer System II for nitrate, ammonium, nitrite, phosphate and silicate (Grasshoff et al. 1983), for phosphate modified by Eberlein and Kattner (1987). Dissolved organic nitrogen (DON) and phosphorus (DOP) were calculated by subtracting the inorganic N and P from total dissolved N and P analysed as nitrate and phosphate after wet combustion by peroxidisulphate (Parsons et al. 1984). Dissolved organic carbon (DOC) was analysed from $HgCl_2$ (0.01% w/v) preserved samples by a DOC-analyser with FID detector (Carlo Erba model TCM 480) after high temperature catalytic oxidation (Raabe et al. 1997).

Particulate organic matter: Particulate carbon and nitrogen (POC, PN) were analysed after degradation to various nitrogen oxides and reduction to N_2 by oxidative combustion catalysed by copper from the residuals of frozen (-20°C) filters with a CHN analyser (Heraeus CHN-O- RAPID). Particulate phosphorus (PP) was measured by an autoanalyser as phosphate after combustion (Kattner and Brockmann 1980).

Dissolved free amino acid (DFAA): After filtering through GF/C filters, samples were fixed with $HgCl_2$ to a final concentration of 0.01% (w/v), and stored dark and cool. The samples were measured by a fluorescence method (Hammer and Luck 1987), based on the orthophthaldialdehyd (OPA) method introduced by Roth (1971).

2.3.3 Biological parameters

Chlorophyll *a*: Two methods were used to measure the concentration of chlorophyll *a*. By Turner fluorescence total chlorophyll *a* was estimated, by 1 Hz fluorometer (BBE, Kiel, Germany) only that of living phytoplankton cells was measured (Moldaenke et al. 1995). Filtered chlorophyll *a*, was measured additionally by HPLC and photometrically (Jeffrey and Humphrey 1975, Sterman 1988) for calibration of the Turner and 1Hz measurements.

Phytoplankton: Water samples for determination of phytoplankton species were taken with a 1 litre DURAN glass bottle from the bags at the depth of 0.5 m, filled into 250 ml polyethylene bottles and fixed with formalin to the final concentration of 1.5% (v/v). Phytoplankton was identified and counted with an inverted microscope according to the method of Utermöhl (1958). For the estimation of biomass parameter a geometrical form was assigned to each species and all necessary dimensions for the determination of the volume were measured (Hillebrand et al. 1999). To convert to carbon biomass the equations according to Eppley et al. (1970b) were used: log C = -0,29 + 0,757 log V for diatoms and log C = -0.6 + 0.94 log V for non-diatoms.

Primary production: Primary production was measured once a day from the main tanks using the light-dark oxygen technique (Gaarder and Gran 1927) based on the classical Winkler (1988) method for the determination of dissolved oxygen modified by Strickland and Parsons (1972).

Water samples from DURAN bottles were carefully sub sampled into 9 100 ml - BOD (biological oxygen demand) glass bottles. To three of them $MgCl_2$ and alkaline iodide solution were added immediately to get the initial oxygen values. Another three bottles were used as light bottles (LB) for measuring the net primary production and the remaining three bottles, wrapped with aluminium foil were used as dark bottles (DB) for measuring the total respiration. LB and DB were fixed near the station at about 0.5 m depth for 9 hours and then stopped by adding $MnCl_2$ and alkaline iodide solution. Titration with thiosulfate was conducted by a Metrohm Titroprocessor 686. The factor of 1.2 to convert the produced oxygen to fixed carbon for marine phytoplankton was used as suggested by Strickland and Parsons (1972).

Table 2-1 Experimental design of the mesocosm experiments at the Research Centre Büsum in spring and summer 1999.

Series	Sequence	Bag	Start	End	Description	Notes
1	A control	1	15/03/99	09/04/99	Main bag [1]	[1] plastic bag (about 2.5 m^3 water volume) [2] rigid circulation tank (about 20 m^3 ent [3] bag was damaged after four days [4] adding of ca. 2 µM l^{-1} P at 26/03/99 [5] Adding: ca. 1 µM l^{-1} P and ca. 15 µM l^{-1} Si at 04/06/99; ca. 0.5 µM l^{-1} P, ca. 15 µM l^{-1} Si and ca. 15 µM $^{-1}$ N at 05/06/99; ca. 0.5 µM l^{-1} P, ca. 15 µM l^{-1} Si and ca. 10 µM l^{-1} N at 06/06/99; ca. 0.5 µM l^{-1} P, ca. 15 µM l^{-1} Si and ca. 20 µM l^{-1} N at 07/06/99; ca. 2 µM l^{-1} P, ca. 15 µM l^{-1} Si and ca. 20 µM l^{-1} N at 08+09/06/99; ca. 2 µM l^{-1} P, ca. 20 µM l^{-1} Si and ca. 20 µM l^{-1} N at 10/06/99; ca. 3 µM l^{-1} P, ca. 20 µM l^{-1} Si and ca. 25 µM l^{-1} N at 11/06/99; ca. 3 µM l^{-1} P, ca. 25 µM l^{-1} Si and ca. 25 µM l^{-1} N at 12/06/99 [6]adding: ca. 3 µM l^{-1} P and ca. 30 µM l^{-1} N at 23/06/99
		3	15/03/99	07/04/99	Additional bag [1]	
		5	15/03/99	09/04/99	Additional bag [1]	
	B (addition of PO_4^{3-})	2	15/03/99	08/04/99	Additional bag [1, 4]	
		4	15/03/99	08/04/99	Main bag [1, 4]	
		6	15/03/99	19/03/99	Additional bag [1, 3]	
	Reference	7	15/03/99	09/04/99	Harbour basin	
2	C Control	8	01/06/99	14/06/99	Main bag [1]	
		9	01/06/99	14/06/99	Additional bag [1]	
		10	01/06/99	14/06/99	Additional bag [1]	
	D (repeated addition of nutrients)	11	01/06/99	14/06/99	Main bag [1, 5]	
		12	01/06/99	14/06/99	Additional bag [1, 5]	
		13	01/06/99	14/06/99	Additional bag [1, 5]	
	Reference	14	01/06/99	14/06/99	Harbour basin	
3	E (single addition of nutrients)	15	15/06/99	28/06/99	Main tank with sediment [2]	
		16	15/06/99	28/06/99	Main bag [1, 6]	
		17	15/06/99	28/06/99	Additional bag [1, 6]	
	F control	18	15/06/99	28/06/99	Main tank with sediment [2]	
		19	15/06/99	28/06/99	Main bag [1]	
		20	15/06/99	28/06/99	Additional bag [1]	
	Reference	21	15/06/99	28/06/99	Harbour basin	

2.4 Conceptual model

2.4.1 Description of the applied model

Fig. 2-3 shows the main flows between the main compartments in the model. The state variables included two groups of phytoplankton: (diatoms and flagellates), herbivorous zooplankton, nutrients (nitrate, nitrite, ammonium, phosphate and silicate), dissolved organic matter (dissolved organic nitrogen and phosphorus), and detritus. The microbial loop was not integrated as such. The turnover of bacteria was included implicitly in some processes, such as, detritus decay, DON demineralisation, pelagic nitrification and denitrification, etc. Mostly the dominant processes were considered.

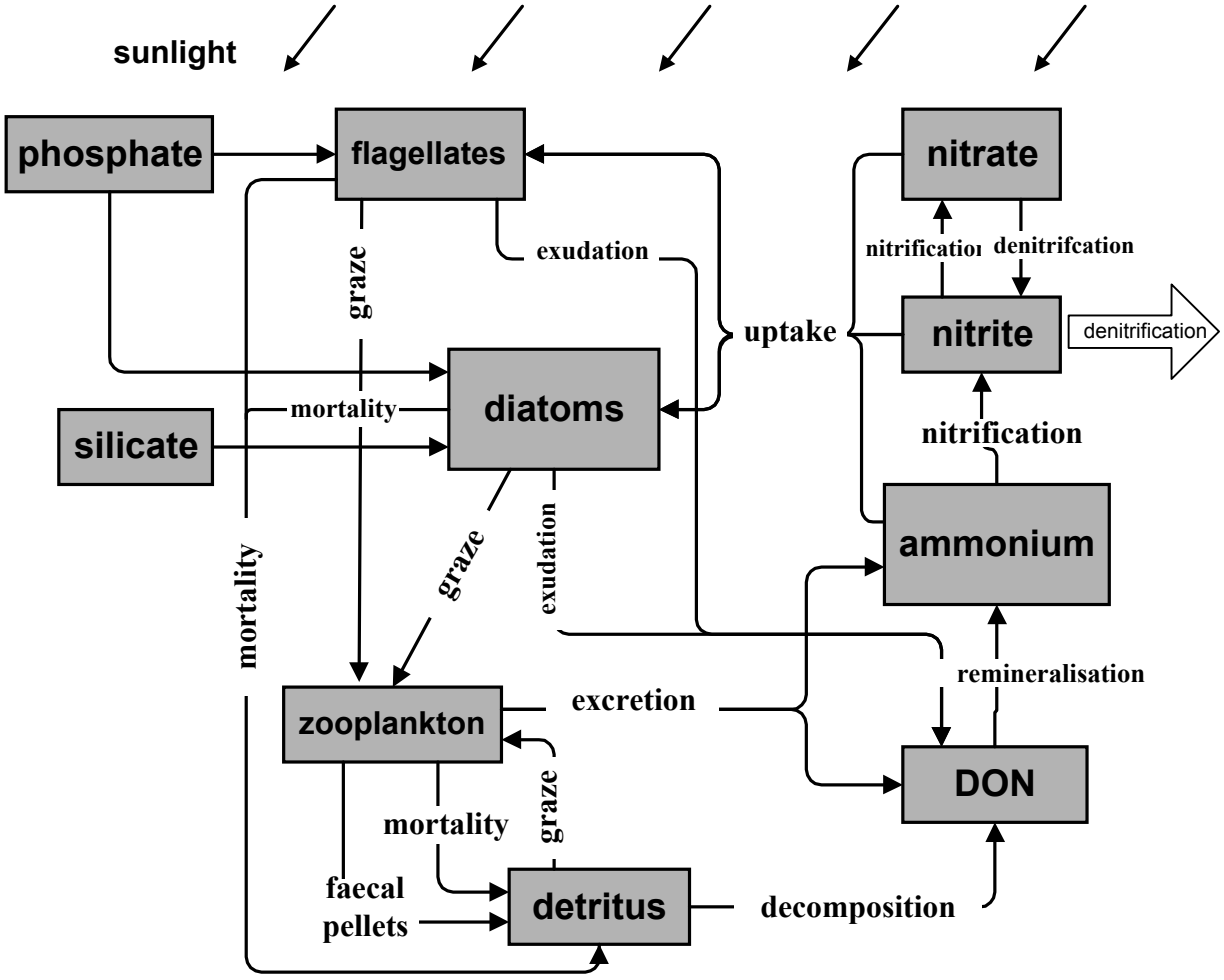

Fig. 2-3 Simplified scheme of modeling pelagic nitrogen cycling in enclosed waters.

2.4.1.1 The nitrogen cycle

2.4.1.1.1 Phytoplankton

The main processes considered in the model are summarized in the following general equation:

Phytoplankton N (diatoms, flagellates) = uptake - DON release - zooplankton grazing - natural mortality - nitrite release

It was assumed in the current model that mainly diatoms utilise silicate in the water column for growth. Though silicoflagellates and radiolarians also require silicon, they were neglected because of less biological importance (Parsons and Harrison 1983). Accordingly, phytoplankton community was simply divided into two groups: diatoms and flagellates, neglecting the different species with its different dynamic characteristics. Our assumption in using the phytoplankton biomass is that the species composition is dominated by two or three species, whose dynamic constants are similar and represent the entire plankton community, as has been practiced in many models (Radach and Moll 1993, Tett et al. 1986, Fasham et al. 1990, Dzierzbicka-Glowacka and Zielinski 1997, Bissett et al. 1999).

Since the enclosed systems were kept homogeneously mixed by pumping air bubbles into the water every minute, each enclosure was treated as one homogeneous box. The variations of both diatom and flagellate standing stocks are controlled by balances between primary production and losses due to zooplankton grazing, phytoplankton release and natural mortality, etc. The following differential equations were used for diatoms and flagellates respectively:

$$\frac{dptpd\_N}{dt} = (1 - Rpexud) \times uptk\_d - G\_pd \times zpt\_N - Pmort - Rno2\_d \quad (1)$$

$$\frac{dptpf\_N}{dt} = (1 - Rpexud) \times uptk\_f - G\_pf \times zpt\_N - Pmort - Rno2\_f \quad (2)$$

$\frac{dptpd\_N}{dt}$, $\frac{dptpf\_N}{dt}$: change of diatom and flagellate biomasses within the time step *t* (µmol N l^{-1} d^{-1}).

ptpd_N, ptpf_N: diatom and flagellate biomass in nitrogen (µmol N l^{-1}, state variables).

ptpd and *ptpf* represent the groups of diatoms and flagellates. *'_N'* refers to nitrogen cycle.

uptk_d, uptk_f: overall uptake rate of diatoms and flagellates, respectively (see equations 3 and 4) (d^{-1}).

Rpexud: specific phytoplankton DOM release rate (d^{-1}).

G_Pd, *G_Pf*: specific zooplankton graze rate on diatoms and flagellates (see equations 23 and 24) (d^{-1}).

Pmort: phytoplankton natural mortality (see equation 20).

Rno2_d, Rno2_f: nitrite release from diatoms and flagellates during luxury nitrate uptake (see equations 18 and 19).

Primary production

The growth of phytoplankton depends on the maximum growth rate under optimal growth conditions, affected by changing water temperature, light and nutrient concentrations:

$$uptk\_d = Rd\max \times Ftemp \times FI \times \min\left(FN, FP, FSi\right) \times ptpd\_N \quad (3)$$

$$uptk\_f = Rf\max \times Ftemp \times FI \times \min\left(FN, FP\right) \times ptpf\_N \quad (4)$$

Rdmax, Rfmax: maximum specific growth rate of diatoms and flagellates (d^{-1}).

Ftemp: temperature limitation function on phytoplankton growth (see equation 5) (dimensionless).

FI: light limitation function on phytoplankton growth (see equation 7) (dimensionless).

FN, FP, FSi: nitrogen nutrient, phosphate and silicate limitation functions on phytoplankton growth (see equations 15, 16 17) (dimensionless).

Temperature effects

The Q_{10} rule was used in the model to describe the temperature effect (*Ftemp*) on phytoplankton growth (Eppley 1972), which is defined as the change of phytoplankton growth rate for temperature increases by 10 °C steps. It is expressed as the equation below:

$$Ftemp = e^{r1 \times temp} \quad (5)$$

$r1$: temperature rate constant ($°C^{-1}$) on phytoplankton growth.

$r1$ is derived from the logarithm of the physiological Q_{10}, given by Kremer and Nixon (1978):

$$r1 = (\ln Q_{10})/10 \quad (6)$$

Q_{10}: the value gives the factor with which the process speed rises when increasing the process temperature by 10 °C (dimensionless).

Light effects

Light is often the ultimate limiting factor and supplies the radiant energy for photosynthesis. The effect of incident radiation on daily phytoplankton photosynthesis rate is described in the Steele equation (Steele 1962) (eq. 7), which involves designation of an optimal light level I_{opt} for photosynthesis. Only a part of irradiance is available for the photosynthesis, which is defined as photosynthesis available radiation (PAR). The ratio of PAR to total irradiance is affected by the zenith angle of the sun, water vapour content and aerosol optical thickness. A constant θ with the value of 0.43 was used as the ratio of PAR on sea surface to global irradiance. λ is set to define the transmittance at the air-water interface (Smith and Baker 1981, Fasham et al. 1990) (eq. 8).

$$FI = \frac{I}{Iopt} \times e^{(1-I/Iopt)} \quad (7)$$

I: the variable incident light intensity in the water column ($W\ m^{-2}$).

I_{opt}: optimum light intensity for phytoplankton photosynthesis (W m^{-2}).

$$Is = \lambda \times \theta \times I_0 \quad (8)$$

Is: photosynthesis available light intensity in the water below the surface (W m^{-2}).

I_0: light intensity measured above the water column (W m^{-2}).

θ: the ratio of photosynthesis available radiation (PAR) to measured light intensity (dimensionless).

λ: the transmittance at the air-water interface (dimensionless).

Light intensity decreases exponentially (eq. 9) with the water depth in correspondence to an extinction coefficient (*Ke*) due to the absorption of water itself K_0, the diffusion by suspended matter, and self-shading of phytoplankton which is dependent on the concentration of chlorophyll *a* (*chl*) in seawater (Kremer and Nixon 1978, Fransz et al. 1991, Chapelle et al. 1994) (eq. 10).

$$I = Is \times e^{-Ke \times z} \quad (9)$$

K_e: overall extinction coefficient of light in the water column (see equation 10) (m^{-1}).

z: the thickness of the water column (m).

$$Ke = K_0 + K_1 \times chl + K_2 \times (chl)^{2/3} \quad (10)$$

K_0: extinction of light intensity in the water column without phytoplankton self-shading (m^{-1}).

K_1: constant for phytoplankton self-shading (m^2 $(chl)^{-1}$).

K_2: constant for phytoplankton self-shading (m $(chl)^{-2/3}$)

Chl: phytoplankton biomass expressed as chlorophyll concentration (μg l^{-1}).

Express of $(K_1 \times chl + K_2 \times (chl)^{2/3})$: extinction of light intensity in the water column related to phytoplankton self-shading.

The overall expression of light intensity effect on primary production is shown in eq. 11, estimating the accumulated effects of non optimum light throughout the water column during a day (Kremer and Nixon 1978).

$$FI\,\mathrm{int} = 0.85 \times e \times f \times \left(e^{-(Is/Iopt) \times e^{-(ke \times z)}} - e^{-Is/Iopt} \right) \Big/ \left(k_e \times z \right) \quad (11)$$

*FI*int: the accumulated limitation function of light throughout the water column during a day (dimensionless).

0.85: correction factor.

e: the base of natural log.

f: the photoperiod as a fraction.

Nutrient uptake

Several laboratory experiments and field investigations showed that NH_4^+ is the most preferential nitrogen source for phytoplankton growth. NO_3^- is not taken up until NH_4^+ concentration drops to a threshold of 1 μM (McCarthy 1981, Dortch et al. 1991). After NO_3^- depletes below to ca. 1 μM, NO_2^- will be taken up in the following as N source for phytoplankton growth (Collos 1982, Raimbault 1986, Collos 1998). The simulation of the uptake of these three nitrogen sources follows the above principles.

The Michaelis-Menten-Monod equations were used here to parameterize the effect of nutrient concentration on nutrient uptake and therefore, assuming balanced growth, on the growth rate. *FN*, with *_a*, *_n* and *_i* representing ammonium, nitrate and nitrite respectively.

$$FN\_a = N\_a/(Ksa + N\_a) \tag{12}$$

$$FN\_n = N\_n \times \exp[(-\varphi 1 \times N\_a)/(Ksn + N\_n)] \tag{13}$$

$$FN\_i = N\_i \times \exp[(-\varphi 2 \times N\_n)/(Ksn + N\_i)] \tag{14}$$

FN_a, FN_n, FN_i: ammonium, nitrate and nitrite limitation functions on phytoplankton growth (dimensionless).

Ksa, *Ksn*, *Ksi*: the half-saturation constants of NH_4^+, NO_3^- and NO_2^- uptake (μmol N l^{-1}).

N_a, N_n, N_i: concentration of ammonium, nitrate and nitrite in the water (μmol N l^{-1}, state variables).

φ1 and φ2: inhibition factors, to allow uptake of NH_4^+ prior to NO_3^- and NO_3^- prior to NO_2^-.

General nitrogen limitation is summed up from these three equations (Fasham et al. 1990, Oguz et al. 1999).

$$FN = FN\_a + FN\_n + FN\_i \tag{15}$$

Functions of PO_4^{3-} and Si to phytoplankton growth (*FP, FSi*) were simplified also by Michaelis-Menten-Monod equation related to the concentration in the water column.

$$FP = P/(Ksp + P) \tag{16}$$

$$FSi = Si/(Kssi + Si) \tag{17}$$

FP, FSi: phosphate and silicate limitation function on phytoplankton growth (dimensionless).

P: phosphorus concentration in the water (μmol l^{-1}, state variable).

Si: silicate concentration in the water (μmol l^{-1}, state variable).

Ksp, *Kssi*: half-saturation constants of PO_4^{3-} and Si uptake (μmol l^{-1})

The Liebig's law was used to define the overall nutrient limitations on diatom and flagellate growth (De Groot 1983, Legovic and Cruzado 1997).

DOM release

DOM release by phytoplankton was observed from previous mesocosm experiments (Brockmann et al. 1983b, 1992) and other field investigations (Bronk et al. 1994, 1999). Phytoplankton releasing dissolved organic nitrogen (DON) was parameterized as a constant fraction of uptake (*Rpexud*: 2%) as in the model of Fasham et al. (1990) and other models (Chappell et al. 1994, Oguz et al. 1996, 1999).

Release of nitrite during phytoplankton nitrate uptake were proved and studied under various experimental conditions (Raimbault 1986, Sciandra and Amara 1994, Collos 1998) as well as in the field (French et al. 1983). The release of nitrite (*Rno2*) is dependent on uptake of nitrate and it could reach up to 27% of nitrate uptake. It is found to be affected by temperature, light and nutrient conditions (Collos 1998). A parameter σ was induced in the model to ioarameterize the fraction of nitrite released during surplus nitrate uptake.

$$Rno2\_d = \sigma \times \frac{FN\_n}{FN} \times uptk\_d \tag{18}$$

$$Rno2\_f = \sigma \times \frac{FN\_n}{FN} \times uptk\_f \tag{19}$$

σ: the fraction of NO_2^- release by phytoplankton during surplus nitrate uptake (dimensionless).

Mortality

Natural mortality of phytoplankton *Pmort* was mainly concerned as physiological process and assumed as certain proportion of plankton biomass related to temperature effects.

$$Pmort = Rpmort0 \times e^{r3 \times Temp} \times ptp\_N \tag{20}$$

Rpmort0: specific phytoplankton mortality rate at 0°C (d^{-1}).

*r*3: temperature rate constant on phytoplankton mortality, similar to *r*1 (dimensionless).

2.4.1.1.2 Zooplankton

For zooplankton, only one state variable was used with main turnover rates related to its biomass. Change of zooplankton standing stock is controlled by zooplankton ingestion, grazing, mortality, faecal pellet production and DOM excretion, summarized by following expression:

Zooplankton N = grazing on diatoms and flagellates + grazing on detritus –

natural mortality – excretion – faecal pellet production

$$\frac{dzpt\_N}{dt} = b1 \times (G\_pd + G\_pf) \times zpt\_N + b2 \times G\_d \times zpt\_N - Zmort - Zexcr \tag{21}$$

$\frac{dzpt\_N}{dt}$: change of zooplankton biomass within the time step *t* (μmol N l^{-1} d^{-1}).

zpt_N: zooplankton biomass in nitrogen (μmol N l^{-1}, state variable).

*b*1, *b*2: zooplankton assimilation efficiency on phytoplankton and detritus (dimensionless).

Zmort: zooplankton natural mortality (μmol N l^{-1} d^{-1}).

Zexcr: zooplankton excretion (μmol N l^{-1} d^{-1}), including NH_4^+ fraction (*Zexcr1*, see equation 34) and DON fraction (*Zexcr2*, see equation 44).

Grazing

Zooplankton grazing was referred to the literature from Oguz et al. (1999), which is a modified version from Fasham et al. (1990). The grazing was represented by the similar Michaelis-Menten-Monod equation, in which the food preferences on diatoms, flagellates and detritus were considered. The total available food source for the whole zooplankton group was defined as:

$$Fz = c1 \times ptpd\_N + c2 \times ptpf\_N + c3 \times D\_N \quad (22)$$

Fz: total available food source (μmol N l^{-1}).

c1, c2, c3: the preference constants of zooplankton grazing on diatoms, flagellates and detritus. Different values are used here to indicate zooplankton grazing preference to phytoplankton in comparison to detritus (Parsons et al. 1984).

The grazing rates on diatoms (*G_pd*), flagellates (*G_pf*) and detritus (G_*d*) were expressed respectively as maximum zooplankton grazing rate, total available food, food preference coefficients and the amount of respective food source.

$$G\_pd = Rgmax \times \frac{c1 \times ptpd\_N}{Kg + Fz} \quad (23)$$

$$G\_pf = Rgmax \times \frac{c2 \times ptpf\_N}{Kg + Fz} \quad (24)$$

$$G\_d = Rgmax \times \frac{c3 \times D\_N}{Kg + Fz} \quad (25)$$

Rgmax: zooplankton maximum specific graze rate (d^{-1}).

Kg: half-saturation constant of zooplankton grazing (μmol N l^{-1}).

The increase of zooplankton body weight is related to metabolic processes and excretion. Different constants have been used to express the diverse assimilative efficiencies (affinity) on different diets for zooplankton with higher efficiency on phytoplankton feeding (*b1*: 0.85) than on detritus (*b2*: 0.6) (Parsons et al. 1984).

Excretion

The principle products of excreted N from zooplankton are NH_4^+ and DON, including urea and amino acids (Parsons et al. 1984). The ratio of excreted NH_4^+ to DON is variable (Jφrgensen et al.

1991). Butler et al. (1970) found from some experiments that the percentage of body nitrogen excreted per day varies from ca. 10% in spring to less than 2% in winter. Nitrogen and phosphate excretion from zooplankton is significantly influenced by temperature, with Q_{10} about 0.8 to 2.7 (Wen and Peters 1994). Zooplankton excretion (*Zexcr*) was thus expressed as a fraction of zooplankton body N in relation to a parameter of excretion rate *Rzexcr* (eq. 26), which is affected by temperature with a coefficient *r6* (eq. 27).

$$Z_{excr} = R_{zexcr} \times zpt\_N \quad (26)$$

$$R_{zexcr} = R_{zexcr0} \times e^{r6 \times temp} \quad (27)$$

Rexcr: specific zooplankton excretion rate (d^{-1}).

Rexcr0: specific zooplankton excretion rate at 0°C (d^{-1}).

*r*6: temperature constant for zooplankton excretion (dimensionless).

Faecal pellet production

The main fates of zooplankton grazing are for growth, metabolism, faecal pellets and grazed by higher trophic predator. The fraction not assimilated was assumed to be returned to the water column as faecal pellets. This fraction can reach 60% and 95% of grazing varying with different food sources (Parsons et al. 1984). Recent measurements showed that the faecal pellet production of copepods varied from 0.34 pellets ind^{-1} h^{-1} to 0.27 pellets ind^{-1} h^{-1} during a diatom bloom in the North Sea Southern Bight (Frangoulis et al. 2001).

Faecal pellet production from copepods varies also with temperature and food concentration. Based on feeding rates between 77% and 187% of the body weight per day, the egestion rates varies between 8% and 25% of body weight with the highest rates recorded at the highest water temperatures and highest food concentration (Burckhardt and Heerkloss 1999). The production rate of faecal pellets measured in the pelagic zone was found to be ca. 5 to 10 times higher than faeces in the water column, indicating very fast turnover of faecal pellets in the water column in relation to remineralisation and filtering graze. Fast remineralisation of faecal pellets was observed, the fraction of faeces broken up and further on remineralised in the mixed water layer could reach up to 99% (Viitasalo et al. 1999).

2.4.1.1.3 Detritus

Terms involved into the pelagic detritus pool were expressed as following:

Detritus = mortality (phytoplankton + zooplankton) + faecal pellet production –

detritus decay - zooplankton grazing

Faecal pellets, constituting the non-assimilated part of ingested food, aggregates of DOM, dead phytoplankton cells and zooplankton bodies as well as moults, are the main sources of the pelagic

detritus pool.

$$\frac{dD\_N}{dt} = Zmort + Pmort + (1-b1)\times(G\_pd + G\_pf)\times zpt\_N - b2\times G\_d\times zpt\_N - Ddecay \quad (28)$$

$\frac{dD\_N}{dt}$: change of detritus contents in the water column within the time step *t* (µmol N l^{-1} d^{-1}).

D_N: detritus content in the water (µmol N l^{-1}, state variable).

$(1-b1)\times(G\_pd + G\_pf)\times zpt\_N$: Faecal pellets, dissimilated fraction of zooplankton feeding on phytoplankton.

$b2\times G\_d\times zpt\_N$: the overall expression of zooplankton filtering feed on detritus and non-assimilated fraction.

Ddecay: fraction of detritus decomposition (see equation 29) (µmol N l^{-1} d^{-1}).

Decay of pelagic detritus is relevant to bacteria, which is a fraction of detritus as well, if they are attached to particles. It has been shown that some bacteria clinging to detritus decompose detritus to DON (Hoppe 1976). Menzel and Goering (1966) found that in samples from 1m depth in the North Atlantic, between 16% and 52% of the detritus are biodegradable. Since bacteria are treated here as an implicit term, this process was simply parameterized by specific decay coefficient of detritus (*Rddecay*) (eq. 29), which is a function of temperature (r7) and detritus concentration (eq. 30).

$$Ddecay = Rddecay\times D\_N \quad (29)$$

$$Rddecay = Rddecay(0)\times e^{(r7\times temp)} \quad (30)$$

Rddecay: specific decomposition rate of detritus (d^{-1}).

Rddecay0: specific decomposition rate of detritus at 0°C (d^{-1}).

r7: temperature constant for detritus composition (dimensionless).

Detritus is also a food source for some filter-feeding animals, grazing of bacterial aggregates, which grow using the detritus as substrates (Seki 1982). Some planktonic herbivores (the cladocere *Evadne tergestina* and the copepoda genus *Acrocalanus*) were found to exhibit a clear tendency to re-ingest their own faecal pellets after a period of starvation (Goes et al. 1999).

2.4.1.1.4 Nitrogen nutrients

NH_4^+, NO_3^- and NO_2^- were considered in the model as the main nitrogen sources for phytoplankton growth. NH_4^+ is supposed to be the first product of nitrogen regeneration, which is mainly related to DON remineralisation and zooplankton related excretion. Bacteria related nitrification and denitrification are processes at the steady equilibrium among the three forms of N in the water.

Nitrification and denitrification in the water column

The processes of nitrification from ammonium to nitrite and from nitrite to nitrate are related to nitrifying bacteria of *Nitrosomonas* and *Nitrobacter* respectively. The oxidation of ammonium to nitrite and nitrite to nitrate follows Michaelis-Menten kinetics (Kaplan 1983). As bacteria were implicated in this model, a fraction of ammonium (nitrification rate) was assumed to be converted to nitrate, but the effect of temperature (*r9*) has to be considered (eq. 33). The optimum temperature for nitrification was found ranging between 25°C and 35°C. The values of Q_{10} vary between 1.3 and 3.0 over a temperature range of 18°C to 28°C (Kaplan 1983), thus, *Rni0* was set as nitrification rate at 15°C.

Denitrification is the main sink of nitrogen in the marine environment besides sedimentation. Data reviewed by Hattori (1983) indicated that water column denitrification and sedimentary denitrification contribute equally to the nitrogen budget in the world oceans. In the water with sufficient oxygen supply, the aggregates of organic matter take the role to supply a micro anoxic environment for denitrifying bacteria to degrade nitrate, nitrite and DON to N_2O and N_2. As pointed out by Jannasch (1960): 'in some aerobic environments, denitrification may occur in the presence of detrital particles'. This is probably due to the formation of anaerobic microzone of bacterial activity within the particles (Parsons et al. 1984).

Denitrification in the water column is related to concentrations of dissolved oxygen, nitrate, nitrite and the abundance of bacteria, which are involved in the different steps of the dissimilatory nitrate reduction: from NO_3^- to NO_2^- and further on from NO_2^- to N_2O and N_2 as well as in the decomposition of dissolved and particulate organic matter (Hattori 1983). In the model, the process is considered as consisting in two steps: from NO_3^- to NO_2^- and from NO_2^- to N_2O and N_2. Both are related to a specific rate and temperature coefficient (*r8, r10*). (eq. 38, 42)

The overall equations of NH_4^+, NO_3^- and NO_2^- are as following:

NH_4^+ - related equations:

Ammonium = - phytoplankton uptake + DON_remineralisation + zooplankton excretion - nitrification

$$\frac{dN\_a}{dt} = -uptkN\_a - Nitri + Zexcr1 + Remin \tag{31}$$

$\frac{dN\_a}{dt}$: change of ammonium concentration in the water column within time step *t* (µmol N l^{-1} d^{-1}).

$$uptkN\_a = \frac{FN\_a}{FN} \times (uptk\_d + uptk\_f) \tag{32}$$

uptkN_a: ammonium by phytoplankton uptake (µmol N l^{-1} d^{-1}).

$$Nitri = Rni0 \times e^{(r9 \times (temp - 15))} \times N\_a \tag{33}$$

Nitr: ammonium loss via nitrification (µmol N l^{-1} d^{-1}).

Rni0: specific nitrification rate (d^{-1}).

*r*9: temperature constant of nitrification (dimensionless).

$$Zexcr1 = \varepsilon \times Rzexcr \times zpt\_N \quad (34)$$

Zexcr1: ammonium regeneration from zooplankton excretion (µmol N l^{-1} d^{-1}).

ε: the fraction of ammonium from zooplankton excretion (dimensionless).

$$R_{emin} = R_{emin(0)} \times e^{(r8 \times temp)} \times DON \quad (35)$$

R_{emin}: remineralisation rate (d^{-1}).

$R_{remin(0)}$ the remineralisation rate at 0°C (d^{-1}).

*r*8: temperature constant for DON remineralisation (dimensionless).

NO_3^- - related equations:

Nitrate = - phytoplankton uptake + nitrification – denitrification to nitrite

$$\frac{dN\_n}{dt} = -uptkN\_n + Nitri - den1 \quad (36)$$

$\frac{dN\_n}{dt}$: change of nitrate concentration in the water column within time step *t* (µmol N l^{-1} d^{-1}).

$$uptkN\_n = \frac{FN\_n}{FN} \times (uptk\_d + uptk\_f) \quad (37)$$

uptkN_n: nitrate loss by phytoplankton uptake (µmol N l^{-1} d^{-1}).

$$den1 = Rden01 \times e^{r10 \times (temp - 15)} \times N\_n \quad (38)$$

den1: specific rate of denitrification $NO_3^- \rightarrow NO_2^-$ (d^{-1}).

Rden01: specific rate of denitrification at 15°C (d^{-1}).

*r*10: temperature constant (dimensionless).

NO_2^- - related equations

Nitrite = - phytoplankton uptake + release during surplus nitrate uptake + denitrification from nitrate - denification to N_2O or N_2

$$\frac{dN\_i}{dt} = -uptkN\_i + Rno2 + den1 - den2 \quad (39)$$

$\frac{dN\_i}{dt}$: change of nitrite concentration in the water column within the time step *t* (µmol N l^{-1} d^{-1}).

$$uptkN\_i = \frac{FN\_i}{FN} \times (uptk\_d + uptk\_f) \quad (40)$$

uptkN_i: nitrite loss by phytoplankton uptake (µmol N l^{-1} d^{-1}).

$$Rno2 = \rho \times uptkN\_n \quad (41)$$

Rno2: nitrite release from phytoplankton (µmol N l^{-1} d^{-1}).

ρ: fraction of nitrite release to nitrate uptake (dimensionless).

$$den2 = Rden02 \times e^{r11 \times (temp-15)} \times N\_i \quad (42)$$

den2: nitrite loss via denitrification $NO_2^- \rightarrow N_2$ (or N_2O) (µmol N l^{-1} d^{-1}).

Rden02: specific rate of denitrification at 15°C (d^{-1}).

*r*11: temperature constant (dimensionless).

2.4.1.1.5 Dissolved organic nitrogen (DON)

Pelagic DON pool balances between production from phytoplankton release, zooplankton excretion, detritus decay and remineralisation. Particularisation and dissolution from detritus by sorption and desorption was assumed to be levelled and was neglected.

DON = phytoplankton release + zooplankton excretion + detritus decay - remineralisation

$$\frac{dDON}{dt} = Zexcr2 + Ddecay + Rpexud \times (uptk\_d + uptk\_f) - Remin \quad (43)$$

$\frac{dDON}{dt}$: change of DON concentration in the water column within time step *t* (µmol N l^{-1} d^{-1}).

DON: dissolved organic nitrogen in the water (µmol N l^{-1}, state variable).

$$Zexcr2 = (1-\varepsilon) \times Rzexcr \times zpt\_N \quad (44)$$

Zexcr2: fraction of DON from zooplankton excretion (µmol N l^{-1} d^{-1}).

2.4.1.2 The phosphorus cycle

P uptake by phytoplankton in the model was related to N uptake. Specified uptake N/P ratio (*Rpn_uptk*) is used for phytoplankton uptake, though the N/P ratio in phytoplankton varied dramatically at different nutrient conditions (Jϕrgensen et al. 1991).

Regeneration of phosphorus is mainly related to zooplankton activities. Butler et al. (1970) reported that during grazing of *Calanus* more than 80% of the consumed phytoplankton phosphorus was released, either as particulate organic phosphorus in faecal pellets or as soluble organic phosphorus from the metabolism (ca. 60%). A small amount of dissolved organic phosphorus can be excreted by phytoplankton but it is generally of minor importance compared to zooplankton production (Parsons

and Harrison 1983). This fraction of P excretion from zooplankton is 5% to 25% of the body phosphorus according to the studies of Harris (1973) and Pomeroy et al. (1963). The N/P ratio in dissolved excreted material is about 5 in spring and 6 in winter (Butler et al. 1970). Thus, in this model the main sources of dissolved organic phosphorus were assumed to originate from zooplankton and detritus decay. Unlike nitrogen, DOP returns directly to the phosphate pool via remineralisation.

The equations of the main phosphorus compartments are represented quite similarly to those of nitrogen, except for some parameters related to regeneration processes, such as zooplankton P excretion (*Rzexcr_P(0)*), P release from detritus decay (*Rddecay_P(0)*), DOP remineralisation (*Rremin_P(0)*).

Phytoplankton P = phosphate uptake - zooplankton grazing - natural mortality

$$\frac{dptp\_P}{dt} = P\_uptk - (G\_pd + G\_pf) \times zpt\_P - P\_Pmort \tag{45}$$

$\frac{dptp\_P}{dt}$: change of phytoplankton biomass in phosphorus within time step *t* (μmol P l^{-1} d^{-1}).

ptp_P: phytoplankton biomass in phosphorus (μmol P l^{-1}, state variable).

$$P\_uptk = (uptk\_d + uptk\_f) \times Rpn\_uptk \tag{46}$$

P_uptk: phytoplankton uptake phosphorus (μmol P l^{-1} d^{-1}).

Rpn_uptk: P/N uptake ratio in atom (μmol P/μmol N).

$$P\_Pmort = Pmort \times Rpn\_ptp \tag{47}$$

P_Pmort: phytoplankton natural mortality in phosphorus (μmol P l^{-1} d^{-1}).

Rpn_ptp: phytoplankton P/N ratio in atom (μmol P/μmol N).

Zooplankton P = grazing on phytoplankton + grazing on detritus

- zooplankton mortality - zooplankton excretion

$$\frac{dzpt\_P}{dt} = b1 \times (G\_pd + G\_pf) \times zpt\_P + b2 \times G\_d \times zpt\_P - P\_Zmort - P\_Zexcr \tag{48}$$

$\frac{dzpt\_P}{dt}$: change of zooplankton biomass in phosphorus within time step *t* (μmol P l^{-1} d^{-1}).

zpt_P: zooplankton biomass in phosphorus (μmol P l^{-1}, state variable).

$$P\_Zmort = Rzmort \times zpt\_P \tag{49}$$

P_Zmort: zooplankton natural mortality in phosphorus (µmol P l^{-1} d^{-1}).

R*zmort*: specific zooplankton mortality rate (d^{-1}).

$$P\_Zexcr = Rzexcr\_P \times zpt\_P \tag{50}$$

P_Zexcr: zooplankton excretion in phosphorus (µmol P l^{-1} d^{-1}).

$$Rzexcr\_P = Rzexcr\_P(0) \times e^{r6 \times temp} \tag{51}$$

Rzexcr_P: specific zooplankton excretion rate in phosphorus (d^{-1}).

Rzexcr_P(0): specific zooplankton excretion rate in phosphorus at 0°C (d^{-1}).

Detritus P = phytoplankton mortality + zooplankton mortality + zooplankton dissimilation - zooplankton grazing - detritus decay

$$\frac{dD\_P}{dt} = P\_Zmort + P\_Pmort + (1 - b1) \times (G\_pd + G\_pf) \times zpt\_P - b2 \times G\_d \times zpt\_P - P\_Ddecay \tag{52}$$

$\frac{dD\_P}{dt}$: change of detritus contents in phosphorus within time step *t* (µmol P l^{-1} d^{-1}).

D_P: detritus contents in the water column (µmol P l^{-1}, state variable).

$$P\_Ddecay = P\_Rddecay \times D\_P \tag{53}$$

$$P\_Rddecay = Rddecay\_P(0) \times e^{(r7 \times temp)} \tag{54}$$

P_Ddecay: detritus decomposition in phosphorus (µmol P l^{-1} d^{-1}).

P_Rddecay: specific detritus decomposition in phosphorus (d^{-1}).

R_ddecay_P(0): specific detritus decomposition in phosphorus at 0°C (d^{-1}).

DOP = zooplankton excretion + detritus decay – remineralisation of DOP

$$\frac{dDOP}{dt} = P\_Zexcr + P\_Ddecay - P\_Remin \tag{55}$$

$\frac{dDOP}{dt}$: change of dissolved organic phosphorus concentration within time step t (µmol P l^{-1} d^{-1}).

DOP: dissolved organic phosphorus concentration in the water (µmol P l^{-1}, state variable).

$$P\_Remin = Remin\_P(0) \times e^{(r8 \times temp)} \times DOP \tag{56}$$

P_Remin: DOP remineralisation to phosphate (µmol P l^{-1} d^{-1}).

Remin_P(0): specific DOP remineralisation rate at 0°C (d^{-1}).

Phosphate = - phytoplankton uptake + remineralisation of DOP

$$\frac{dP}{dt} = -P\_uptk + P\_remin \quad (57)$$

$\frac{dP}{dt}$: change of phosphate concentration within time step *t* (µmol P l^{-1} d^{-1}).

2.4.1.3 The silicon cycle

The silicate cycle is the simplest compared to nitrogen and phosphorus. Silicate in seawater is mainly taken up by diatoms, though a few other classes of phytoplankton (e.g. silicoflagellates) and protozoa (e.g. radiolarians) also require silicon. However, silicate will also be absorbed by diatom cells below the euphotic zone (Rey and Skjoldal 1987, Wassmann et al. 1997). Not any known organic forms are of biological importance. Thus, the main cycling pathway of silicate is from dissolved inorganic to particulate and back to the inorganic form (Parsons and Harrison 1983). The rate of silicate remineralisation is slow compared to nitrogen and phosphorus (Dugdale 1972). In the model, it is assumed that only a certain fraction of incorporated silicate is regenerated and returned to the silicate pool (Eppley et al. 1978, Parsons and Harrison 1983).

Silicate = - diatom uptake + regeneration

$$\frac{dSi}{dt} = Si\_uptk + Si\_regn \quad (58)$$

$\frac{dSi}{dt}$: change of silicate concentration within time step *t* (µmol Si l^{-1} d^{-1}).

$$Si\_uptk = uptk\_d \times Rsn\_uptk \quad (59)$$

Si_uptk: Silicate by phytoplankton uptake (µmol Si l^{-1} d^{-1}).

Rsn_uptk: Si/N ratio for diatom uptake in atom (µmol Si/µmol N).

$$Si\_regn = \xi \times Si\_uptk \quad (60)$$

Si_regn: regenerated silicate (µmol Si l^{-1} d^{-1}), expressed as a fraction of taken up silicate.

ξ: the fraction of regenerated Si to uptake (dimensionless).

2.4.2 Forcing variables

The model was physically driven by irradiance and water temperature. These data were measured during the experiments. The time steps of the model were one hour. Hourly integrated means of irradiance were induced to the model. Water temperature was measured every 2 hours. Hourly data were linearly interpolated between two measurements.

2.4.3 Initial values

Most initial values of the model compartments were taken from measurements such as inorganic

nutrients, dissolved organic matters. Initial values of diatoms, flagellates, zooplankton and detritus were estimated from measured particulate matter as follows: phytoplankton nitrogen and phosphorus were calculated from measured living chlorophyll *a* (1 Hz) via ratios of phytoplankton N/chl*a* and P/chl*a* under similar conditions. Accordingly, the proportions of phytoplankton N and P to total particulate N and P were calculated. The initial diatoms/flagellates ratio to phytoplankton N and P, and zooplankton/detritus ratio to total particulate N and P were then assumed according to their abundance from microscopic observations (Dürselen, personal communication). The initial values of all state variables in spring and summer were listed in table 2-2.

Table 2-2 The main compartments (state variables) and respective initial values in the model.

Compartments	**Symbols**	**Initial values**	
		Spring (μM)	Summer (μM)
Diatom nitrogen	*ptpd_N*	0.5	1.6
Flagellate nitrogen	*ptpf_N*	0.13	0.4
Zooplankton nitrogen	*zpt_N*	0.6	2
Detritus nitrogen	***D_N***	5.0	5.2
Nitrate	***N_n***	143.0	25.32
Ammonium	***N_a***	12.0	13.85
Nitrite	***N_i***	2.68	0.74
Dissolved organic nitrogen	DON	22.57	22.0
Phosphate	P	1.65	1.84
Phytoplankton phosphorus	*ptp_P*	0.03	0.075
Zooplankton phosphorus	*zpt_P*	0.01	0.05
Detritus phosphorus	***D_P***	0.64	0.38
Dissolved organic phosphorus	DOP	10	2.0
silicate	Si	88	10.2

2.4.4 Sensitivity analysis

Sensitivity analysis of parameter was carried out by changing the parameters, then the corresponding response on the selected state variables was observed.

For parameter P, the sensitivity is *Sp*, thus following equation was used (Jϕrgensen 1994):

$$Sp = \left[\frac{\partial X}{X}\right] \Big/ \left[\frac{\partial P}{P}\right] \tag{61}$$

X is the state variable considered.

For detailing the above equation, following equation may be clearer:

$$Sp = \left(\frac{\left(E(p) - Es\right)}{Es} \right) \Big/ \left(\frac{\left(P - Ps\right)}{Ps} \right) \tag{62}$$

Es is the value of a given statistic for the standard case with parameter value *Ps*, and *E(p)* is the value for the case when the parameter is given the value *P*. This index measures the fractional change in the statistic for a fractional change in the parameters.

In this model for sensitivity analysis, integrated amounts of chosen state variables during the whole period of the experiment were considered by a different value of a chosen parameter. Based on the knowledge of the parameter, the relative variation of a parameter was chosen at ±10% or ±50% of it, according to the uncertainty of the parameter.

2.4.5 Software environment

ModelMaker 3 (Cherwell Scientific Company) was used for mathematical calculations.

3 RESULTS

3.1 Mesocosm experiments

3.1.1 Spring experiment (Series 1)

Sub-systems: Sequence A: Control bags are indicated as T1, T3*, T5;

Sequence B: Experimental bags are indicated as T2, T4*, T6;

Reference: Harbour water is indicated as T7.

Due to good reproducibility of the mesocosms for most monitored parameters, only the developments in the main bags (T1 and T4) are presented and mainly discussed considering their more frequent sampling.

3.1.1.1 Physical boundary conditions

Light (Fig. 3-1A)

The field data of irradiance during the spring experiment were integrated and calculated to hourly and daily means. Hourly irradiance variation showed the expected diurnal rhythm with the highest values between 12:00 and 14:00 and close to zero at night-time 18:00 to 06:00. The highest values changed between 320 W/m^2 and 480 W/m^2 in the first week and increased to 550 to 660 W/m^2 during the following two weeks except for two days, 24th and 26th, lower than 300 W/m^2. Irradiance in the last 4 days varied strongly between 120 W/m^2 up to 683 W/m^2.

Daily mean irradiance showed variations between 75 W/m^2 and 135 W/m^2 in the first week, followed by two weeks with a daily mean irradiance between 130 and 200 W/m^2 except for two days with lower than 70 W/m^2. During the succeeding 6 days, the daily mean irradiance varied strongly between 40 W/m^2 up to 180W/m^2.

Water temperature (Fig. 3-1B)

During the experiment, temperature in the three bags increased in parallel from about 4°C at the beginning to 10°C with diurnal variation in the range of 0.6 to 1.0°C.

Salinity (Fig. 3-1C)

The salinity in the plastic bags remained constant at 19.1 to 19.2 at the beginning and started from 01/04 to increase up to 20.0 at the end. In the harbour, salinity was higher than in the bags and increased gradually from 19.4 to 21, showing short-term fluctuations due to tidal action.

Turbidity (Fig. 3-1D)

Turbidity fluctuated in T1 and T4 between 6.0 NTU and 9.0 NTU during the first three days. Afterwards it remained around 5.5 to 6.0 until 30/03, increased for about 1.0 NTU within one day and fluctuated in the range of 6.0 to 7.0 NTU after 01/04. Turbidity in the harbour showed larger variation especially during the first half period from about 6.0 NTU to more than 15.0 NTU. During the second half period, turbidity varied in the range of 3.7 NTU to 9.0 NTU.

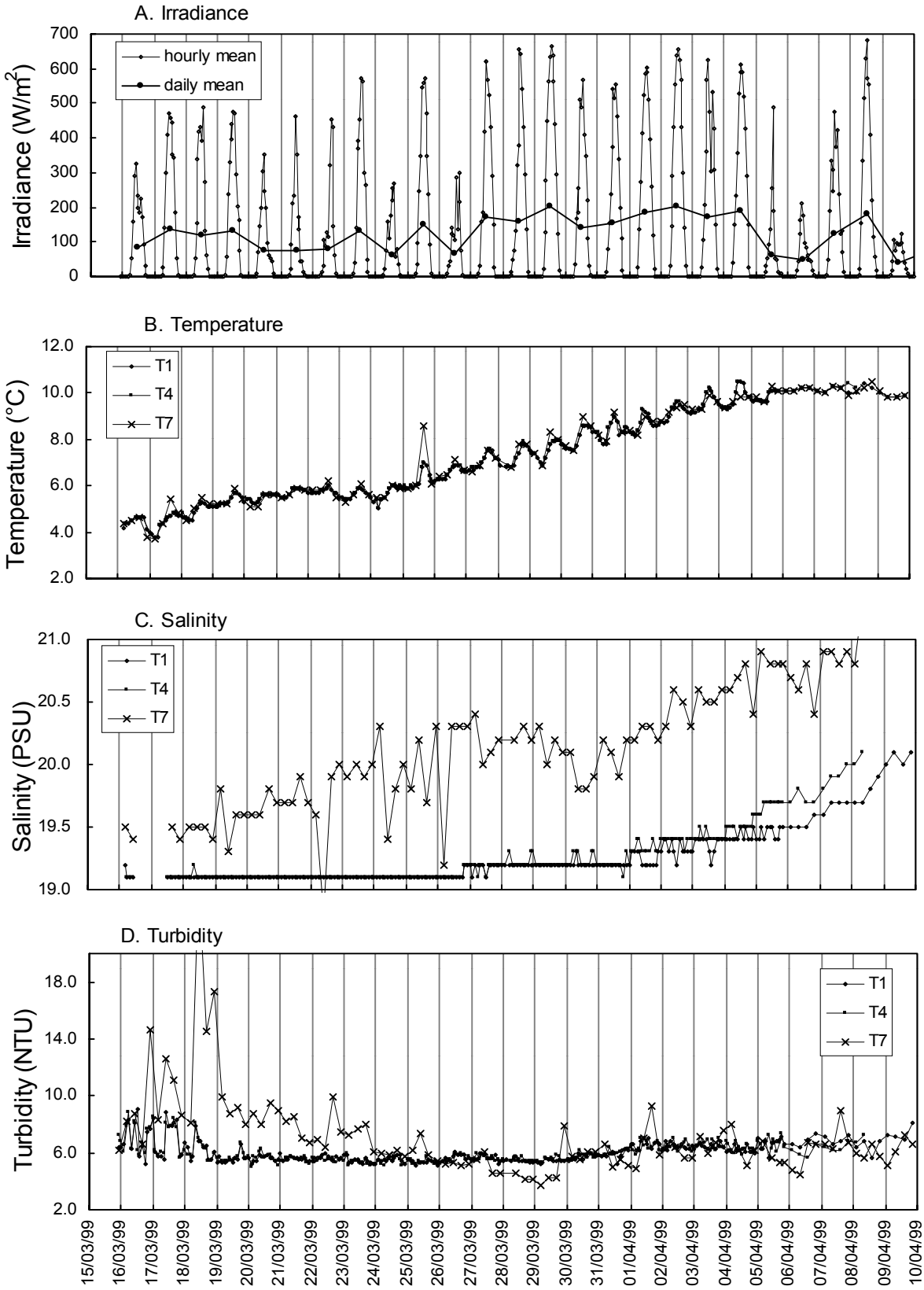

Fig. 3-1 Physical parameters in the spring experiment (Series 1, Büsum, Mar./Apr., 1999) (T1: the main bag of sequence A; T4: the main bag of sequence B; T7: the harbour water)

3.1.1.2 Chemical parameters

Nutrients (Fig. 3-2)

In the control bag (T1), ammonium decreased from about 12 µM at the beginning of the experiment to a minimum of 0.3 µM within 12 days until the midday of 27/03 (Fig. 3-2A). Then it increased slightly to 0.8 µM, and fluctuated around 0.8 to 1.0 µM until the end of the experiment. In the experimental bag (T4), ammonium developed quite similarly as in T1. NH_4^+ concentrations in the harbour were around 12 µM at beginning and fluctuated between 9 and 15 µM during the first 15 days. After that, they gradually decreased from 14 µM to the lowest of 6 µM during the following 6 days. During the last 5 days, they remained around 8 µM. All periods were characterised by maxima, reaching more than 20 µM.

Nitrate in T1 remained constant during the first 12 days in the range of 142 to 145 µM (Fig. 3-2B). It started to decrease after the depletion of ammonium on 27/03, and declined to about 85 µM on 03/04, then remained at this value until the end. Nitrate in T4 was nearly constant around 142 to 145 µM during the first 12 days and started to decrease at 28/03, from 141 µM to 48 µM on 03/04. Afterwards, it stagnated in the range of 47 µM to 49 µM within the following two days. It then increased slightly since 06/04 from 50 µM to 58 µM at the end of the experiment. In the harbour, NO_3^- varied around 140 µM for most of the time. During the last 4 days, it decreased gradually to 125 µM.

Nitrite in T1 varied between 2.65 to 2.70 µM from the beginning to 26/03, followed by a decrease to about 2.60 µM until 03/04, and then increased succeedingly up to 2.75 µM on 09/04 (Fig. 3-2C). Nitrite in T4 fluctuated mostly between 2.65 µM and 2.70 µM until 29/03. It increased to a maximum of 2.85 µM on 30/03, and varied with significant diurnal fluctuation during the next three days. There was a decrease of 0.1 µM within the last 7 days. In the harbour, NO_2^- decreased from 2.6 µM at the beginning to 2.5 µM during the first 6 days. It then increased to 2.7 during the next 6 days and continued to increase to 2.9 µM within the following 6 days. During the last 5 days it fluctuated around 2.8 µM.

PO_4^{3-} concentrations in T1 decreased gradually from 1.65 µM to 1.6 µM during the first 8 days (Fig. 3-2D). It then dropped below 0.1 µM within the next 6 days and remained around 0.05 µM during the rest of experimental period. In T4, PO_4^{3-} was added on 26/03 reaching 3.5 µM. Added PO_4^{3-} was depleted quickly within the next 5 days and remained around 0.05 µM during the following 8 days. In the harbour, PO_4^{3-} showed an inconsistent development: it increased gradually from 1.65 µM at the beginning to about 2.5 µM during the first 15 days. Following a decrease to 1.75 µM during the next 6 days, an increase of 0.5 µM occurred during the last 5 days and PO_4^{3-} reaching about 2.2 µM until the end.

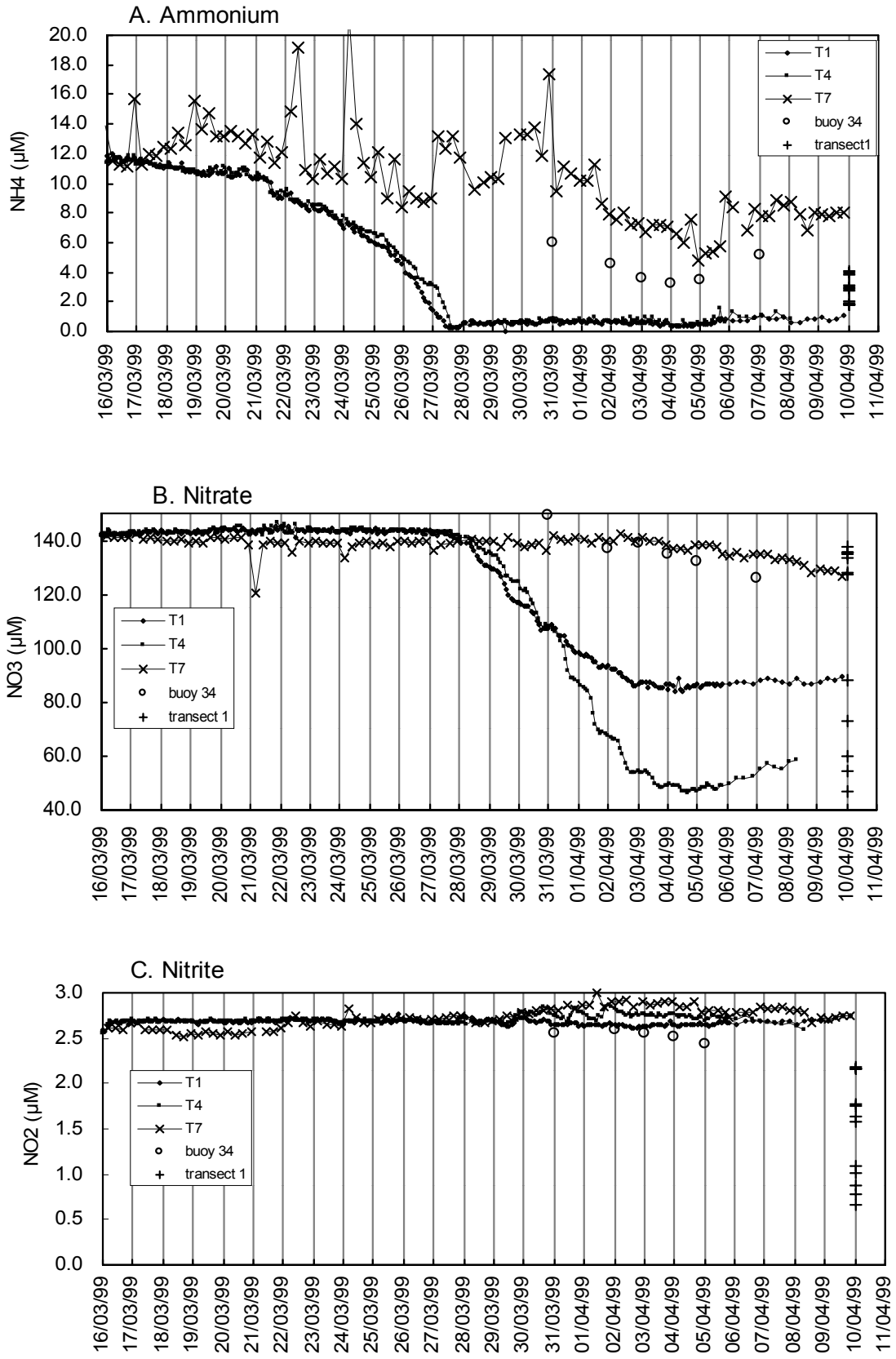

Fig. 3-2 Nutrients in the spring experiment (Series 1, Büsum, Mar./Apr., 1999)
(to be continued)

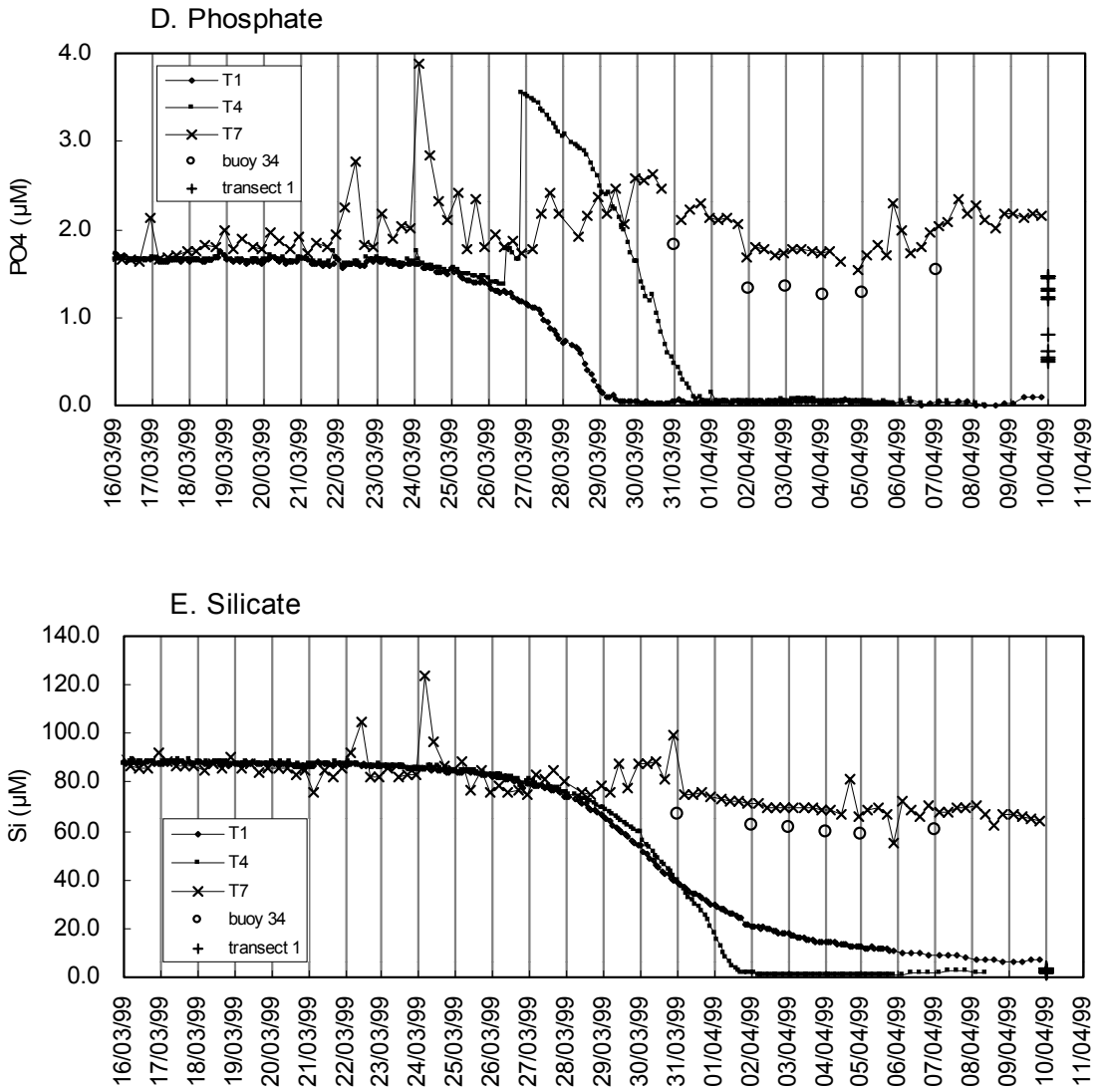

Fig. 3-2 Nutrients in the spring experiment (series 1, Büsum, Mar./Apr., 1999) (T1: the main bag of sequence A; T4: the main bag of sequence B; T7: the harbour water)

Silicate in T1 decreased slowly from 88 µM to 82 µM within the first 10 days, followed by a faster decrease of 50 µM to 31 µM within 6 days (Fig. 3-2E). After that, it decreased gradually to about 7 µM during the last 10 days until the end. With 90 µM at the beginning, silicate in T4 decreased very slowly until the exponential growth phase started on 29/03. Then it was exhausted within three days on 01/04. Due to phosphate addition the exponential growth of diatoms was prolonged. Stagnation took place around 1.0 µM during the next 4 days. A slight increase of 1 µM was detected during the last 2 days. In the harbour water, silicate decreased slowly from 88 µM to 64 µM at the end with various fluctuations between 1µM and more than 40 µM during the observed course of time.

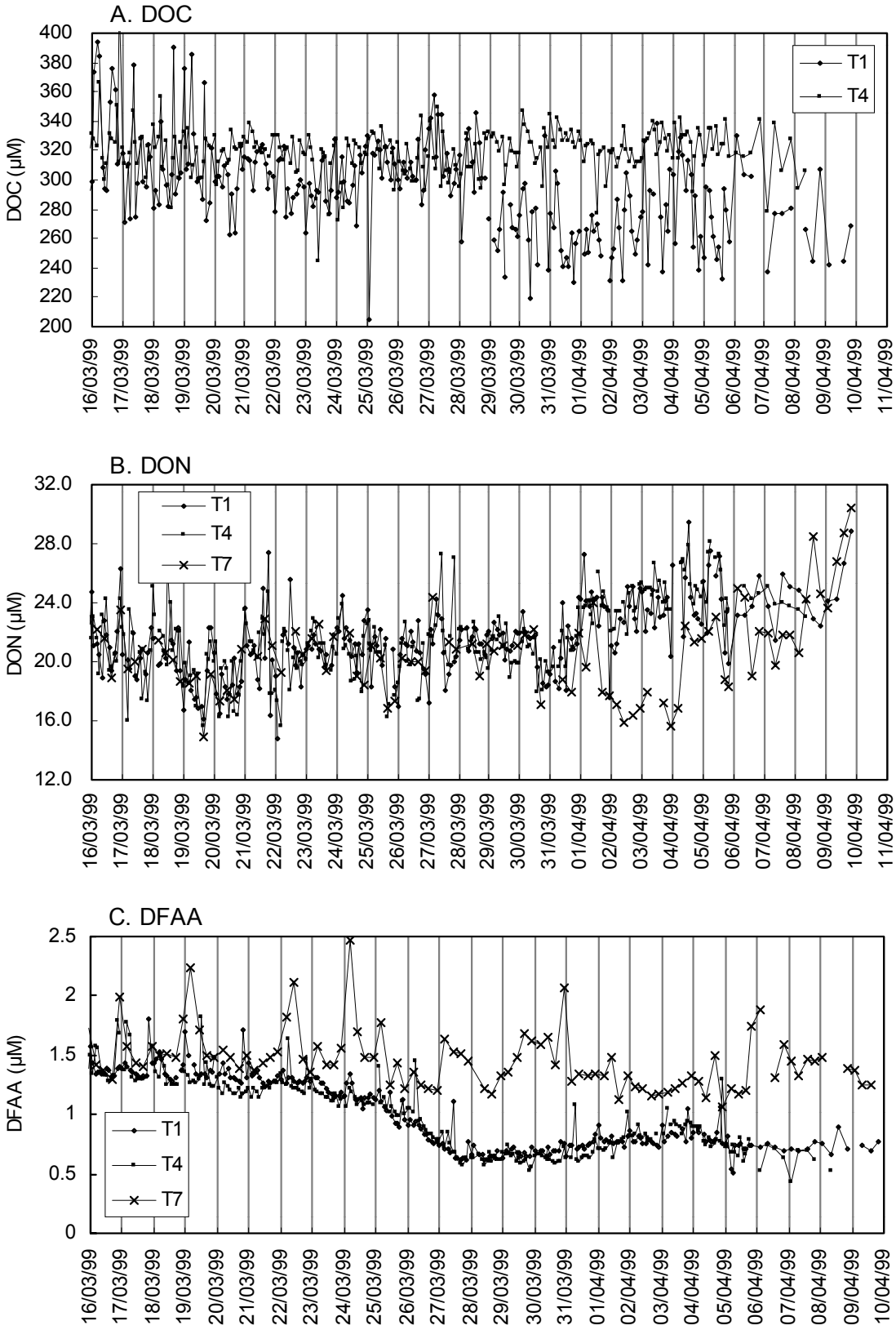

Fig. 3-3 Dissolved organic matter in the spring experiment (Series 1, Büsum, Mar./Apr., 1999) (T1: the main bag of sequence A; T4: the main bag of sequence B; T7: the harbour water)

Dissolved organic matter (Fig. 3-3)

The development of dissolved organic carbon (DOC) in T1 showed strong fluctuations of 10 to 100 µM. Generally, it varied between 290 to 310 µM during the first week and increased by 10 µM during the following 2 days. After this period it decreased to the range of 250 to 280 µM within the next 5 days. Finally a small increase was observed during the last 8 days with fluctuations between 250 to 320 µM (Fig. 3-3A). DOC in T4 fluctuated between 300 µM and 340 µM most of the time with variations of 10 µM to 30 µM within one day.

Dissolved organic nitrogen (DON) concentrations in T1 remained constant between 16 to 25 µM from 16/03 to 30/03 (Fig. 3-3B). A slight increase to the range of 25 to 29 µM was observed from 31/03 until the end. Large variations in the range of 2 to 8 µM were found within one day besides contamination. DON in T4 remained between 16 to 24 µM from 16/03 to 30/03. It slightly increased to 28 µM during 31/03 to 05/04, and decreased to 23 µM until the end. As in T1, large variations in the range of 2 to 10 µM were found within one day except events of contamination. DON in harbour water showed nearly similar variations as in the bags. In the harbour only some lower values were detected between 01/04 and 05/04.

Dissolved free amino acid (DFAA) in both T1 and T4 bags developed in parallel (Fig. 3-3C). It decreased from 1.5 µM to 1.1 µM during the first 9 days until 24/03. Faster decrease from 1.1 µM to 0.5 µM was detected during the following 3 days (25/03 to 27/03), followed by a slow increase to 0.9 µM on 03/04. Afterwards, it decreased slightly and remained around 0.7 µM in the last 6 days. In the harbour, DFAA varied between 1.4 µM and 2.4 µM with larger variation compared to that in the bags. Slight decrease to 1.1 µM was detected during the last week.

Particulate organic matter (Fig. 3-4)

Particulate organic carbon (POC) in T1 increased slowly from 110 µM to about 200 µM within the first 12 days (Fig. 3-4A). From 28/03, POC increased exponentially and reached 660 µM on 02/04 with significant diurnal variation. It fluctuated in the range of 600 to 680 µM during the last 7 days. POC in T4 increased from about 90 µM at the beginning of the experiment to about 140 µM until 27/03. After then, it increased exponentially to about 1000 µM within 9 days followed by a decrease to about 800 µM during the last 4 days. The short-term variation of POC showed diurnal fluctuations with maximum differences of about 50 µM.

Particulate organic nitrogen (PN) in T1 showed a slight increase from 5.0 µM up to 18 µM during the first 12 days (Fig. 3-4B). After this, phytoplankton started its exponential growth and PN in T1 increased by more than 39 µM during the following 5 days to 57 µM on 02/04. The concentrations remained constant around 58 µM during the following stationary phase. PN in T4 increased gradually from 5.0 µM up to 18 µM during the first 12 days (Fig. 3-4B). From 28/03 to 03/04, it continued to increase to 90 µM. In relation to the decrease of NO_3^-, the increase of PN was about 25 µM lower during this period of time. PN fluctuated between 84 µM and 95 µM from 04/04 to the end.

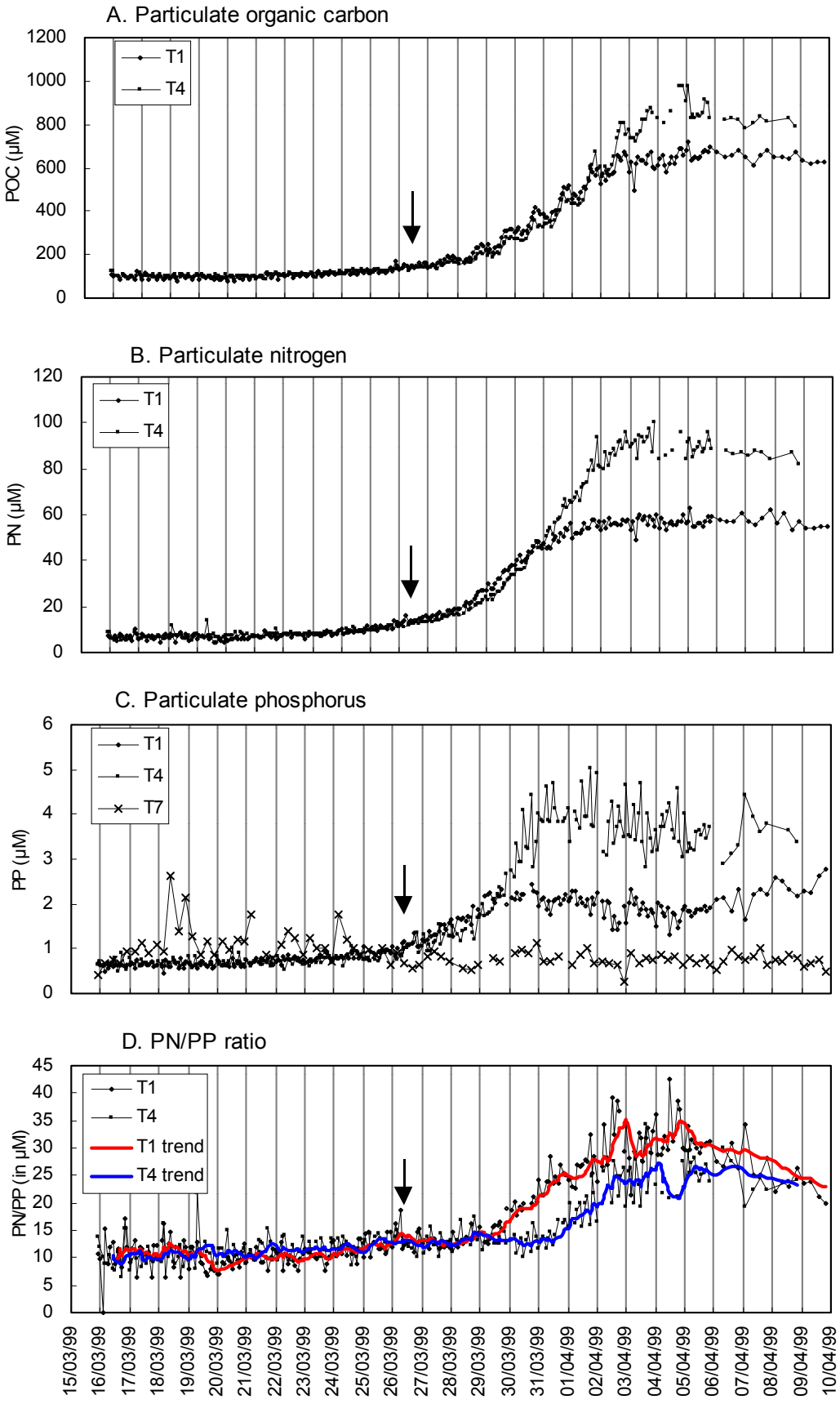

Fig. 3-4 Particulate organic matter in the spring experiment (Series 1, Büsum, Mar./Apr., 1999) (Arrow marked as phosphate addition. T1: the main bag of sequence A; T4 (upper line in D, following 30/03): the main bag of sequence B; T7: the harbour water)

Particulate organic phosphorus (PP) in T1 increased slightly from 0.6 µM to 0.9 µM within the first 10 days, followed by about three days exponential increase and reached 2.2 µM on 29/03. It then decreased to 1.6 µM until 06/04. Gradual increase was detected afterwards reaching 2.7 µM at the end. PP concentration in T4 was about 0.5 to 0.8 µM at the beginning. It then increased very slowly and reached 1.0 µM until 25/03. Afterwards it increased exponentially for two days longer than in T1 and reached the highest value of about 5.0 µM. Then it decreased to 3.0 and to 3.4 µM with short-term fluctuations until the end. In the harbour water, PP varied between 0.6 to 1.2 µM with some particular deviations of more than 2.5 µM.

PN/PP ratio varied between 10 to 15 (M/M) during the first 12 days in both T1 and T4 (Fig. 3-4D). It increased during the exponential phase and reached up to 38 in T1 and 27 in T4 at the end of the exponential phase. Afterwards it decreased gradually to about 22 in both bags.

3.1.1.3 Plankton development

Chlorophyll *a* (Fig. 3-5)

Chlorophyll concentration measurements by the 1 Hz fluorometer only started on 24/03, though measurements by the Turner fluorometer covered all the time. Because the former reflects more bioactive chlorophyll, here the results from 1 Hz were chosen to be presented. The correlation of these two data sets was near to 1 (Fig. 3-5, attached figure).

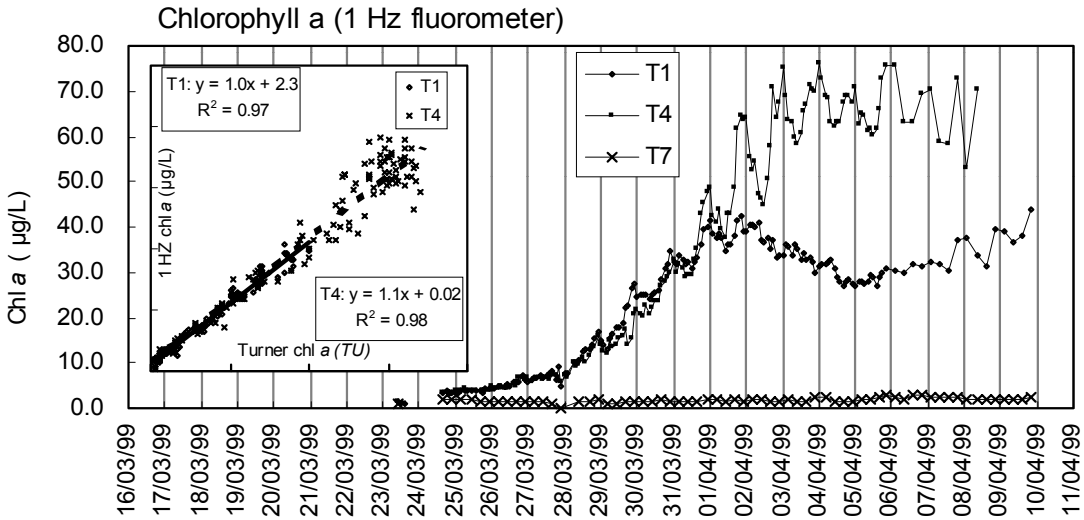

Fig. 3-5 Chlorophyll a in the spring experiment (series 1, Büsum, Mar./Apr., 1999) (T1: the main bag of sequence A; T4: the main bag of sequence B; T7: the harbour water, the attached figure show the correlations between 1 Hz measurements and Turner measurements.)

In both T1 and T4, chlorophyll showed very low values of 3.5 µg/L even 9 days after the start. Afterwards it exponentially increased up to 40 µg/L during the following 8 days until 02/04. Chlorophyll developments in both bags were parallel. In T1, chlorophyll a started to decrease afterwards and reached a lower value of 29 µg/L on 05/04. An increase by 14 µg/L was detected

during the last 5 days. In T4, chlorophyll continued to increase with significant diurnal variation and reached the maximum value of 76 µg/L on 03/04. No significant decrease was detected until the end. In the harbour, chlorophyll remained at very low concentrations in the range of 1.2 to 2.8 µg/L all the time with a slight increasing trend.

Species succession (Fig. A, B in appendix)

In spring, at the beginning of the experiment and in the long slow exponential growth phase, *Asteroplanus karianus (GRUNOW) GARDNER ET CRAWFORD* dominated the phytoplankton community in both control and experimental bags, followed by *Thalassiosira angulata (GREGORY) HASLE*, *Odontella aurita (LYNGBYE) C.A. AGARDH* and *Thalassiosira levanderi (VAN GOOR).* Flagellates were quite minor (Dürselen et al. 2002a).

During the exponential growth phase, diatoms grew fast in all bags. In T1, *A. karianus* still kept large numbers, whereas the other diatoms *T. angulata, O. aurita* and *T. levanderi* increased fast. In T4, except *A. karianus*, *T. angulata*, especially *Thalassiosira punctigera (CASTRACANE) HASLE* and *T. levanderi* grew very fast. Unlike the development in T1, *O. aurita* kept relatively low numbers (Dürselen et al. 2002a).

In the stationary phase, *A. karianus*, *T. levanderi* and *O. aurita* in T1 started to decrease under P depletion. *T. angulata* was detected to be dominant instead. In T4, *A. karianus* still kept large numbers, *T. punctigera*, *T. levanderi* and *T. angulata* all decreased at the end of the experiment (Dürselen et al. 2002a).

3.1.2 Summer experiment (series 2)

Sub-systems: Sequence C: Control bags are indicated as T8*, T9, T10;
Sequence D: Experimental bags are indicated as T11*, T12, T13;
Reference: Harbour water is indicated as T14.

Due to good reproducibility of the mesocosms for most parameters, only the developments in the main bag of each sequence are represented here. T8 for sequence C; T11 for sequence D.

3.1.2.1 Physical boundary conditions

Light (Fig. 3-6A)

According to the hourly means, the highest irradiance during the summer experiment occurred mostly between 12:00 and 14:00. Lower incident irradiance at noon was also detected at some days 04/06 - 06/06, 08/06 and 10/06, reflecting the local climate. The highest hourly irradiance varied between 600 to 850 W/m^2 for most of the measured days except three days with 450 W/m^2 on 05/06 and 10/06, and 340 W/m^2 on 08/06.

Daily mean irradiance during the summer experiment varied between 100 W/m^2 and 320 W/m^2. It decreased from 300 W/m^2 to 110 W/m^2 during the first 5 days, followed by an increase to

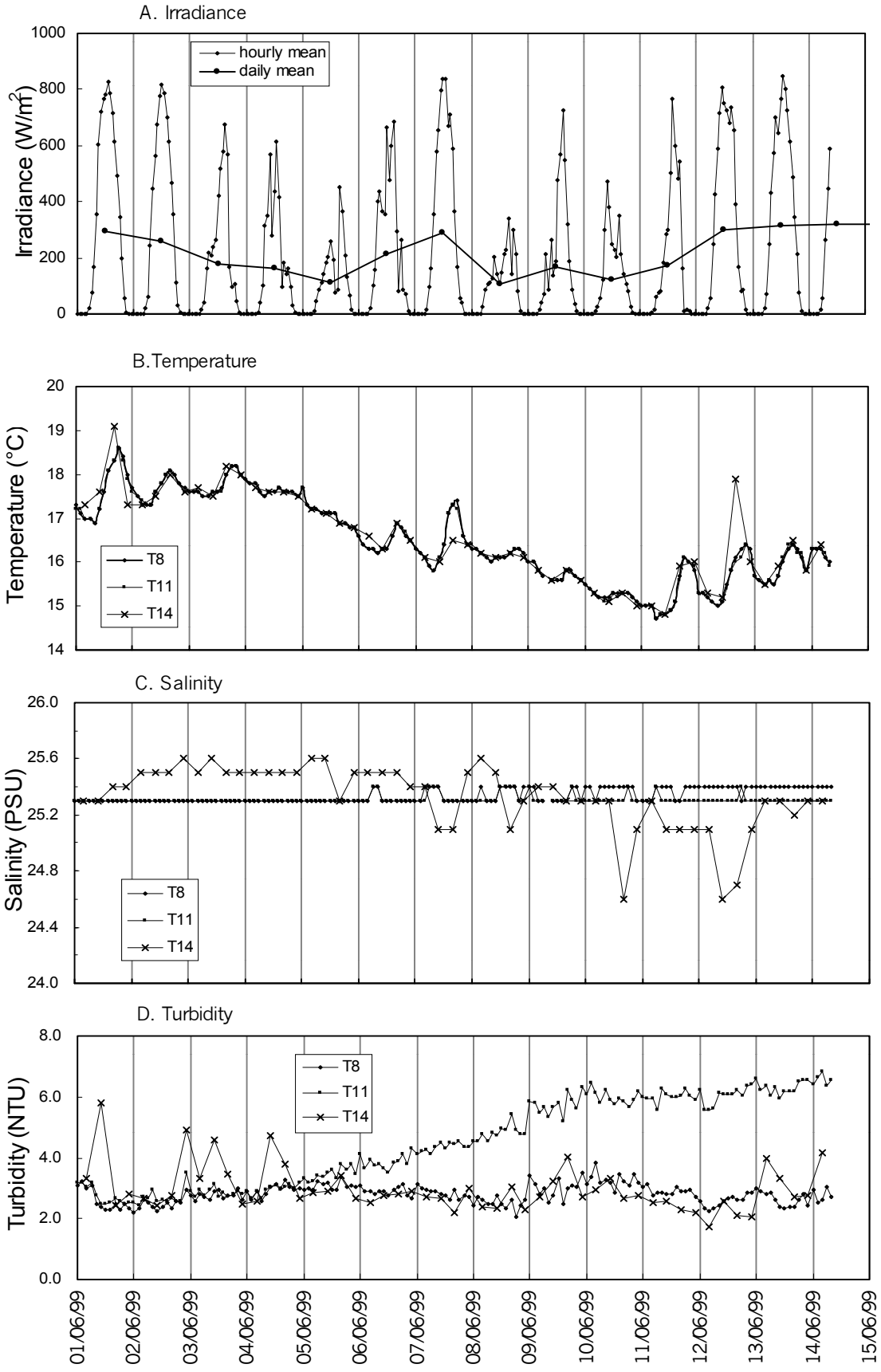

Fig. 3-6 Physical parameters in the summer experiment (Series 2, Büsum, Jun., 1999). (T8: the main bag of sequence C; T11: the main bag of sequence D; T14: the harbour water)

about 300 W/m^2 on 07/06. Afterwards it decreased to 100W/m^2 and remained between 100 W/m^2 and 170 W/m^2 during the following 4 days. Finally it increased again and remained higher than 300 W/m^2 until the end.

Water temperature (Fig. 3-6B)
The development of temperature in both the control bag (T8) and experimental bag (T11) as well as in the harbour (T14) were consistent during the whole sampling period with diurnal fluctuations. Overall, temperature decreased from 18.0 °C to less than 15 °C until 11/06 when it increased to 16 °C during the last 4 days.

Salinity (Fig. 3-6C)
Salinity in both T8 and T11 remained in the range of 25.3 PSU to 25.4 PSU. In the harbour, salinity varied largely from 25.6 PSU to 24.6 PSU due to the effects of tide, exchanges with the water outside the harbour.

Turbidity (Fig. 3-6D)
Turbidity in T8 and T11 was quite similar during the first 5 days varying between 2.5 NTU and 3.0 NTU. Afterwards in T8, it fluctuated between 2.5 and 3.5 NTU until the end. In T11, it steadily increased to 6.5 NTU on 10/06 with a slight decrease of 0.9 NTU afterwards and finally ended at 6.8 NTU. Turbidity in the harbour varied largely up to 5.8 NTU during the first 5 days. Afterwards it remained mostly between 2 NTU and 4 NTU. Large fluctuations were again detected during the last 4 days.

3.1.2.2 Chemical parameters

Nutrients (Fig. 3-7)
In T8, NH_4^+ decreased from 14 µM below 1.0 µM within the first two days and remained in the range of 0.5 to 0.9 µM until the end (Fig. 3-7A). The development of NH_4^+ in T11 was similar to that in T8. In the harbour, NH_4^+ decreased from 16 µM to 9.2 µM during the first 3 days. It gradually increased to 17 µM and remained at this level afterwards except for some lower values around 08/06 and higher values around midnight of 12/06.

In both bags, nitrate remained constant at 25.3 µM during the first day (Fig. 3-7B). It started to decrease at noon of 02/06 to lower than 1.0 µM at noon of 04/06. Afterwards, NO_3^- fluctuated in the range of 0.1 µM to 0.5 µM until the end. Daily addition of nitrate to T11 was started on 05/06. The added nitrate was mostly exhausted within the succeeding 4 hrs and remained around 1.0 µM afterwards before another addition followed. NO_3^- concentration in the harbour increased gradually and ended at 26 µM.

Nitrite in T8 varied between 0.71 µM and 0.74 µM during the first 2 days (Fig. 3-7C). A slight increase of 0.04 µM was detected during 03/06 to 04/06. It decreased below 0.1 µM on 05/06 and fluctuated within 0.3 to 0.8 µM to the end. In T11, NO_2^- varied similarly to T8 before nitrate additions. It increased periodically, coupled with NO_3^- additions and decreased soon after NO_3^- depletion. In the harbour, NO_2^- showed a slight increase from 0.7 µM at the beginning to 1.2 µM until the end.

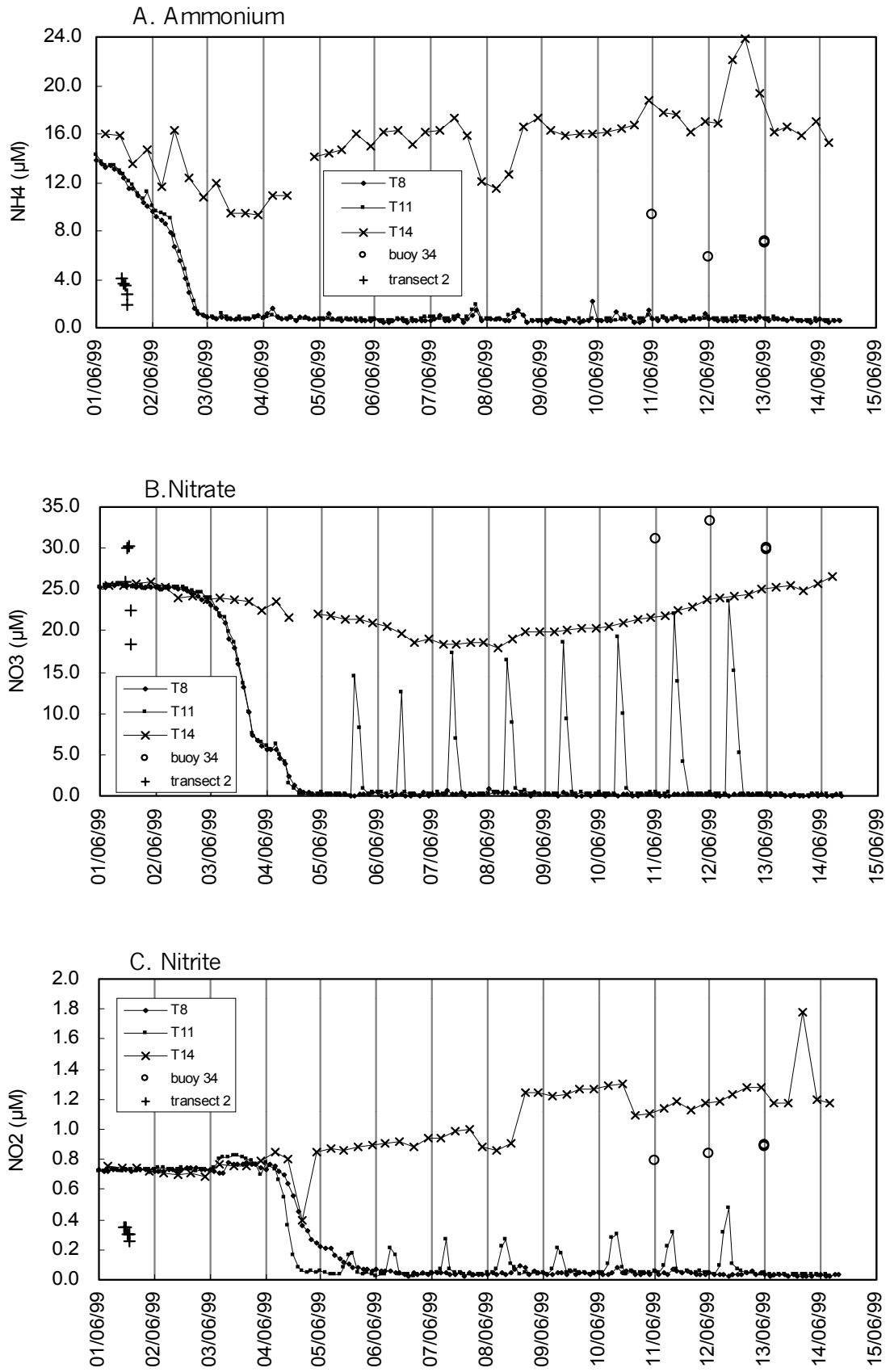

Fig. 3-7 Nutrients in the summer experiment (Series 2, Büsum, Jun., 1999) (to be continued)

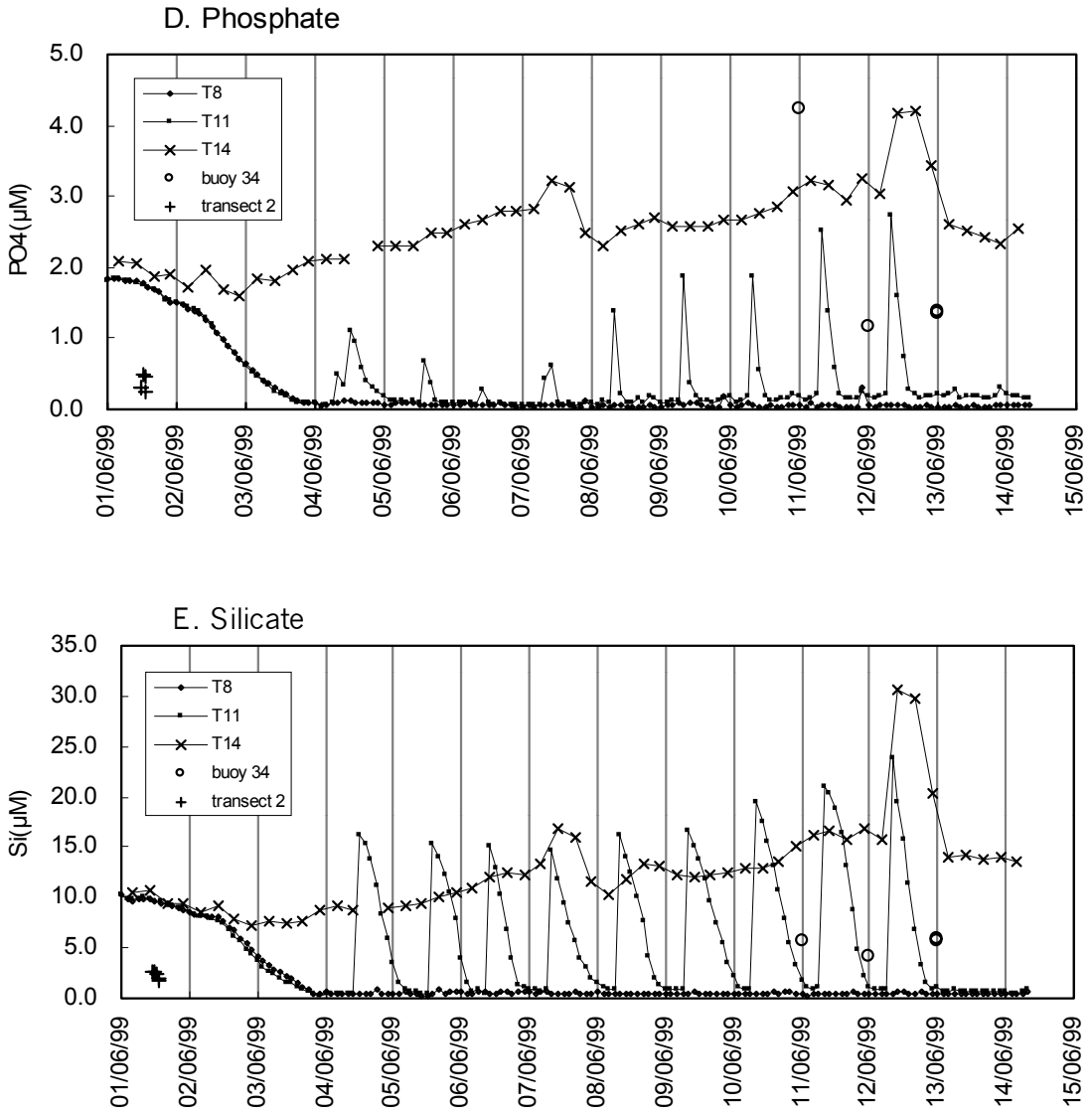

Fig. 3-7 Nutrients in the summer experiment (series 2, Büsum, Jun., 1999) (T8: the main bag of sequence C; T11: the main bag of sequence D. T14: the harbour water)

Phosphate in T8 and T11 decreased from 1.8 µM to < 0.1 µM within the first three days. In T 8 it remained around 0.05 µM until the end (Fig. 3-7D). To the T11, PO_4^{3-} was added from 04/06 on. The added PO_4^{3-} was consumed quickly within the succeeding 4 hrs and dropped to 0.1 µM. In the harbour, PO_4^{3-} increased slightly from 1.6 µM to 2.5 µM until the end. Some higher concentrations of 4.2 µM were detected around midnight of 12/06.

In both bags, Si decreased from 10 µM at the beginning to < 1 µM within the first three days. In T8 Si fluctuated around 0.5 µM until the end (Fig. 3-7E). In T11, added Si was taken up gradually within the succeeding 12 hours. In the harbour, the concentrations of Si increased from 10 µM up to 15 µM at the end. A maximum of 30 µM was detected at midnight of 12/06.

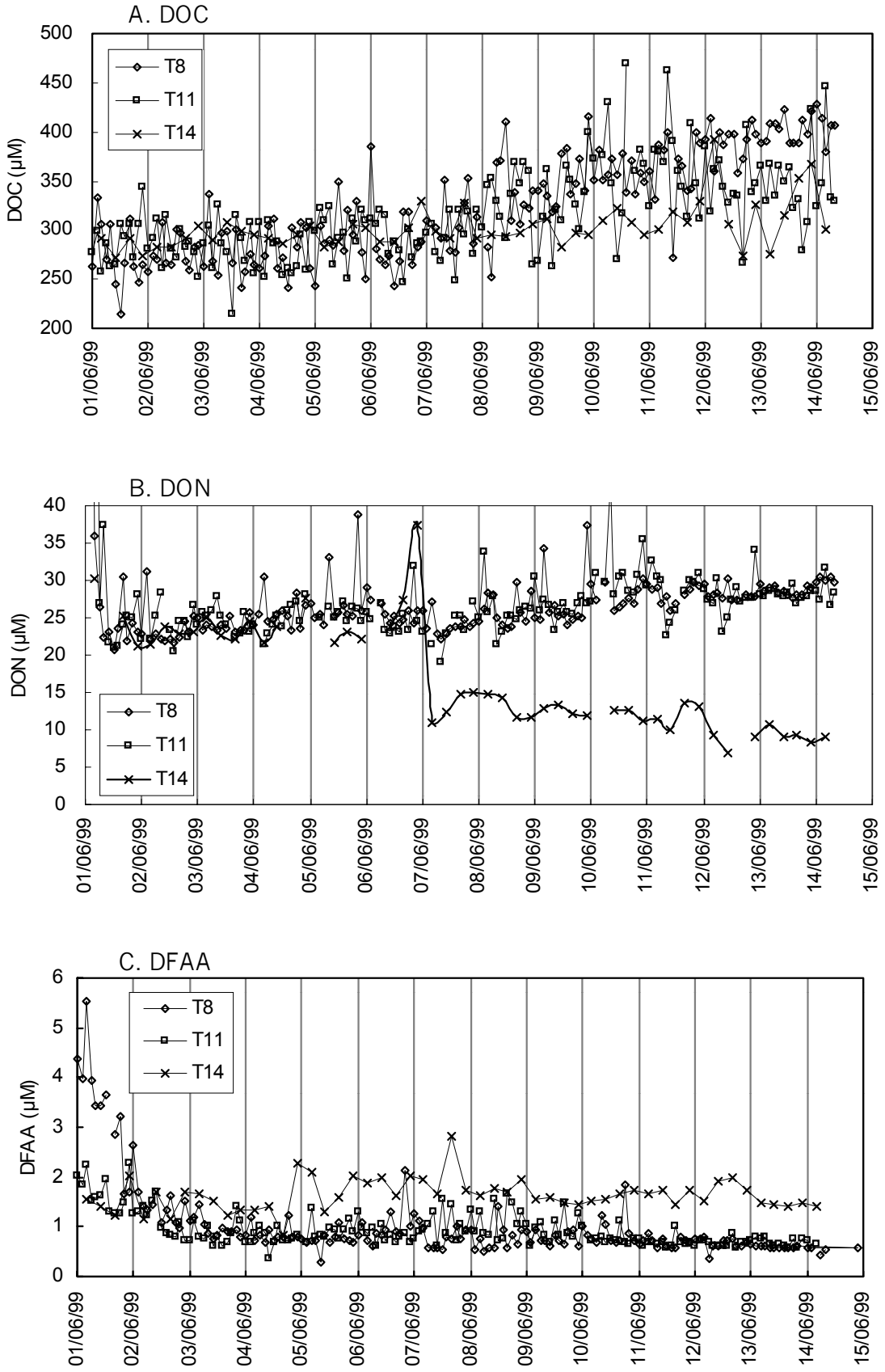

Fig. 3-8 Dissolved organic matter in the summer experiment (Series 2, Büsum, Jun., 1999) (T8: the main bags of sequence C; T11: the main bag of sequence D. T14: the harbour water)

Dissolved organic matter (Fig. 3-8)

DOC showed a high variability. In T8 it fluctuated between 245 µM and 332 µM during the first week with highest fluctuations of 90 µM. A slight increase was detected afterwards and DOC reached more than 420 µM at last (Fig. 3-8A).

DOC in T11 varied in the range of 257 µM to 340 µM with short-term variation of about 60 µM during the first week. Slight increase with a maximum of 450 µM was detected afterwards with larger variation of 100 µM to 150 µM during the second week (Fig. 3-8A). DOC in the harbour varied in the same range as in T8 during the first week and remained between 270 µM and 390 µM till the end (Fig. 3-8A).

DON concentrations in T8 dropped from 110 µM to 21 µM within the first 8 hours. Afterwards, it varied between 21 µM and 24 µM during the first 9 days. Then it slightly increased to 30 µM (Fig. 3-8B). DON in T11 fluctuated around 25.0 µM during most of the experimental period with a slight increase of 2 to 3 µM during the last three days (Fig. 3-8B). In the harbour, DON remained around 25.0 µM during the first 7 days. After 07/06, it decreased to 10.0 to 11.0 µM and remained at this concentration during the succeeding 8 days (Fig. 3-8B).

In summer, high concentrations of DFAA (5.5 µM) were detected at the beginning in T8. It then decreased to 0.8 µM within the first 2 days and mostly fluctuated between 0.5 and 0.8 µM until the end of the experiment. However, in T11, the initial value was about 2.0 µM and it varied in the range of 0.7 to 1.2 µM after the first 2 days. Higher values and larger variations were detected in T11 especially during the period of nutrient additions. In the harbour, DFAA fluctuated mostly between 1.4 µM and 2.0 µM with some values up to 2.3 µM.

Particulate organic matter (Fig. 3-9)

In T8, POC increased from 85 µM to 480 µM on 06/06, that was about 20 µM/d (Fig. 3-9A). After remaining around 500 to 540 µM during the next three days, POC decreased slowly afterwards to about 340 µM at the end. In T11, POC increase continued one day longer than in T8 and reached up to 1000 µM on 07/06. It fluctuated in the range of 900 to 1154 µM during the following 6 days with an increasing tendency. The development of POC in both bags showed significant day-night periodical variations, with higher values at daytime.

Development of PN in both bags was quite consistent during the first 4 days (Fig. 3-9B), increasing from 8 µM up to 40 µM late on 04/05. In T8, it decreased slightly to about 35 µM until the end. In T11, it increased linearly to 150 µM on 12/06. Within the last two days PN decreased by 20 µM. There are no available data of PN in the harbour.

In both bags, PP increased from 0.3 µM at the beginning up to 1.6 µM within the first three days. Afterwards, PP in T8 fluctuated in the range of 1.1 to 2.0 µM until 10/06 and slightly decreased to 1.0 µM at the end. In T11 with nutrient enrichments, PP increased linearly up to 11 µM until 11/06, followed by a fluctuation between 6.0 and 11.0 µM until the end.

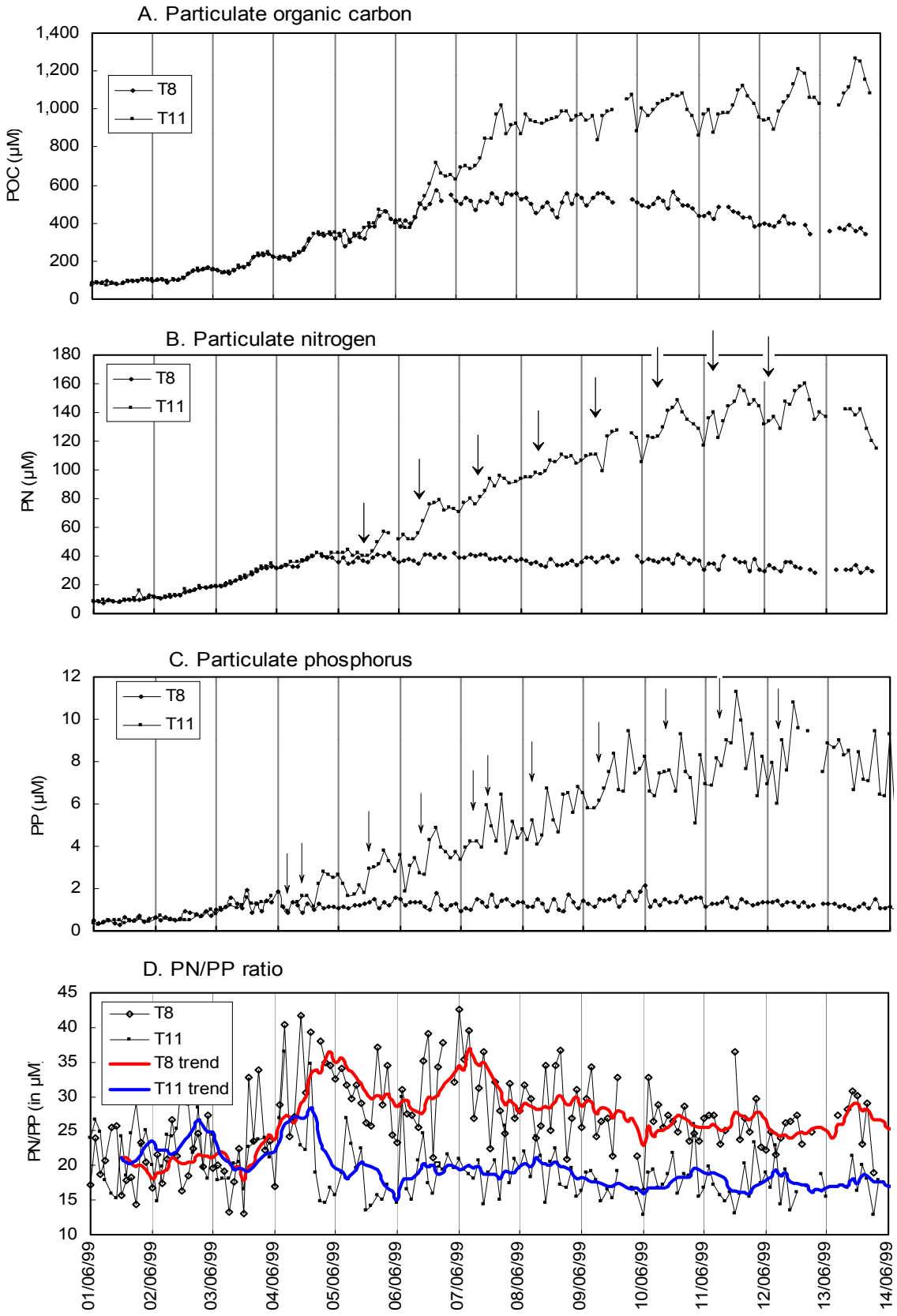

Fig. 3-9 Particulate organic matter in the summer experiment (Series 2, Büsum, Jun., 1999, arrows marked the nutrient additions) (T8: main bag of sequence C (upper line in D, following 04/06); T11: main bag of sequence D; data in the harbour water missed.)

PN/PP ratio fluctuated in the range of 20 to 25 (M/M) in both bags (T8 and T11) during the first 3 days (Fig. 3-9D). In T8, it then increased to 40 on 04/06 and fluctuated between 25 to 40 until 07/06, and decreased gradually afterwards to 23 at the end. In T11, it increased slightly to 30 on 04/06 and then decreased a little and fluctuated around 14 to 24 in the rest period of experiment.

3.1.2.3 Plankton development

Chlorophyll *a* (Fig. 3-10)

1 Hz chl*a* in T8 increased from 6 µg/L up to 75 µg/L within three days with diurnal variations. It decreased gradually afterwards to about 15 µg/L in the end.
In T11, the increase of chl*a* measured by the 1 Hz fluorometer beginning at 8 µg/L was continued up to 520 µg/L during the first 9 days. Then, it decreased to about 200 µg/L during the succeeding 4 days with diurnal variations of 140 to 180 µg/L.
In the harbour, initial concentrations of chlorophyll *a* from 1 Hz measurement were about 5 µg/L. The values mostly fluctuated in the range of 8 to 15 µg/L during the experiment with some extreme data above 20 µg/L.

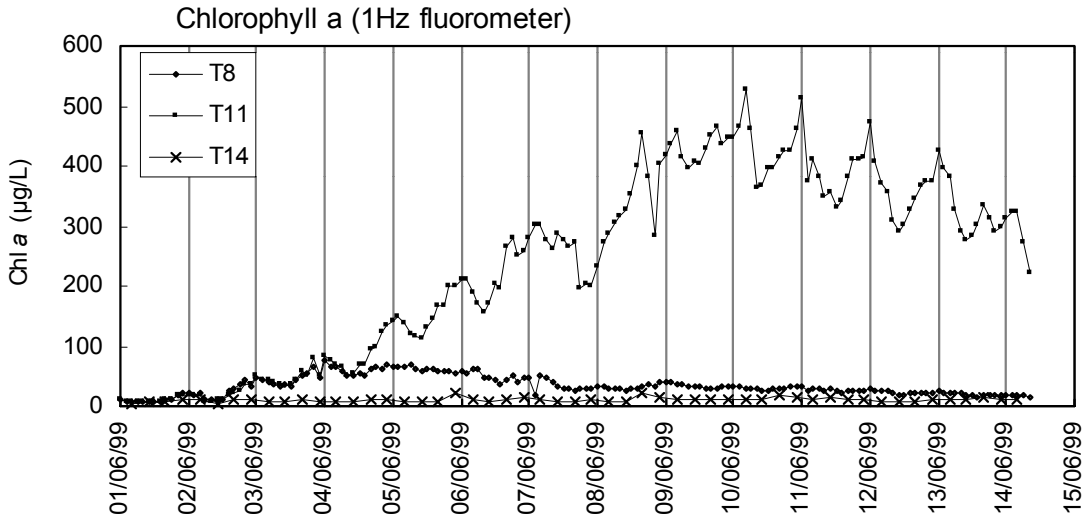

Fig. 3-10 Chlorophyll *a* in the summer experiment (series 2, Büsum, Jun., 1999) (T8: main bag of sequence C; T11: main bag of sequence D; T14: harbour water)

Species succession (Fig. C, D, E, F in appendix)

From the counted cell numbers, the diatom *Lauderia annulata (CLEVE)* dominated the whole period in T8, followed by *Thalassionema nitzschioides (GRUNOW) GRUNOW* and *T. levanderi*, *Guinardia delicatula (CLEVE) HASLE* and *T. angulata* (Dürselen et al. 2002b). Nearly all diatom species reached their maximum concentrations on the 3rd day with cell numbers more than 50 times higher than at the beginning. The diatom numbers decreased afterwards. Some dinoflagellates and other flagellates also grew faster during the first three days and reached their maximum at this time. Unlike

diatoms, flagellates kept high cell numbers during most of the experiment.

In T11 with nutrient enrichments, diatoms were continuously increasing during the experiment. Only a slight decrease was observed during the last two days. The dominant species were *T. punctigera*, *L. annulata*, and *T. nitzschioides*. The latter grew faster during the second period of the experiment and dominated during the last three days reaching its highest numbers of more than 1000 times higher than the initial numbers (5×10^6 cells/L). Dinoflagellates like *Prorocentrum micans (EHRENBERG)* and cryptophytes in T11 grew during the whole experiment. Their cell numbers reached at last more than 100 time higher numbers (1.7×10^6 cells/L), compared to the beginning (Dürselen et al. 2002b).

3.1.3 Nutrient uptake

3.1.3.1 Uptake ratio

In order to analyse details of nitrogen uptake by the phytoplankton exclusively in the spring and summer experiments, correlations of chlorophyll *a* with NH_4^+, NO_3^-, PO_4^{3-} and Si were plotted from both experiments (In spring, chl*a* from Turner measurements were used, considering it was whole duration measured and its correlation to 1 Hz measurements was close to 1, see Fig. 3-5). With this, the diurnal variation of all related parameters was supposed to be excluded. Accordingly, different phases of N uptake were distinguished and the decrease ratios of nitrogen, phosphate and silicate (ΔDIN: ΔP: ΔSi), as well as increase ratio of POC to chlorophyll (ΔPOC/Δchl*a*) were calculated from the respective slopes. Furthermore, the increase ratios of POC, PN and PP (ΔPOC/ΔPN, ΔPN/ΔPP) were also estimated from the correlation of PN to POC and PP, respectively (Fig. 3-11 to Fig. 3-16).

Spring experiment

In spring, significant correlations of chl*a* with NH_4^+ and NO_3^- showed that NH_4^+ uptake occurred at first in both T1 and T4, covering the N-demand of the phytoplankton during the slow growth phase. NO_3^- uptake occurred between 28/03 and 31/03 in T1 and 28/03 to 02/04 in T4, covering the exponential growth phase (NO_3^- uptake). In between, parallel uptake of NH_4^+ and NO_3^- occurred but only for 1 day (co-uptake of NH_4^+ and NO_3^-) (Fig. 3-11, 3-13).

From the correlations between chlorophyll *a* and nutrients, it is shown that the slopes of the chl*a*-NH4 curve (ΔNH4/Δchl*a*) in both T1 and T4 were about 5.6 µM/(µg/L), which were close to those of the chl*a*−PN curve (ΔPN/Δchl*a*) during the same period (Fig. 3-11 to 3-14: A-1). During nitrate uptake, ΔNO3/Δchl*a* were much lower than these of ΔNH4/Δchl*a*, around 1.5 to 1.6 µM/(µg/L). ΔPN/Δchl*a* decreased to 1.3 and 1.4 µM/(µg/L) in T1 and T4, respectively (Fig 3-11 to 3-14, B-2). Different to the NH_4^+ uptake phase, there were differences between ΔPN/Δchl*a* (1.3) and ΔNO3/Δchl*a* (1.5) in the NO_3^- uptake phase. Similarly, ΔPO4/Δchl*a* and ΔSi/Δchl*a* in the NH_4^+ uptake phase were higher than those in the NO_3^- uptake phase by about 1 and 1.5 times in both bags (Fig. 3-11, 3-13).

ΔPOC/Δchl*a* in the NH_4^+ uptake phase reached up to 400 (µg/L)/(µg/L). This was much higher than

that in the NO_3^- uptake phase, which were only 120 in both bags. In both NH_4^+ uptake and NO_3^- uptake phases, ΔPOC/ΔPN varied in the same range, from 6.7 to 7.7 μM/μM in T1 and 8.1 to 6.9 in T4. ΔPP/ΔPN changed from 0.03 to 0.02 μM/μM in T1 and was higher in T4 due to PO_4^{3-} addition, varying from 0.04 to 0.03 μM/μM in T4 in the two phases (Fig. 3-12, 3-14).

Generally, in both bags, the correlations had higher significance in the NO_3^- uptake phase than in the NH_4^+ uptake phase, as indicated by the R-squared (R^2) values.

Summer experiment

In summer, significant succession of NH_4^+, NO_3^- and NO_2^- uptake was followed by the plots, with and without their relations to chlorophyll *a* (Fig. 3-15, 3-16). In both T8 and T11, NH_4^+ uptake occurred for 2 days (01/06 to 02/06). Nitrate uptake covered nearly one and half day (03/06 to 04/06). Actually, there was also very short period of 6 hours co-uptake of NH_4^+ and NO_3^-, which can be deduced from the simultaneous decrease of NH_4^+ and NO_3^-. Nitrite uptake only lasted 1 day (05/06). The related ratio calculations in the periods of the co-uptake and nitrite uptake were omitted due to the short period. In T11, the related ratios of ΔPOC/ΔPN, ΔPN/ΔPP and ΔPOC/Δchl*a* in the period of nutrient additions were calculated as one phase.

Compared to spring, the slopes of chl*a*-nutrient curves were all lower in summer (Fig. 3-15, 3-16). The changes of NH_4^+ and chlorophyll a (ΔNH4/Δchl*a*) in both bags were only around 0.34 to 0.39 μM NH4/(μg/L chl*a*). In the same phase, ΔPN/Δchl*a* were around 0.28 μM PN/(μg/L chl*a*), lower than that of ΔNH4/Δchl*a*. ΔNO3/Δchl*a* was 0.46 μM NH4/(μg/L chl*a*) and 0.39 μM NO3/(μg/L chl*a*) in T8 and T11, respectively, while ΔPN/Δchl*a* were quite close in both bag, with 0.32 μM PN/(μg/L chl*a*). Due to the very short exponential period (3 days), correlations of chla with phosphate and Si could not be distinguished for the different N nutrients. ΔPO4/Δchl*a* and ΔSi/Δchl*a* had similar values in both bags with 0.035 μM PO4/(μg/L chl*a*) and 0.18 μM Si/(μg/L chl*a*), respectively (Fig. 3-15, 3-16).

In T8, ΔPOC/Δchl*a* both for NH_4^+ and NO_3^- uptake were similar, varying around 25 (μg/L)/(μg/L), which was much slower than that in spring. ΔPOC/ΔPN was lower than in spring, changing from 6.4 to 5.8 μM/μM from NH_4^+ uptake phase to NO_3^- uptake phase. ΔPP/ΔPN in the NH_4^+ uptake phase was 0.04 μM/μM. During the NO_3^- uptake phase, nearly no significant correlation between PN and PP was traced as detected from R^2 (Fig. 3-15).

In T11, except for the NH_4^+ uptake and NO_3^- uptake phases, the period of nutrient enrichment was treated as another phase for the correlations of chl*a* with POC, and PN with POC and PP (Fig. 3-16). In both the NH_4^+ and NO_3^- uptake phases, ΔPOC/Δchl*a* (31 to 37), ΔPOC/ΔPN (5.7 to 5.6) and ΔPP/ΔPN (0.022 to 0.023) had similar values. Among these, PN—PP correlation was less significant. The slopes in the nutrient addition phase were different from those in the previous phases, with the specific values of 23 (ΔPOC/Δchl*a*), 6.8 (ΔPOC/ΔPN) and 0.059 (ΔPP/ΔPN), separately. PP—PN correlation in the nutrient addition phase had higher significance than during the previous phases, with high R^2 of 0.82.

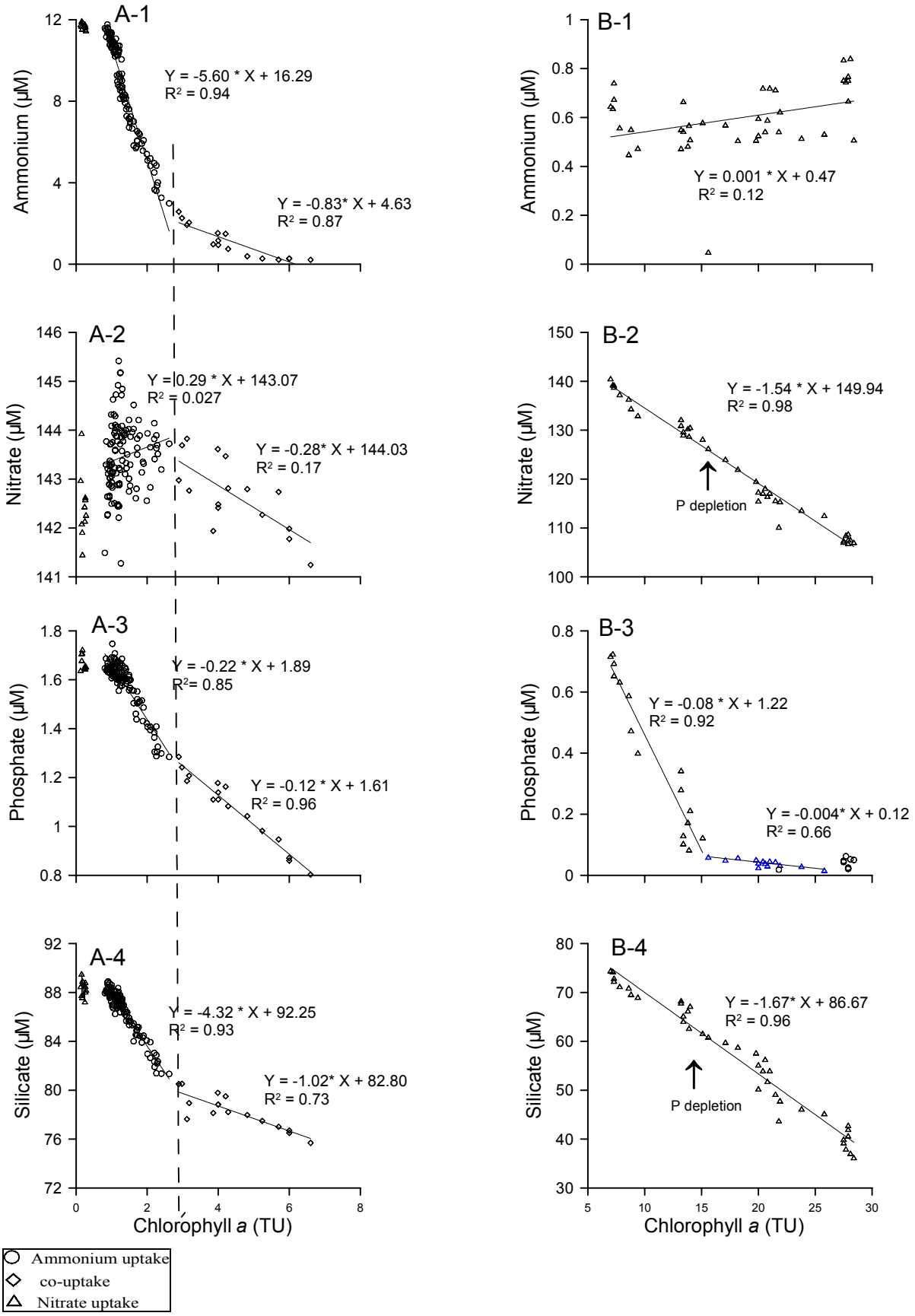

Fig. 3-11 Correlation of chlorophyll with nutrients in the spring experiment (T1, amplified the slow exponential growth phase16/03 to 27/03 in line A; the exponential growth phase 28/03 to 31/03 in line B)

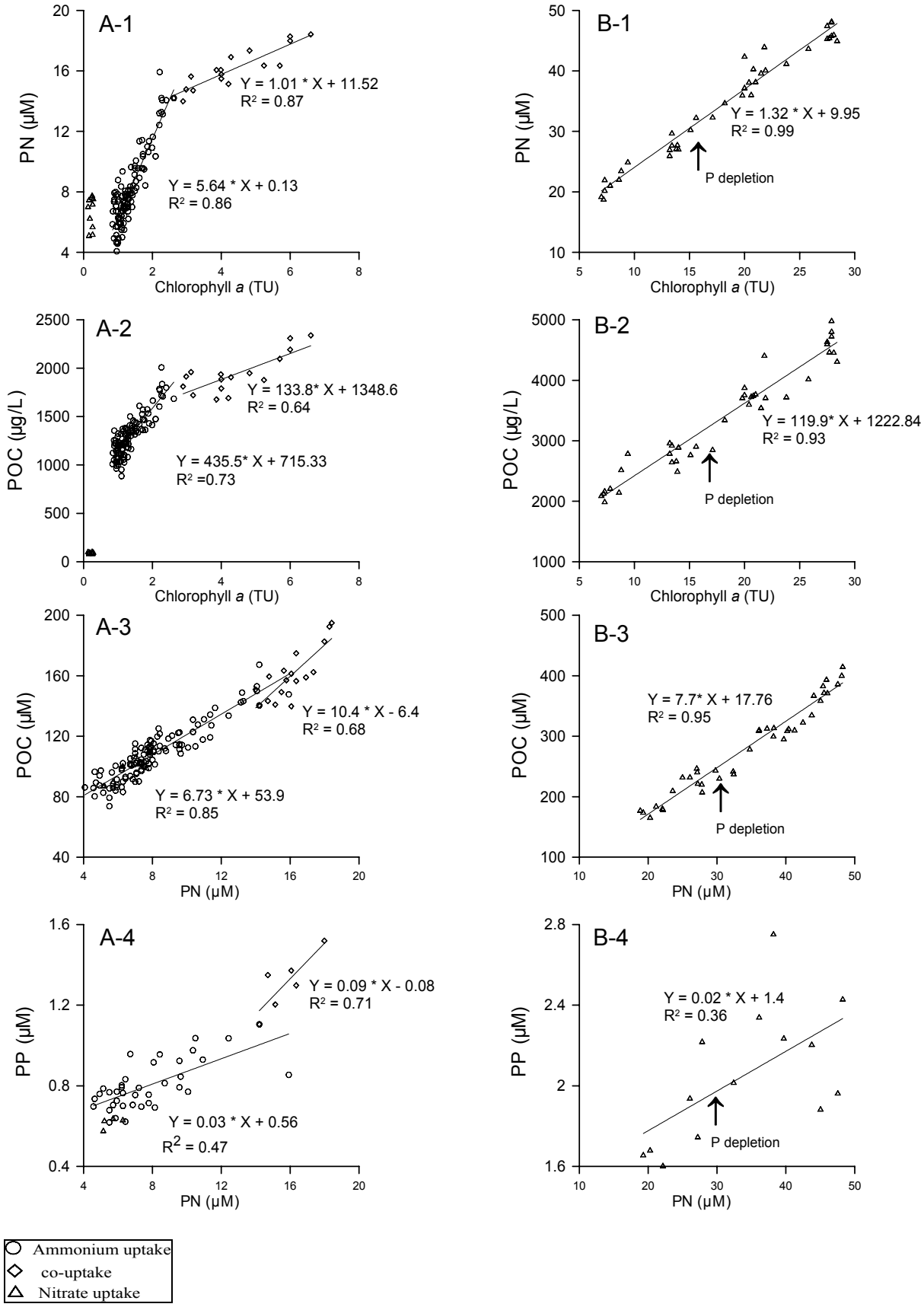

Fig. 3-12 Correlation of chl*a* with PN and POC, and PN with PC and PP in spring experiments (T1, amplified in two phases: A. 16/03-27/03, B: 28/03-31/03)

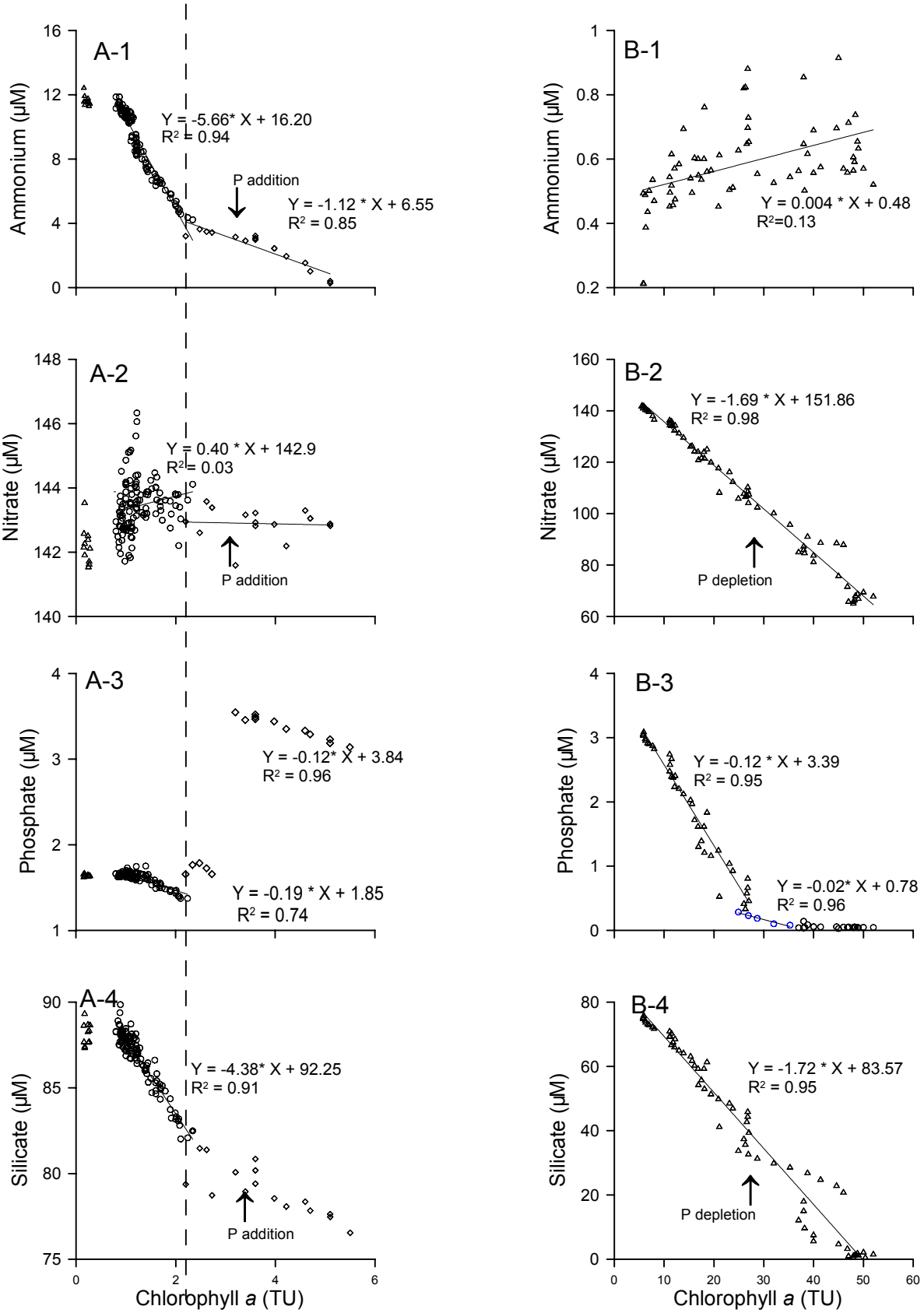

Fig. 3-13 Correlation of chlorophyll with nutrients in the spring experiment (T4, amplified the slow exponential growth phase16/03 to 27/03 in line A; the exponential growth phase 28/03 to 02/04 in line B. legend is the same as Fig. 3-11)

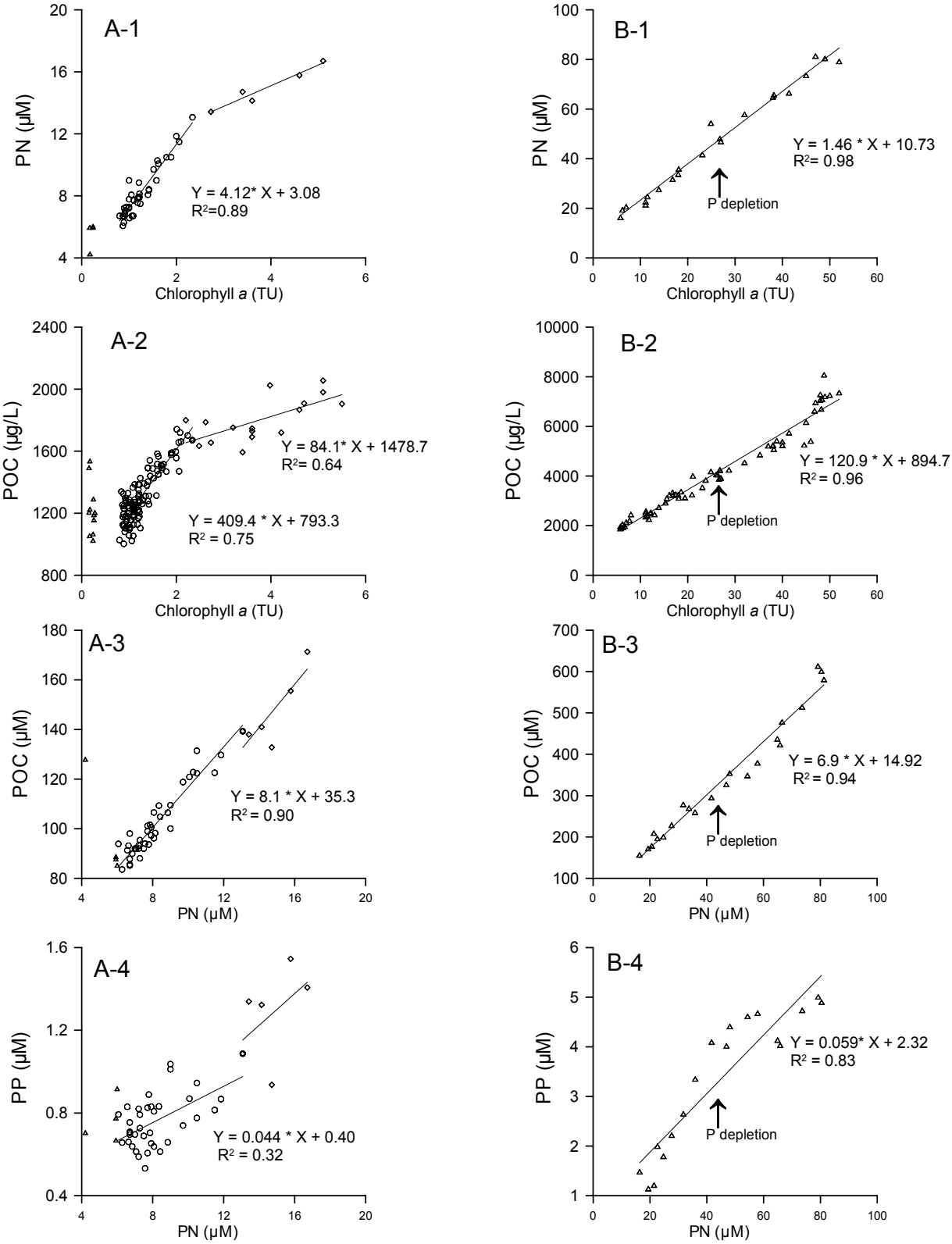

Fig. 3-14 Correlation of chl*a* with PN and POC, and PN with PC and PP in spring experiments (T4, amplified in two phases: A. 16/03-27/03, B: 28/03-02/04. Legend is the same as Fig. 3-12)

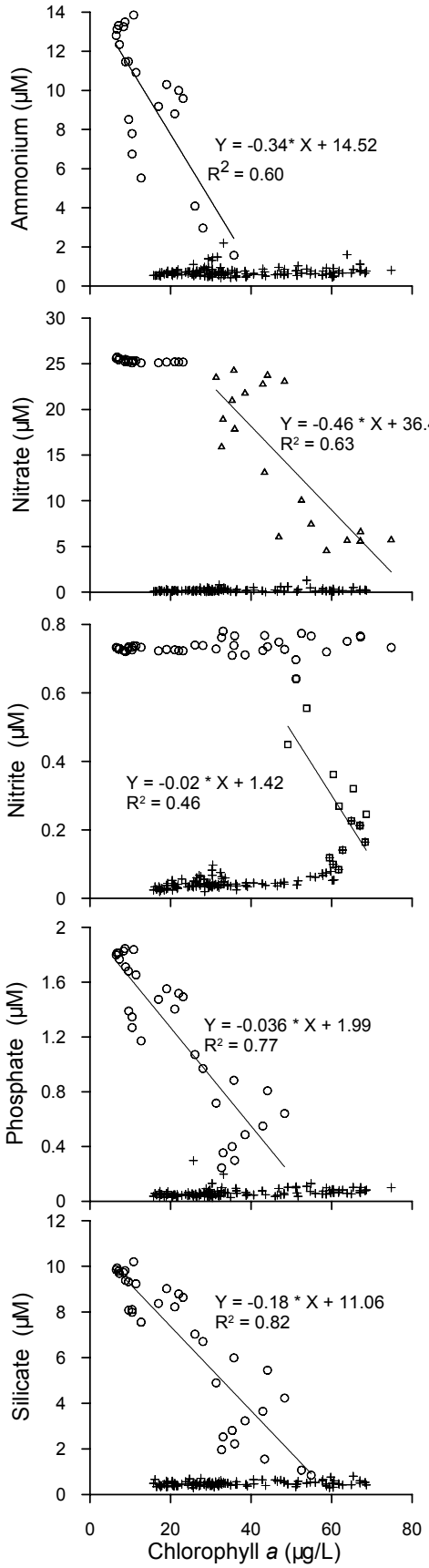

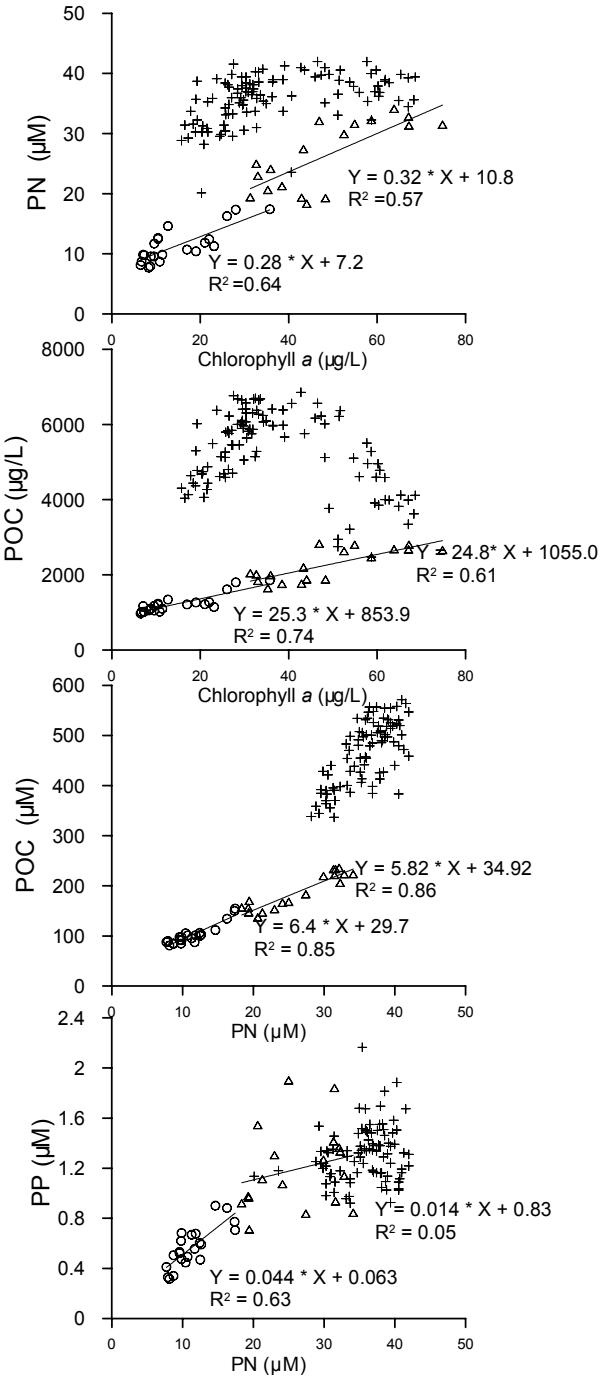

Fig. 3-15 Correlations of chlorophyll *a* with nutrients, PN with POC and PP in the summer experiment (T8)

○ Ammonium uptake

△ Nitrate uptake

□ Nitrite uptake

\+ decay phase

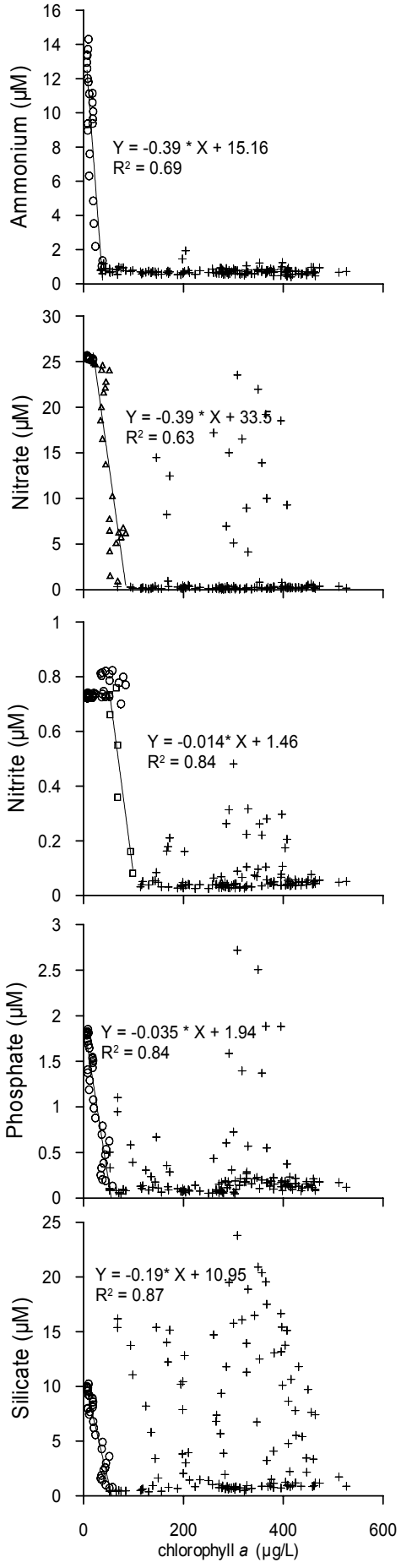

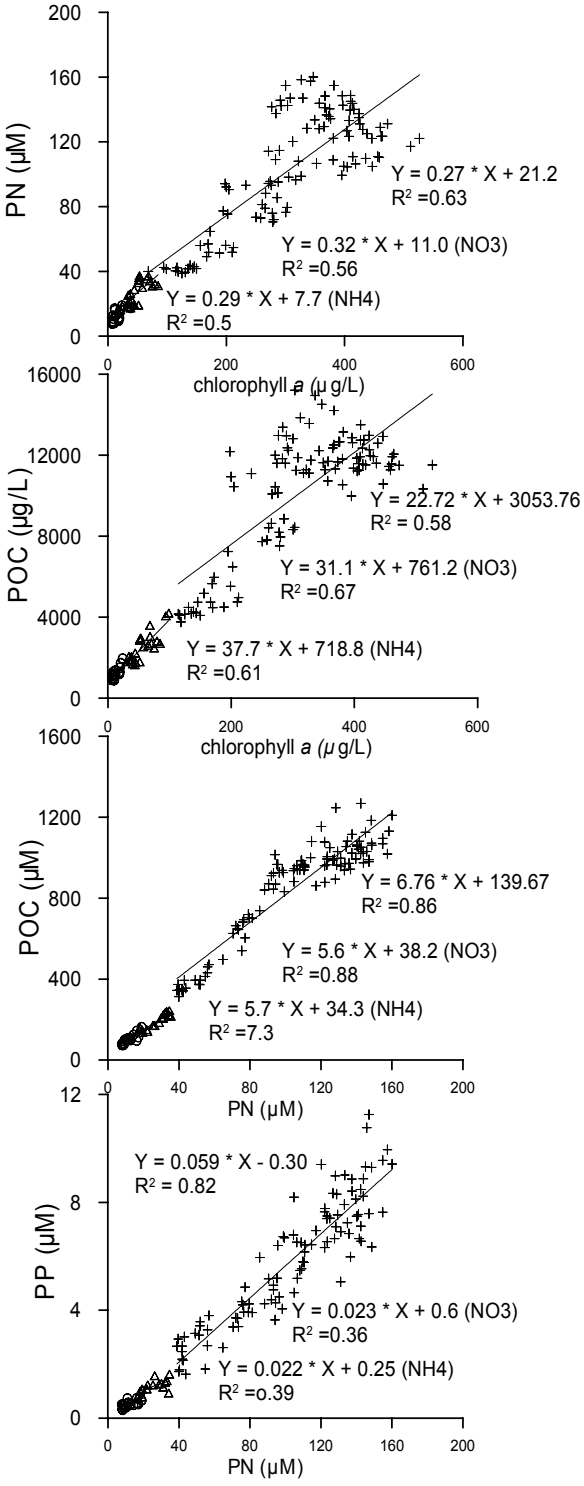

Fig. 3-16 Correlations of chlorophyll *a* with nutrients, PN with POC and PP in the summer experiment (T11)

○ Ammonium uptake

△ Nitrate uptake

□ Nitrite uptake

\+ nutrient addition

The uptake ratios in different phases in both spring and summer mesocosm experiments were calculated and summarized in table 3-1.

Table 3-1: Nitrogen nutrient uptake in the spring and summer experiments.

The ΔDIN: ΔP: ΔSi decrease ratios were calculated from the slopes of ΔDIN/Δchl*a*, ΔP/Δchl*a* and ΔSi/Δchl*a,* according to the correlation of chlorophyll *a* to nutrients (Fig. 3-11, 3-13 for spring and Fig. 3-15, 3-16 for summer). ΔPOC/ΔPN, ΔPN/ΔPP were calculated from the correlations of PN to POC and PP. ΔPOC/Δchl*a* and ΔPN/Δchl*a* were calculated from correlation of chl*a* to POC and PN (Fig. 3-12, 3-14 for spring and Fig. 3-15, 3-16 for summer). (The according calculations excluded diurnal variations.)

Spring experiment (Series 1)

	ΔDIN : ΔP : ΔSi by atoms	**ΔPOC/ΔPN** by atoms	**ΔPN/ΔPP** by atoms	**ΔPOC/Δchl*a*** (μg/L)/(μg/L)	**ΔDIN/Δchl*a*** μM/(μg/L)	**ΔPN/Δchl*a*** μM/(μg/L)
NH_4^+ uptake	25 : 1 : 20 (T1) 29 : 1 : 23 (T4)	6.7(T1) 8.1(T4)	33(T1) 23(T4)	435(T1) 409(T4)	-5.6 (T1) -5.7 (T4)	5.6 (T1) 4.1 (T4)
$NH_4^+ + NO_3^-$ uptake	Not calculated due to short period					
NO_3^- uptake	19 : 1 : 21 (T1) 15 : 1 : 15 (T4)	7.7(T1) 6.9(T4)	50(T1) 33(T4)	120(T1) 121(T4)	-1.5 (T1) -1.7 (T4)	1.3 (T1) 1.4 (T4)

Summer experiment (Series 2) (with *: calculations from the period of nutrient additions)

	ΔDIN : ΔP : ΔSi by atoms	**ΔPOC/ΔPN** by atoms	**ΔPN/ΔPP** by atoms	**ΔPOC/Δchl*a*** (μg/L)/(μg/L)	**ΔDIN/Δchl*a*** μM/(μg/L)	**ΔPN/Δchl*a*** μM/(μg/L)
NH_4^+ uptake	13 : 1 : 4 (T8) 10 : 1 : 5 (T11)	6.4(T8) 5.7(T11)	90(T8) 45(T11)	25(T8) 38(T11)	-0.34 (T8) -0.39(T11)	0.28 (T8) 0.29 (T11)
$NH_4^+ + NO_3^-$ uptake	Not calculated due to short period					
NO_3^- uptake	12 : 1 : 4 (T8) 12 : 1 : 5 (T11)	5.8(T8) 5.6/6.8*(T11)	70(T8) 45/17*(T11)	25(T8) 31/23*(T11)	-0.46 (T8) -0.39(T11)	0.32 (T8) 0.32 (T11)
NO_2^- uptake	Not calculated due to short period.					

3.1.3.2 Calculated conversion rates

Spring experiment

Specific uptake rates (SUR) of N nutrients were calculated as daily nutrient disappearance divided by daily mean PN (Fig. 3-17).

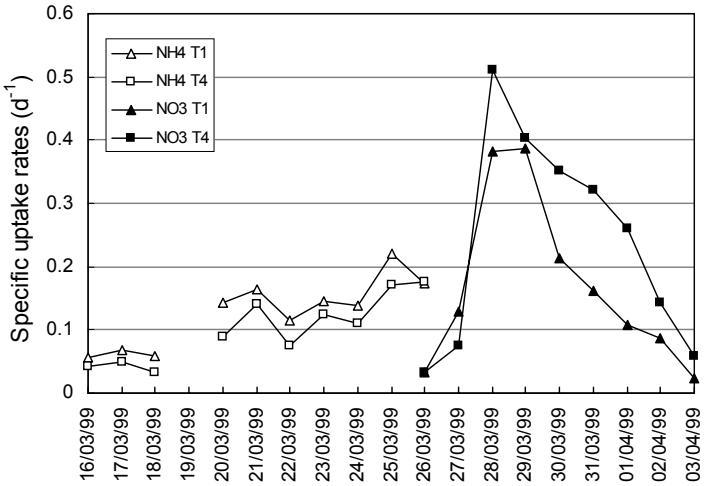

Fig. 3-17 Specific ammonium and nitrate uptake rates in T1 and T4 in the spring experiment. (Calculated from nutrient disappearance divided by mean PN within one day.

During the spring experiment, in the NH_4^+ uptake phase, specific ammonium uptake rates (NH_4^+-SUR) in the T1 increased gradually from 0.05 d^{-1} at the beginning to a maximum value of 0.22 d^{-1} on 25/03. In T4, it increased parallel to T1 to 0.18 d^{-1} on 26/03 (Fig. 3-17).

Daily NO_3^--SUR in T1 increased from 0.03 d^{-1} on 26/03 to the highest of 0.38 d^{-1} on both 28/03 and 29/03 and then decreased to 0.2 d^{-1} and reached 0.02 d^{-1} on 03/04. In T4, NO_3^--SUR increased from identical rate on 26/03. The highest rates occurred on 28/03 with 0.5 d^{-1} and decreased slowly afterwards to 0.26 d^{-1} and reached 0.05 d^{-1} on 03/04.

Summer experiment

During the summer experiment, all N nutrients were exhausted within the first 4 days. NH_4^+, NO_3^- and NO_2^- were utilised successively (Fig. 3-18). In T8, NH_4^+-SUR increased from 0.3 d^{-1} at the beginning up to 0.8 d^{-1} on 02/06. NO_3^--SUR fluctuated in the range of 0 to 0.1 d^{-1} during ammonium uptake. It then started to increase when NH_4^+ -SUR reached the maximum from 0.2 d^{-1} to the maximum of 0.9 d^{-1} on 03/06. At last it dropped near to zero until 04/06. NO_2^- -SUR fluctuated between –0.001 d^{-1} and 0.002 d^{-1} during the ammonium uptake. In the following nitrate uptake phase, NO_2^- -SUR reached the maximum value in minus (-0.005 d^{-1}), showing NO_2^- increase in the water. NO_2^--SUR started to increase after NO_3^- uptake reached the peak and the maximum SUR was 0.02 d^{-1}. It declined nearly to zero until 05/06.

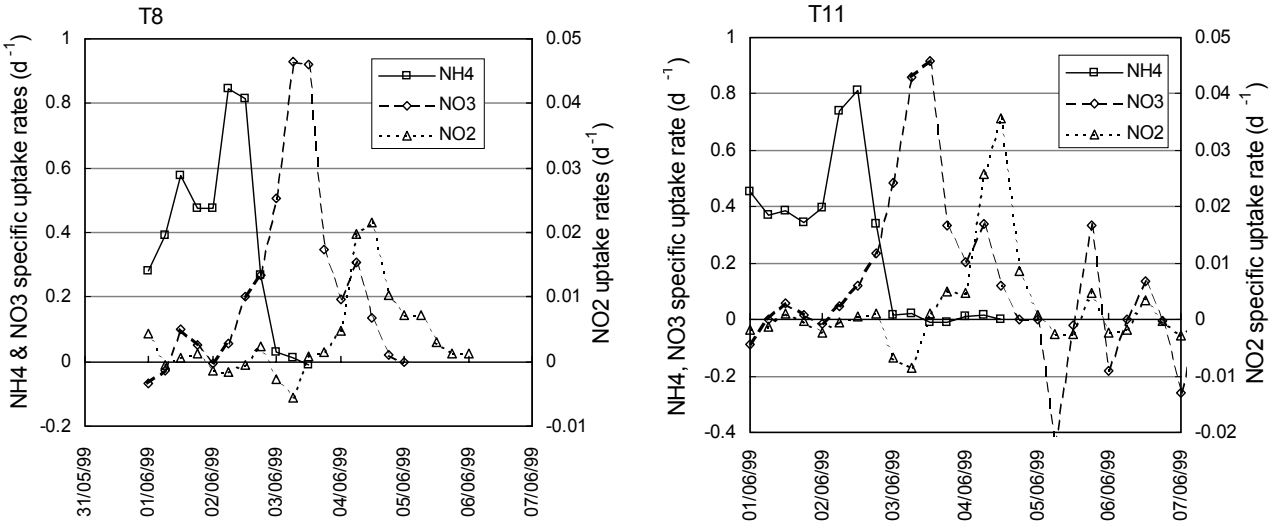

Fig. 3-18 N nutrient uptake rates in the summer experiment (Series 2, Büsum, Jun., 1999, Calculated from nutrient disappearance divided by mean PN within one day)

In T11, nutrient uptake was divided into two phases. The first phase included the first 4 days before nutrient enrichments. The second phase was characterised by nutrient enrichments. The uptake succession and rates during the first 4 days in T11 were quite similar to those in T8, except for NO_2^-, with nearly twice as in T8 (Fig. 3-18).

Detected from nutrient concentrations, there was nearly 24 hours N, 10 hours P and 16 hours Si starvation for phytoplankton cells before the first enrichment. Added nutrients were consumed rapidly within hours. In order to differentiate short-term variation of nutrient uptake during this period, hourly mean specific uptake rates were calculated from nutrient disappearance every 2 hours divided by average PN (Fig. 3-19). All nutrients showed higher short-term uptake rate after the first and second addition compared to the first phase.

Mostly, the added NO_3^--SUR reached 1.8 and 2.3 d^{-1} on the first two days of enrichments. It decreased to 1.5 and 1.0 d^{-1} during the next days. The highest rate, occurring on 06/06 during the enrichment phase was 1.5 times higher than in the first phase.

The added PO_4^{3-} was mostly exhausted within the first 2 to 6 hours, coupled with the highest uptake 0.15 d^{-1} (09/06), which was twice as high than that of the first period (02/06).

The uptake of the added Si was lasting longer in comparison to NO_3^- and PO_4^{3-}. The time-dependent uptake rate reached the highest value of 0.9 d^{-1} (04/06), which was twice the value of the first phase (02/06).

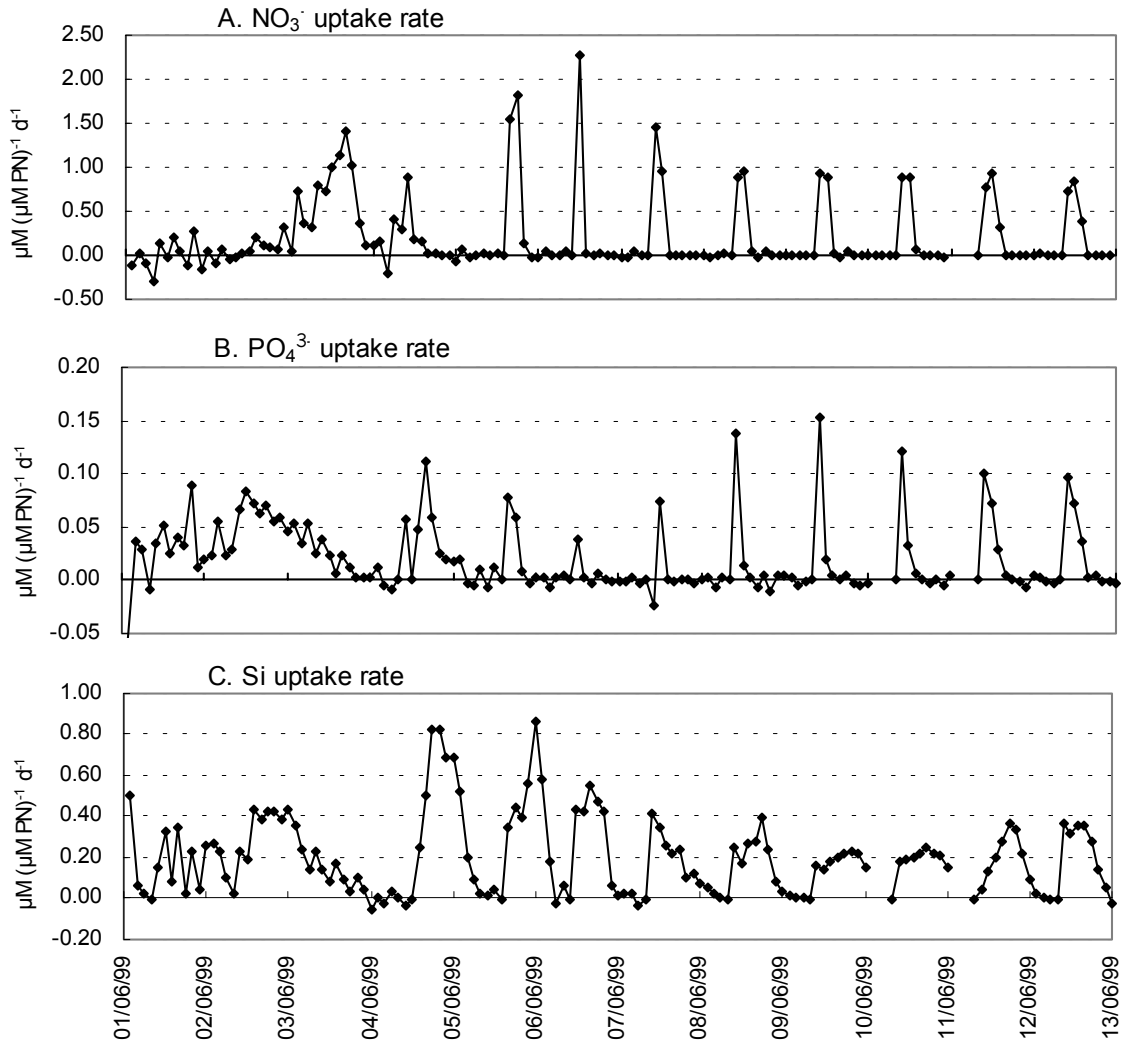

Fig. 3-19 Short-term uptake rates in summer experimental bag (T11)
(After 04/06, NO_3^-, PO_4^{3-} and Si were added.)

3.1.4 Nitrogen mass balance and fractions

3.1.4.1 Spring experiment

N mass balance

The initial N pools were quite similar in both bags with the amount of 183 to 184 µM. In T1, TN fluctuated in the range of 180 µM to 185 µM until 28/03. TN decreased gradually after 29/03, when NH_4^+ was exhausted and NO_3^- started to be taken up, from 183 µM to 170 µM (-7%) until 04/04. Afterwards it stagnated between 170 µM and 173 µM after 04/04 until the end (Fig. 3-20A). In T4, TN started to decrease at the same time as in T1 and reached the minimum of 167 µM (-9%) on 04/04. It then remained around 168 µM until the end (Fig. 3-20B).

Thus, the N loss during the whole period of the experiment reached about 12 µM and 14 µM in T1 and T4 respectively, corresponding to 7% and 9% of the initial TN.

Contributions of different N fractions

Contributions of DIN (NH_4^+, NO_3^- and NO_2^-), PN and DON in T1 and T4 are calculated as percentage of initial TN (Fig. 3-21). At the beginning, DIN occupied the major part of TN with 85%, among which NO_3^- contributed 77%, followed by NH_4^+ and NO_2^- with 6.5% and 1.5% respectively. DON contributed 12% to TN and PN the last 3% in both bags.

In T1, NH_4^+ decreased to 0.2% on 28/03. Correspondingly PN increased to 9% of TN during the same period. NO_3^- started to decrease from 29/03, reaching 47% of TN on 04/04. Correspondingly PN increased to 31% of TN. There was a difference of about 8% of TN between NO_3^- decrease and PN increase. After 04/04, NH_4^+ increased slightly to 0.5% until the end, while NO_3^- and PN remained around 47% and 30%, respectively. NO_2^- remained constant with 1.5% of TN during the whole experiment due to its low concentration. DON remained nearly constant at about 12% from the beginning to 31/03. A slight increase of 2 to 3% was detected from 01/04 (Fig. 3-21A).

In T4, similar to T1, NH_4^+ decreased from 6.5% in the beginning to 0.2% until 28/03 and remained around 0.5% until the end, corresponded with the increase of 6% in PN. NO_3^- decreased from 29/03 to 26% on 04/04, while PN increased from 9% to 49% during the same time. There was 11% of difference between NO_3^- decrease and PN increase. NO_3^- finally remained at 30% and PN at 47% until the end. NO_2^- remained around 1.5% all the time. DON stagnated constant at 12% from the beginning to 31/03, with a slight increase of 2 to 3% starting from 01/04, and remained between 13 and 14% to the end (Fig.3-21B).

Thus, it is evident that N loss mostly occurred during NO_3^- uptake.

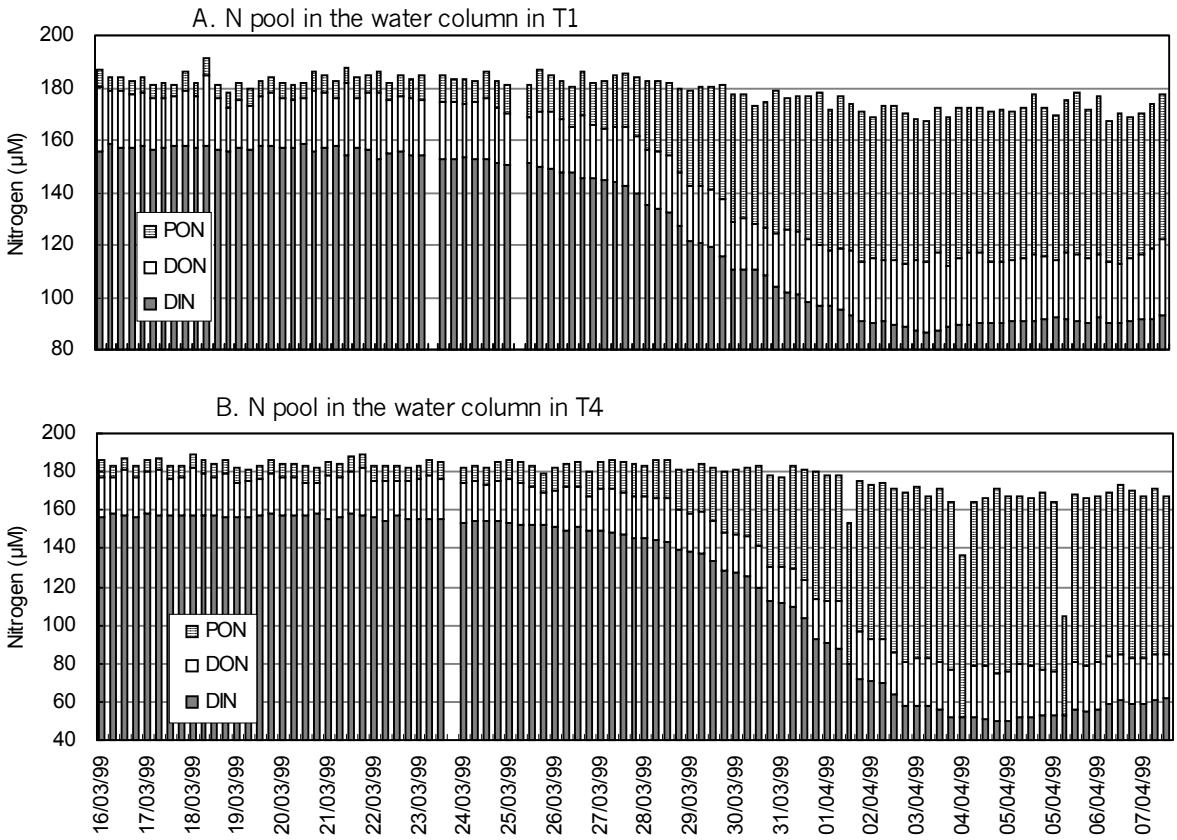

Fig. 3-20 Mass-balance of nitrogen in T1 and T4 during the spring experiments (series 1, Büsum, Mar./Apr., 1999)

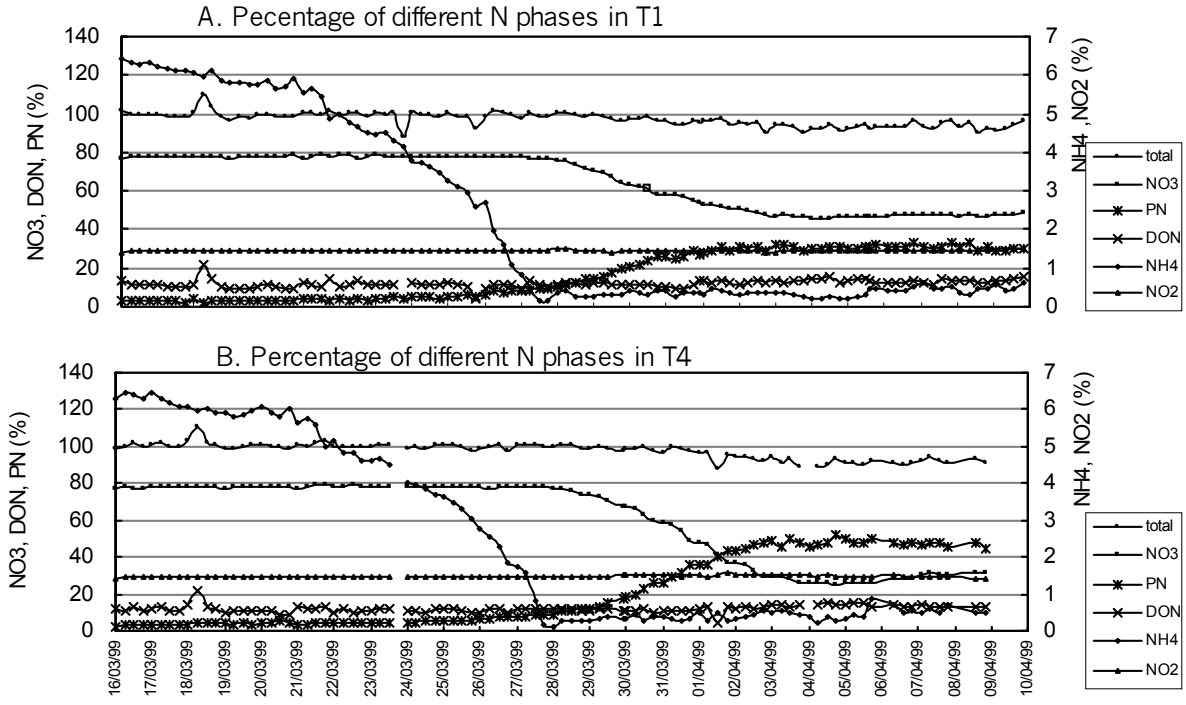

Fig. 3-21 Fractions of different N phases in the spring experiment (Series 1, Büsum, Mar./Apr., 1999. All contributions calculated from the initial total N pool in the water column.)

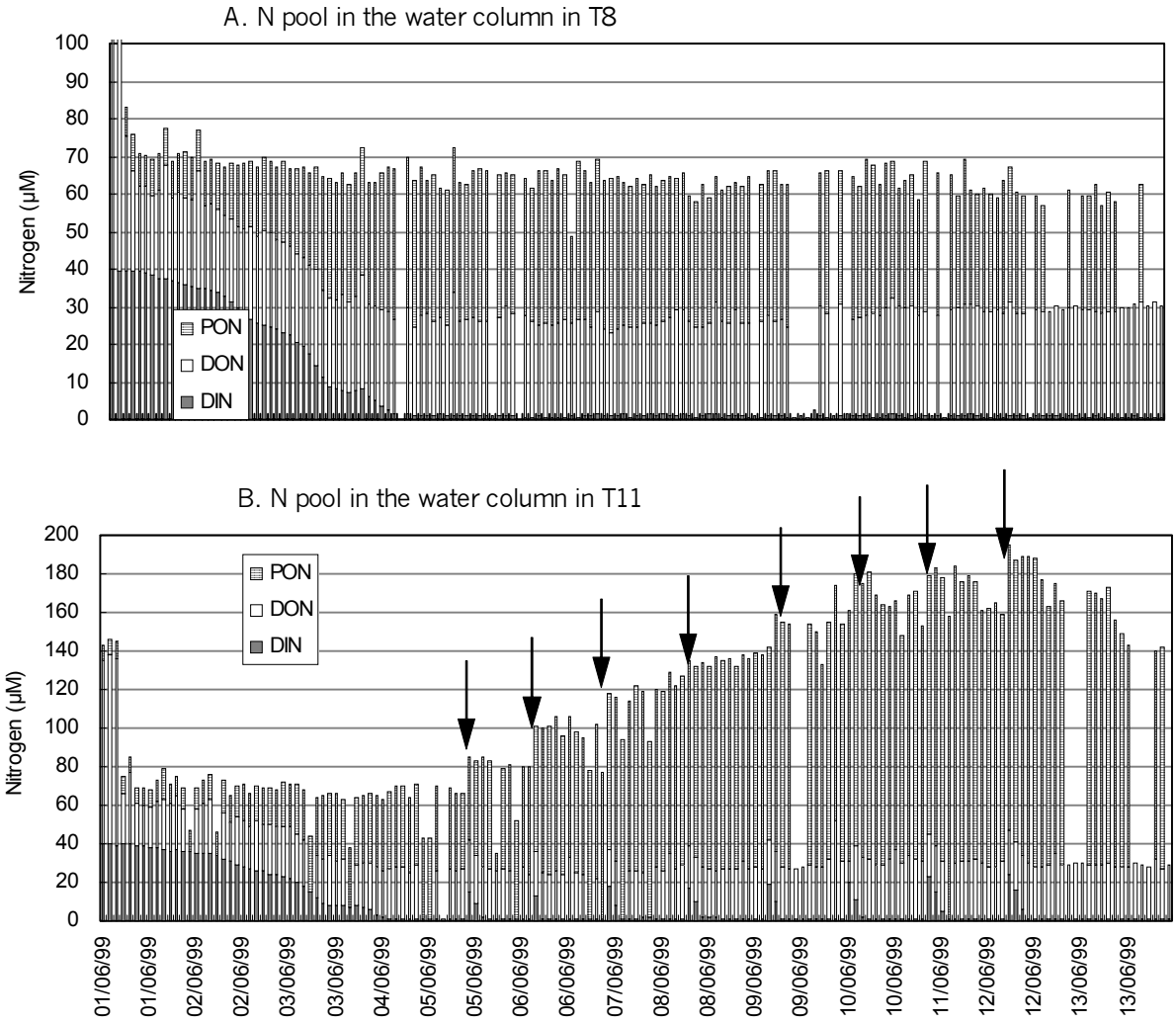

Fig. 3-22 Mass-balance of nitrogen in T8 and T11 during the summer experiment (Series 2, Büsum, Jun., 1999, the moments when nitrate was added are marked with arrows).

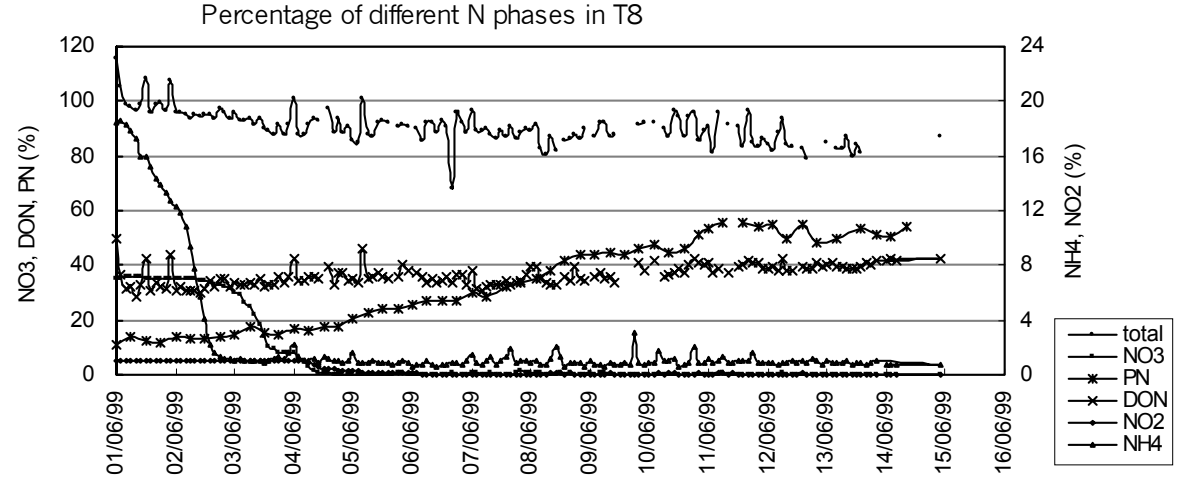

Fig. 3-23 Fractions of different N phases in the summer experiment (Series 2, Büsum, Jun., 1999. All contributions calculated from the initial total N pool in the water column.)

3.1.4.2 Summer experiment

N mass balance

In T8, the TN pool remained around 71 μM during the first 2 days. It started to decrease on 03/06 to 60 μM at the end (Fig. 3-22A). Accordingly, it is estimated that about 15% of the initial N were lost during the whole experiment.

In T11, the initial TN pool was about 72 μM. Totally about 155 μM nitrate was added during the whole experiment. Measured TN on 12/06 was 190 μM (daily average). There were about 20% of TN lost until 12/06 (Fig. 3-22B).

Contributions of different N fractions

Here only T8 was specified to calculate the contributions (Fig. 3-23). Compared to the initial values, DIN in summer amounted to 55%, among which NO_3^- took 35%, NO_2^- took 1% and NH_4^+ 18%. At the same time, DON and PN amounted to 30% and 11%, respectively.

Within the first two days, NH_4^+ decreased to about 0.8% of TN. Afterwards, NO_3^- decreased to 0.1% of TN on 03/06 followed by NO_2^- decrease to 0.1% of TN on 05/06. Correspondingly PN increased to 55% until 05/06, which resulted in a difference of 9% of initial TN. A slight increase to 0.3% of TN in NO_3^- was detected, NO_2^- decreased to 0.03% until the end. PN also declined after 05/06 and remained between 42% and 45% until the end.

The percentage of DON showed slight increase from 30% to 43% at the end. Overall, comparing the final total and the initial TN pool, about 13% of TN were lost in T8, which mostly occurred during the exponential growth phase and the decay phase.

3.1.5 Diurnal variations

In order to study the daily variability, at first trends were calculated, which were used for calculating from the differences of the short time (diurnal) variation, e.g., concentrations of nitrate and nitrite were smoothed by 24 hours running averages, based on the 2-hourly measurements:

$$X(t_i)=(X(t_{i-n})+X(t_{i-n+1})+\ldots+ X(t_i)+ X(t_{i+1})+\ldots+ X(t_{i+n}))/(2n+1)$$

Where t_{i-n}, t_{i-n+1},…,t_i,…,t_{i+n-1}, t_{i+n} are 13 successive sampling times. These means were used for calculating short-term variations of the difference between measurements and corresponding means.

3.1.5.1 Diurnal variation of chlorophyll *a* and photosynthesis

Both in spring and summer experiments, concentrations of chlorophyll *a* showed significant diurnal periodicity, especially during the exponential growth phase (Fig. 3-24, 3-25 and 3-26).

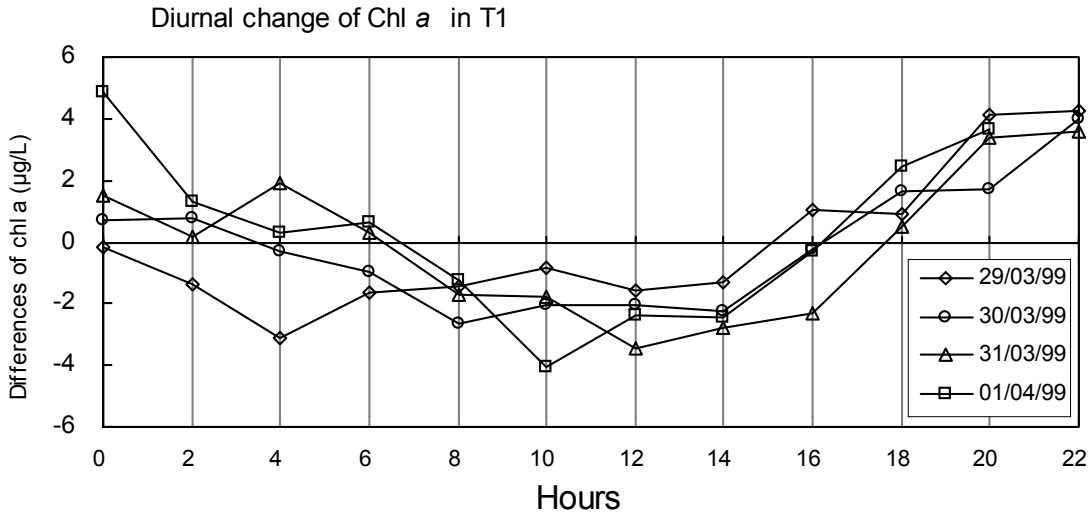

Fig. 3-24

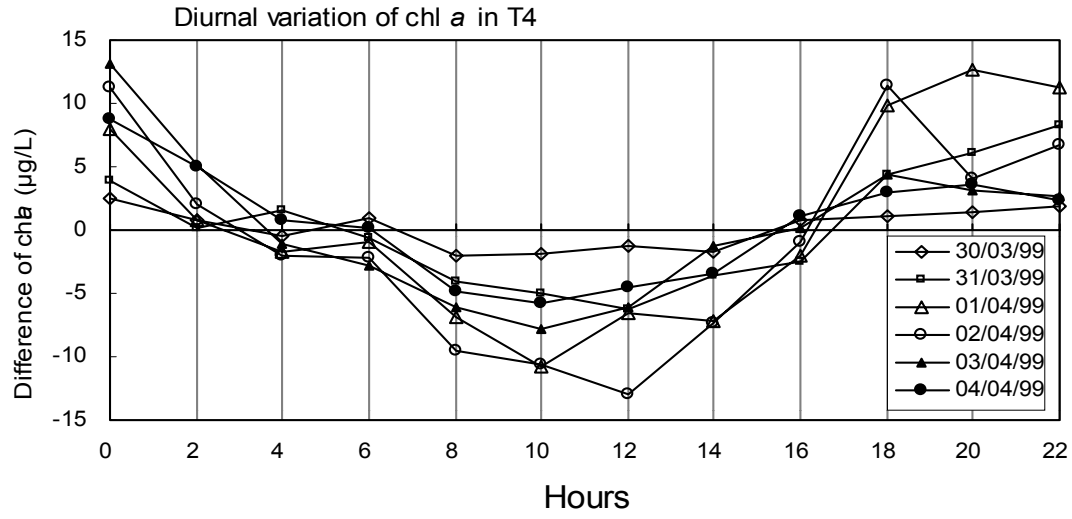

Fig. 3-25

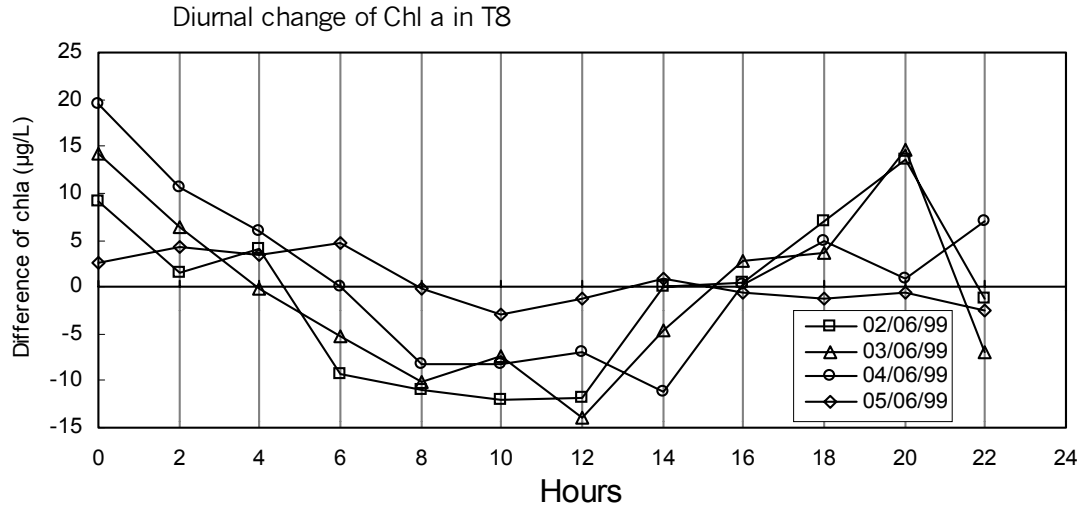

Fig. 3-26

Fig. 3-24 to Fig. 3-26 Diurnal changes of chlorophyll *a* in the spring and summer experiments. The differences were calculated from the measurements and running means of 13 values each.

During spring, in both T1 and T4, chl*a* reached the maximum values at midnight. Afterwards, it decreased gradually and reached its minimum mostly between 10:00 to 12:00 followed by the increase in the afternoon. In T1, the greatest differences occurred during the days of 30/03 to 01/04, being in the exponential phase. The maximum difference reached up to 10 µg/L (±1 to ±5µg/L) (Fig. 3-24). In T4, the maximum difference occurred during the exponential phase (31/03 to 02/04). The difference reached up to 20 µg/L (±10 µg/L) (Fig. 3-25).

In the summer experiment (series 2), chl*a* concentrations showed the highest values at midnight and decreased in the morning as that in spring (Fig. 3-26). The minimum occurred between 10:00 and 12:00. Short-term variation showed greater differences on 02/06 to 04/06 with up to 30 µg/L.

Specific rates of photosynthesis were calculated from the increase of POC during a period of 6 hours divided by the average concentration of chlorophyll *a* during the same period (µg POC (µg chl*a*)$^{-1}$ h^{-1}). Thus, for every day, there are 4 points of photosynthesis rates. Every point represents the average rate within the 6 hours (Fig. 3-27 and 3-28).

It is shown that in spring, the highest photosynthetic rates occurred in the afternoon, with about 5 to 8 µg POC (µg chl*a*)$^{-1}$ h^{-1} in T1 and 3 to 5 µg POC (µg chl*a*)$^{-1}$ h^{-1} in T4. The lowest rates occurred at night with about –2 µg POC (µg chl*a*)$^{-1}$ h^{-1} in both bags (Fig. 3-27).

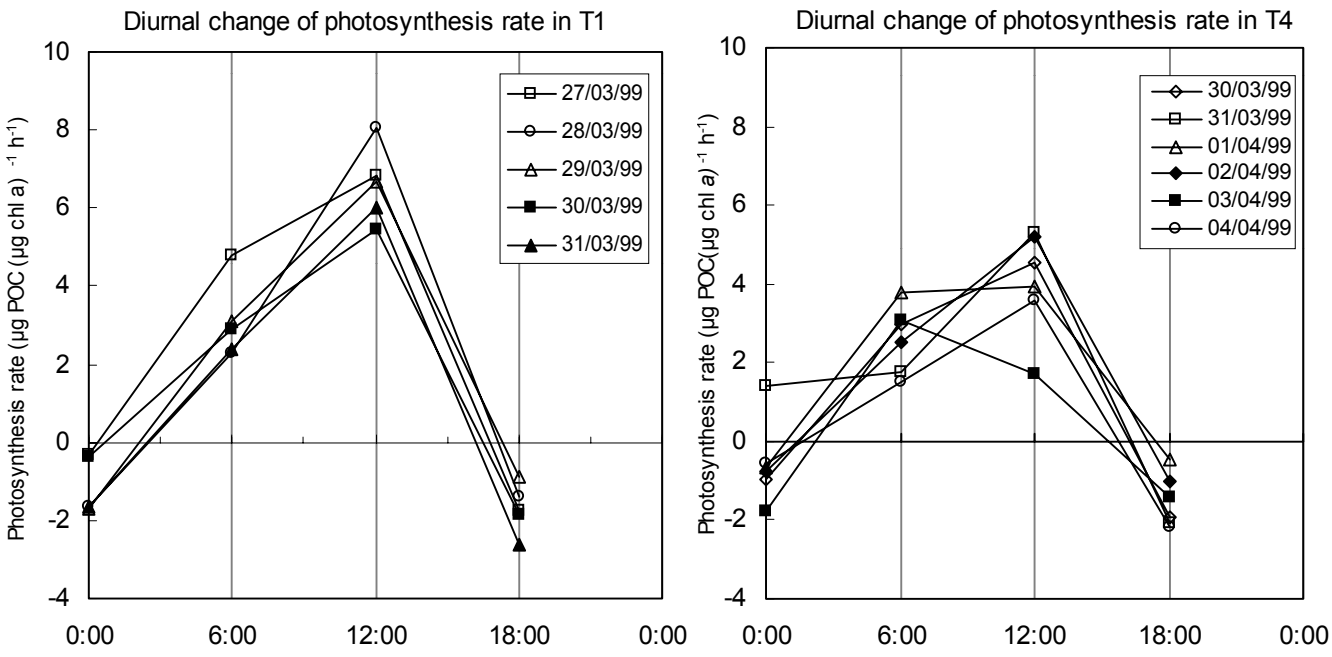

Fig. 3-27 Diurnal changes of photosynthesis rates in the spring experiment (series 1, Büsum, Mar./Apr., 1999. Calculated from variations of POC during a period of 6 hrs divided by mean chlorophyll concentrations during the same period, thus, every value represents the rate during the 6 hrs.)

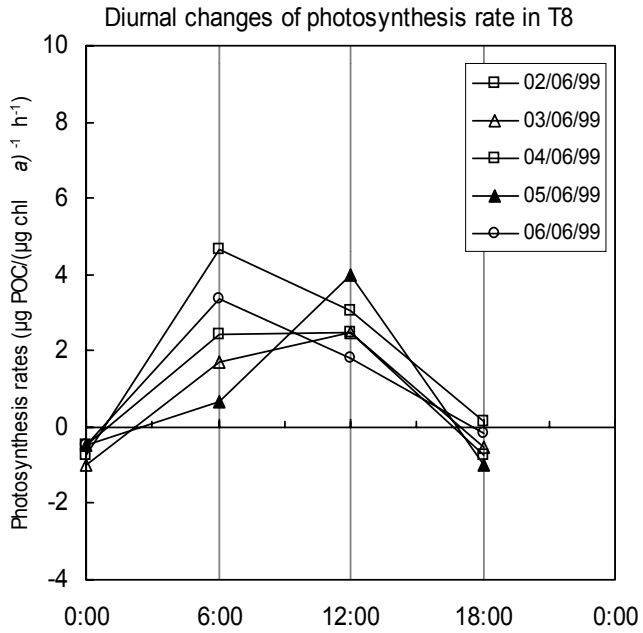

Fig. 3-28
Diurnal changes of photosynthesis rates in the summer experiment (Series 2, Büsum, Jun., 1999. Calculated as for Fig. 3-27.)

During the summer experiment (Fig. 3-28), on 03/06 and 05/06, the highest specific photosynthesis occurred in the afternoon with 2 µg POC (µg chl*a*)$^{-1}$ h^{-1} and 4 µg POC (µg chl*a*)$^{-1}$ h^{-1} respectively. On the days of 02/06, 04/06 and 06/06, the photosynthesis rates were higher in the morning with 2.0 to 4.5 µg POC (µg chl*a*)$^{-1}$ h^{-1}. The rates decreased to around –1.0 µg POC (µg chl*a*)$^{-1}$ h^{-1} at night.

Changes of POC in relation to chl*a* also showed some diurnal periodicity. It is shown that short-term variation was negative between midnight and morning, which indicated a relative decrease of carbon content in the phytoplankton cells. Increase of C content occurred mainly in the afternoon (Fig. 3-29A, B). This character was more significant during the exponential growth phase. In T1, the highest values were observed in the early evening with a difference of up to 10 (µg POC)/(µg chl*a*). The lowest values appeared in the early morning with –20 (µg POC)/(µg chl*a*) (Fig. 3-29A). In T4, strongest increases mostly occurred in the afternoon with differences of about 20 (µg POC)/(µg chl*a*), or even 40 (µg POC)/(µg chl*a*), and decreases around midnight with differences of –20 (µg POC)/(µg chl*a*). On 30/03 and 04/04, the start of the exponential and stationary phase, the highest increase occurred in the early evening with values up to 10 (µg POC)/(µg chl*a*) (Fig. 3-29B).

Diurnal changes of POC/chl*a* in T8 are shown in fig. 3-29C. Only in the exponential growth period of 02/06 and 03/06 showed similar variation as in spring.

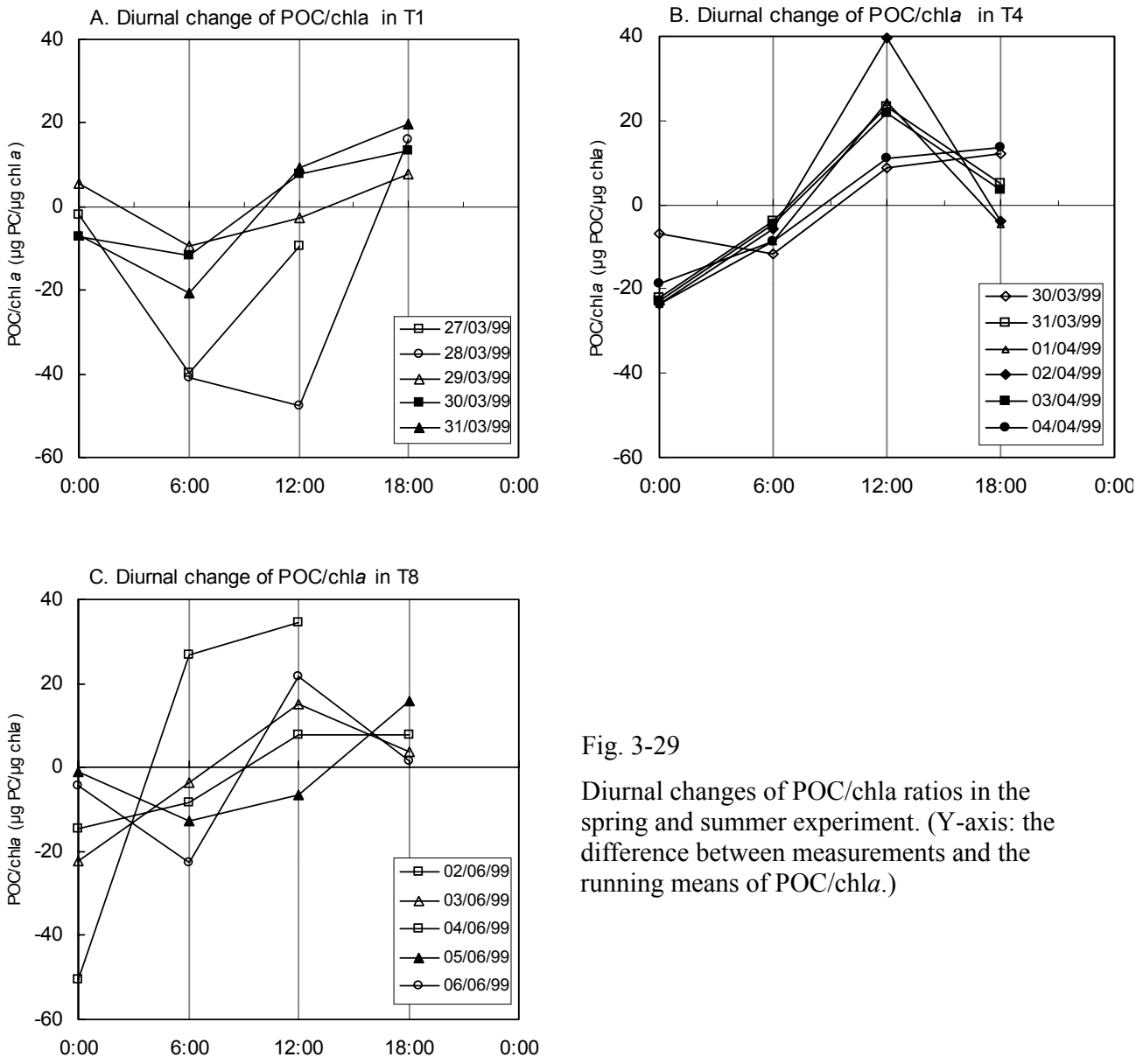

Fig. 3-29

Diurnal changes of POC/chla ratios in the spring and summer experiment. (Y-axis: the difference between measurements and the running means of POC/chl*a*.)

3.1.5.2 Diurnal variation of nutrient uptake

Ammonium

Short-term variation of NH_4^+ in spring revealed that during the first 5 days (16/03 to 20/03) there was no significant diurnal variation. After 21/03 the variation showed a regular periodic diurnal character with decreases at daytime due to the uptake by phytoplankton and increases at night resulting from remineralisation. These diurnal changes were only detectable when the phytoplankton biomass had reached a significant level of ca. 2 µg/L chlorophyll (Fig. 3-30).

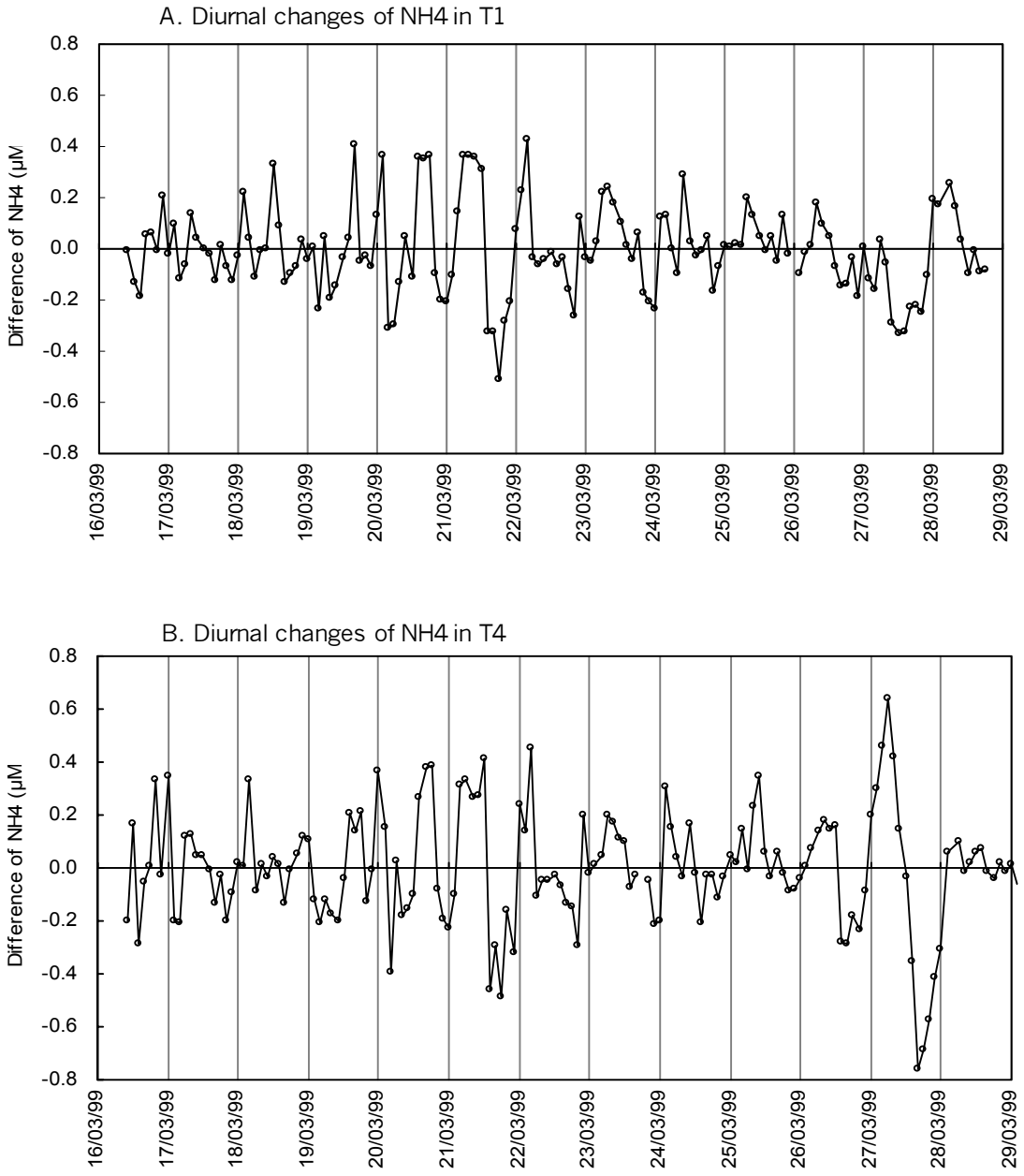

Fig. 3-30 Diurnal changes of ammonium concentrations in the spring experiment (Series 1, Büsum, Mar./Apr., 1999. Y-axis: the difference between the measurements and the running means.)

Nitrate

During the exponential phytoplankton growth phase, nitrate concentrations showed significant diurnal variations both in T1 and T4 as shown in Fig. 3-31. Nitrate decreased mainly at daytime between 8:00 and 18:00 due to light-dependent phytoplankton uptake, and increased during nights from 18:00 to the next morning about 6:00 due to stagnating concentrations, and nitrification resulting in the maximum at 8:00 and minimum at the beginning of the dark period.

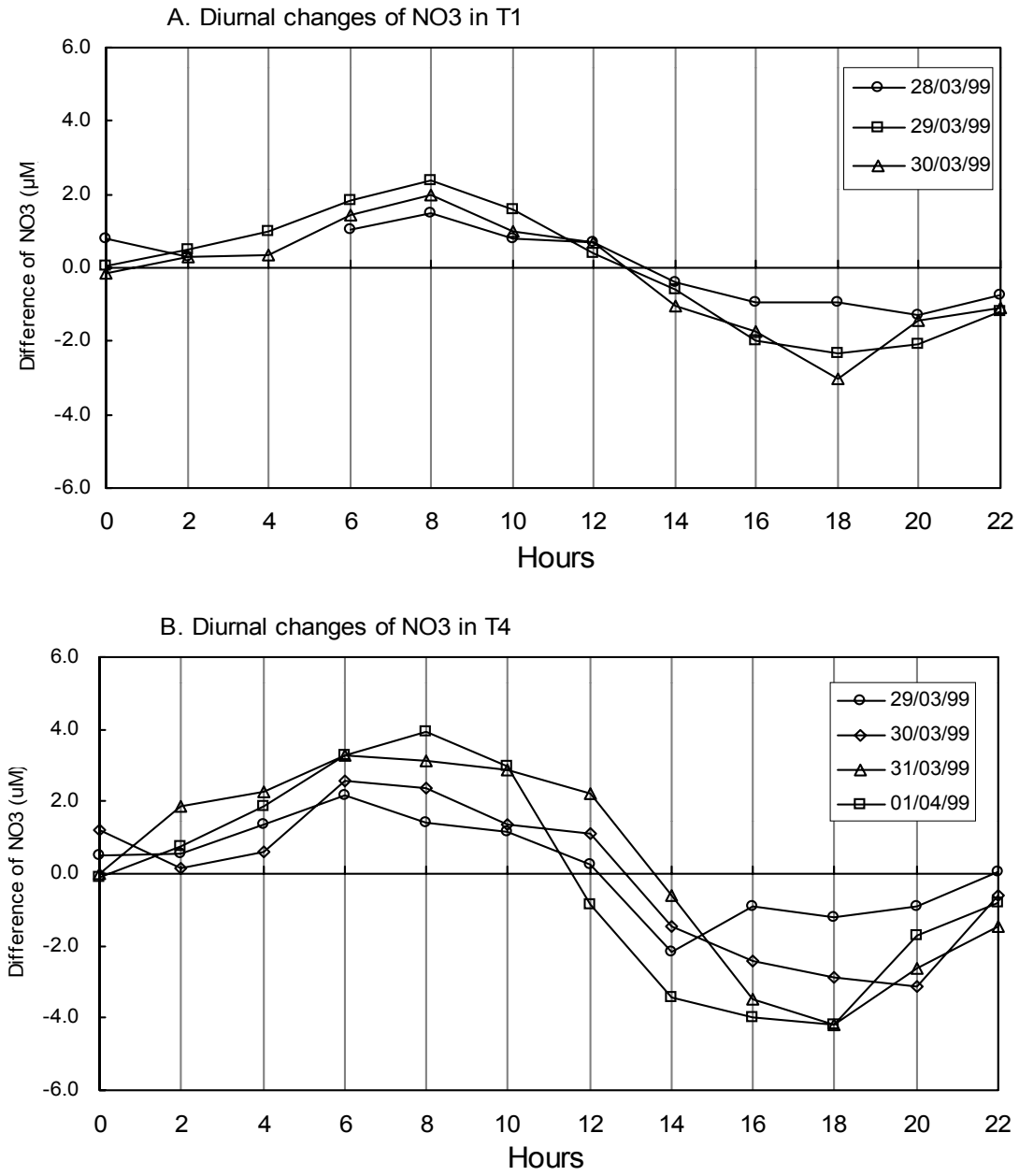

Fig. 3-31 Diurnal changes of nitrate in the spring experiment (Series 1, Büsum, Mar./Apr., 1999, Y axis: the differences between the measurements and the running means.)

Nitrite

Short-term variations of nitrite in T1 and T4 are shown in Fig. 3-32. The concentrations of nitrite increased after 12:00 and were highest around 18:00, in T 1 by 0.02 to 0.04 µM, in T 4 up to 0.08 µM. Minima were observed near noon which were in the same order of magnitude as the maxima. There was a delay between the nitrate minima and nitrite maxima of about 2 to 4 hrs.

In summer, the fast uptake of NO_3^- and NO_2^- prevented this diurnal periodicity. Only on 04/06, a slower decrease of NO_3^- was detected from the plot both in T8 and T11, indicating slow uptake by phytoplankton at night (Fig. 3-7B).

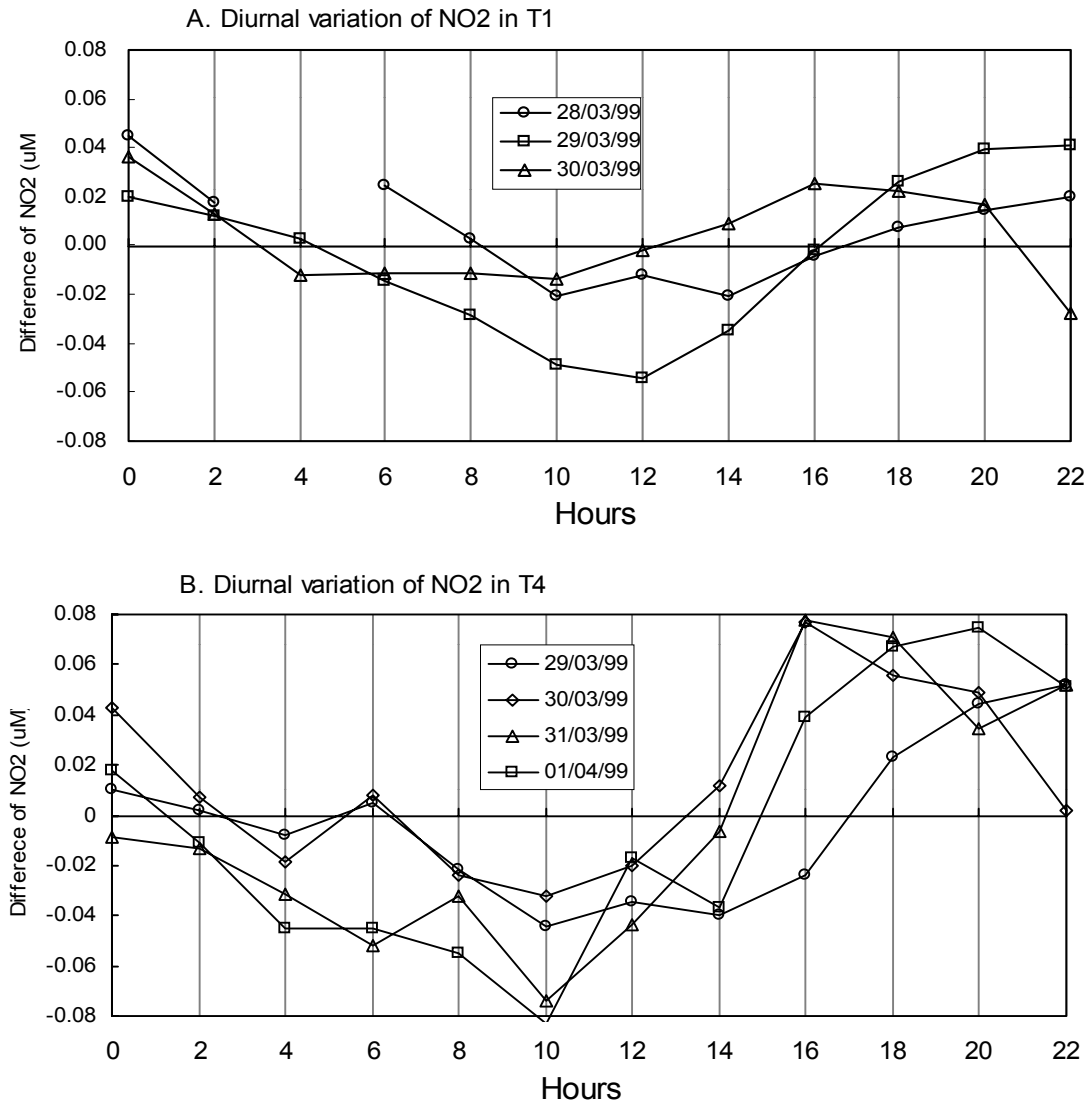

Fig. 3-32 Diurnal changes of nitrite concentrations in the spring experiment (Series 1, Büsum, Mar./Apr., 1999, Y axis: the differences between the measurements and the running means.)

3.2 Model simulations

3.2.1 Model procedures

Mesocosm experiments with very good reproducibility and representativity of the natural systems supplied complete data sets for model simulations. In the bags of the spring and summer experiments, identical ecological and chemical processes in the planktonic system were included. However, the spring and summer series were independent because the initial chemical and biological conditions were different due to the seasonal change in the natural system. Moreover, seasonal temperature and light climate as well as different nutrient manipulations drove the two series to be differently developed. For this reason, the systematic data from the spring and summer control bags were used to calibrate and validate the model.

At first, the model was run to reproduce the measurements from the spring control experiment with the given forcing data (water temperature and global radiation) and initial values of the state variables. A set of parameter values was resulted from this calibration process. This given set of parameter values, together with the forcing functions and initial conditions, constitute the so-called "standard model". Parameters related to processes and relationships, used in standard runs were mostly derived from literature except for some cases when it was impossible, then a reasonable guess was assumed. Small adjustment has been done during the model runs.

After calibration, the model was adapted to simulate the development in the summer control bag with the purpose of model validation. During this procedure, some parameters were modified in order to reproduce the development of the main compartments better. Those parameters included the maximum specific growth rate of flagellates (*Rfmax*), zooplankton maximum graze rate (*Rgmax*), detritus decomposition rate (*Rddecay(0)*, *Rddecay_P(0)*) and DOM remineralisation rate (*Rremin(0)*, *Rremin_P(0)*). The values of all parameters both after calibration and validation are as shown in table 3-3.

Based on calibration and validation, the model was finally applied to reproduce the development of the spring and summer experimental bags, by introducing the addition manipulations as events and keeping the forcing factors (temperature and light climate) and initial values the same as in the respective control system. Because the measurements were prior to the model simulations, the simulations for the experimental system were called 'hindcast', distinguished from forecast, which is normally defined when the simulation is in advance of measurements. The data sets used for modelling procedures are listed in table 3-2.

Table 3-2 Data sets for modelling procedures

Model procedures	**Data sets**	**enclosure number**
Calibration	Spring control bag	T1
Validation	Summer control bag	T8
Hindcast (verification)	Spring experimental bag Summer experimental bag	T4 T11

Table 3-3: Parameters in the model and the values in standard run. (with '-': dimensionless)

Symbol	Unit	meaning	values	
			spring	summer
R*dmax*	d^{-1}	Diatom maximum specific growth rate	2.4	2.4
R*fmax*	d^{-1}	Flagellates maximum specific growth rate	2.4	2.8
r1	Q_{10}=1.65	Temperature coefficient for diatom and flagellate growth	0.05	0.05
I_{opt}	W/m^2	Optimal photosynthesis radiation	70	70
λ	-	Transmission of light at air-sea interface	0.94	0.94
θ	-	Fraction of PAR to global radiation	0.43	0.43
e	-	The base of natural log	2.72	2.72
K0	m^{-1}	Extinction coefficient without chl*a*.	0.8	0.8
K1	$m^2(mgchl)^{-1}$	Constant for phytoplankton self-shading	0.0088	0.0088
K2	$m\ (mgchl)^{-2/3}$	Constant for phytoplankton self-shading	0.054	0.054
Ksa,Ksn,Ksi	$mmolN/m^3$	Half-saturation for phytoplankton N uptake	0.5	0.5
$\varphi 1, \varphi 2$	$(mmolN)^{-1}$	NH_4^+ (NO_3^-) inhibition constant for phytoplankton uptake NO_3^- (NO_2^-)	1.5	1.5
Ksp	$mmol\ P/m^3$	Half-saturation constant for phytoplankton P uptake	0.1	0.1
Kssi	$mmol\ Si/m^3$	Half-saturation constant for phytoplankton Si uptake	0.5	0.5
qac	(g chl)/(g C)	Chl/C ratio in weight for phytoplankton	0.02	0.02
qcn	(g C)/(g N)	C/N ratio of phytoplankton in weight	6±1	6±1
Rpn_uptk	mol/mol	The ratio of N/P for phytoplankton uptake	16	16
Rpexud	-	Phytoplankton release fraction of primary production	2%	2%
Rpmort(0)	d^{-1}	Phytoplankton specific natural mortality rate at 0°C	0.01	0.01
r3	Q_{10}=1.92	Temperature coefficient for phytoplankton. natural mortality	0.065	0.065
H	m	Water depth	3	3
b1,b2	-	Zooplankton assimilation efficiency on phytoplankton and detritus	0.85,0.6	0.85,0.6
c1,c2,c3	-	Food preference of zooplankton on diatoms, flagellates & detritus	0.7, 0.6, 0.2	0.7,0.6, 0.2
Rgmax	d^{-1}	Maximum specific grazing rate of zooplankton	0.12	0.2
Kg	$mmol\ N/m^3$	Half-saturation of zooplankton grazing	0.5	0.5
Rzmort(0)	d^{-1}	Zooplankton natural mortality rate at 0°C	0.01	0.01
r5	Q_{10}=2.01	Temperature coefficient for zooplankton natural mortality	0.07	0.07
Rzexcr(0)	d^{-1}	Zooplankton N excretion rate at 0°C	0.02	0.02
Rzexcr_P(0)	d^{-1}	Zooplankton P excretion rate at 0°C	0.02	0.02
r6	Q_{10}=1.65	Temperature coefficient for zooplankton excretion	0.06	0.06
Rddecay(0)	d^{-1}	Specific decomposition rate of detritus in N	0.05	0.15
Rddecay_P(0)	d^{-1}	Specific decomposition rate of detritus in P	0.03	0.10
r7	Q_{10}=1.65	Temperature coefficient for detritus breakdown	0.05	0.05
qnd	(g N)/(g detritus)	N/detritus in weight	0.08	0.08
Rni0	d^{-1}	Specific ammonium nitrification rate at 10°C	0.001	0.001
r9	Q_{10}=1.65	Temperature coefficient for ammonium nitrification	0.05	0.05
Rden0	d^{-1}	Denitrification rate from NO_3^- to NO_2^- at 10°C	0.0001	0.0001
r10	Q_{10}=1.49	Temperature coefficient of NO_3^- to NO_2^-	0.04	0.04
Rden02	d^{-1}	Denitrification rate from NO_2^- to N_2O or N_2	0.005	0.005
R11		Temperature coefficient of NO_2^- to N_2O or N_2	0.06	0.06
Rremin(0)	d^{-1}	DON remineralisation rate at 0°C	0.005	0.015
r8	Q_{10}=1.49	Temperature coefficient for DON remineralisation	0.04	0.04
ε	-	Ammonium fraction of zooplankton excretion	75%	75%
σ	-	Fraction of nitrite release during nitrate uptake	0.002	0.01
Rremin_P(0)	d^{-1}	Remineralisation rate of DOP at 0°C	0.002	0.008
ξ	-	Regenerated silicate fraction of total uptake silicate	0.02	0.02
Rsn_uptk	mol/mol	Ratio of N/Si by diatom uptake	1	1
Pi	-		3.1415	3.1415

3.2.2 Model results

3.2.2.1 Simulations of the spring control bag

3.2.2.1.1 Primary productivity and the control factors

The simulated primary productivity varied from 0.5 μg N l^{-1} h^{-1} to 18.0 μg N l^{-1} h^{-1} in spring (Fig. 3-33A). These data are comparable to the *in situ* measurements, which showed that the gross primary productivity varied from 20 μg C l^{-1} h^{-1} to 180 μg C l^{-1} h^{-1} during spring in T1 (Fig. G in appendix).

The limitation function of temperature varied between 1.25 and 1.85, corresponding to the temperature increase of 6°C (Fig. 3-1) during the whole spring experiment. Exponential correlation between growth rates and temperature was significant from model simulation (Fig. 3-33B).

The theoretical light limitation function for growth rates varied between zero to 1, with the optimum for $I/I_{opt} = 1$ (Fig 3-33C). Light showed strict limitation to the primary productivity in the spring control bag with the highest values of the overall light limitation function within one day varying between 0.3 to 0.2 in the control bag, integrated over the day and the water column (Fig. 3-33C).

Nutrient limitation was only considered in relation to transient concentrations, which gave a limitation of 1 when a nutrient was relatively high in correspondence to the other elements, assuming that the nutrient with the lowest factor limits the growth according to Liebig's law.

In the spring control bag, nitrogen, phosphate and silicate had high limitation functions close to 1 during the first 12 days, as shown from the simulation (Fig. 3-33D). There was a decrease of the nitrogen limitation function on day 10 to 11 when ammonium was depleted. The phosphorus limitation function decreased quickly after day 13, corresponding to the decrease of phosphate in the water column (Fig. 3-2D). Si limitation functions kept around 1.0 over the experiment, corresponding to high silicate concentrations in the water column.

3.2.2.1.2 Simulations of the main compartments

The simulated results of the main compartments in the model were plotted together with the respective measurements (Fig. 3-34).

Nutrients

The simulated NH_4^+ was generally in coincidence with the measurements as shown in Fig. 3-34A. The model simulated well the exhausting point of NH_4^+. The accumulation of NH_4^+ during the last week was also reflected in the model. However, simulated NH_4^+ concentrations were about 0.5 μM higher during the first 8 days and lower concentrations during the last 12 days, compared to the measurements.

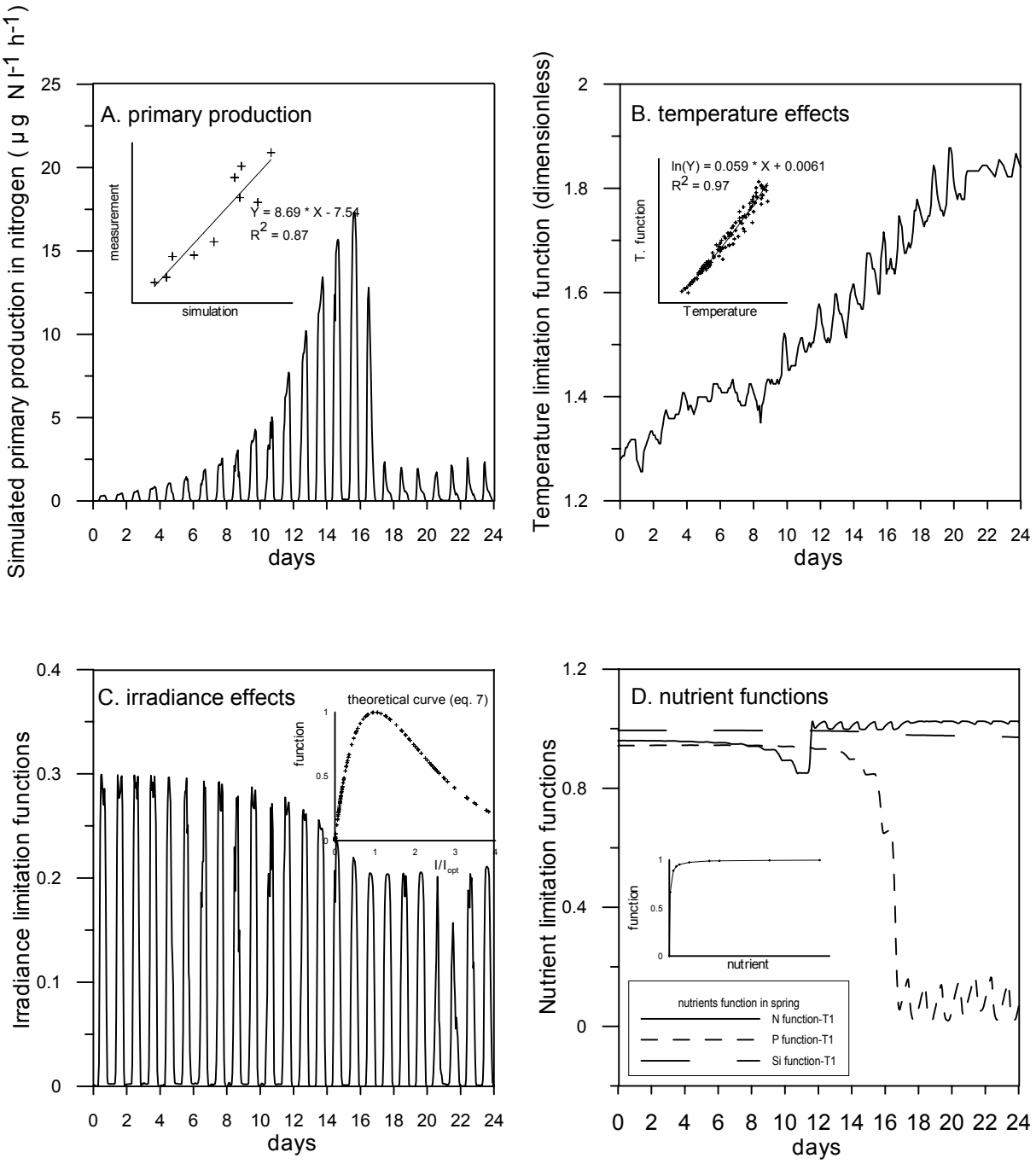

Fig. 3-33 Simulated primary production and temperature, irradiance and nutrients functions on primary production in the spring control system (T1, calculated from the model)
For the values of the nutrient limitation function, the value of 1 represents no limitation; lower values represent the increasing limitation of nutrient.
The complementary plot in A shows the correlation of simulative primary production with measured primary production; complementary plots in B, C, and D show the theoretical curve of respective limitation function.

The point from which nitrate started to be taken up by phytoplankton was consistent with the measurements (Fig. 3-34B). The model reproduced well ammonium preference and inhibition of nitrate. Significant day-night periodicity in nitrate variation showed both from the model and the measurements. However, the exponential uptake in the model stopped about two days earlier compared to the measurements. At last, nitrate remained at the level of several μM higher than the measurements.

Different developments of NO_2^- in the bags of the same sequence, such as T1 and T3 were detected from the measurements (Fig. 3-34C). The simulated nitrite fitted more the measurements from T3 with slight increase during the first 12 days. However, the fast decrease of nitrite during the night was not obviously simulated.

The development of phosphate from simulation had similar curve to that from measurements. However, there was slightly higher in simulations compared to the measurements during the first 8 days. The time delay of PO_4^{3-} simulation from half to two days in the simulation occurred in the exponential growth phase and increased over the time (Fig. 3-34D).

The simulated Si was generally consistent with the measurements (Fig. 3-34E), except a little faster decrease during the first 12 days. Similar to nitrate, Si uptake stopped two days earlier and finally remained at higher concentrations compared to the measurements.

The simulated development of DON was well consistent with the measured highly variable data in the general developing trend (Fig. 3-34 J).

Particulate matter

Compared to the measurements, the model simulated the main features of PN development, including the slower exponential growth phase, which lasted about 11 days, the starting-points of the exponential growth and stationary phases (Fig. 3-34F). The modelled development of PN showed significant diurnal variation, especially in the exponential phase.

Diatoms significantly dominated the phytoplankton community, covering more than 90% of phytoplankton N (Fig. 3-34G). Flagellate N remained at very low concentrations all the time. The initial zooplankton nitrogen biomass was quite low (0.6 μM). It increased exponentially over the time to 2.3 μM at the end (Fig. 3-34H). Mostly, the increase of detritus occurred during the last 10 days and reached 13 μM in the end (Fig. 3-34I).

PP increased from 0.7 μM to 2.3 μM with an exponential increase of 1.5 μM mainly between days 11 to 17 (Fig. 3-34K). The simulated curve was similar with the measurements. However, there was a time delay of half to two days in the exponential growth phase in the simulations, which is consistent with PO_4^{3-} simulations.

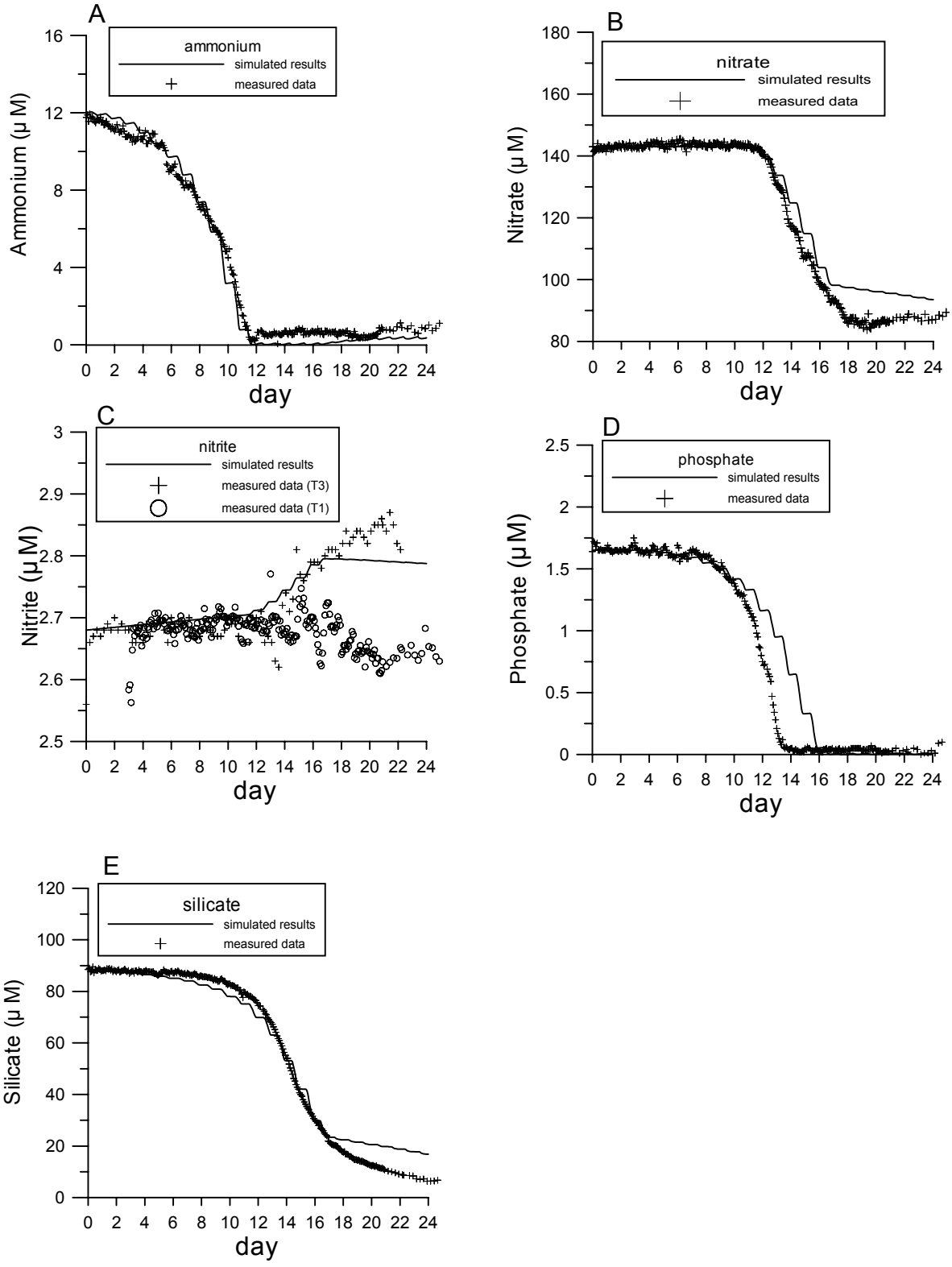

Fig. 3-34 Outputs of main compartment simulations in spring control system (T1, nutrients. Crosses: measurements; line: simulations) (to be continued)

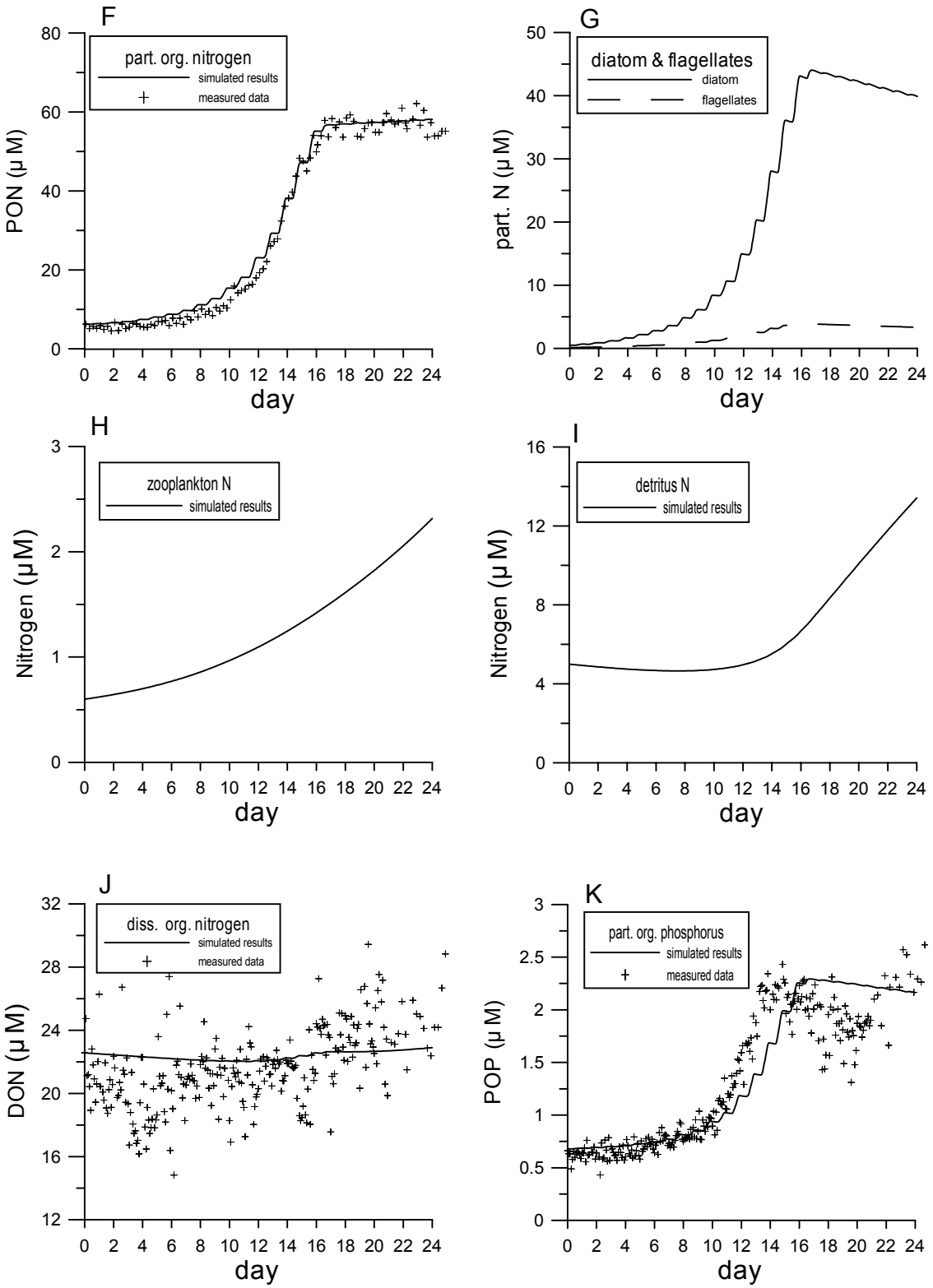

Fig. 3-34 Outputs of main compartment simulation in the spring control system (T1, dissolved and particulate matter. Crosses: measurements; line: simulations)

3.2.2.2 Simulations of the summer control bag

3.2.2.2.1 Primary productivity and the control factors

The simulated primary productivity in the summer control bag varied as N equivalents from 4.0 µg N l^{-1} h^{-1} to 23 µg N l^{-1} h^{-1} (Fig. 3-35A), comparable to the *in situ* measured gross primary productivity varying from 33 µg C l^{-1} h^{-1} to 250 µg C l^{-1} h^{-1} (Fig. H in appendix).

The temperature limitation function was higher than that in spring. However, over the whole experiment, it decreased from 2.5 to 2.1, corresponding to temperature decrease of 4°C (Fig. 3-35B).

Light limitation function varied from 0 to maximum 0.3 after integrated over the day and water column (Fig 3-35C). The overall limitation functions decreased from 0.3 to 0.22 within the first 4 days with phytoplankton growing.

During the first two days, all nutrients (N, P, Si) had very loose limitations to primary production with high values of limitation functions (Fig. 3-35D). Silicate limitation function decreased first quickly on day 3. Soon after, the N and P limitation functions also decreased to 0.3 and remained at this level until the end.

3.2.2.2.2 Simulations of the main compartments

The simulated results of the main compartments in the summer control bag were plotted together with the measurements in Fig. 3-36.

Nutrients

The simulated development of DIN in the summer control bag was mostly consistent with the measurements. Compared to spring, the turnover of phytoplankton growth and nutrient uptake was faster, occurring in the first 4 days. The model was able to reproduce the patterns of DIN utilisations by phytoplankton, not only ammonium preference and inhibition of nitrate uptake as reflected in spring, but also nitrate preference and inhibition of nitrite uptake when nitrate was depleted to <1.0 µM (Fig. 3-36A, B). Nitrite accumulation during nitrate uptake was obviously reflected (Fig. 3-36C). However, compared to the measurements, the exhausting point of ammonium showed a delay of several hours, which was also reflected in the nitrate uptake. The delays of the NO_3^- depleting point and the starting-point of NO_2^- utilisation compared to the measurements were in the same range as the ammonium delay.

From simulation, PO_4^{3-} was exhausted within 4 days (Fig. 3-36D). Again, as in spring, the simulation showed a time delay of half to one day during PO_4^{3-} uptake period, shorter than that in spring.

The simulated development of silicate, which was exclusively related to diatoms, fitted the measurements better compared to spring (Fig. 3-36E).

DON simulation reflected the trend of the real development in the bags, the simulated curve is smooth compared to the high deviation of the real data (Fig. 3-36J).

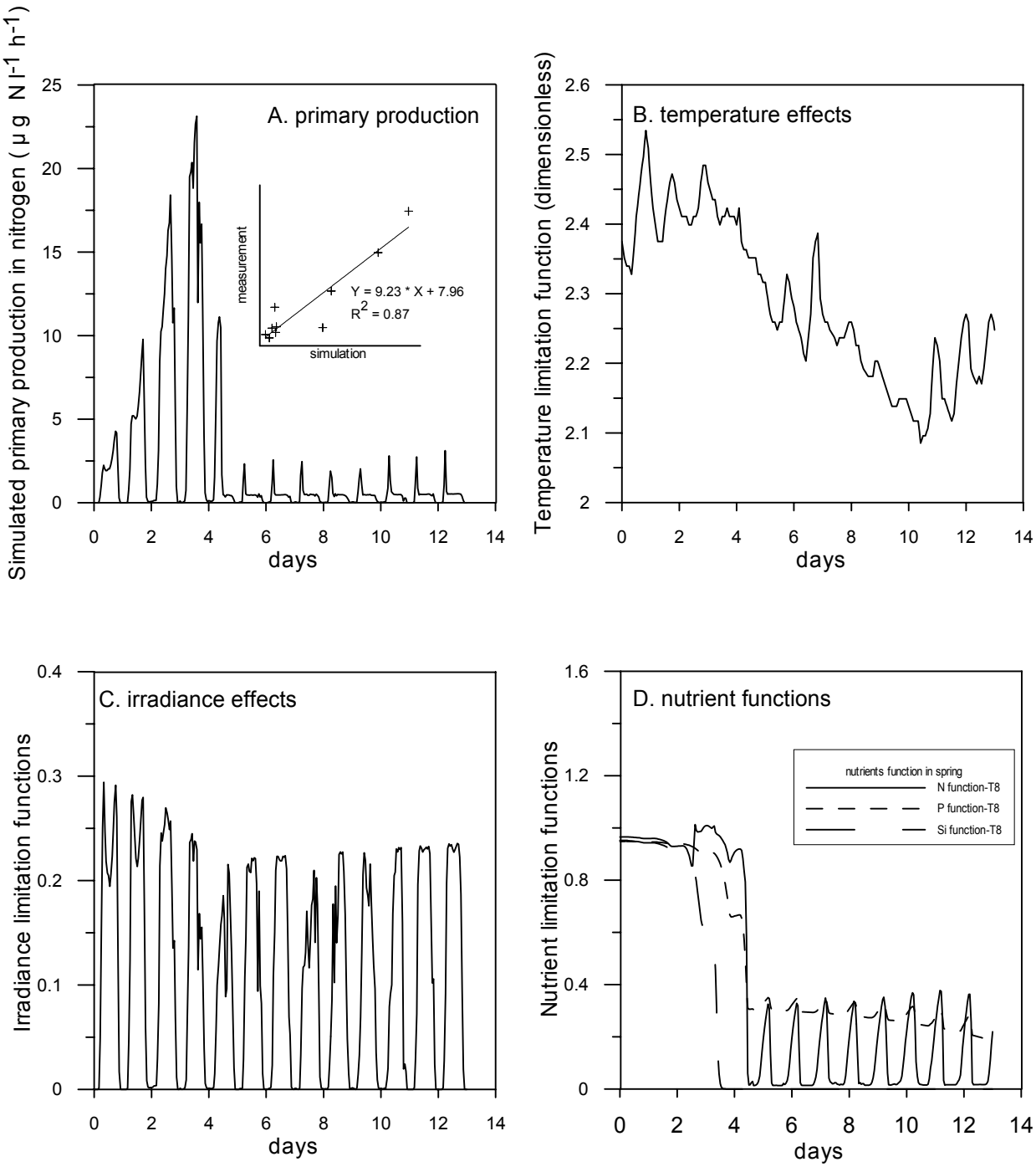

Fig. 3-35 Simulated primary production and temperature, irradiance and nutrients functions on primary production in the summer control system (T8, calculated from the model)
For the values of the nutrient limitation function, the value of 1 represents no limitation; lower values represent the increasing limitation of nutrient. The complementary plot in A shows the correlation of simulative primary production with measured primary production.

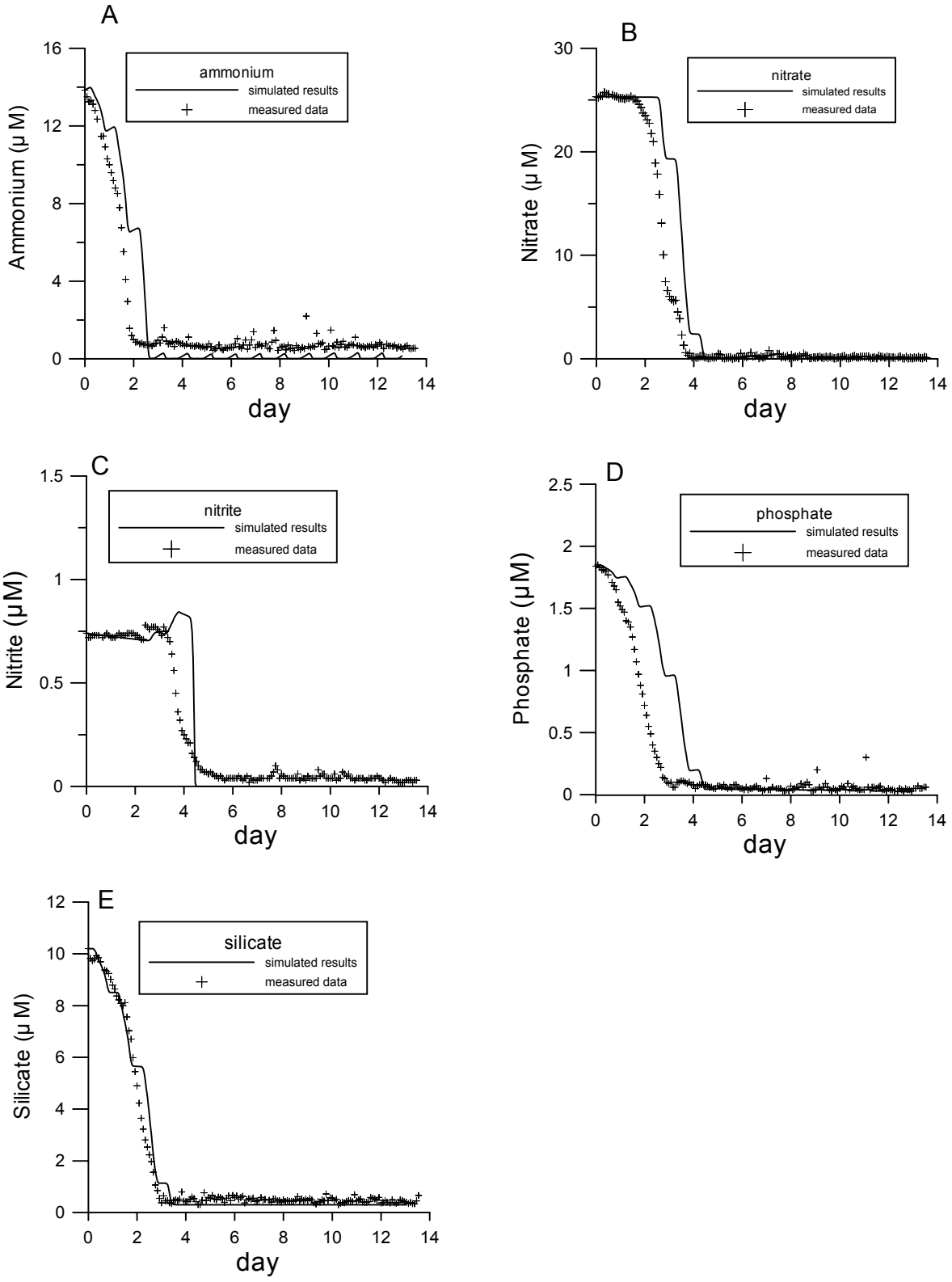

Fig. 3-36 Outputs of the main compartment simulations in the summer control system (T8, nutrients. Crosses: measurements; line: simulations)

(to be continued)

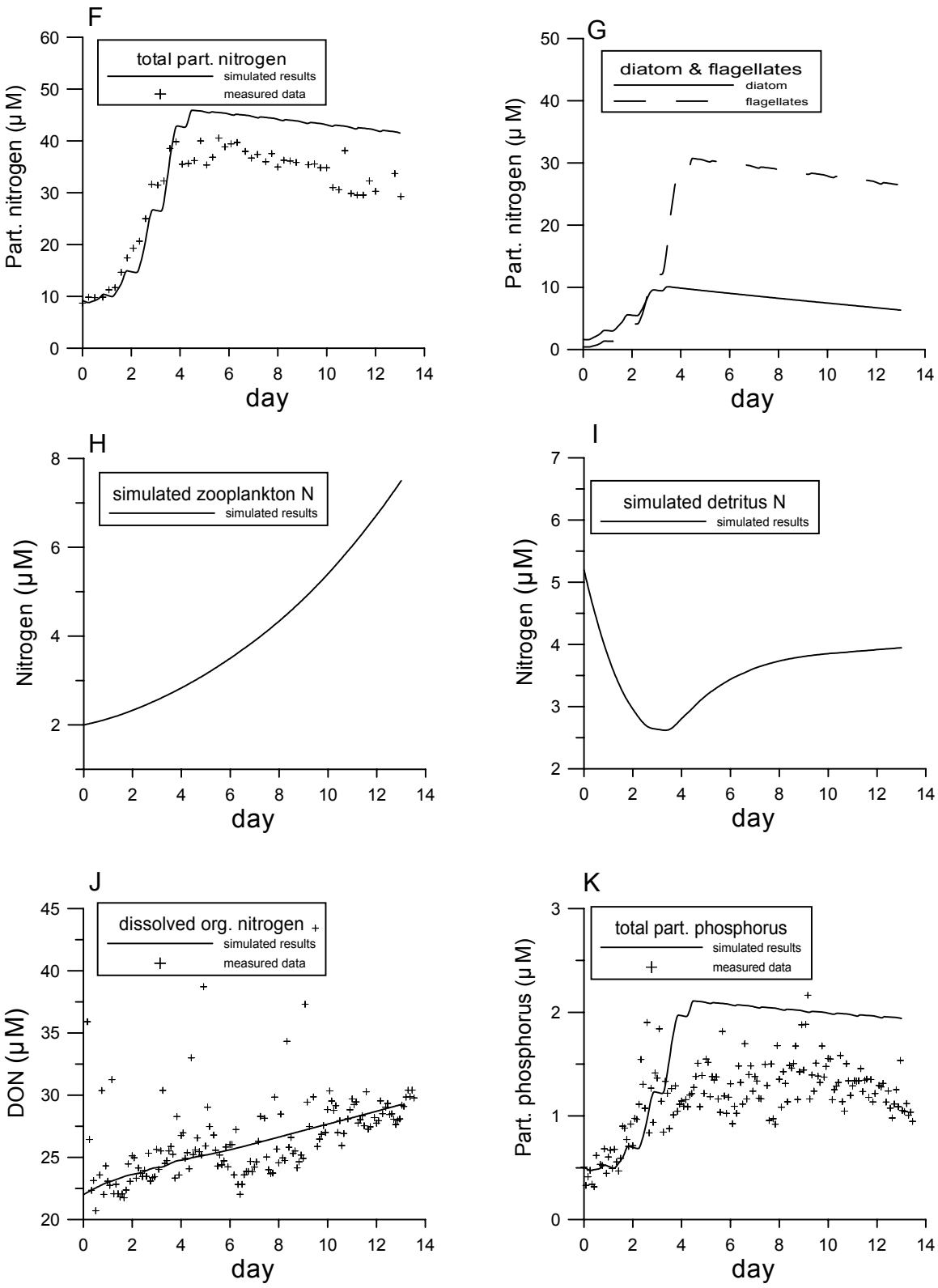

Fig. 3-36 Outputs of the main compartment simulations in the summer control system (T8, dissolved and particulate matter. Crosses: measurements; line: simulations)

Particulate matter

Simulated PN was generally consistent with the measurements (Fig. 3-36F), especially in the exponential phase, increasing fast from 9 μM to about 46 μM. However, there was about 5 to 10 μM higher in simulations than the measurements during the last 10 days.

According to the model simulation, diatoms dominated phytoplankton N during the first three days, reaching the maximum of 10 μM N. The growth of flagellates lasted 2 days longer than diatoms and dominated the phytolankton N pool with the highest of 30 μM N (Fig. 3-36G).

Simulated zooplankton N increased from 2 μM up to 7 μM at the end (Fig. 3-36H).

Simulated detritus N decreased by about 2.3 μM within the first two days, which was different with that in spring (Fig. 3-36I). Afterwards it remained at a low level of 4 μM until the end.

The model results of PP increased from 0.5 μM up to 2.1 μM during the first 4 days and decreasing by 0.2 μM within the following 9 days. The difference between simulated and measured PP during the exponential increase could be expected from the time delay in phosphate simulations. Similar to the PN simulations, the model had overestimated by 0.5 μM of PP during last 10 days (Fig. 3-36K).

3.2.2.3 Simulations of the spring experimental bag

3.2.2.3.1 Primary productivity and the control factors

In the experimental bag (T4), by the phosphate addition, the exponential increase of primary productivity was prolonged for two days and reached 23 μg N l^{-1} h^{-1} (Fig. 3-37A), corresponding to the *in situ* measured gross primary productivity of 215 μg C l^{-1} h^{-1} (Fig. G in appendix)

The temperature limitation function in the experimental bag was the same as the control bag (Fig. 3-37B). But the overall light limitation functions decreased to <0.18 during the experiment, corresponding to the continuing increase of chlorophyll *a* concentrations (Fig. 3-37C).

N limitation was quite similar to the control bag (T1). The P addition increased the phosphorus limitation function by 0.04 compared to T1. Unlike in T1, the silicate limitation function decreased near to zero in the last week, resulting from Si consumption by the higher diatom standing stock in the water column (Fig. 3-37D).

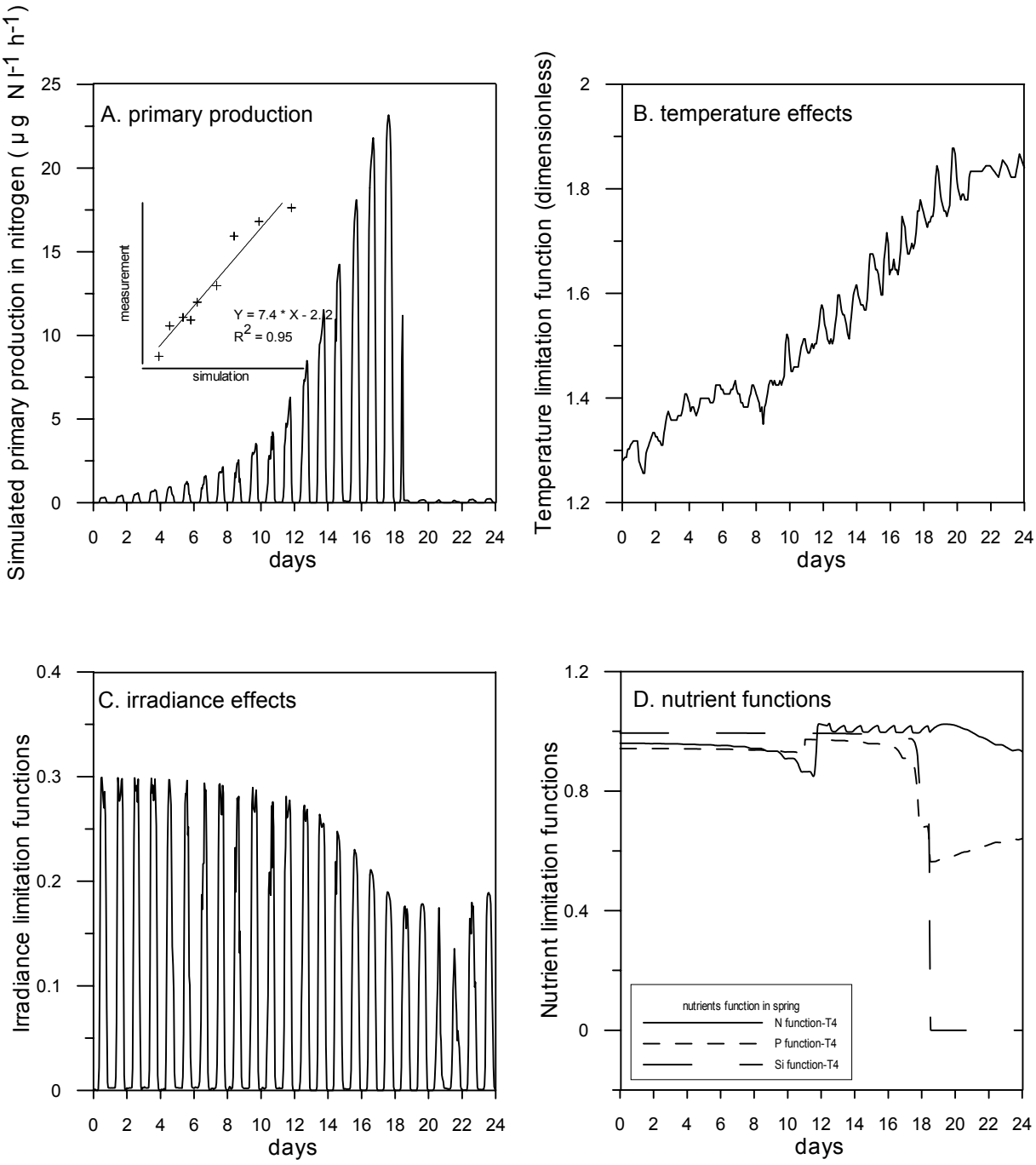

Fig. 3-37 Simulated primary production and temperature, irradiance and nutrients functions on primary production in the spring experimental system (T4, calculated from the model)
For the values of the nutrient limitation function, the value of 1 represents no limitation; lower values represent the increasing limitation of nutrient. The complementary plot in A shows the correlation of simulative primary production with measured primary production.

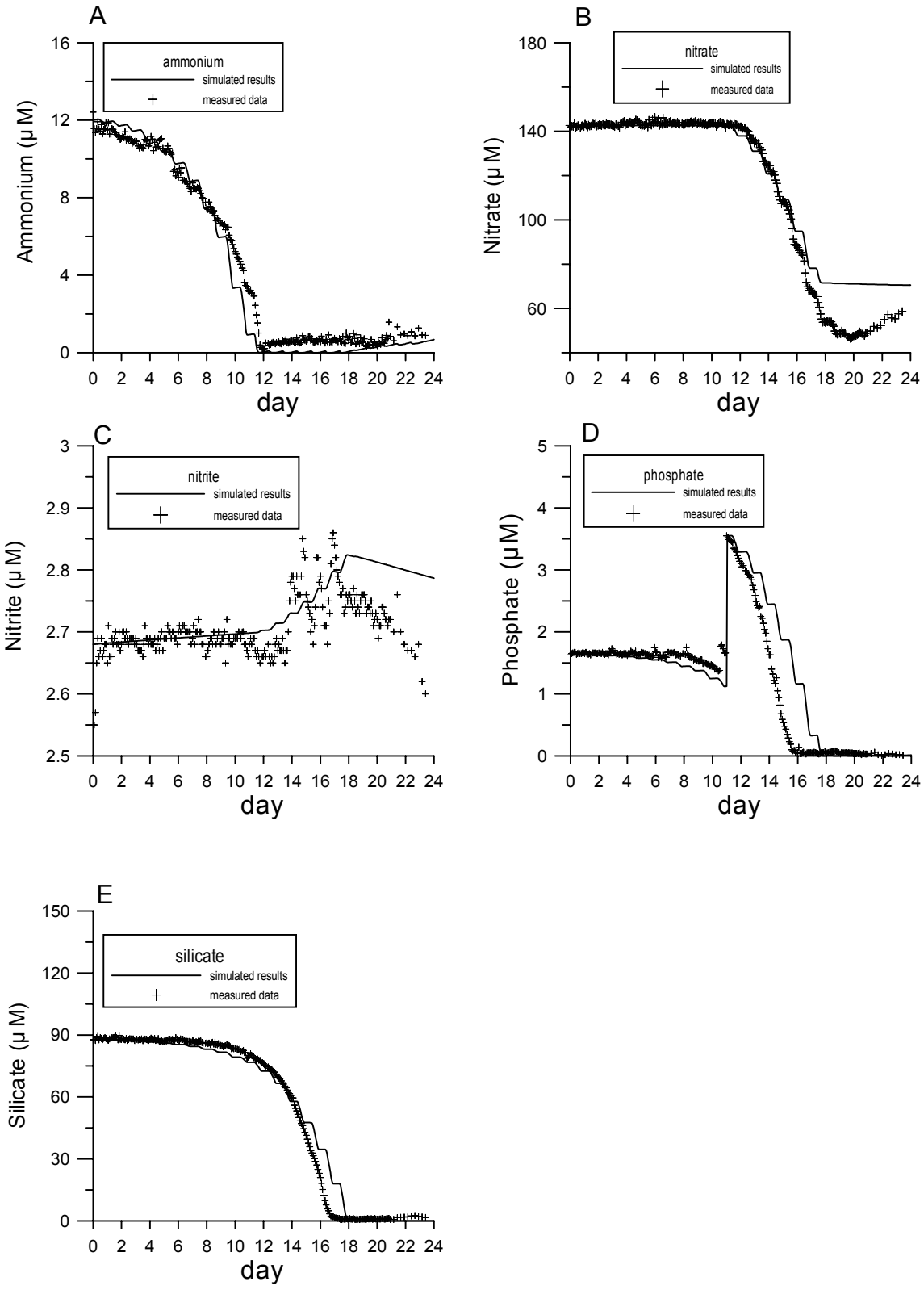

Fig. 3-38 Outputs of the main compartment simulations in the spring experimental system (T4, nutrients. Crosses: measurements; line: simulations) (to be continued)

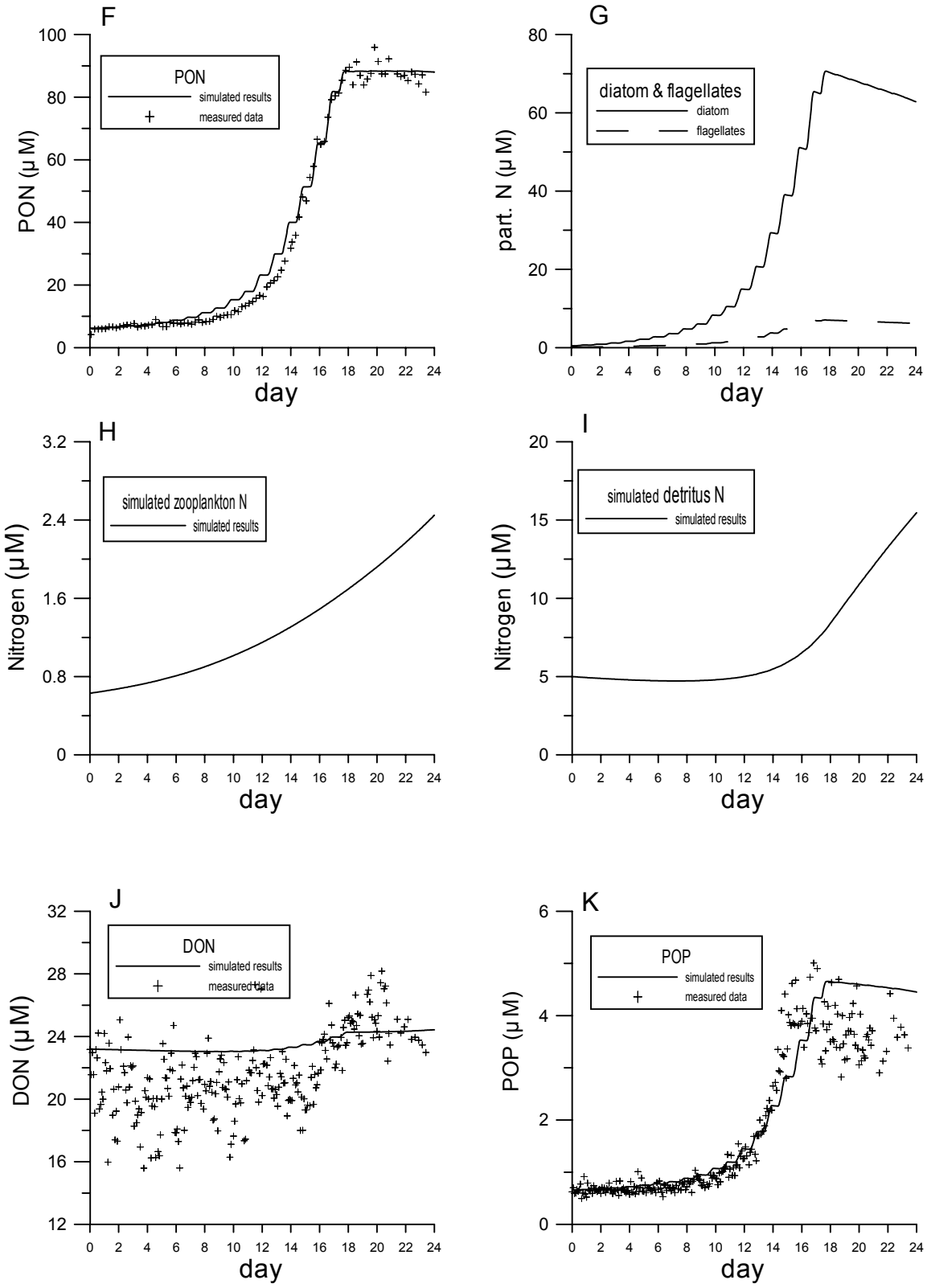

Fig. 3-38 Outputs of the main compartment simulations in the spring experimental system (T4, dissolved and particulate organic matter. Crosses: measurements; line: simulations)

3.2.2.3.2 Simulations of the main compartments

Nutrients

From the comparison of the simulated and measured data sets, it is evident that the model reproduced the main features of the development of aimed nutrients (Fig. 3-38).

Compared to T1, NO_3^- uptake lasted nearly 2 days longer and resulted in lower nitrate concentrations in the water column (Fig. 3-38B). But, as the same in T1, the depletion of phosphate in the water resulted in an earlier stop of NO_3^- uptake and NO_3^- remained at higher concentrations than the measurements. NO_2^- increased higher in the exponential phase and decreased quickly during the last 5 days (Fig. 3-38C).

Still, there was a delay of half to two days in the phosphate simulations compared to the measurements, similar to T1 (Fig. 3-38D).

The model reproduced the development of Si quite well, except the fast decrease around the day 10 and time delay around the day 16 (Fig. 3-38E).

Particulate matter

Very good coincidence for PN was reached between model simulations and the measurements (Fig. 3-38F). The exponential growth of diatoms lasted two days longer and diatom N increased by 40% compared to the control bag. The diatom bloom decayed under the Si depletion, different to the spring control system.

However, for PP, there was still a time delay of half to two days in simulations compared to the measurements. This corresponded to phosphate simulations.

3.2.2.4 Simulations of the summer experimental bag

3.2.2.4.1 Primary productivity and the control factors

The increase of simulated primary productivity in the summer experimental bag (T11) lasted 8 days longer than the control bag (T8) and reached up to 70 μg N l^{-1} h^{-1} in T11 in relation to the nutrient enrichments (Fig. 3-39A). This was comparable with the *in situ* measurements of gross primary production up to 399 μg C l^{-1} h^{-1} (Fig. H in appendix).

Temperature limitation function was the same as that in T8 (Fig. 3-39B). The light limitation functions decreased from 0.3 to 0.1, only half of that in T8 (Fig. 3-39C).

During the first 3 days, N, P and Si functions were high, similar with those in the control bag. The periodic enrichments of N, P and Si significantly increased all nutrient limitation functions. The N limitation function varied from 0 to 1 due to the restricted daily single NO_3^- additions (Fig. 3-39D). P and Si functions kept at high level of 0.9 related to high phosphate and silicate concentrations from the simulations.

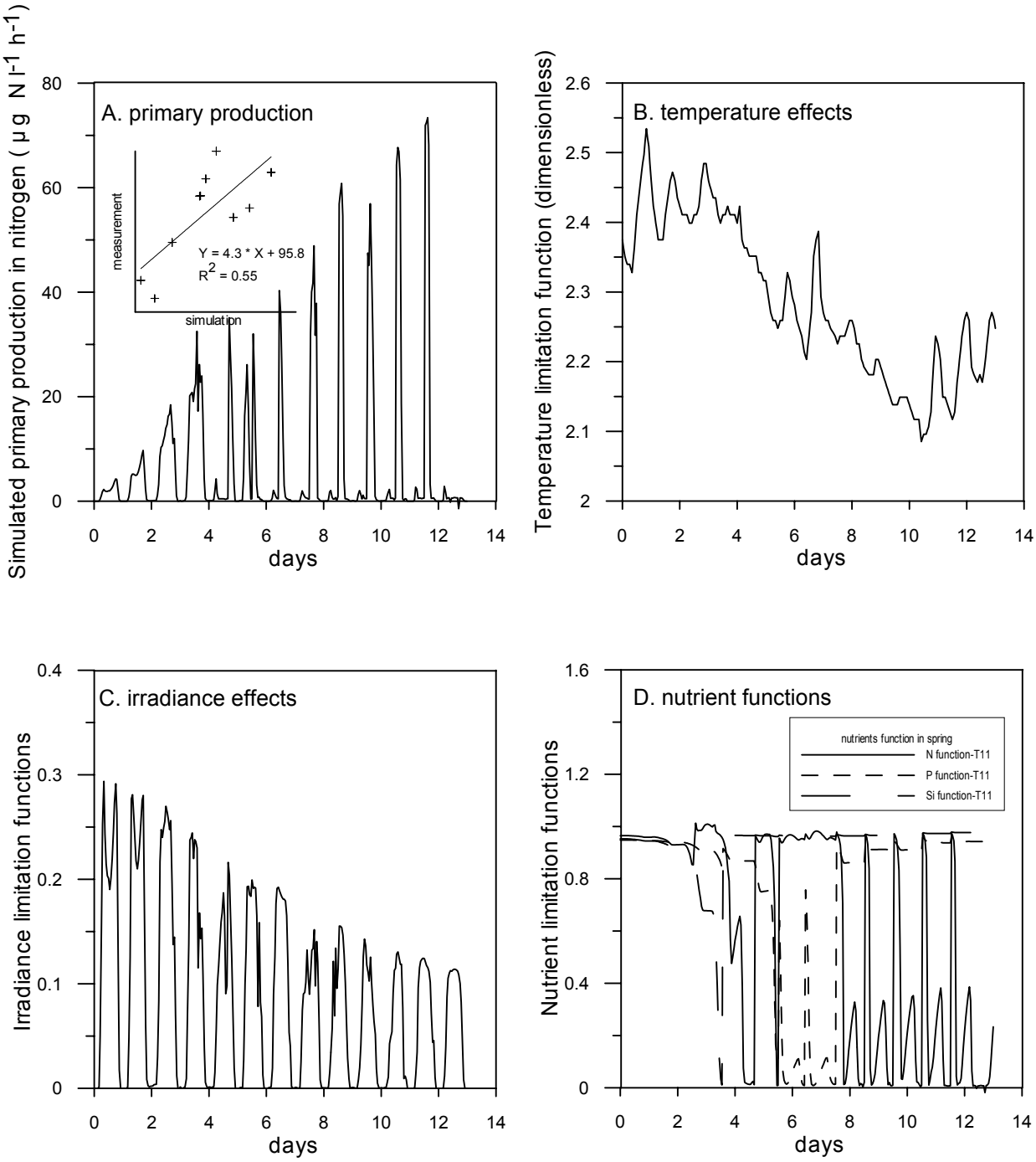

Fig. 3-39 Simulated primary production and temperature, irradiance and nutrients functions on primary production in the summer experimental system (T11, calculated from the model)

For the values of the nutrient limitation function, the value of 1 represents no limitation; lower values represent the increasing limitation of nutrient. The complementary plot in A shows the correlation of simulative primary production with measured primary production.

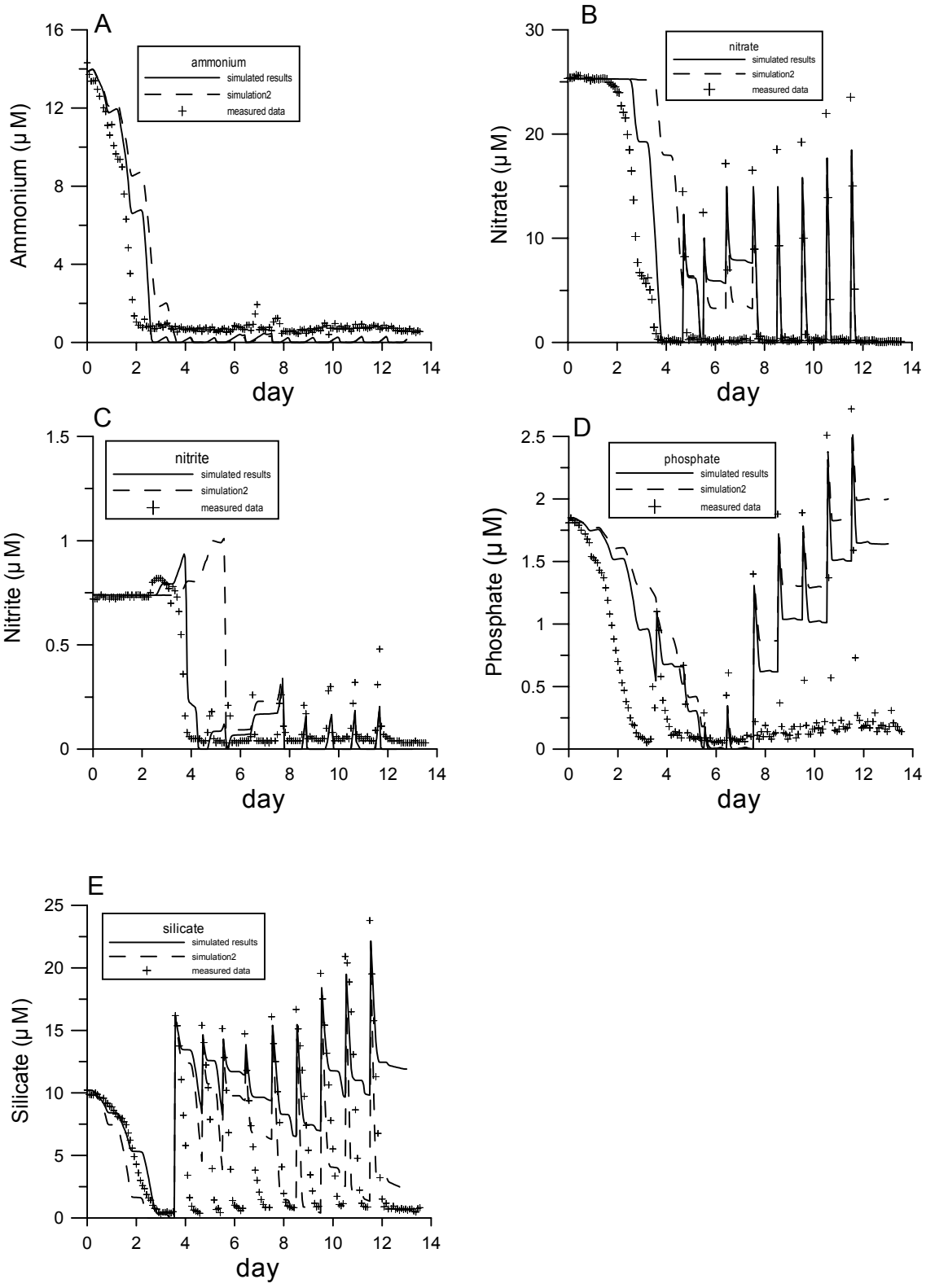

Fig. 3-40 Outputs of the main compartment simulations in the summer experimental system (T11, nutrients. Crosses: measurements; line: simulations, Simulation2 with changed max. growth rates of diatoms and flagellates, see discussion 4.3.3.1) (to be continued)

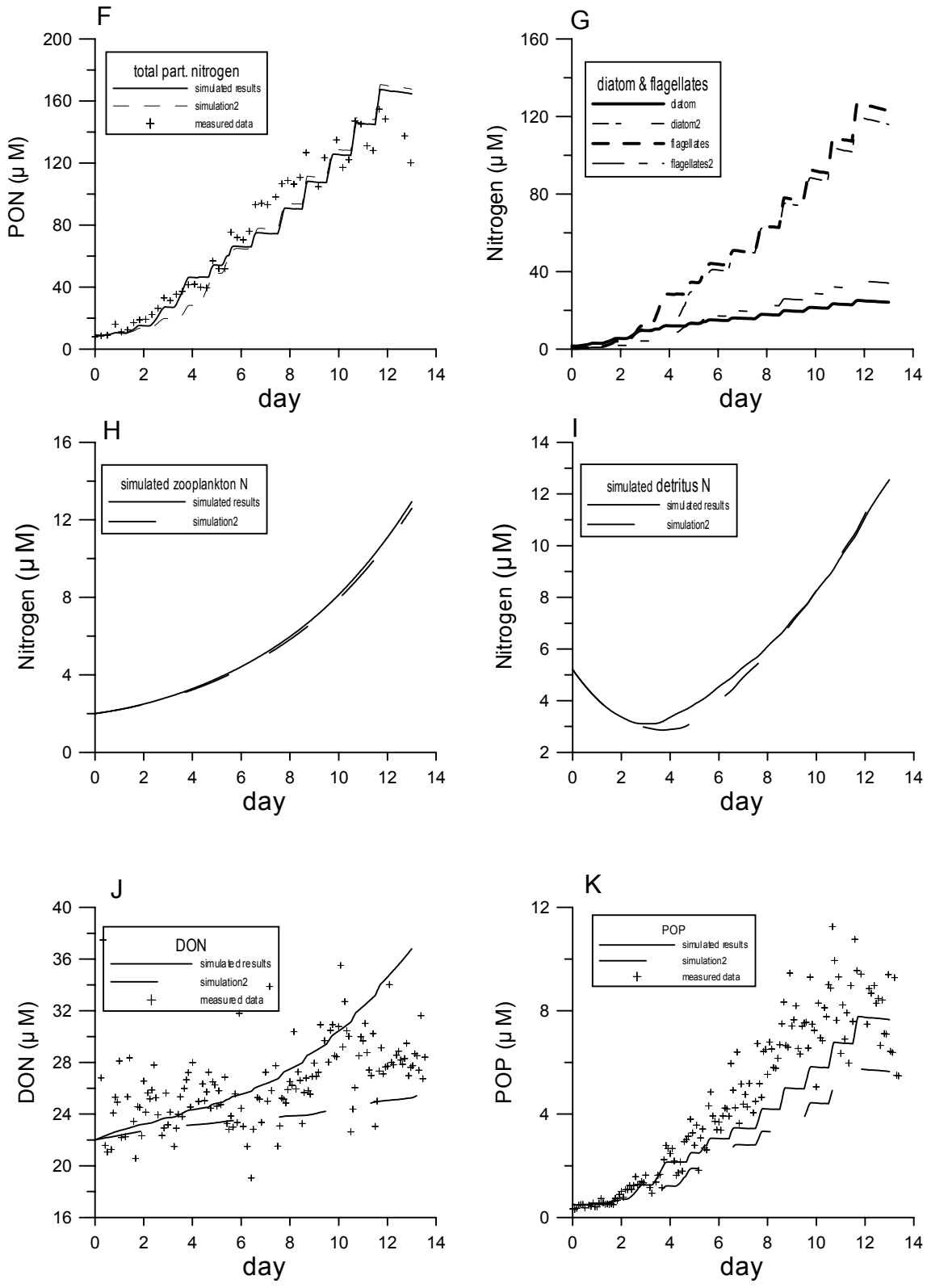

Fig. 3-40 Outputs of the main compartment simulations in the summer experimental system (T11, dissolved and particulate organic matter. Crosses: measurements; line: simulations. Simulation2 with changed max. growth rates of diatoms and flagellates, see discussion 4.3.3.1)

3.2.2.4.2 Simulations of the main compartments

The simulated results of the main compartments in the summer experimental bag were plotted together with the measurements in Fig. 3-40.

Nutrients

The development of nutrients in T11 could be separated into two phases. One was the phase during the first 4 days without nutrient manipulation; the other was the phase with nutrient manipulation. The simulation in the first phase was the same as T8 with good consistence with the measurements.

For the second phase, the model was successful to simulate the development of nitrate with great fluctuation due to the addition and fast consumption (Fig. 3-40B). Nitrite was also well simulated on its release during nitrate uptake and utilisation by phytoplankton (Fig. 3-40C). Compared to nitrate simulations, there was some under-estimation for phosphate (Fig. 3-40D) and silicate (Fig. 3-40E) in comparison to the measurements.

Particulate matter

The model successfully simulated the development of PN, which increased linearly up to 170 μM due to nutrient enrichments with significant diurnal periodicity (Fig. 3-40F). Compared to those in the control bag, diatoms and flagellates continued to growth until the end. Flagellates dominated the phytoplankton N with about 83% and diatoms covered only 17% (Fig. 3-40G).

Compared to the measurements, simulated PP had about 1 μM of under-estimation, mostly during nutrient enrichments in relation to the under-estimation of phosphate simulations (Fig. 3-40K).

3.2.3 Sensitivity analysis

3.2.3.1 Sensitivity analysis of initial values

In the model, initial values of diatom and flagellate biomass as well as zooplankton and detritus were set from estimation according to measurements and referencing ratios (section 2.4.3). Sensitivity analysis of the initial values were carried out by setting different ratios of diatoms to flagellates and zooplankton to detritus and comparing the respective outputs of the main compartments (Figs 3-41, 3-42 and 3-43, 3-44).

Generally, the development of diatom and flagellate biomass is sensitive to the initial values. In spring, lower initial values of diatoms resulted in slower growing. The integrated diatom biomass over the duration of the whole experiment (24 days) decreased by 12% compared to the standard run when the initial value decreased by 40% of that in the standard run. However, the final standing stock of diatoms kept in the same range in spite of the changed initial values. In contrast to the diatoms, the final standing stock of flagellates reached 3 to 7 times of the standard run when the initial values increased by 2 and 4 times (Fig. 3-41) and the corresponding integrated biomass increased to 2.5 and 5 times compared to the standard run.

In summer, diatoms were highly sensitive to the initial values. The highest biomass of diatoms only reached to 1/3 and 1/5 of the standard run when the initial values were 2/3 and 1/3 of the standard run (Fig. 3-43), and the integrated biomass decreased by 30% and 77%. The highest biomass of flagellates increased by 13% and 26%, with the integrated biomass increasing by 15% and 33%, when the initial values of flagellates increased by 1.5 and 3 times.

Both in spring and summer, the development of main inorganic nutrients showed similar trends, but different variations were significant during uptake duration. The silicate variation was sensitive to the initial values of diatoms.

In spring, the system did not change significantly when initial values of zooplankton varied within a limited scale of 2% of the sum of zooplankton and detritus (Fig. 3-42). However, phytoplankton growth was inhibited significantly and even completely when initial zooplankton/detritus ratio was high (1:1 and 4:1). Zooplankton growth is sensitive to its initial values. The final standing stock and integrated biomass of zooplankton reached to one sixth and 4 times respectively of those in the standard run when the initial values were set to one sixth and 4.7 times of those in the standard run. But higher initial values (9 times of the standard run) led to lower final standing stock, though at the beginning zooplankton grew faster.

The changes of initial values of zooplankton and detritus in summer did not change the development of phytoplankton and nutrients strongly except for DON (Fig. 3-44). Zooplankton growth and biomass increased with increasing initial values with the same proportion (e.g. the final standing stock and integrated biomass reached 1.7 and 2.7 times respectively, when the initial values were set to 1.7 and 2.7 times of those in the standard run).

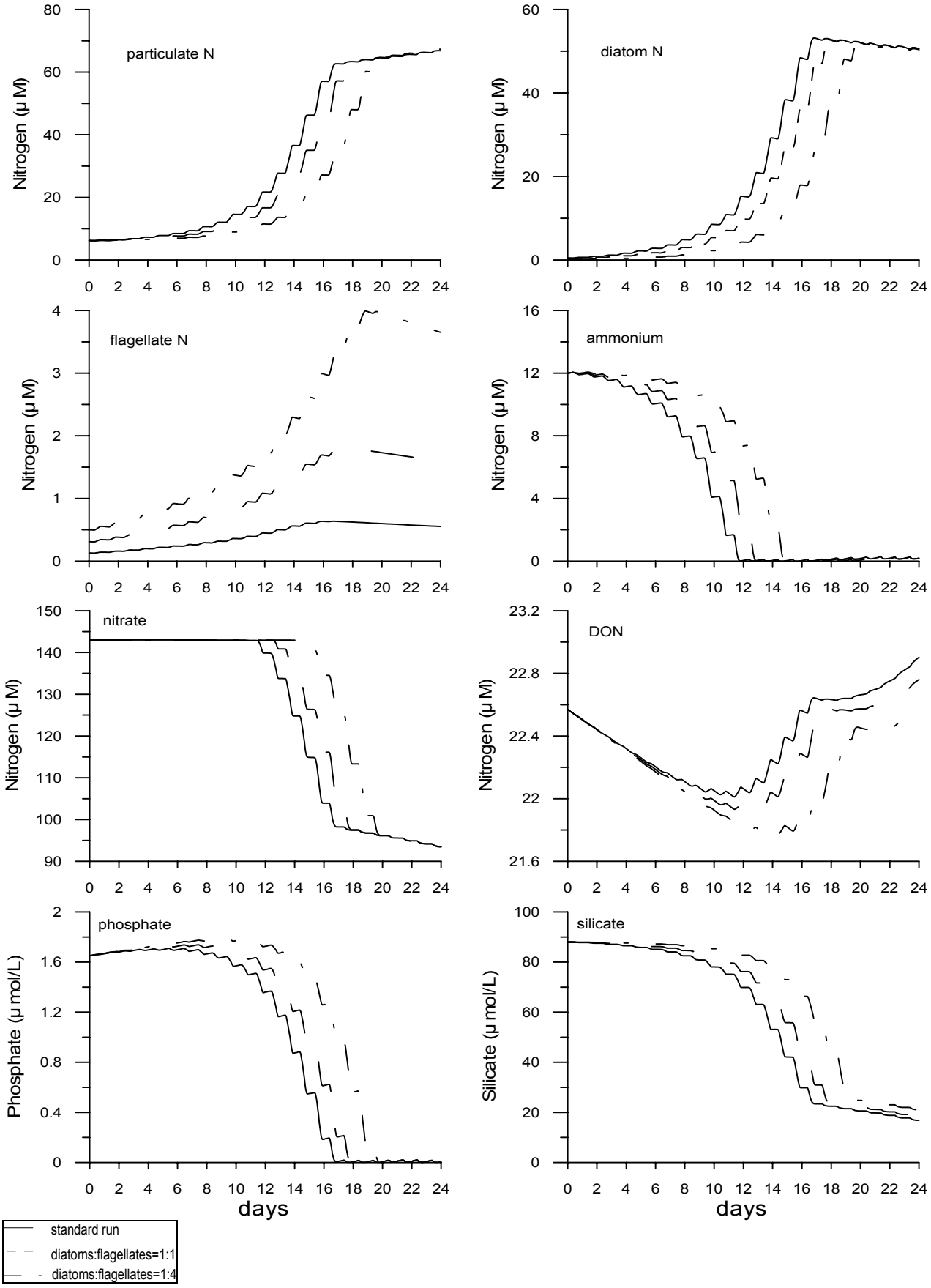

Fig. 3-41 Model outputs of some compartments to different initial values of diatoms and flagellates in spring (T1)

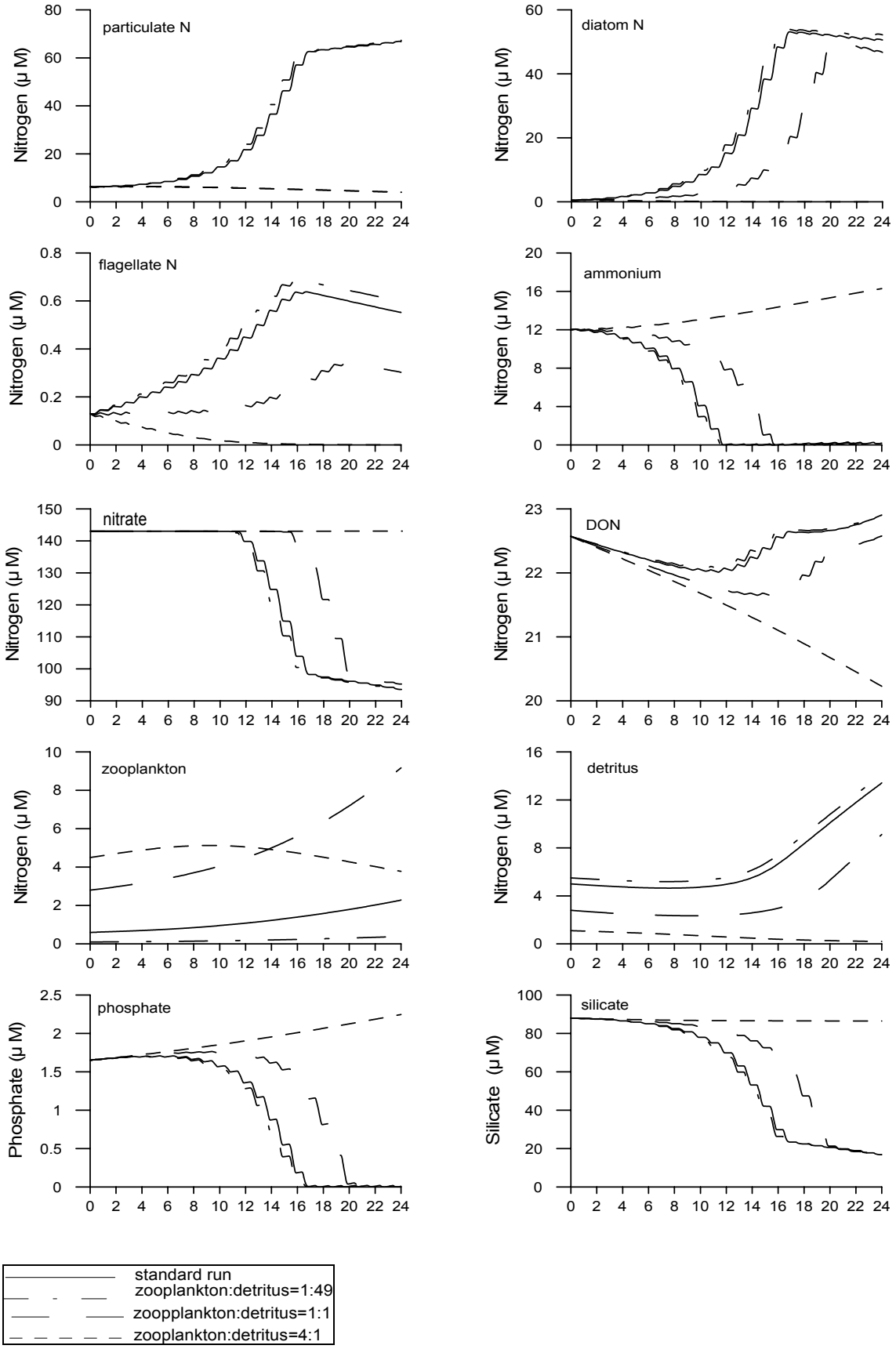

Fig. 3-42 Model outputs of some compartments to different initial values of zooplankton and detritus in spring (T1)

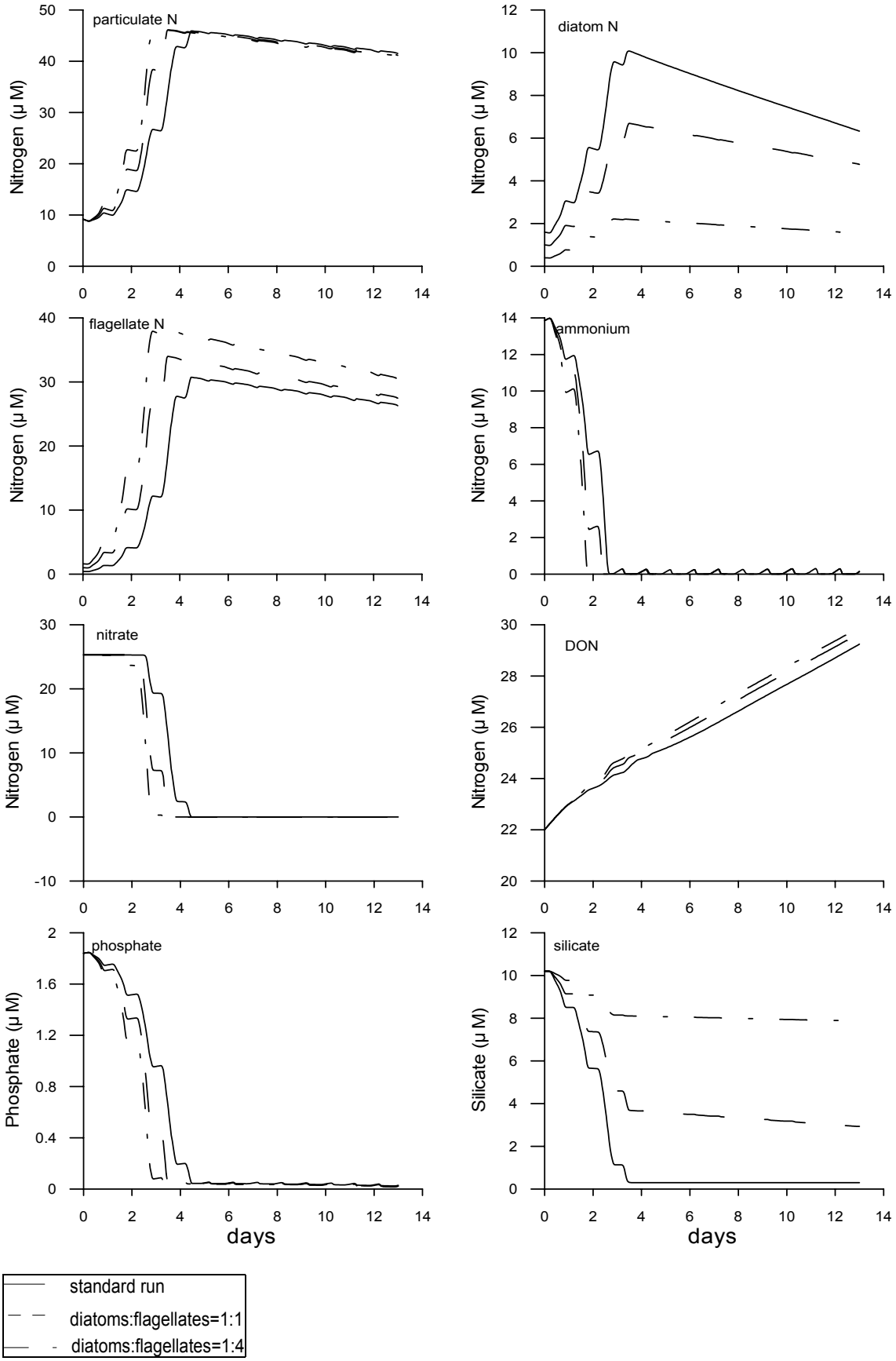

Fig. 3-43 Model outputs of some compartments to different initial values of diatoms and flagellates in summer (T8)

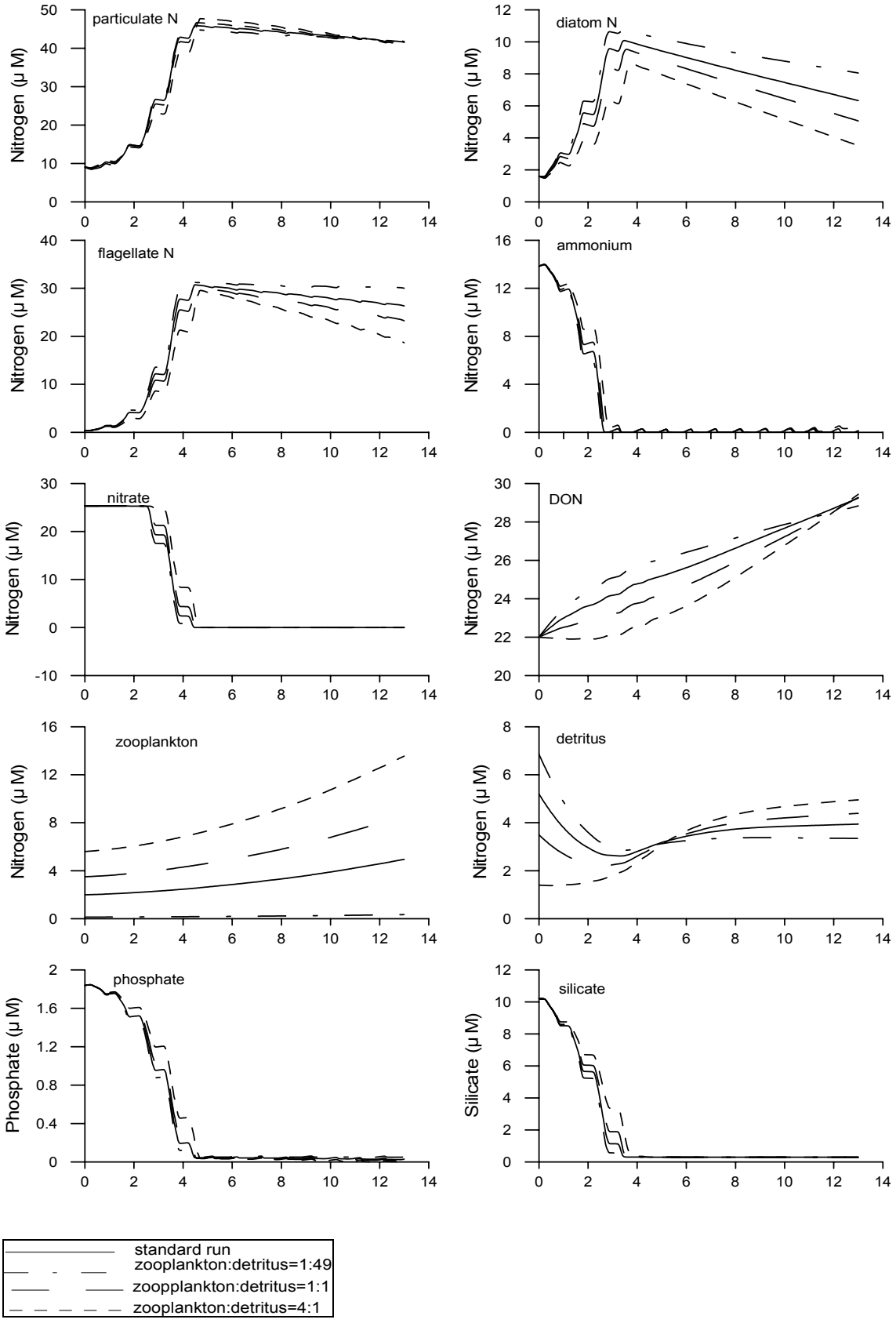

Fig. 3-44 Model outputs of some compartments to different initial values of zooplankton and detritus during summer (T8)

3.2.3.2 Sensitivity analysis of parameters

The results of parameter sensitivity analysis in spring and summer are listed in table A and B (in appendix), respectively. It was supposed that those parameters with the values of *Sp* >0.5 are very sensitive to the model output. Those between 0.2 to 0.5 are sensitive parameters and those < 0.2 are not so sensitive. The outputs of some sensitivity analysis with different *Sp* values are shown in Fig. I (in appendix) as an example.

The maximum growth rates of diatoms and flagellates (*Rdmax, Rfmax*) having a direct control on the growth of diatoms and flagellates showed very strong influences on the model outputs both in the spring and summer experiments. In spring the change of *Rdmax* and *Rfmax* strongly affected the model solutions of nutrients (NH_4^+, PO_4^{3-} and Si). High values of either parameter caused the related phytoplankton component to bloom earlier in spring and the other reduced or delayed. On the contrary, low values caused the delay of the related phytoplankton component bloom. Zooplankton and detritus were also significantly affected when these two parameters modified in the consideration of food sources.

The light extinction coefficient (K_0) was a sensitive parameter to influence the growth of diatoms and their nutrient uptake through photosynthesis especially in spring when the irradiance was somehow low.

The Michaelis-Menten limitation terms for phytoplankton growth set the differential ability of diatoms and flagellates to growth under nutrient stress. The half-saturation constants for the various nutrients have hardly noticeable effects in the phytoplankton and nutrient distributions both in spring and summer.

The ammonium and nitrate preference coefficients ($\varphi 1$ and $\varphi 2$) set the weight that ammonium and nitrate concentrations exerted over these of nitrate and nitrite uptake, respectively. The effects of changing these parameters on the phytoplankton biomass were negligible.

The ratios of P and Si to nitrogen were fixed in the nutrient uptake terms by their respective quota. In both seasons, changing the maximum allowable nutrient quotas in phytoplankton uptake drastically changed the P and Si variations.

For zooplankton, the assimilation coefficient (*b1*) and maximum grazing rate (R*gmax*) were more sensitive than others were. High grazing rate resulted in high suppression of phytoplankton growth.

4 DISCUSSION

During spring the large amounts of the discharged nutrients, being especially high during this season due to high precipitation, will be converted to biomass by the phytoplankton spring bloom, which will finally be limited by silicate depletion. The succeeding phytoplankton utilising the surplus nitrogen and phosphorus will be formed by flagellates, including harmful species like *Phaeocystis*. For this reason, the reaction potential of the hypertrophic coastal water was studied during this season. Even during early spring at calm weather conditions plankton blooms can be formed in the tidal flats as has been observed in 1996 (Brockmann et al. 1999a). During summer nutrients will be remobilised from sediments and tidal flats (Dick et al. 1999) and will enhance eutrophication effects occurring mostly during this season (Gerlach 1990). For this reason, it was important to study the reaction potential of the river plume water, spread along the shallow coast, where tides and waves keep a high load of particulate material in suspension, causing a high turbidity which limits primary production in this area. However, when this plume water, conditioned by the high loads of suspended matter, enters the clearer coastal water, production will be accelerated. Therefore, the turbid nutrient-rich plume water in the tidal flats can be seen as a short time pool for nutrients, which may be supplied to coastal production, enforcing the eutrophication, at different time scales: hours to days by tidal action; days to weeks by wind driven advection and turbulent diffusion.

4.1 Mesocosm experiments

4.1.1 Reproducibility

The reproducibility of mesocosm experiments can be detected in terms of the parallel developments in replicate bags. Generally excellent reproducibility was achieved during both spring and summer experiments, according to the correlation of most parameters in parallel bags except for nitrite, DON and turbidity (Table 4-1, Brockmann et al. 2002).

Nitrite, as a minor fraction of DIN in the water, is a very sensitive parameter from the processes of nitrification and denitrification, as well as phytoplankton release due to luxury nitrate uptake. The deviation mostly occurred during the second half of the experiment in spring and summer. Combined with bacteria increase at the same time, it is evident that nitrite was significantly involved in microbial activities.

DON as a bulk parameter, including the wide spectrum of molecular weight organic matter, showed a less significant correlation, due to its more complex generation from phytoplankton release (Myklestad 2000), zooplankton excretion, and loss during grazing, bacterial decomposition, and interaction with the particulate phase including lysis and sorption processes.

Table 4-1 Enclosure experiments in Büsum 1999, series 1 and 2: coefficient of determination, R^2

	T1 - T5	T4 - T2	T8 - T9	T8 - T10	T9 - T10	T11 - T12	T11 - T13	T12 - T13
number of datapoints	63-100	59-95	48-54	47-54	47-54	40-54	40-54	45-54
nitrate	0.9911	0.9990	0.9993	0.9952	0.9934	0.9715	0.9824	0.9673
nitrite	0.3254	0.6238	0.9965	0.9807	0.8330	0.9144	0.9320	0.9519
ammonium	0.9624	0.9986	0.9954	0.9946	0.9886	0.9912	0.9927	0.9971
phosphate	0.9956	0.9962	0.9967	0.9980	0.9963	0.8400	0.9637	0.9741
silicate	0.9972	0.9976	0.9968	0.9955	0.9963	0.8957	0.9638	0.9559
diss.inorg.nitrogen	0.9934	0.9991	0.9994	0.9968	0.9957	0.9797	0.9882	0.9777
diss.org.nitrogen	0.3849	0.5658	0.4117	0.5829	0.5829	0.5075	0.3061	0.7437
diss.org.phosphorus	0.7986	0.7729	0.8088	0.6138	0.6138	0.8883	0.6472	0.8285
dry weight	0.6709	0.7282	0.4331	0.1508	0.2599	0.5537	0.3806	0.4247
turbidity	0.1801	0.7001	0.3428	0.5797	0.1655	0.9413	0.9606	0.9540
part. nitrogen	0.9624	0.9917	0.8786	no data T10	no data T10	0.9480	no data T13	no data T13
part. carbon	0.9712	0.9809	0.9572	no data T10	no data T10	0.9637	no data T13	no data T13
part.carbohydrates	0.9749	0.9591	0.9153	0.9403	0.8672	0.9122	0.9415	0.9580
part.phosphorus	0.9213	0.9362	0.2484	0.3156	0.6743	0.8022	0.7713	0.8469
pH	0.9200	0.9721	0.9143	0.8980	0.8301	0.9718	0.9796	0.9943
Turner - fluorescence	0.9200	0.9981	0.9508	0.9787	0.9747	0.9718	0.9664	0.9809
1Hz-chlorophyll	0.9131	0.9815	0.4871	0.9145	0.6706	0.9761	0.9758	0.9916
1Hz-transmission	0.5045	0.6349	0.0149	0.6920	0.0991	0.9702	0.9720	0.9895

Turbidity was controlled by plankton growth as well as by the artificially created turbulence pulses. This enhances the formation of patches of particulate material of which the variability in the open water is also higher than that of the dissolved constituents.

Particulate organic compounds also showed significant correlations during spring and summer. The reason is that the concentration of biomass was mainly controlled by the plankton growth and that other factors were of second order. During summer, particulate phosphorus showed a less significant correlation between the replicates. However, the deviations were mainly caused by higher individual variability than by systematic differences.

Very good reproducibility thus can be concluded from the mesocosm experiments. This high reproducibility of natural ecosystems indicates that the enclosed systems were not significantly contaminated from the surrounding harbour water and represented independent systems.

4.1.2 Representativity

The representativity or field validation of mesocosm experiments can be demonstrated via (i) comparing the mesocosm results with the key parameter concentrations and changes in the natural system during the experiment considering the variability of the open system; (ii) comparing the experimental results with process data from field studies to prove causal relationships and predictive capability, as shown for some mesocosm experiments (Takahashi et al. 1975, Oviatt 1984).

The comparison with the harbour water allows a comparison of concentrations and their changes,

besides a control of possible contamination of the exposed fragile systems. Since the shallow (4 to 6 m) harbour was frequently flushed by tides (3.2 m tidal level), the harbour water was also representative for the water masses passing the coastal area. This was proven by some stations and transect measurements offshore (Brockmann and Topcu 2001). Changes in the harbour water mostly reflect modified gradients, passing this area because of the short residence time.

In spring, the temperature in the bags increased consistently as that in the harbour over the experiment indicating complete heat exchange between bags and surrounding natural water mass (Fig. 3-1). Since tidal flats dominate the coast off the harbour, it can be assumed that during the whole period with dominating westerly winds, river plume water was moving along the coastal line keeping the salinity mostly below 21 PSU. Gradual increase over the time indicated a decrease of river discharge. The natural variation of turbidity was high, which can be expected in relation to tide movements, and it remained in the same range as in the bags by artificial mixing.

Starting conditions regarding the nutrients were identical to those in the harbour. NH_4^+ in the harbour fluctuated above 5 µM due to events like sediment effluxes in the outdoor tidal flats from remineralisation and decreased due to utilisation by bacteria (nitrification) and phytoplankton. The decrease of ammonium after 01/04 might indicate the diatom growth in a patch in the open water passing the harbour, combined with decreases of nitrate, phosphate and Si, and increase of chlorophyll *a* during the same time (Fig. 3-2). Nitrate and Si remained constant for a long period of 14 days at the same level as the initial values. Slight increase of phosphate was detected probably due to P release in estuary areas (Brockmann et al. 1994). Nitrite concentrations increased over the time, indicating on-going nitrification processes with the temperature increasing.

Comparison of chl*a* concentrations in the mesocosm system with the harbour water, revealed that the starting points of chl*a* development were quite similar, which implies identical triggering factors. No significant bloom was detected in the harbour resulting from the frequent water exchange with deeper turbid areas. It is assumed that the light climate in the whole spring duration was not sufficient enough to trigger a widespread bloom in the adjacent open water including the harbour. Turbidity behaved mostly similar in the open system as in the bags, larger variation resulted from resuspension of particulate matter from sediment surface due to regular (tides) and occasional (wind forces) turbulence and the shallow water.

In summer, the development of water temperature measured in the bags was consistent with that in the harbour (Fig. 3-6). Higher salinity compared to spring resulted from lower freshwater discharge of the Elbe. Some fluctuations in the harbour indicated advection of different water masses.

The initial concentrations of nutrients as well as chlorophyll *a* were identical with those in the harbour (Fig. 3-7). The conditions in the plastic bags were comparable with the situation in the stratified river plume, also containing high nutrient concentrations but providing a stable light climate in the mixed layer, as has been studied in the Elbe river plume during drift experiments (Brockmann et al. 1999b). The developments in the plastic bags corresponded to those in stratified

coastal waters. Light climate (in the catched water masses, exposed at the surface), together with sufficient nutrients, enabled a net primary production in the mesocosms within a few days, leading to nutrient depletion. In the harbour, no detectable phytoplankton bloom developed and chlorophyll concentrations remained quite low. All main nutrients thus were kept at high concentrations. In open system, strong vertical mixing including deep tidal channels in the coastal water prevented the formation of phytoplankton bloom by severe light limitation in spite of similar transmission in the harbour and at the outer buoy station with that in the enclosures.

Since, NH_4^+, PO_4^{3-} and Si were higher in the harbour water than at the outer buoy station, a release from the sediment and an export to the coastal water was indicated. The release of phosphorus from the Wadden Sea during summer due to exhausted storage capacity of the surface sediments has been discussed (Dick et al. 1999, Pohlmann et al. 1998, van Beusekom et al. 1998). Contrarily, nitrate was higher at the outer station than in the harbour, indicating adsorption by anoxic sediment surfaces, being frequently eroded by tidal currents. Generally the concentrations in the open water and in the enclosures remained in the same magnitude. The gradients of most nutrients reflected the influence of the river plume in the open water, as well as local processes.

Due to the fact that the plastic bags were floating, the mixing depths were reduced to the upper few meters, keeping the phytoplankton permanently within the euphotic zone. This was not the case in the turbid open waters, where the tidal action mixed the water column, causing light limitation from high turbidity.

4.1.3 Nutrient uptake in enclosed ecosystems

4.1.3.1 Uptake ratio

Spring experiment

Since in both the control and experimental bags (T1 and T4), the decrease of N/P ratios (ΔDIN/ΔP) during ammonium uptake (25 and 29 by atoms) were higher than that during nitrate uptake (15 and 19 by atoms) (Table 3-1), it can be assumed that ammonium was partly utilized by nitrification. Though total bacteria biomass was at a low level that time, nitrifying bacteria could take high proportion of the total bacteria community and converted ammonium to nitrate even at low temperature. However, the contribution of the process to nitrate pool was not detectable due to extremely high nitrate concentrations in the Elbe River plume. On the other hand, high ΔNH4/ΔP could also imply a competition of bacteria to ammonium uptake (Wheeler and Kirchman 1986). The bacteria uptake of NH_4^+ could occur even at low bacterial abundance during a rich phytoplankton bloom (Tupas et al. 1994). Though preference of DFAA for bacteria over ammonium was documented (Middelburg and Nieuwenhuize 2000), the simultaneous uptake of NH_4^+ and DFAA could still happen because DFAA concentration was low in the spring enclosures (<1.5 µM, fig. 3-3C) (Goldman and Dennett 2000). This could be deduced from the similar trends of development of ammonium and DFAA. At sufficient N (or ammonium) concentrations, N/P ratio of bacteria could reach as high as 25 (Chrzanowski and Kyle 1996), which is closed to the calculated ΔNH4/ΔP

removal ratio, implying the optimum uptake of bacteria.

However, the high significance (R^2=0.94) of the correlation between chlorophyll and ammonium during the period of ammonium uptake (Fig. 3-11, A-1; Fig. 3-13, A-1) indicates the dominance of ammonium uptake by phytoplankton. Phytoplankton uptake could also cause a higher ΔNH4/ΔP ratio, because marine phytoplankton is able to take up NH_4^+ for short period of time (seconds to minutes) at rates far in excess of that required to balance growth (McCarthy and Goldman 1979; Glibert and Goldman 1981, Goldman and Glibert 1982, Parslow et al. 1984a, 1985, Zehr et al. 1988). This ability was found to be greatly enhanced at low relative growth rates (Goldman and Glibert 1982) and also at low temperature, when phytoplankton N uptake relies more on ammonium at low temperature because ammonium uptake is much less temperature dependent than nitrate uptake (Reay et al. 1999).

This combination of all these conditions were found during the beginning of the spring experiment.

The nitrate decrease in relation to phosphate decrease (ΔNO3/ΔP) were close to the Redfield ratio (Redfield 1958) (Table 3-1), indicating the utilisation of both nutrients by phytoplankton, because nitrate uptake lasted during the whole exponential growth phase both in T1 and T4 and nutrient decreases fitted well (R^2: 0.98 and 0.95 for nitrate, 0.92 and 0.89 for phosphate) with the biomass increase, which was significantly correlated (R^2=0.99) with the chlorophyll increase (Fig. 3-12, B-2; Fig. 3-14, B-2).

ΔPOC/ΔPN increase ratio in the two bags were quite close to Redfield ratio as well (6.7 and 7.7 in T1; 8.1 and 6.9 in T4. Table 3-1), indicating neither carbon nor nitrogen limited phytoplankton growth. Slight difference between the periods of NH_4^+ uptake and NO_3^- uptake may reflect changing species composition of phytoplankton community in these two phases (Fig. A, B).

Compared to ΔPOC/ΔPN, ΔPN/ΔPP was more variable as indicated by lower R^2 (Fig. 3-12; Fig. 3-14). All calculated ΔPN/ΔPP are higher than 16, indicating that phytoplankton growth were under P limitation (Redfield 1958, Goldman 1980). In T4, PO_4^{3-} addition decreased P limitation as was reflected by much lower ΔPN/ΔPP of 23 compared to that in T1. In both bags, P limitation became more severe with phytoplankton growth due to higher biomass accumulation. Cellular phosphorus contents decreased, resulting in an increase of ΔPN/ΔPP during the transition from ammonium uptake phase to nitrate uptake phase. Because the enclosures were nitrate rich, it is assumed that average phosphorus cell quota for NO_3^- uptake decreased by 1.5 times in comparison to the NH_4^+ uptake phase.

ΔNO3/ΔSi, close to 1, indicated a typical diatom bloom in the two bags, because diatoms utilise nitrate and silicate with a ratios of 1 as documented from field investigations and laboratory experiments (Brzezinski 1985, Dugdale and Wilkerson 1998, Dunne et al. 1999). A little higher ΔNH4/ΔSi resulted than ΔNO3/ΔSi from the same processes as supposed for higher ΔNH4/ΔP ratio.

During the whole experiment, significant correlations of silicate with nitrogen and phosphate (r^2=0.99, 0.95, respectively) indicated that diatoms dominated the phytoplankton assemblage in the

spring enclosures and converted the largest portion of DIN to PN. In T1, the ammonium removal to chl*a* increase ratio (ΔDIN/Δchl*a)* was quite comparable to PN increase (ΔPN/Δchl*a)* (Fig. 3-11 A-1; Fig. 3-12 A-1)*,* indicating a complete conversion from DIN to PN production. In T4, lower ΔPN/Δchl*a* ratio compared to ΔDIN/Δchl*a* might be related to P addition. Excretion and release might have occurred while nutrient addition manipulating. During NO_3^- uptake, lower ratios in (ΔPN/Δchl*a)* compared to (ΔDIN/Δchl*a)* in both bags indicate that 14% to 16% of NO_3^- taken up by phytoplankton, were probably returned to the water column. This fraction of N, released by phytoplankton cells as mostly dissolved organic nitrogen (DFAA), which has been observed also during blooms (Brockmann et al. 1983b, 1992, Bronk et al. 1994, 1999, Raimbault et al. 2000).

Summer experiment

In summer, correlations (R^2: 0.6 to 0.87) of chlorophyll *a* with all nutrients (Fig. 3-15; Fig. 3-16) indicate that nutrient uptake by phytoplankton was dominating process in the enclosures. However, fast increase of free and attached bacteria and their high activity (Dürselen 2002) also influenced the change of nutrients not only by remineralisation processes (Chrzanowski and Kyle 1996), but also by utilisation, competing with phytoplankton (Danovaro 1998, Middelburg and Nieuwenhuize 2000). Because the small size of most of the bacteria and high temperature, these processes are supposed to be very patchy. This was also reflected by more scattering in the correlation curves and lower significance of correlations compared to spring.

Compared to spring, the decrease ratio of ΔDIN/ΔP were much lower during both NH_4^+ and NO_3^- uptake phases in both bags, in the range of 10 to 13, which is lower than Redfield ratio (Table 3-1). Low ΔNH4/ΔP indicates fast turnover of ammonium because ammonium can directly regenerated from zooplankton excretion (Parsons et al. 1984), detritus dissolution and DON remineralisation related to bacteria (Koike et al. 1982) and will be take up immediately after release. At high temperature, these processes will be accelerated. Low ΔNO3/ΔP than in spring could indicate strong nitrification processes in the water column, contracting to the nitrate uptake in summer due to high temperature and more abundant nitrifying bacteria. This could have been detected during NH_4^+ uptake phase, however, this fraction of ammonium might have been replenished by the fast regenerated ammonium.

Lower ΔDIN/ΔP ratio could also be a result from bacterial utilisation of phosphorus, using for N organic sources. Compared to spring, ammonium and nitrate were much lower and the competition of N utilisation became stronger. In this case, bacteria were revealed to have much greater potential to adjust their cell N/P composition ($Q_{N:P}$) to low as 8 (Chrzanowski and Kyle 1996), implying that they are likely to uptake nitrogen and phosphorus with such low ratio.

High removed NH_4^+/Si ratio as well as NO_3^-/Si (up to 2, Table 3-1) probably resulted from the Si production of thinner cell walls by summer species. It also indicates competition for nitrogen sources by flagellates. Compared to spring, if those ratios are referred to the spring experiment, it implies that only 38% of ammonium in T8 and 56% of ammonium in T11, and 34% of nitrate in both

bags were taken up by diatoms.

Low ΔPOC/ΔPN (5.8 to 6.4) indicates high N utilisation and conversion to phytoplankton biomass. It was also a result from high respiration of the planktonic community due to high temperature.

ΔPN/ΔPP ratio in both bags of the summer experiment varied in a large scale (45 to 90, Table 3-1). Higher ratios compared to spring indicate severe P limitation. Considering low ΔDIN/ΔP removal ratios, high ΔPN/ΔPP indicates fast turnover of particulate phosphorus to dissolved organic phosphorus by release and excretion (Benitez-Nelson and Buesseler 1999).

In T11, during the nutrient additions, the correlations of PN with PC and PP were highly significant and consistent during this phase with ΔPOC/ΔPN of 6.8 and ΔPN/ΔPP of 17, close to the Redfield ratio (Fig. 3-16), in spite of the different ratios of added NO_3^-: PO_4^{3-}: Si (Table 4-2). It indicates that the fertilized nutrients were mostly converted to phytoplankton biomass with maximum assimilation rates rather than to bacteria, as documented by other authors (Goldman and Dennett 2001).

Compared to spring, the differences between DIN removal and PN biosynthesis, in terms of the ratios of ΔDIN/Δchl*a* and ΔPN/Δchl*a* (Table 3-1), were found not only during nitrate uptake but also ammonium uptake. This indicates that DON release could have occurred during ammonium uptake because the exponential phytoplankton production started bloom from the beginning of the experiments. It also implies that some bacteria, which completely kept on the filters used for PN analyses, but were transferred to the DON pool.

4.1.3.2 Interactions of the uptake of different N nutrients

4.1.3.2.1 Ammonium inhibition of nitrate uptake

It is shown both from the spring and summer experiments that ammonium was the most preferential N nutrient for phytoplankton growth and it inhibited NO_3^- uptake though the initial concentrations of nitrate was higher than those of ammonium by 12 times in spring and 2 times in summer. This reflects the fact that among all available inorganic forms of N sources, NH_4^+ is the most preferential for a natural phytoplankton assemblage (Dugdale and Georing 1967, McCarthy 1981, Wheeler and Kokkinakis 1990). The mechanism of NH_4^+ inhibition of NO_3^- uptake was studied in laboratory experiments by Syrett (1981) who assumed that inhibition of membrane transport of NO_3^-, inhibition of NO_3^- reductase, and repression of NO_3^- reductase synthesis are involved. However, the exact concentration at which the inhibition occurs is still of disputation and may be different for different species and their preconditioning (Dortch 1990). Eppley et al. (1969) pointed out that the synthesis of nitrate reductase is inhibited by the presence of ammonium at concentrations between 0.5 to 1 μM. McCarthy (1981) and Wheeler and Kokkinakis (1990) also suggested that nearly complete inhibition of NO_3^- assimilation occurred at NH_4^+ concentrations of around 1 μM or even lower in the open sea. However, some authors argued that a complete inhibition rarely happened, since there is co-uptake of ammonium and nitrate instead of complete inhibition (Dortch 1990, 1991, Yin et al. 1998, Lomas and Glibert 1999).

The stagnation of nitrate shows that NH_4^+ with concentration higher than 3.0 µM completely inhibited NO_3^- uptake (Fig. 3-11 and Fig. 3-13). NO_3^- was taken up simultaneously afterwards until ammonium concentrations were depleted below 1.0 µM. Ammonium concentrations finally remained around 0.8 to 1.0 µM for a long time both in spring and summer. It resulted from the balance of remineralisation and utilisation, because ammonium turnover time was several hours (Kanda et al. 1990). From the spring experiment, turnover time of 10 hrs could be detected when ammonium concentrations remained lower than 0.3 µM, before it increased to more than 0.6 µM (Fig. 3-2A). This was not the case in summer. Much faster turnover due to higher temperature kept ammonium at around 1.0 µM. Ammonium regeneration rate can reach a magnitude of 1.52 µM m^{-2} d^{-1} (Parsons and Harrison 1983). If this value was referenced, it could be assumed that regenerated ammonium was used by growing phytoplankton even at higher nitrate concentrations as in spring. This assumption was supported by calculated NH_4^+ limitation from the model simulation (Fig. 4-4).

Thus, it can be concluded that complete inhibition of NO_3^- uptake could happen when ammonium concentration was higher than 3.0 µM. Threshold of NH_4^+ uptake is proven to be about 1.0 µM. When NH_4^+ concentrations are in the range of 1.0 to 3.0 µM, co-uptake occurs by natural phytoplankton assemblages (Ren et al. 2002b).

The possible explanation for the different findings of ammonium inhibition (Eppley 1969, McCathy 1981, Dortch 1991) is that preference and inhibition of ammonium varies with species and various environmental conditions, such as light intensity and temperature. Lower temperature, especially lower light intensity at the beginning of the spring experiments also inhibited nitrate uptake of algae because nitrate uptake is mostly light-dependent (Malone et al. 1975, Varela and Harrison 1999). It was found by Lomas and Glibert (1999) that diatoms had higher inhibition half-saturation than flagellates for both uptake and assimilation under changing temperature. Complete inhibition could be defined for one certain species under controlled condition during lab experiments (Eppley 1969, Syrett 1981). But, for the natural assemblage of phytoplankton, it is difficult to ascertain a general threshold. It was pointed out that at the enzymatic level, the inhibitory mechanism of NO_3^- assimilation is similar among species, but at the cell level, may be regulated by species-specific differences in the accumulation of internal metabolic pools and pathways (Lomas and Glibert 1999).

Parallel nitrate and ammonium uptake could happen especially during summer, when ammonium was produced but not increasing in its concentrations. This point has been reflected from the model simulations (Fig. 4-4).

4.1.3.2.2 Nitrite release and utilisation by phytoplankton

Nitrite release during luxury nitrate uptake by phytoplankton has been reported from previous experimental studies (Anderson and Roels 1981, Collos 1982, Raimbault 1986) and in field observations (French et al. 1983, Collos 1998). It is due to the limitation of nitrite reduction in phytoplankton cells. The transient accumulation of nitrite in the free water during the growth of alga on nitrate has been documented especially for diatoms. In cultures of *Thalassiosira pseudonana*,

Prorocentrum minimum and *Skeletonema costatum*, it can represent up to 25, 45 and 50% of nitrate uptake, respectively.

Nitrite production is coupled to the nitrate uptake and it is apparently stimulated by light, and may be accelerated by nitrate uptake (Wada and Hattori 1991). From the spring experiments, it can be seen that nitrite fluctuated nearly diurnal in relation to nitrate concentrations (Fig. 4-1), indicating a dominance of nitrite release during the nitrate uptake at daytime. Nitrite release reached about 1% of nitrate uptake according to the slope of the correlation. At night slower nitrate uptake, coupled with carbohydrate dissimilation, resulted to minor nitrite release. Consequently nitrite decreased with decreasing nitrate due to the dominance of denitrification during the night reduced always kept until late morning (10:00), whereas, diatom release dominated in the afternoon.

Nitrite is an alternative N source for phytoplankton growth when nitrate concentrations drop below 1.0 µM, as identified from mono species incubations (Collos 1982, Raimbault 1986). In spring this process was totally missed because the system was nitrate-rich during the whole experiment. In summer nitrite uptake was evident in both the control and experimental bags (T8 and T11), occurring on day 4 after nitrate was depleted to about 1 µM. Moreover, during the periodic NO_3^- enrichments in experimental systems, dominating NO_2^- release in the morning and NO_2^- uptake after NO_3^- depletion in the afternoon could be observed, in spite of the fast turnover. These processes increased with growing phytoplankton biomass (Fig. 3-7B, C). Thus, our results clearly showed the pattern of alternative uptake of different N forms under nearly natural conditions.

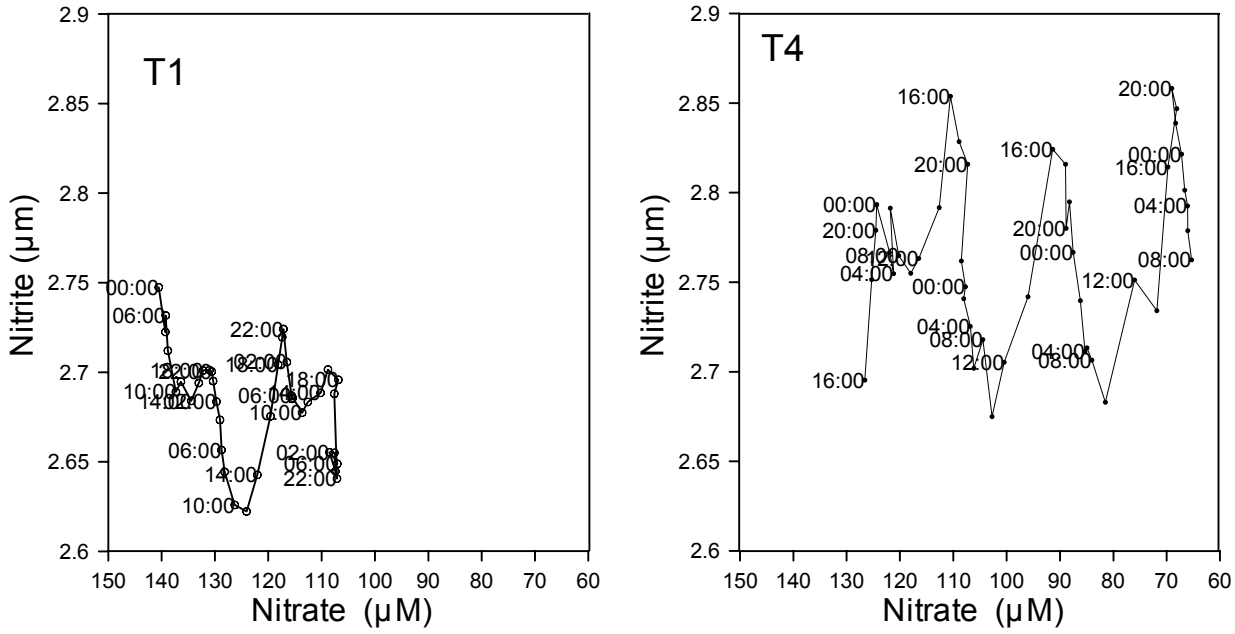

Fig. 4-1 Correlation between nitrate and nitrite during nitrate uptake in the spring experiment (note that the labels of X-axis descend in both plots)

4.1.3.3 DON dynamics

DON, which contains various kinds of substances from small molecules like urea and amino acids up to higher molecules like peptides and proteins, plays a key role in N cycling in the marine environment and seasonally it may replace inorganic nutrients in the N-budget (Butler et al. 1979). DON variation is related not only to biological activities by phytoplankton, zooplankton and bacteria but also controlled by physico-chemical sorption-desorption processes, controlling the phase transfer between detritus and dissolved compounds. 'Concentrations of DOM at a distinct time only represent the steady state of different compounds in the complex marine ecosystem under the given conditions' (Brockmann et al. 1983b).

Both in spring and summer, DON showed similar concentrations (20 to 30 µM) as from the field investigations (Brockmann et al. 1998), indicating that most of DON in the inner German Bight is refractory (Brockmann et al. 1994). Except for a slight increase observed during the spring (T1 and T4) and summer (T8 and T11) experiments (Fig. 3-3B, Fig. 3-8B), DON remained at equilibrium between the processes of production and loss during most of the experiments.

DON can be formed by detritus dissolution and partial decomposition related to bacterial activity and exoenzymes. This could account for a large amount of DON production especially in summer due to higher bacteria biomass and their increased activity at higher temperature (Bronk and Ward 1999).

Another path of DON production is release by phytoplankton cells. This DON release is demonstrated to occur not only under the nutrient depletion (Sharp 1977) but also during the exponential growth phase (Mague et al. 1980, Fogg 1983a,b, Brockmann et al. 1983b, 1992, Hammer et al. 1981, 1983, Myklestad 2000). It is shown that 'in oceanic, coastal and estuarine environments, an average of 25 to 41% of dissolved inorganic nitrogen (NH_4^+ and NO_3^-) taken up by phytoplankton is released as dissolved organic nitrogen (DON)' (Bronk et al. 1994). It is evident that the amount of released DOM could be higher during a phytoplankton bloom than in its stationary phase (Myklestad 2000). Cellular release of DON during phytoplankton growth may have significantly contributed to the observed increase of 5 µM during spring (Fig. 3-3B). However, in summer, this process had minor effects in the enclosed water masses because of the short growth phase and high bacteria biomass. A slight increase of DON occurred during the last days (Fig. 3-8B), indicating decomposition related to microbial activity because of the increase of some free bacteria as well as high biomass of attached bacteria (Dürselen 2002).

Increased release during nutrient limitation (P depletion in spring and all nutrients during summer) may mainly concern carbohydrates, which will be synthesized for some days during nutrient depletion as had been observed by Ittekkot et al. (1981). This situation was simulated in T11 by slower increase of total dissolved carbohydrates and the lower maximum concentration in T11 than in T8 (Fig. J in appendix) (Starke et al. 2002).

DON production from zooplankton excretion accounts for e.g. urea, which can be utilized easily by

the phytoplankton (Bidigare 1983). Zooplankton was found only at a low level during the spring and summer experiments (Meng et al. 2002). Thus, it was assumed that the contribution of zooplankton excretion to the DON pool was of minor importance.

Besides bacteria utilising DON (Billen et al. 1990), also phytoplankton was found to utilise DON, e.g. urea and free amino acids (DFAA), as N source for growth in some areas when the available DIN is exhausted (Eppley et al. 1971, Carpenter et al. 1972, Paul 1983). This could only occur during summer, when DIN was frequently exhausted. However, the small fluctuations of DON did not show any relationship to N-depletion.

To some extent, these processes of DON production and utilisation are related more to low molecular DON forms within a short period (Brockmann et al. 1983b, 1992, Hammer et al. 1981, 1983). Thus, DFAA could be a more sensitive parameter to trace phytoplankton release of nitrogen compounds and bacteria utilisation.

Due to the high DIN during spring, uptake of DFAA by phytoplankton cells can be neglected at that season. However, during summer, when DIN was exhausted, DON, as well as DFAA became a potential N source for phytoplankton growth (Paul 1983, Bronk and Glibert 1993, Maestrini et al. 1999).

Both in spring and summer experiments, DFAA covered only a minor fraction of DON (about 2 to 6% in spring and 2 to 10% in summer).

In spring, faster decrease of DFAA between 25/03 and 27/03 at rates of 0.2 µM d^{-1} than the former days (0.03 µM d^{-1}) (Fig. 3-3C) was related to the fast increase of bacteria at that time (Dürselen 2002), indicating that DFAA was utilized preferably by bacteria. Afterwards, with the start of exponential growth of phytoplankton, DON including DFAA was released as has been observed before (Brockmann et al. 1983b, Hammer et al. 1981, 1983) and supplied a major source of DON for bacteria (Billen et al. 1990). For this reason, in spite of high bacteria biomass at the same time, slight increase of DFAA was detected. Bacteria utilisation and decrease of cell release during the stagnating phytoplankton development (Myklestad 2000) resulted in DFAA stagnation at 0.7 µM.

In summer, continuous decrease of DFAA during the first 2 days indicated the fast utilisation by bacteria in the bags (Dürselen 2002). The following stagnation of DFAA in both T8 and T11 until the end of the experiments (Fig. 3-8C) indicates a steady state of DFAA between bacteria utilisation and production by growing algae and lysis of dying algae due to nutrient limitation. As DON increased slightly during the experiment (Fig. 3-8B), it can be deduced that produced DON was mainly of polymeric organic matter (Billen et al. 1990), with longer turnover time. At last, in both control and experimental bags, DFAA reached the balanced concentration of 0.5 µM to 0.8 µM, which is quite comparable to the spring experiments as well as the field data from summer investigation in German Bight (Baraniok 1994), indicating a possible threshold DFAA for pelagic bacteria utilisation.

4.1.3.4 Effects of nutrient enrichments

The continental coastal water of the North Sea receives a number of nutrient inputs from several large rivers, which are anthropogenically influenced. Increased nutrient inputs had caused the increase of algae biomass, a decrease in diatoms during late summer in coastal areas (Hickel et al. 1995), the formation of harmful blooms and accumulation of organic material in the bottom water of stratified areas may cause oxygen depletion (Gerlach 1990, Zevenboom 1994). Especially the effects and fates of nitrogen and phosphorus discharged by the Elbe River into the German Bight is of importance for the understanding of phasing of discharges and eutrophication effects.

Various mesocosm experiments (Jacobsen et al. 1995, Escaravage et al. 1996**,** Schlüter 1998, Egge and Jacobsen 1997, Rick 1999) and field investigations (Raabe et al. 1997, Brockmann and Kattner 1997, Brockmann et al. 1999a, 1999b) have been conducted to study the effects of nutrient discharges on species composition and growth rate of phytoplankton communities, as well as the succeeding reactions in the coastal ecosystem. Primary production in response to nutrient fertilisation or reduction have been intensively studied especially during the last 10 years (Jacobsen et al. 1995, Taylor et al. 1995, Escaravage et al. 1996, Egge and Jacobsen, 1997, Schlüter 1998, Sϕndergaard et al. 2000). Recently the contribution of the tidal flats surrounding the German Bight, which was the experimental site for this investigation, have been investigated because here suspended organic matter discharged by the rivers or synthesised in the coastal water from discharged nutrients is trapped seasonally or for longer time periods (Postma 1984). The remineralised nutrients will be remobilised during summer mostly (Dick et al. 1999). One main question was to which degree nutrients are utilized in the shallow turbid coastal water in the tidal flats. For this reason the reaction potential was studied in enclosed water columns, to which nutrients were added, simulating remobilisation from the sediment (Brockmann et al. 2002).

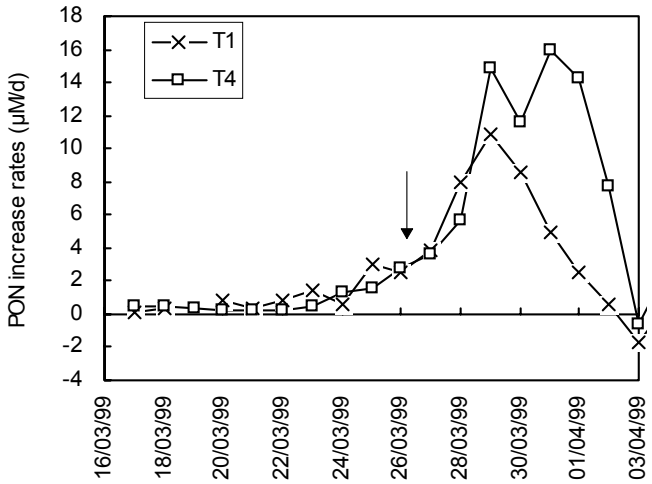

Fig. 4-2

Daily increase rates of particulate organic nitrogen in the spring experiment (T1 & T4, arrow: phosphate addition.)

The effects of nutrient enrichments in the experiments varied with different initial phytoplankton composition and nutrition conditions (Mozetic et al. 1997). In the spring experiments, P addition resulted in significant increase of phytoplankton biomass due to imbalanced nutrient discharges by the river Elbe which contains higher nitrate loads, caused especially during spring by high freshwater discharges (ARGE 1999) resulting in a N/P ratio of about 80. Compared to the control

bags, biomass of phytoplankton after P addition reached 160% of chlorophyll *a*, 130% of PC, 155% of PN and 210% of PP at the end of the exponential growth (Fig. 3-4). It can be assumed that phosphorus will limit the reaction potential of Elbe River plume water in the early spring bloom and in the German Bight as suggested by Philippart and Cadèe (2000). Increase of phosphorus input will significantly lead to a prolonged diatom growth and a higher standing stock, furthermore to silicate exhaustion, which at last leads to an earlier out-burst of dinoflagellates and harmful algae such as *Phaeocystis*. Since the phytoplankton uptake rates (Fig. 3-17) and biomass increase rates (Fig. 4-2) did not show significant differences from the control bags, it is assumed that there was only a quantitative but no qualitative effect during spring. Only with a lag of 3 days, the increase rate in the fertilised bags exceeded that in the control bags.

In the summer experimental bag, nitrate, phosphate and silicate were added after several hours starvation as described in section 3.1.3.2. During the transient depletion of nutrients, phytoplankton was supposed to continue its growth for a certain period, however, which will lead to decrease of cell quota finally (Parslow et al. 1984b). The reduction of cell quota will result in high nutrient uptake capacity of cells (Droop 1968). It has been verified from the batch cultures of marine diatom *Thalassiosira pseudonana* by Parslow et al. (1984a, 1984b), that the specific uptake rates of nutrient depleted cells could reach several times higher values than the maximum uptake rates. The increase of nutrient uptake rates after nutrient addition from our experiment were not as much as those from culture experiments. Compared to mono-cultures, the responses of natural phytoplankton communities to fluctuating nutrient addition were influenced by more complicated extrinsic factors, such as incidental temperature and light conditions as well as physiological factors of various species because nutrient addition might only fertilise some specific species (Dunstan and Tenore 1974).

The ratios of N:P:Si varied in the experimental bags from 40:1:30 to 8:1:6 during the second half of the manipulation (Table 4-2), indicating that the enclosed systems changed from P limitation to N limitation. Increased P addition resulted in lower PN/PP ratio compared to the beginning, being close to 15 (Fig. 3-9D). In spite of variable NO_3^-/PO_4^{3-} ratios, no significant scattering in short-term variation of PN/PP was detected additionally compared to that in the first 4 days, which suggests the uncoupling of general nutrient uptake and assimilation. The supplementary NO_3^- and PO_4^{3-}, taken up fast by phytoplankton were most probably stored in the cells for periods of several hrs as inorganic form (Dortch 1982) and served as nitrogen and phosphorus supply for photosynthesis when the extracellular NO_3^- and PO_4^{3-} concentrations were exhausted. However, bacteria utilise nutrients (Wheeler and Kirchman 1986, Fuhrman et al. 1988, Horrigan et al. 1988, Lebo 1991, Groenlund et al. 1996) and at least for phosphate sorption by the walls of the plastic bags should also be considered.

The maximum chlorophyll contents of the experimental bags were at the end of the exponential growth 6 times higher than in the control bags. The maximum POC, PN and PP in manipulated bags were 200%, 300% and 500% of that in the control bags (Fig. 3-9). Lower increase in POM pool

compared to chlorophyll increase indicates low percentage of phytoplankton in the total particulate matter in the water column. In the summer experiment, higher initial amount of enclosed zooplankton with higher activity and growth rate caused higher grazing pressure to phytoplankton than in spring. On the other hand, bacteria, mostly attached to detritus also contributed to the fraction of the POM pool. It is expectable that the total POM pool did not increase as much as phytoplankton (which was determined by chlorophyll).

Compared to spring, the much lower increase in percentage of POC to chlorophyll can be attributed to lower ΔPOC/Δchl*a* in summer, according to the calculations from the correlation of chlorophyll a with POC (Fig. 3-12, 3-14, 3-15 and 3-16).

Large variations in ΔPOC/Δchl*a* were detected from spring (120 to 435, by weights) in comparison to summer (25 to 38, by weights, Table 3-1). In spring, ΔPOC/Δchl*a* of 120 reflected mostly the high activity of phytoplankton during its exponential growth (NO_3^- uptake phase). However, the calculated ΔPOC/Δchl*a* not only reflects the activity of phytoplankton cells but also is interfered by co-varying processes, such as phytoplankton cell release, bacteria turnover, detritus decomposition and formation e.g. by flocculation as well as by zooplankton production in the same water mass (Banse 1976). Carbon is usually lost from the cells as carbohydrates (Brockmann et al. 1979, Ittekkot et al. 1981), which led to higher carbohydrate concentration in the water column during decomposition phase in the control bags. Because particulate C is more related to the degradation processes, lower ΔPOC/Δchl*a* in summer, compared to spring, indicates the faster decomposition of particulate C especially concerning detritus, which covered up to 55% of total particulate matter at the beginning of the experiment (from microscopic observation, Dürselen, personal communication). The decomposition could have been fastened in the experimental bag due to higher bacteria biomass, because both free bacteria (rods) and algae attached bacteria increased by a factor of 3 and 8, respectively in the main control bag (T8) in comparison to the experimental bag (T11) (Dürselen 2002). At the same time, zooplankton may have taken a very important role in converting POC to DOC and CO_2 by excretion and respiration.

Table 4-2 Nutrient additions to the bags of sequence D in the summer experiment. (N: nitrate; P: phosphate; Si: silicate)

Time of adding	04/06 06:00	04/06 10:00	05/06 12:00	06/06 08:00	07/06 07:30	07/06 09:30	08/06 07:30	09/06 07:30	10/06 07:30	11/06 07:30	12/06 07:30
N:P:Si	only P	P:Si=1:15	30:1:30	20:1:30	40:1:30	only P	10:1:8	10:1:8	10:1:10	8:1:6	8:1:8

Similarly, the different increases in percentage of PN and PP are also supposed to correspond to respective turnover processes between the particulate and dissolved pools.

Assimilated nitrogen can be released from phytoplankton cells as DON and ammonium under rapid increase of irradiance (Lomas et al. 2000). Phytoplankton was found to contribute as much as

zooplankton to the DON turnover (Parsons and Harrison 1983, Hasegawa et al. 2000). However, phosphorus is mostly recycled by zooplankton excretion and its release from phytoplankton is of less importance compared to nitrogen (Parsons et al. 1984). Thus, it is deduced that flux from PP to DOP might be low due to low biomass of zooplankton (see section 3.2.2.2).

It was shown that 78% of totally added N and 61% of totally added P was converted to particulate matter compounds. Lower assimilation of phosphorus compared to nitrogen indicated another path of P being removed from the water column, in addition to biological utilisation by microalgae attached to the plastic material (polyethylene) of the bag.

The smoothed linearly increase of PN and PP (Fig. 3-9) indicated that the added nutrients were mostly consumed for the biomass increase. It was observed microscopically that the cell volumes of the dominant phytoplankton increased in the manipulated bags in comparison to the control bags (Dürselen et al. 2002b). It is likely that through this increased cell volume the biomass increased without changes of relative growth rate (Hein and Riemann 1995).

4.1.4 Fate of N, loss from the water column

In spring, N loss was found to occur mostly when nitrate was the main N source for phytoplankton. Imbalance between nitrate uptake and phytoplankton production has been observed from field investigations and various experiments (Raimbault et al. 2000). It was shown that the differences between nitrate decrease and particulate nitrogen (phytoplankton) increase were higher than the overall N loss in both the control and experimental systems (8% and 11% in T1 and T4, respectively). This indicated that the nitrate taken up was converted additional to PON to other N forms such as DON and NO_2^- via phytoplankton cell releases (Bronk et al. 1994, 1999, Raimbault 1986, Collos 1998). However, DON was found to increase by only 2% of total N during nitrate uptake in the spring experiment (Fig. 3-21), accounting for a minor fraction of N loss as suggested by Raimbault et al. (2000). Short-term variation of NO_2^- indicated obvious cell release of NO_2^- during luxury NO_3^- uptake at daytime. However, NO_2^- release was two magnitudes lower than NO_3^- uptake (Fig. 4-1) and nitrite remained at low concentrations all the time because it was utilized finally as well, so that its contribution did not show significant variation during the whole experimental period. Thus, other processes would have been involved in N loss. It should be noticed that the bacteria biomass increased significantly during nitrate uptake (Dürselen 2002). For this reason, denitrification could be an essential process to convert nitrate and nitrite to N_2O and N_2, escaping from water column. This was reflected by the fact that nitrite significantly decreased at night and was not accumulated in the water (Fig. 3-2C).

During the summer experiments, fast uptake and turnover processes made it difficult to separate different DIN utilisation by phytoplankton in comparison to spring. Rough estimates showed that N losses during nitrate uptake (02/06 to 03/06) were lower than overall N losses when nitrate was the main N source (Fig. 3-23). Among overall N loss, about 4 to 5% of total N was accounted for DON increase from phytoplankton production. It is concluded that nitrite release was significant.

However, the amount was lower than in spring. Different to the spring experiments, N loss occurred continuously during the whole experiment in the control system. Combined with the increasing bacteria, it is presumed that denitrification was the main process resulting in N loss from the water column.

Another sink of N from water column is sedimentation. In the two experimental bags, the whole water system was kept homogeneous by frequent bubbling. Only little sediment was detected at the bottom and nearly no biogenic coating on the wall of the bags after the experiments. Thus, the contribution from this part was assumed to be minor.

It is concluded that denitrification related to bacterial activity in anaerobic microzones within detritus particles (Jannasch 1960, Dürselen 2002) mainly accounted for the N loss of about 7% of the initial N in the control bags in spring and 13% to 14% of initial N pool in the control bags in summer as from the overall estimation (Fig. 3-21, 3-23). These corresponded to the denitrification rates of 1.5 mmol m^{-2} d^{-1} in spring and 2.5 mmol m^{-2} d^{-1} in summer. By higher temperatures during summer denitrification rate were increased to about 2 times (Hattori 1983).

In winter the N:P ratio is lower in many areas of the southern North Sea than in any of the source waters. The deficit in the load of nitrate N relative to that which would be present assuming conservative mixing of river and ocean waters is 580 ktonnes (Hydes et al. 1999). This is probably due to denitrification. Considering the flushing rate it is equivalent to a maximum rate of 0.7 mmol N m^{-2} d^{-1} for the southern North Sea. Our estimation is twice to triple as this value.

On the other hand, the production of organic matter in the enclosures has enhanced the formation of anoxic microzones within particles. In field, faecal pellets with including anoxic microzones could be concentrated at the thermocline, resulting in denitrification of N. In most estuaries, denitrification is the major process responsible for removing N, and the fraction of total N input that is denitrified appears to be directly proportional to the log mean water residence time (Nixon et al. 1996).

4.1.5 Diurnal processes

4.1.5.1 Diurnal change of phytoplankton photosynthesis

Both in spring and summer experiments, short-term variation of chl*a* concentrations showed a diurnal periodicity with maximum concentrations at midnight and minimum concentrations at midday. This diurnal rhythm was also observed in previous measurements and it is supposed to be a result of both biosynthesis and decomposition (Raymont 1980).

Photosynthesis activity (detected from the calculated photosynthetic rates) related to phytoplankton biomass (mg C/L) as well as to the relative C contents per unit chl*a.* Both showed the highest values in the afternoon (Fig. 3-27), indicating significant net photosynthesis. At night-time the negative values of photosynthesis rates imply net C decomposition due to respiration, cell excretion and cell division of some species at night (Sournia 1974). Comparing the variation of photosynthesis rates in summer with those in spring, there were shifts of the maximum rates from afternoon to later morning

on some days (Fig. 3-27, 3-28). These shifts are so called ‘afternoon’ and ‘midday depressions’ (Sournia 1969) and caused by photoinhibition to photosynthesis, which can occur in the afternoon when irradiance reach the highest values (Fig. 3-6). This photoinhibition in summer was also indicated by the model analyses (Fig. 3-35C, 3-39C).

4.1.5.2 Diurnal change of nutrient uptake

Ammonium uptake itself is supposed to be not light-dependent (Cabrita et al. 1999), because the reduced form of nitrogen can immediately enter the amino acid synthesis, which is not directly coupled with photosynthesis. On the other hand, ammonium is often the first product from regeneration (deammonification). Ammonium turnover in the water column via remineralisation can reach an amount of about 1.52 μM m^{-2} day^{-1} (Parsons and Harrison 1983). For this reason, it is assumed that ammonium uptake was much higher than the calculated daily uptake rates, because parallel to the uptake, remineralisation may occur which was not detected (Fig. 3-30). The uptake of up to 2 μM/d can be assumed to be in the same order as undetected remineralisation rates.

Regeneration of ammonium in the water column occurs as a result of two largely separate processes: excretion from zooplankton and release during decomposition of organic detritus and dissolved organic matter via bacteria (Bidigare 1983, Gotschalk and Alldredge 1989).

The fraction especially from microzooplankton excretion has been shown to be of importance in coastal water (Koike et al. 1982, Parsons and Harrison 1983). Ammonium release from microbiological activities could be two times that from zooplankton (Blackburn and Sϕrensen 1988). In our spring experiments, zooplankton biomass was low in enclosures and additionally grazing was also low due to low temperature. For this reason, ammonium excretion from zooplankton can be neglected compared to bacterial remineralisation. During the stationary phase, increase of ammonium resulted from decomposition of dying cells and detritus (Fig 3-2A). Very weak diurnal variability again indicates parallel uptake and release processes. This assumption was confirmed by the fact that ammonium was kept around 1.0 μM, which is the threshold for ammonium uptake by phytoplankton.

For many species, nitrate uptake is light-dependent (Berges et al. 1995, Cochlan et al. 1991, Varela and Harrison 1999). The estimated night-time uptake rates were about 16 to 51% in T1 and 12 to 35% in T4 of those of daytime uptake (Fig. 4-3). These values are comparable to the results from upwelling nitrate rich plumes (Eppley et al. 1970a, Cochlan et al. 1991). The conclusion that nitrate uptake by phytoplankton in nitrate rich waters has its maximum during the first half of the light period, as documented by former authors (Eppley et al. 1970a, Malone et al. 1975, Cochlan et al. 1991) was again confirmed from our mesocosm experiments by coastal phytoplankton assemblages.

Nitrate assimilation by phytoplankton is limited by nitrate reductase activity (NRA) during the first step and the latter is inhibited by darkness and stimulated by light (Wheeler 1983). Vergara et al. (1998) examined NRA in the diatom *Thalassiosira weissflogii*, and showed that nitrate reductase had a peak at midday, a decrease towards the end of the photoperiod and an increase in activity near the end of the dark period. The daytime NRA could reach up to 30 fold values in comparison to the night phase’ (Lopes et al. 1997). Thus a lower uptake rate of nitrate at night can be corresponded to

lower activity of NRA at night. Decline of uptake rates at night led to slower decrease of nitrate concentrations. At night, bacteria related nitrification could be a source for nitrate, which would be predominant as shown in former continuous experiments (Malone et al. 1975). But this was not the case in our spring experiment. Very low ammonium and nitrite concentrations made this contribution negligible compared to high nitrate contents.

The concentrations of nitrite increased (0.1 µM/h) in the afternoon due to phytoplankton excretion as shown in fig. 3-32, and reached ca. 1% of the nitrate uptake. It decreased during nights due to the nitrification from nitrite to nitrate by nitrifying bacteria. The delay of 2 to 4 hrs implied the turnover time for the metabolic processes of nitrate being reduced to nitrite and nitrite being released via cell membrane.

In both bags (T1, T4), during the exponential phase, the correlation between nitrate and nitrite was very significant fluctuating short-term positive and negative (Fig. 4-1), indicating the dominance of nitrite excretion during the nitrate uptake at daytime and nitrite oxidation to nitrate by nitrifying bacteria in seawater during darkness.

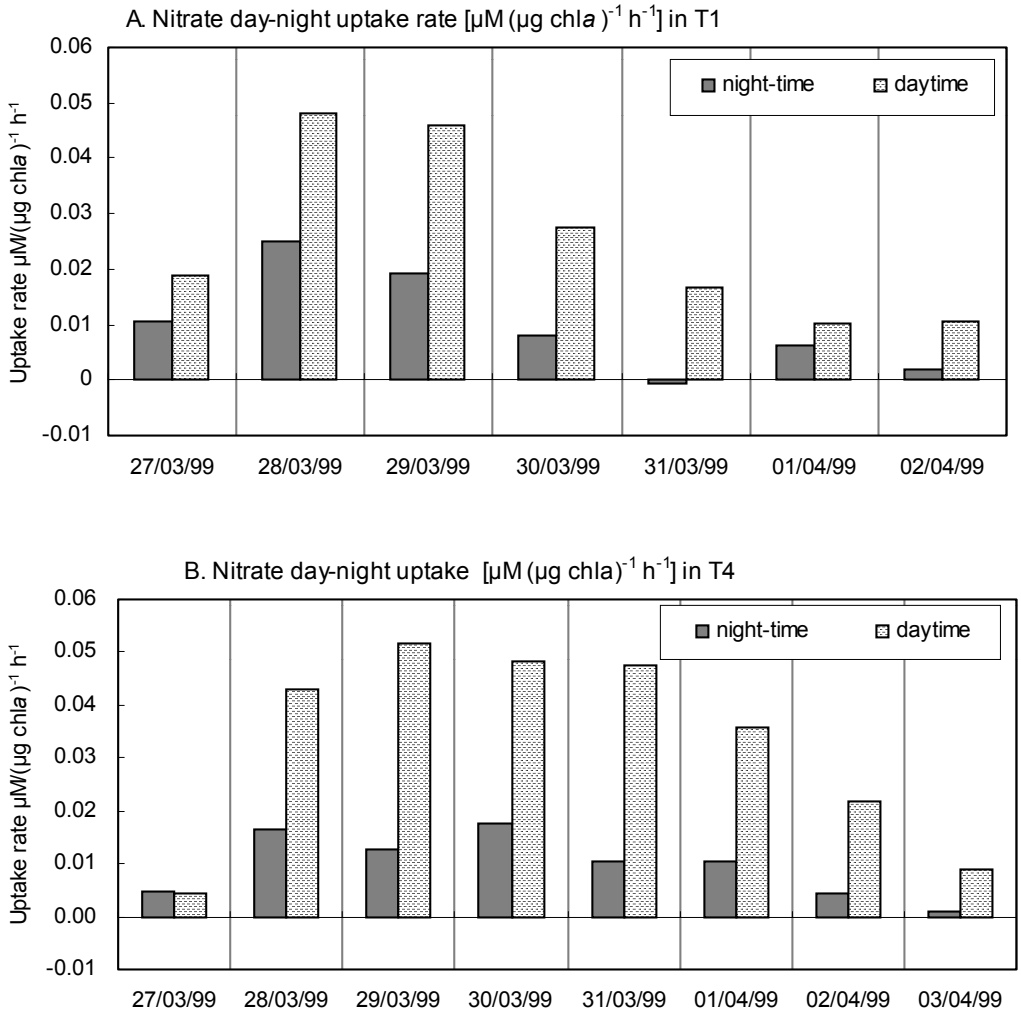

Fig. 4-3 Nitrate uptake rates in the spring experiments (T1& T4, averaged from 2 hour calculation, night-time: 20:00-08:00; daytime: 10:00-18:00. Darkness: 20:00-06:00)

Generally, this diurnal rhythm can be recognised for marine phytoplankton, independent of biomass or pigment changes, because it reflects internal biochemical mechanisms (Raymont 1980). Various factors could lead to diurnal periodicity, such as light intensity (the time of day), chl *a* content and the availability of nutrients, as well as species-specific processes, for example, different duration of cell division (Sournia 1974). The diurnal periodicity might also result from obvious physiological changes in photosynthesis, which may effectively slow down any potential increase in the phytoplankton standing stock during different parts of the day (Parsons et al. 1984). The effects from temperature could be attributed finally to diurnal change of light intensity. It can be assumed that the periodicity of phytoplankton activity brings the diurnal variation of nutrients uptake thus further to produce a diurnal change in nutrients concentrations in the medium.

4.2 Model simulations

4.2.1 Model validation

The step of model validation follows the calibration, which we have done with the data of the spring control bag. Validation requests the model to be tested against an independent set of data to observe how well the model simulations fit these data (Jϕrgensen 1994). Thus, it is very essential to get data, which are entirely different from those used in the calibration. For this reason, the data from the summer control bag was used to carry out the step.

At first, the whole set of parameters from the standard run was directly applied to simulate the development of the summer control bag. It was found that NH_4^+, NO_3^- and PO_4^{3-} uptake was delayed compared to the measurements, as well as PN and PP. In order to adapt the model to fit better the summer control system, following parameters have been changed accordingly.
Because Si simulation was in good agreement with the measurements, which indicates diatom simulations were reasonable, only the maximum growth rate of flagellates (*Rfmax*) was changed by being set 20% higher than that in the standard run (2.8 d^{-1}). The modification was based on the observation that in summer, various dominant species of flagellates kept higher growth rates than in spring. In spite of the increase, the overall growth rates of flagellates at daytime under the *in situ* temperature, light climate and nutrient conditions were around 1.0 d^{-1} and still in the range of experimental results (Jϕrgensen et al. 1991).

A great range in measurements of zooplankton grazing rates (*Rgmax*) was reported, as summarized by Jϕrgensen et al. (1991), which partly reflects the real variations in spite of those differences in experimental technique, food type, organism size, location and so on. The response of *Rgmax* to temperature is assumed to be an exponential relation according to the van't Hoff rule (Kremer and Nixon 1978). In the current model, the temperature effect was not explicitly parameterized and only one constant was used as *Rgmax* for the whole experimental duration. The increase of *Rgmax* from 0.12 d^{-1} in spring to 0.2 d^{-1} in summer was made according to the measurements from Petipa (1966) in consideration of different dominant species in the enclosed water column in summer compared to spring. Sensitivity analysis showed that *Rgmax* had more influence on diatoms and flagellates than on the other model outputs (Table A and B in appendix).

Detritus decomposition rates (*Rddecay(0)*, *Rddecay_P(0)*) and DOM remineralisation rates (*Rremin(0), Rremin_P(0)*) in the simulation of the summer control bag were increased in consideration of higher bacteria activity compared to spring. Because bacteria were not explicitly included in the current model, the faster turnover of decomposition and remineralisation processes related to increased bacteria biomass in the water column was thus reflected by increasing the values of these relative parameters. The sensitivity analysis shows that *Rddecay(0)* was a sensitive parameter to detritus variation and *Rremin(0)* was more to DON, but had no significant influence on most of the model outputs (Table A, B in appendix).

4.2.2 Model insights into enclosed pelagic ecosystem

4.2.2.1 Primary production and phytoplankton growth

Temperate shallow shelf seas such as the North Sea are characterised by high rates of primary production. There are many factors to control phytoplankton primary productivity in specific areas, such as: temperature, light climate, tidal action, current, wave and wind forces, advection and other hydrodynamic processes, nutrient supplies, as well as grazing, lysis and decomposition. The mesocosm experiments supplied a good chance to analyse the factors controlling the primary productivity, eliminating the physical effects, such as tidal action, current, advection etc. As the model reproduced the key points in development of nutrients and aimed particulate matter in both the spring and summer enclosures, it provides us with some considerable insights into primary production and N cycling in the pelagic system by numerical way.

In this section, the classical key factors in primary production, such as temperature, light and nutrients in spring and summer are discussed according to the model simulations.

Spring experiment

In the spring experiment, one of the interesting features was the extended period with very slow growth rates before the phytoplankton spring bloom. This phenomenon was rarely observed in previous experiments. Thus, it brings interests for us to study the reasons for this extended period and the trigger of the spring bloom in the German Bight.

Over the whole slow growth phase before bloom, all macronutrients were at high concentrations and hardly limited the phytoplankton growth as shown from the model calculations by high limitation functions (Fig. 3-33D). Meanwhile, zooplankton in the enclosure remained very low biomass due to winter and the filtration. For this reason, the top-down control was supposed to be weak.

Light climate is considered to be the most important factor especially in shallow turbid coastal waters, such as the German Bight due to high load of suspended matter (Postma 1984, Van Haren et al. 1998). Meanwhile, turbulence, tidal action and wind force also enhance the light extinction in the water column and lead to high extinction coefficient (K_0). The measured incident daily irradiation fluctuated between 60 and 140 W/m^2 during the extended slow growth phase. It has to be mentioned that these values represent the irradiance on the water surface. About 4% of photosynthesis available radiation (PAR) will be reflected on the air-sea interface (Lalli and Parsons 1997) and light intensity decreases exponentially with water depth (Steele 1962). Thus, depth mean light intensity of the whole column was only about 42% of measured irradiance and fluctuated mostly lower than 50 W/m^2 in the extended phase, as calculated from model. Diatoms dominated the phytoplankton community in the spring enclosures from the beginning (Dürselen et al. 2002a). The threshold of irradiance for diatom growth is 0.03 gcal cm^{-2} min^{-1} (Riley 1957), equivalent to 50 W m^{-2} day^{-1}. Thus, low could have limited diatom photosynthesis. Very strict limitation of irradiance was shown by the low limitation functions (Fig 3-33C, 3-37C). Model simulations also showed that decrease of K_0 in

the model resulted in earlier burst of phytoplankton bloom. In the inner area of the German Bight, a longer period of calm weather could also trigger large phytoplankton blooms in February as have been detected (NSTF 1993).

Temperature might not be such a critical factor for the spring bloom as light climate in the German Bight. But, it is generally one of the key factors for determining the biological interactions between the trophic levels in an ecosystem (Van Beusekom and Diel-Christiansen 1994). It determines individual physiological rates, such as growth, reproduction, metabolism etc., and also affects species composition within the plankton community because different species grow optimally under specific temperatures (Eppley 1972). The continuing increased temperature activised phytoplankton growth as showed by the increase of its limitation functions (Fig. 3-33B, 3-37B).

Thus, it can be concluded that the trigger of the spring bloom was the co-effect of light availability and temperature conditions.

Self-shading is one of the main light absorbing components in seawater, as a feedback of phytoplankton to light condition in the water column. It was estimated that in productive oceanic waters with 1 mg m^{-3} or more chlorophyll *a* the phytoplankton became a major contributor to light absorption (Kirk 1992). Though, in the coastal water, this contribution might not be such significant, it still gives the hint that in our enclosure system, phytoplankton itself, represented by chlorophyll, is a very important factor to control the light penetration in the water column over the experimental duration. In the experimental bag, light extinction through the water column resulted from self-shading was more significant compared to the control bag due to further growth of algae by phosphate addition (Fig. 3-37C).

During the whole period of the spring experiments, N did not limit phytoplankton as shown by high N limitation functions (Fig. 3-33D, Fig. 3-37D). The pattern of ammonium and nitrate utilisation can be reflected by the different contributions of nitrate and ammonium to the total nitrogen uptake (eq. 15) by respective uptake functions (eq. 12, 13) (Fig. 4-4A). Slight decrease of N limitation functions around day 11 implies some species shifts when nitrate had not been adopted by some species, due to the different mechanisms of nitrate and ammonium utilisation (Carpenter and Capone 1983). Increasing ammonium contribution in the last week (03/04 to 09/04) (Fig. 4-4A) gives us a signal that regenerated ammonium contributed to primary production, as formerly assumed (section 4.1.3.2).

Phosphorus limitation to phytoplankton growth was indicated not only by high DIN/P ratios in the water from the measurements but also from model calculations, which showed that phosphorus gave the lowest function of all the three nutrients in the most time of the experiment (Fig. 3-33D, 3-37D). In the control bag, the exhaustion of transient phosphate in the water column (Fig. 3-34D) resulted in a very low phosphorus limitation function (Fig. 3-33D) and strictly limited nitrogen and silicate uptake as well as phytoplankton growth.

From the calculations, it is shown that the values of the limitation functions of one nutrient remained

constant with the concentrations of this nutrient decreased but was still above certain values, as shown from the values of P limitation functions (Fig.3-33D, 3-37D). Around these values, the limitation functions varied largely and dropped to very low level in short time afterwards. In other words, in certain range of concentrations, phytoplankton uptake rates are strongly dependent on nutrient concentrations. Under certain point of concentration, nutrient uptake will stop. This phenomenon was at first demonstrated by Ketchum (1939), using the diatom, *Nitzschia closterium* and found the uptake of nitrate was concentration dependent over an approximate range from 1 to 7 μM. Under the range, phytoplankton uptake will stop. This also indicates the minimum nutrient concentration for phytoplankton growth. From the physiological view, this minimum nutrient concentration may reflect the diffusion transport of nutrient ions to the external surface of cells (Raymont 1980). This minimum nutrient concentration at which a species can grow was reflected by the half-saturation constant (*Ks*) in the Michaelis-Menten-Monod equation (Parsons et al. 1984).

According to the theory, it can be derived from the simulations that for phosphate, when the concentrations are in the range from 0.01 to 1.2 μM, the phosphate uptake strongly depends on the concentration of phosphate in the water. It can also be expected that if phosphate is added when the original content is above the range, it will not influence the uptake rates so much. This was verified from the experimental bag, into which phosphate was added when the original PO_4^{3-} was as high as 1.4 μM. As a consequence, the P limitation functions were identical in both control and experimental bags from model calculations (Fig. 3-33D, Fig 3-37D). Moreover from the measurements, the nutrient uptake rates and phytoplankton growth rates did not show much change compared to the control bag (Fig. 3-17, Fig. 4-2).

In spite of little change in P limitation after addition, the prolongation of the exponential growth in the experimental bag was significantly attributed to complementary phosphate. Nitrate uptake thus lasted and led to lower concentrations. As diatoms dominated the phytoplankton assemblage in spring, the fast growing diatoms soon exhausted silicate in the experimental bag. Because silicate is essential to diatom growth, the depletion of Si resulted in diatom stagnation, as also indicated by very low Si limitation function (Fig. 3-37D). This result was consistent not only with our measurements (Dürselen et al. 2002a), but also with the results from mesocosm experiments by Escaravage et al. (1994) and the conclusions from Smayda (1990) and Schöllhorn and Graneli (1993) about the selective role of silicate for the diatom/flagellate balance.

Thus, it is shown that the growth of phytoplankton in spring enclosures were more controlled by nutrient availability (bottom-up).

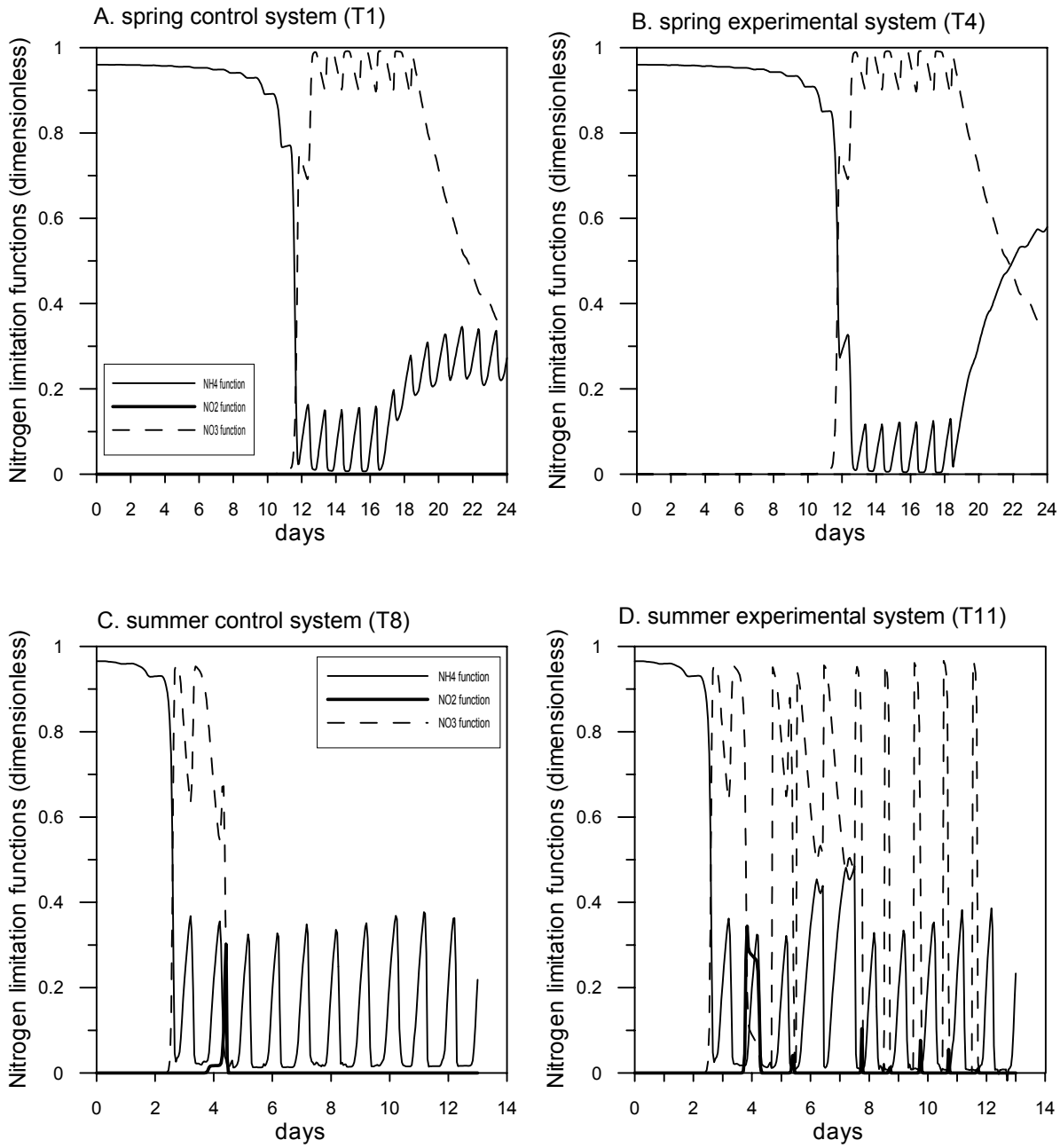

Fig. 4-4 Simulated limitation functions of ammonium, nitrate and nitrite on phytoplankton N uptake in the spring and summer experiments.
In the model, the total N function (eq. 15) was summed up by the respective functions of ammonium (eq. 12), nitrate (eq. 13) and nitrite (eq. 14), so for the above function values of respective N: the value of 0 represents no contribution; higher values represent the increasing contribution to the total N function.

Summer experiment

In summer, compared to spring, temperature increased by about 8 to 10 °C, which indicates that the growth rate of phytoplankton increased by about 1.5 times (Q_{10}=1.65) under the similar light and nutrient conditions. This can be reflected by higher temperature functions (Fig. 3-35B). At the same time, incidental irradiance was higher than that in spring, supplying sufficient light intensity to photosynthesis. Temperature and light conditions, together with low zooplankton graze pressure resulted in the exponential growth of phytoplankton in the enclosures from the very beginning. However, with the growth of phytoplankton, increase of self-shading made the overall irradiance limitation functions decrease during the first 4 days. Compared to spring, light inhibition showed more significant, as indicated by the much lower values of limitation functions at noon with high incidental irradiance from measurements (Fig. 3-35A).

Nutrient functions were all close to 1 during the first 3 days, indicating that all nutrients were sufficient to phytoplankton growth (Fig. 3-35D). The contributions of NH_4^+, NO_3^- and NO_2^- showed significant patterns of utilisation (Fig. 4-4C). After day 3, very low values of Si function indicated that the diatom growth was strictly Si-limited for the rest of the experiment. Because Si turnover is slower than N and P, diatoms soon decayed due to the Si depletion. Relatively, N and P functions remained higher than Si, implying the N, P sources for phytoplankton from internal regeneration.

NH_4^+ is supposed to be the first regenerated product of nitrogen and a very important N source after the original nutrients were exhausted. NH_4^+ can be directly regenerated from zooplankton excretion production and DON remineralisation. In summer, the turnover of these processes is enhanced due to high temperature.

Generally, P has faster turnover time because phosphorus is readily hydrolysed from organic compounds, either by hydrolysis at the alkaline pH of sea water or by phosphatases, which are hydrolytic enzymes present in many bacteria and on the surface of some phytoplankton, particularly those from environments low in phosphate (Parsons et al. 1984).

These regenerated N and P were mostly utilised by flagellates after the diatom bloom decayed due to silicate depletion (Veldhuis et al. 1986), as indicated by continuing increase of flagellates (Fig. 3-36G). However, it was obvious that the regenerated N and P could not support high growth of flagellates and started to decay soon.

It is assumed that nutrient limitations were the most essential to phytoplankton growth in summer, although temperature and light functions both decreased over the experiment. This assumption can be verified by the development of phytoplankton in the experimental bag.

It is no doubt that the continuing increase of primary productivity in the experimental bag under the same temperature and light conditions as the control bag was caused by the periodic additions of N, P and Si, which significantly increased all nutrient limitation functions (Fig. 3-39D). The N limitation function varied from 0 to 1 due to the restricted daily single NO_3^- additions. Succeeding extraordinarily fast uptake by starved phytoplankton cells (Zevenboom and Mur 1979, Goldman and

Glibert 1982, Lehman and Sandgren 1982, Riegman and Mur 1984) exhausted the supplemented nutrient pool before the next addition. Compared to the control bag, the light functions decreased over the experiment, resulting from the self-shading by increasing chlorophyll.

4.2.2.2 Fluxes and nitrogen transformation

From the model simulations which were in good agreements with the measurements, fluxes between every state variable were calculated. The detailed diagram of nitrogen transformations in the enclosed water columns allows direct comparisons of the contribution of the single processe with corresponding measurements. Daily conversion rates between the main compartments were calculated for the different growth phases of phytoplankton both in spring and summer. These rates can be used for comparisons with findings described in the literature and can be used for an independent validation. Daily averaged net fluxes between nutrients, phytoplankton-nitrogen (diatoms and flagellates), zooplankton, detritus and DON were calculated from the model outputs for different phases of phytoplankton development (Table 4-3). In addition, the fluxes integrated from daily average over the whole duration of the experiments were calculated for total N budgeting. These data are given in italic style. The results are shown in the figs 4-5 to 4-8. For the explanation of the figures, the different processes are indicated in the Fig. 4-5.0 (see also Fig. 2-3 in section 2.4).

Spring experiment

The whole period was differentiated into three phases according to the development of chl*a* from measurements (section 3.1.1.3). The first phase was a pre-exponential growth phase (or slow growth phase) which lasted about 12 days from 16/03 to 27/03 (Fig. 4-5 and 4-6). The second phase was the exponential growth phase, lasting for 5 days in the control bag (T1) (from 28/03 to 01/04) and 7 days in the experimental bag (T4) (from 28/03 to 03/04). The third phase, the stationary phase, started from 02/04 in T1 and 04/04 in T4 till the end of measurements. The calculated daily conversion rates are shown in Fig. 4-5 and Fig. 4-6.

In the control bag (T1), the net fluxes (gains and losses) show that in the slow growth phase, phytoplankton biomass was accumulating nitrogen at the rate of 1 µM/d (Table 4-3) utilising mostly NH_4^+ with a daily uptake rate of 1.1 µM/d in T1 (Fig. 4-5). The biomass was mostly formed by diatoms. In this phase, the average uptake rate of NO_3^- was 0.38 µM/d. Actually, NO_3^- was mostly taken following 27/03 when NH_4^+ decreased below 3.0 µM with a rate of 4.3 µM/d (data with # in hexagon in Fig. 4-5), whereas the rate during the first 11 days was only 0.03 µM/d (data with * in hexagon in Fig. 4-5).

The accumulation of phytoplankton mainly occurred in the exponential growth phase and the daily net flux reached up to 6.91 µM/d in T1 (Table 4-3), mainly supplied by nitrate. Daily uptake of NO_3^- by phytoplankton reached 7.95 µM/d (Fig. 4-5). Diatoms still formed the majority of phytoplankton community. Net decrease rates of NO_3^- exceeded diatoms and flagellates biomass (PN) increases (Table 4-3) indicating nitrogen transfer to the other forms such as NO_2^- and DON as detected from the positive net flux of DON at the same time. NH_4^+ was taken up at the rate of 0.17 µM/d mostly

from simultaneous DON remineralisation (Fig. 4-5).

In the stationary phase, nutrient limitation and zooplankton grazing resulted in the decrease of phytoplankton-N. The total N assimilation rate was only 0.8 μM/d for diatoms. Overall, phytoplankton biomass was decomposed at 0.3 μM/d (Table 4-3) due to mortality (0.9 μM/d) and zooplankton grazing (0.2 μM/d) (Fig. 4-5). Meanwhile, NO_3^- still showed negative net fluxes (Table 4-3), resulting from weak phytoplankton uptake and denitrification.

Phytoplankton cell release of nitrogen compounds was highest in T1 (0.16 μM/d) during the exponential growth phase as has been reported before (Hammer et al. 1981, Brockmann et al. 1982b, Brockmann 1992, Myklestad 2000). Cell release in the stationary phase was quite low compared to the experimental results (Myklestad 2000). It indicated that the compounds exudated by phytoplankton are largely non-nitrogenous (Fogg 1983b). On the other hand, DOM release from physiologically old cells at the end of a phytoplankton bloom (Ittekkot et al.1982) and release via cell lysis under nutrient depletion were not considered in the current model, which could have resulted in the gap.

Although zooplankton grazing on phytoplankton in the pre-exponential phase was only 0.06 μM/d, due to the low biomass of zooplankton and phytoplankton as well, it accounted for 5% of phytoplankton production. The daily grazing rate increased continuously over the experiment and reached 0.2 μM/d in the third phase. The increase of zooplankton grazing during the different phases is related to growing zooplankton stock.

DON remineralisation rates were mostly in the same range, from 0.14 to 0.17 μM/d over the whole experiment. Slight increase over the experiment indicates the effect on bacterial activity, triggered by increasing temperature. Detritus mostly consisted of phytoplankton dead cells especially after the blooming period, reached to about 1 μM/d, 17% of which was decomposed to the DON pool.

In the experimental bag (T4), the daily conversion rates of most processes were at the same range as those in the control bag (T1) (Fig. 4-6). Only for the exponential phase, P addition caused an extension of diatom NO_3^- uptake by 20%, and the net flux of diatom biomass increased by 1 μM/d compared to T1 (Table 4-3). On the other hand, during the longer exponential growth Si was exhausted as well, which resulted in lower uptake rate (0.28 μM/d) and higher mortality rate (1.24 μM/d) of diatoms in the third phase in comparison to those in T1. Diatom biomass decreased at a net rate of 1.18 μM/d (Table 4-3).

NO_2^- release occurred mostly in the exponential growth phase, as detected from both T1 and T4. Higher NO_3^- uptake rate in T4 resulted in higher NO_2^- release than that in T1. From overall estimation, in spring, phytoplankton NO_2^- release took 0.2% of the NO_3^- uptake.

From integrated fluxes (Fig. 4-5, data in italic), it is shown that in T1, diatoms dominated the phytoplankton community, utilising the majority (92%) of total DIN loss. NH_4^+ contributed about 23% and nitrate covered 77%. Flagellates were competed out in spring and consumed minor DIN,

8% of total DIN consumption. These results were supported by observations from the phytoplankton analyses (Dürselen et al. 2002a).

In T1, the main losses of phytoplankton N were mortality and zooplankton grazing, accounting for about 16% and 4% of total phytoplankton N respectively. The model simulations revealed that zooplankton fed on diatoms, flagellates and detritus in a ratio of 14:1:2, indicating that diatoms were the main food source for zooplankton.

About 14% of the total grazed nitrogen in T1 returned to the water column as ammonium and DON by excretion with a NH_4^+/DON ratio of 3/1 (ratios taken from Jϕrgensen et al. 1991), and 13% was lost as faecal pellets and dead individuals. Thus, nearly 27% of zooplankton uptake returned to the water column This is only 50% of ratios Steel (1974) calculated for the North Sea ecosystem. This value is also lower than the estimation of 41% from Dagg (1976) at 15°C. The difference might be due to the lower metabolism at the lower temperature (4-10°C) in our experiment.

In T1, the major sources of the pelagic detritus pool in the model were dead phytoplankton cells (92%), zooplankton moulting and faecal pellet fragments (4%) and mortality (4%). 21% of gained detritus N was dissolved to DON by lysis or bacterial activity.

NH_4^+ regeneration was assumed (Butler et al. 1970, Parsons et al. 1984, see also section 2.4.1.1.2) by DON remineralisation (91%) and zooplankton excretion (9%). As discussed in section 4.2.2.1, regenerated ammonium was still taken up by phytoplankton in the course of nitrate uptake.

In the experimental bag (T4), P addition increased the diatom and flagellates production (N uptake) by 29% and 58% of those in T1. The increase of assimilated N was mainly caused by nitrate uptake into phytoplankton biomass. The simulated mortality of phytoplankton increased, but took only 10% of the increase of diatom N and 12% of that of flagellate N. Additionally, phytoplankton cell release and zooplankton grazing increased accounting for 2% and 1% of increased N assimilation, respectively (Fig. 4-6, data in italic style).

From the calculation, it is shown that the nutrient addition did not change much the fluxes of regeneration-related processes, such as detritus decomposition, DON remineralisation and nitrification/denitrification.

Summer experiment

According to the development of chl*a* in the control bag (T8) of the summer experiment (Fig. 3-10), the growth of phytoplankton was differentiated into two phases: the exponential growth phase which started immediately at the beginning of the experiment till 03/06; and the decomposition phase which lasted from 04/06 to 14/06. In the experimental bag (T11), the exponential growth lasted 6 days more due to the nutrient enrichments. The phytoplankton development in T11 was divided into three phases: the first phase, the exponential growth phase as in T8, covered from 01/06 to 03/06 when phytoplankton growth was depended on the originally enclosed nutrients; the second phase was the growth based on frequent nutrient additions, covering from 04/06 to 09/06; the third phase

was the decomposition phase from 10/06 to the end (14/06). The daily conversion rates in the different phases in these two bags were calculated and shown in Fig. 4-7 and Fig. 4-8, respectively.

In the first phase, the rate of NH_4^+ contribution to primary production in T8 was 5.2 µM/d, which was equally assimilated by diatoms and flagellates (Fig. 4-7). Parallel, NO_3^- contributed with the rate of 2.1 µM/d, with one third to diatoms and two third to flagellates accumulation. The different proportions of NH_4^+ and NO_3^- flowing to diatoms and flagellates resulted from the fact that NH_4^+ was taken up within the first two days when diatom growth was supported by sufficient Si (>1 µM), whereas NO_3^- was mainly taken up between 03/06 and 04/06 when the growth of diatoms was limited due to the exhaustion of Si on 03/06. For this reason, the calculation of uptake rates of NO_3^- was reduced to the period during 03/06 and 04/06 (data with * in Fig. 4-7). It reached up to 11 µM/d with only 1 µM/d to diatoms and 10 µM/d to flagellates. It indicated that in this phase, diatom growth was strongly limited by Si. From the average of three days in the first phase, the N assimilation rates of diatoms and flagellates were at the same range of 3.2 µM/d and 4.1 µM/d respectively. The net growth of diatoms and flagellates were 2.8 µM/d and 3.8 µM/d respectively (Table 4-3). But flagellates grew 1 day longer than diatoms. Flagellates show strong ability to utilise low concentration N and P in the water (Harrison and Turpin 1982, Escaravage et al. 1996). Thus, the daily average N uptake rate of flagellates reached 7.2 µM/d (in the double line circles). Overall, in this phase, diatom biomass formation only took 46% of total N uptake.

In the decomposition phase, the average NO_3^- uptake rate was 1.8 µM/d. But, considering that NO_3^- was intensively taken up on 03/06 and 04/06 (11 µM/d), the calculated uptake rate of NO_3^- for the rest of the time (after 05/06) was only 0.28 µM/d. NH_4^+ uptake rate was still 0.78 µM/d, most by flagellates, indicating high ability of flagellates to utilise the regenerated N in this phase. Different to spring, not only DON but also NH_4^+ showed positive net fluxes in the decomposition phase (Table 4-3), which indicated the enhanced regeneration processes in summer due to increased turnover rates by higher temperature (Rivkin et al. 1996, Sommaruga and Conde 1997). Positive net flux of NH_4^+ also reflects the high activity of zooplankton (Parsons et al. 1984, Alcaraz 1988, Alcaraz et al. 1994) as shown by its increasing NH_4^+ excretion rate (Fig. 4-7).

Zooplankton grazed more on diatoms (0.2 µM/d) than on flagellates (0.1 µM/d) in the first phase, whereas in the decomposition phase, flagellates were grazed by zooplankton at a high rate of 0.48 µM/d and diatoms only at a rate of 0.16 µM/d due to its low biomass. Totally, the rates of zooplankton grazing on phytoplankton were higher in the decomposition phase (up to 0.65 µM/d) than that in the growth phase, related to increasing zooplankton biomass over the experiment.

Detritus were decomposed at the rate of 1 µM/d, close to the sum of gains, which indicated very high bacterial activity in summer, as was also shown by DON remineralisation rates of 5 to 6 times higher than those in spring.

In the experimental bag (T11), the daily conversion rates of most processes in the first phase were the same as those in T8 (Fig. 4-8). Due to P and Si addition on 04/06 (see page 108), NO_3^- uptake rate

calculated from 03/06 to 04/06 (data with * in Fig. 4-8) increased by 1.3 μM/d compared to T8.

In the second phase, phytoplankton was kept growing due to nutrient enrichments. NO_3^- was daily added and taken up by phytoplankton by the rate of 13.2 μM/d. Uptake rate of NO_3^- by diatoms was kept at the rate of 2 μM/d, the same level as that in the first phase, whereas flagellates uptake increased to 11 μM/d. This was due to the continuous growth of flagellates which was not limited by Si depletion after noon 03/06. Although Si was added every day since 04/06 (table 4-2), the model has a deficit of simulating the rehabilitation of diatoms following new Si additions.

Phytoplankton extracellular release was significantly enhanced three times (0.28 μM/d) in comparison to the control mostly from flagellates contributing to the DON pool. Zooplankton grazing on diatoms remained the same as during the first phase of 0.2 μM/d, whereas grazing on flagellates increased up to 0.5 μM/d.

The decomposition phase in T11 was found to start from 10/06 in terms of chl*a* decreasing, whereas nutrient addition lasted until 12/06. So, in spite of the decrease of chl*a*, NO_3^- was still taken up at the rate of 14 μM/d, mostly by flagellates. Meanwhile, NH_4^+ was taken up at 0.86 μM/d, close to DON remineralisation rate. Both zooplankton grazing and phytoplankton mortality increased by 2 times compared to the second phase. Detritus decomposition rate enhanced to 2.5 μM/d.

In summer, NO_2^- release from phytoplankton reached up to 1% of NO_3^- uptake, averaged over the whole period of NO_3^- uptake, which was close to the estimation from the measurements (Table 4-4). NO_2^- was taken up at the maximum rate of 0.14 μM/d by diatoms and 0.58 μM/d by flagellates on 04/06 in T11.

From the overall integration, in T8, flagellates assimilation covered 80% and diatoms 20% of the total DIN consumption in the control bag (Fig. 4-7). Ammonium and nitrate contributed 50% and 48% of the total N source, respectively. Different to spring, nitrite was also taken up, which reflects well the measurements though its contribution was quite less (2% of the total N uptake).

In T8, mortality and zooplankton grazing covered 29% and 23% of diatom N uptake, and 21% and 13% of flagellate N uptake. DON release represented about 2% of the total phytoplankton N production.

In the model simulation of T8, regenerated ammonium was mostly originating from DON remineralisation and amounted to 90% of total regenerated NH_4^+, whereas zooplankton excretion covered 10%. Regenerated ammonium is often supposed to support phytoplankton growth especially in summer (King et al. 1987). However, the fraction excreted by the zooplankton can be quite variable from 5% to 31% (Carter et al. 1986, Alcaraz 1988). In the coastal areas, this fraction could reach more than 43% (Alcaraz et al. 1994). The value (10%) from the current model is in this range, but relatively low.

Zooplankton was feeding on flagellates, diatoms and detritus with the ratio of 13: 6: 1. Flagellates contributed more due to its high biomass. Among total zooplankton N gains, loss via mortality and

faecal pellet production amounted to 22% and 15% respectively, and 15% was lost to the dissolved phase as NH_4^+ and DON by excretion.

By the assumed mortality of phytoplankton the major part of pelagic detritus was formed, reaching 78% of total detritus sources. Of which, 80% was converted to DON via bacterial activity.

In T11 diatoms increased by 2 times and flagellates by 2.5 times in comparison to T8. 14% of N uptake by diatoms and 11% by flagellates flowed to detritus by mortality. Except this, phytoplankton cell release was enhanced by 3 times compared to the control bag. However, this fraction only took 2% of added N. Zooplankton grazing on phytoplankton increased by 50% of that in the control bag, as well as its excretion and faecal pellet production. Detritus decomposition increased by 34% and DON remineralisation by 5% of that in the control bag (T8). Increase of biomass indicated that in the T11 enclosure, phytoplankton growth was dominantly limited by nutrients and not controlled by graze pressure (Perez-Martinez et al. 1994, Strauss et al. 1994).

From these calculations, it is concluded that phytoplankton biomass formation was the main process in the enclosures. The results are consistent with the measurements, as detected from nutrient uptake ratios (section 4.1.3.1). In spring, in T1, 77% of primary production remained as increased biomass. 4% contributed to zooplankton biomass built-up. Remineralisation to NH_4^+ accounted for 6% of primary production and 13% of primary production was lost to the detritus pool. In T4, P addition enhanced the percentage of phytoplankton biomass by 2%. In summer, in the control system (T8), the biomass formation covered 60% of primary production. 8% of primary production were converted to zooplankton biomass increase. Remineralisation in T8 reached 22% of primary production, 6% were contributed to the DON pool and only 4% remained in detritus. In the experimental system (T11), the added nutrients were mostly transferred to phytoplankton N. The biomass formation corresponded to 76% of primary production and 4% of zooplankton biomass increase. Remineralisation to NH_4^+ and DON increase accounted for 7% and 9% of primary production, respectively. 4% of primary production flowed to the detritus pool. This is in coincidence with results from other experiments, which showed that with increasing nutrient concentrations, the largest fraction is fixed by phytoplankton (Suttle et al. 1990, Goldman and Dennett 2001). It is furthermore indicated by the results that in eutrophic coastal areas, the further addition of nutrients cause an increase of phytoplankton biomass, and only a small part of it will be transferred to the next trophic level as has also been observed in field observations as well (Madhupratap et al. 1992).

Nitrification in the enclosure experiments was not significantly detected. In spring, very high concentrations of nitrate made it neglect in inorganic nitrogen conversion. In summer, very fast phytoplankton uptake exhausted all DIN within 3 to 4 days. Very low concentrations of NH_4^+, NO_3^- and NO_2^- make it assumable that either nitrification was quite low or the nitrified nitrate was supplied to simultaneous denitrification. However, quite amount of N loss both in spring and

summer was owed to denitrification in the water column (see also section 4.1.4).

From model simulation as shown in Fig 4-5 to 4-8, simulated N loss by denitrification in spring was only at the rate of 0.01 μM/d, corresponding to 0.24 μM nitrogen over the whole period. In summer, denitrification rates varied from 0.001 μM/d to 0.04 μM/d, corresponding to 0.2 μM N loss in total. Compared to the measurements, N loss was underestimated in the current model.

Denitrification in the water column is especially related to specific anoxic microzones created by aggregate-associated bacteria, significantly distinguished from the surroundings (Jannasch 1960, Shankes and Trent 1980, Grossart and Simon 1993, Grossart and Ploug 2001). This brings large difficulties to numerical simulation. In the model, denitrification was set to be related to nitrate and nitrite concentrations only. These processes are extremely sensitive to nitrite simulations (not shown). In summer simulated denitrification was high in the first phase due to high temperature and became very low in the decomposition phase due to NO_3^- exhaustion (Fig. 4-7 and 4-8).

The denitrification rates in the water column and sediments varied in very large scales varying with seasons and environments (Helder et al. 1981, Hattori 1983, Lohse et al 1993, Kerner 1996, Lohse et al. 1996, Barnes and Owens 1998, Hydes et al. 1999). The simulated denitrification rates were in the range of minimum published values.

Table 4-3 Daily net changes of N (μM/d) in the spring and summer experiments. (Spring: slow growth phase: 16/03 to 27/03; exponential growth phase: 28/03 to 01/04; stationary phase: 02/04 to 09/04 (08/04 for T4). Summer (for T8): exponential growth phase: 01/06 to 03/06; decomposition phase: 04/06 to 13/06.)

	bags	slow-growth phase [μM/d]	exponential phase [μM/d]	stationary phase [μM/d]
Diatoms (part. N)	T1	1.19	6.91	-0.29
	T4	0.96	7.87	-1.18
	T8		2.76	-0.38
	T11		2.60	1.19*
Flagellates (part. N)	T1	0.16	0.46	-0.07
	T4	0.14	0.74	-0.006
	T8		6.63	-0.18
	T11		6.83	8.82*
NH4	T1	-0.98	-0.0068	-0.0069
	T4	-0.98	-0.015	-0.078
	T8		-4.50	0.046
	T11		-4.50	0.14*
NO3	T1	-0.38	-7.95	-0.65
	T4	-0.12	-9.60	-0.17
	T8		-5.57	-1.85
	T11		-6.25	-13.61
DON	T1	-0.043	0.10	0.029
	T4	-0.052	0.14	0.047
	T8		0.41	0.37
	T11		0.56	1.27

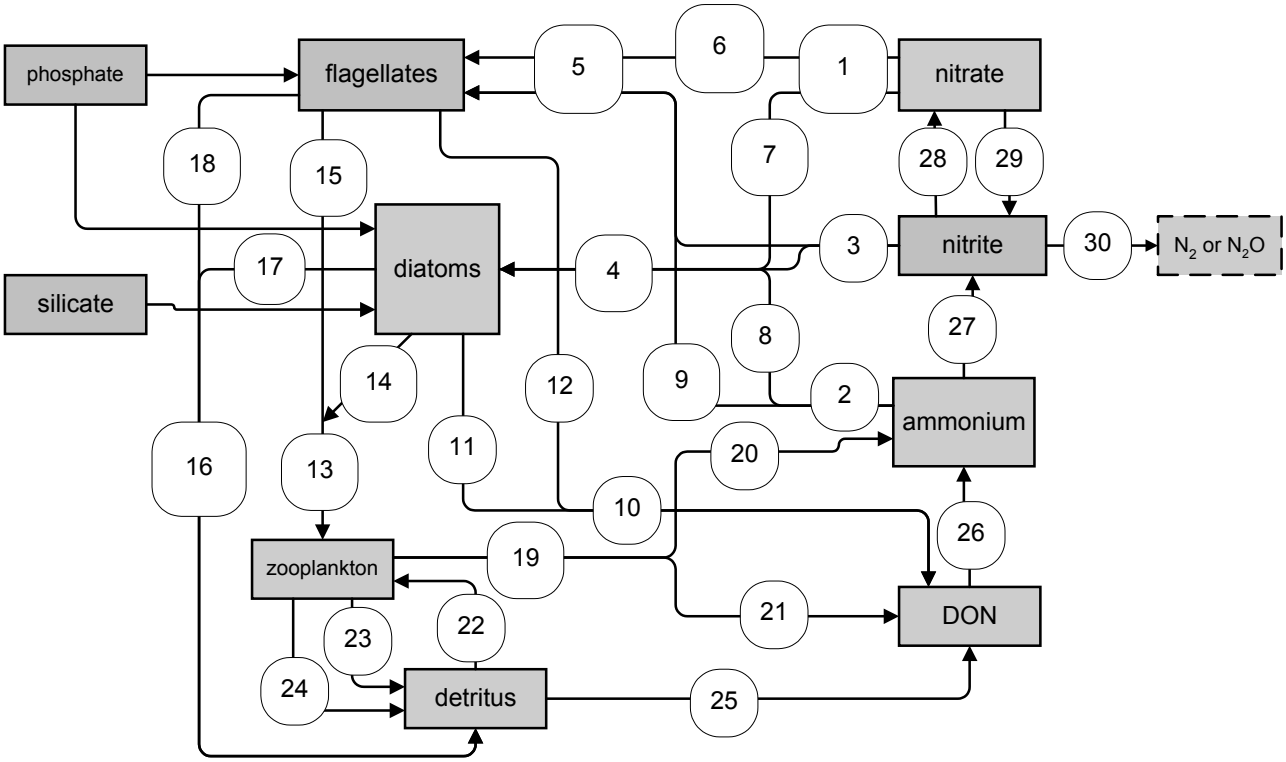

Fig. 4-5.0: Diagram of the processes for flux calculation. (For the explanation of the following figures (Fig. 4-5 to Fig. 4-8), the different processes are indicated, see also Fig. 2-3 in section 2.4)

Process indications:

1. nitrate uptake by phytoplankton (diatoms and flagellates)
2. ammonium uptake by phytoplankton (diatoms and flagellates)
3. nitrite uptake by phytoplankton (diatoms and flagellates)
4. N (ammonium+nitrate+nitrite) uptake by diatoms
5. N (ammonium+nitrate+nitrite) uptake by flagellates
6. nitrate uptake by flagellates
7. nitrate uptake by diatoms
8. ammonium uptake by diatoms
9. ammonium uptake by flagellates
10. phytoplankton (diatoms+flagellates) extracellular release
11. diatoms extracellular release
12. flagellates extracellular release
13. zooplankton grazing on phytoplankton (diatoms+flagellates)
14. zooplankton grazing on diatoms
15. zooplankton grazing on flagellates
16. phytoplankton (diatoms+flagellates) natural mortality
17. diatoms natural mortality
18. flagellates natural mortality
19. zooplankton excretion
20. ammonium fraction of zooplankton excretion
21. DON fraction of zooplankton excretion
22. zooplankton grazing on detritus
23. zooplankton mortality
24. zooplankton faecal pellets
25. detritus decomposition
26. DON remineralisation
27. ammonium nitrification to nitrite
28. nitrification from nitrite to nitrate
29. denitrification from nitrate to nitrite
30. denitrification from nitrite to N_2 or N_2O

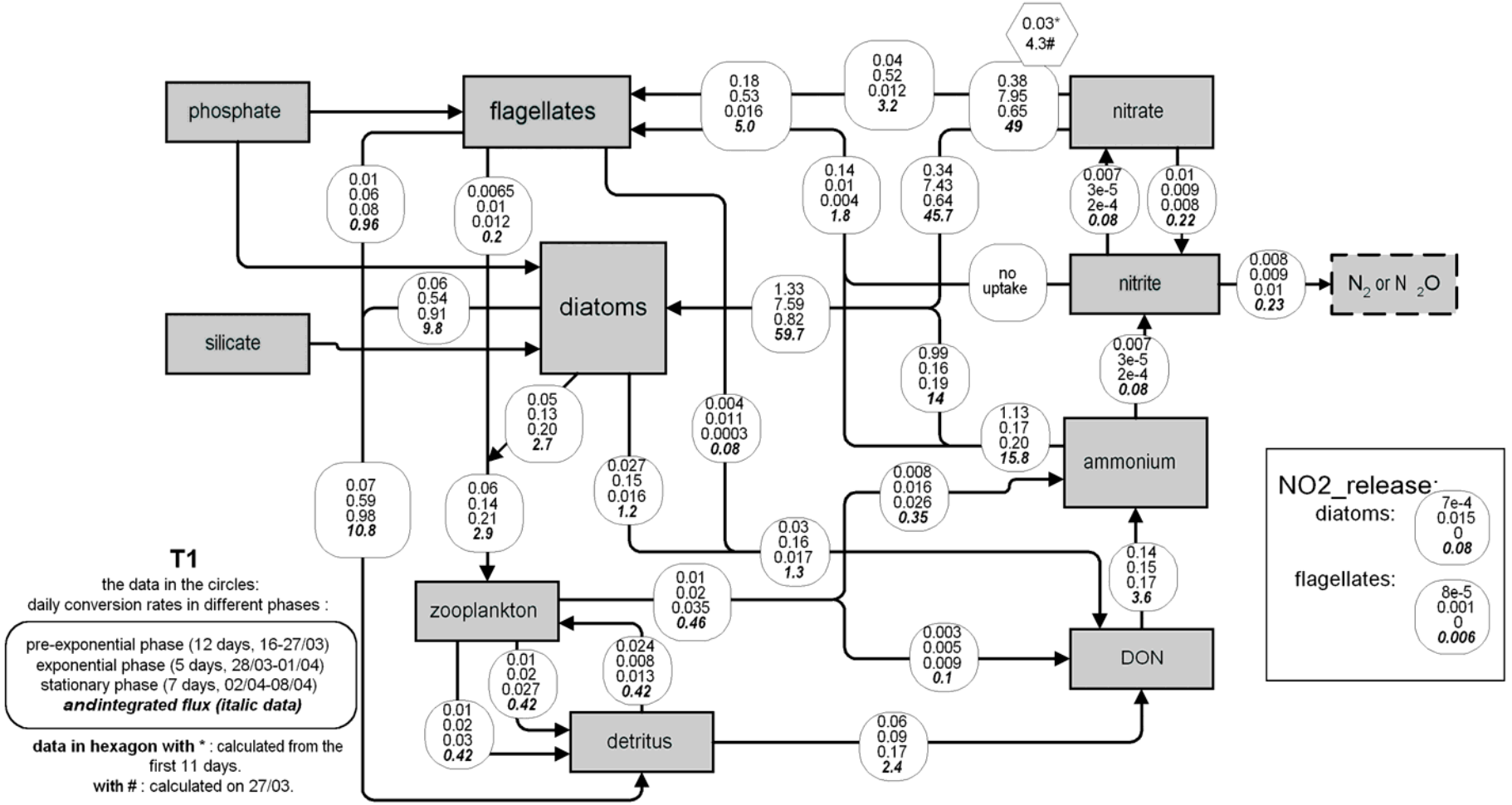

Fig. 4-5 Simulated daily conversion rates (in μM/d) between the main compartments during the different growth phases of the spring control system (T1) and integrated N-fluxes (in μM, integrated over the whole duration of 24 days, data in italic style). (data in hexagon are recalculated NO3 uptake rates in the pre-exponential phase distinguished the day of 27/03 (with #) from the first 11 days (with *)).

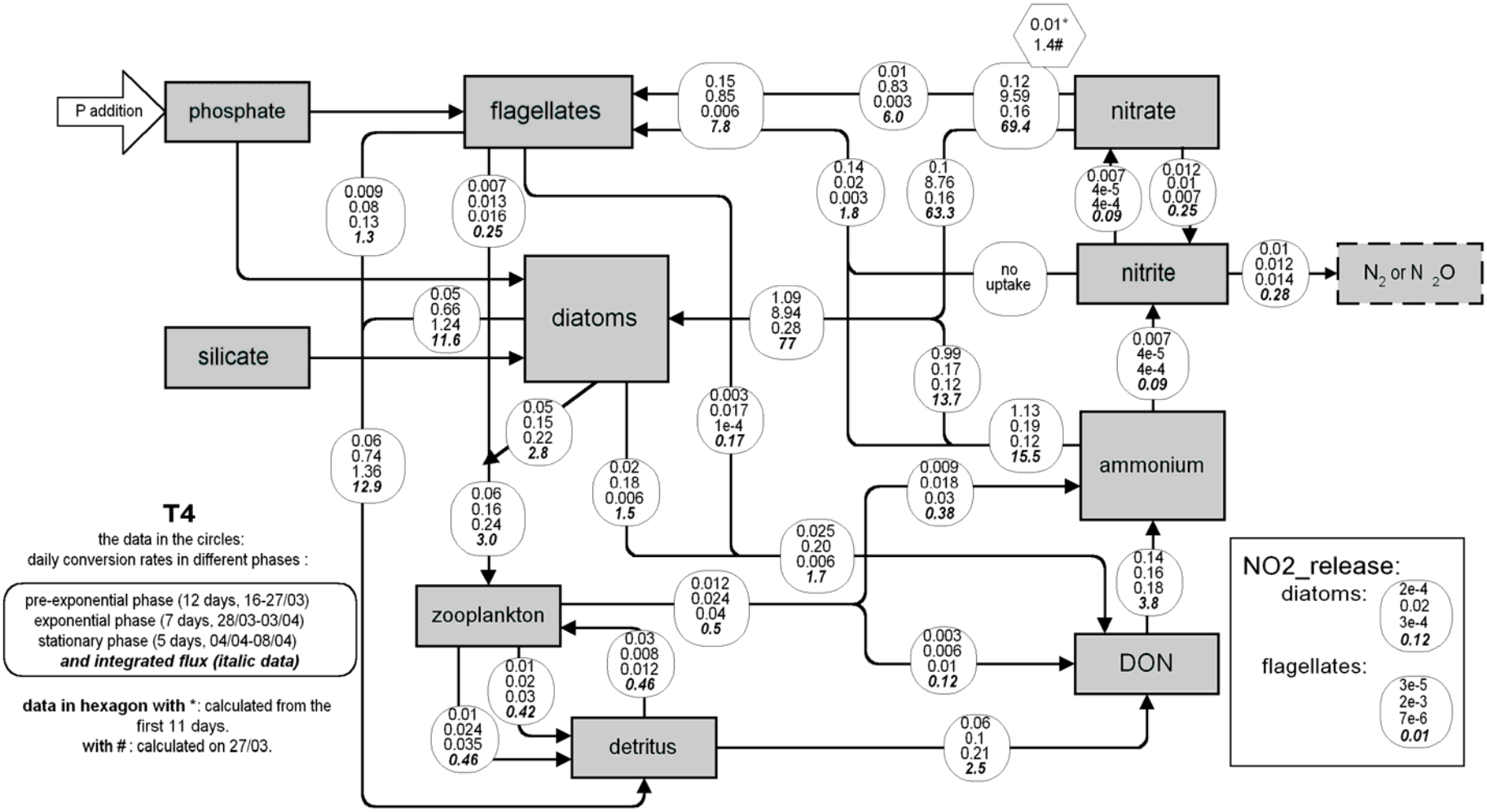

Fig. 4-6 Simulated daily conversion rates (in μM/d) between the main compartments during the different growth phases of the spring experimental system (T4) and integrated N-fluxes (in μM, integrated over the whole duration of 24 days, data in italic style). (data in hexagon are recalculated NO3 uptake rates in the pre-exponential phase distinguished the day of 27/03 (with #) from the first 11 days (with *)).

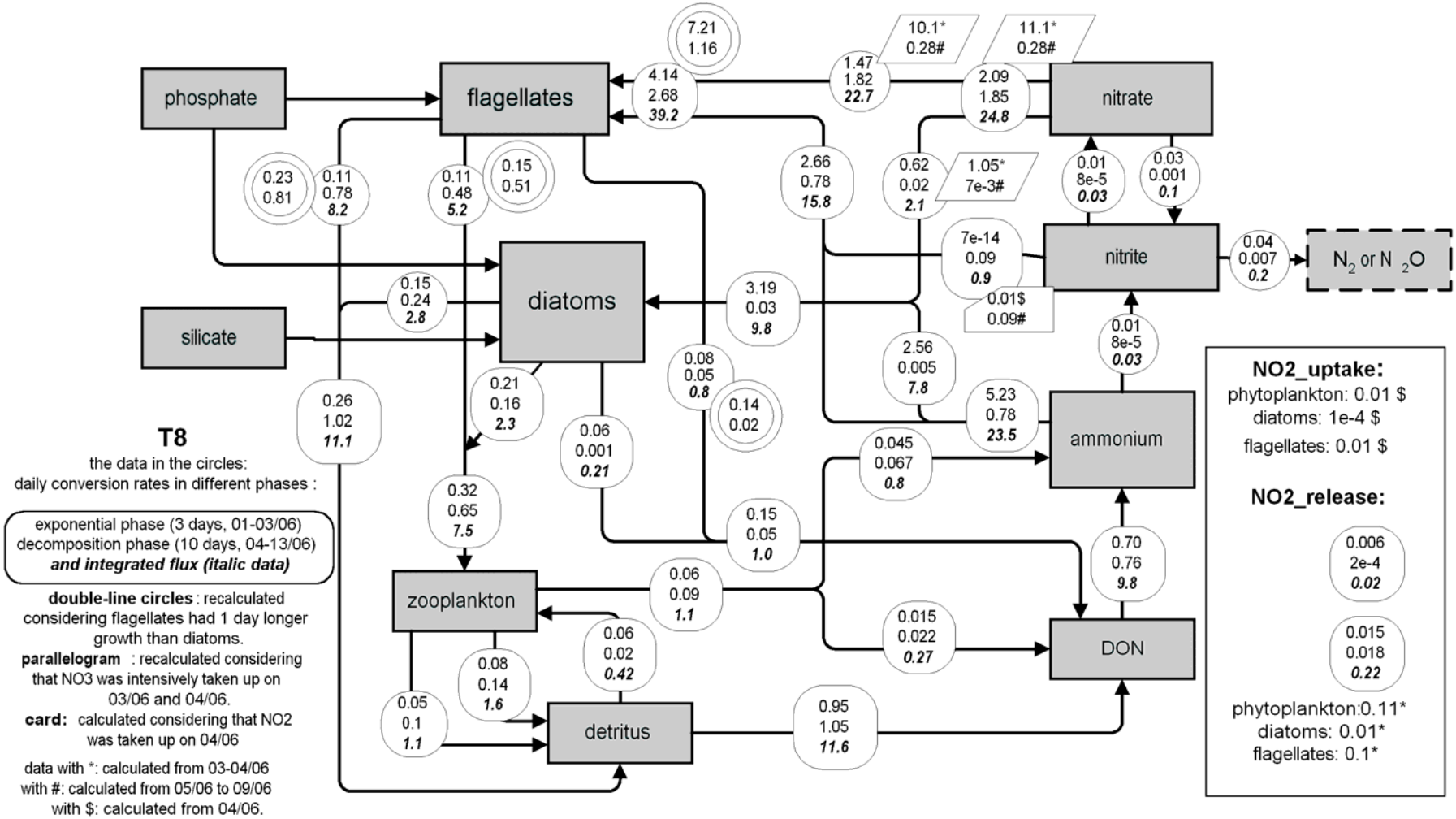

Fig. 4-7 Simulated daily conversion rates (in μM/d) between the main compartments during the different growth phases of the summer control system (T8) and integrated N-fluxes (in μM, integrated over the whole duration of 13 days, data in italic style). (data in the double-line circles: the daily conversion rates re-calculated considering that flagellates had 1 day longer exponential growth than diatoms; data in the parallelogram: the daily conversion rates re-calculated considering that NO3 was taken up intensively on 03/06 and 04/06; data in the card: the daily conversion rates re-calculated considering that NO2 was intensively taken up on 04/06.)

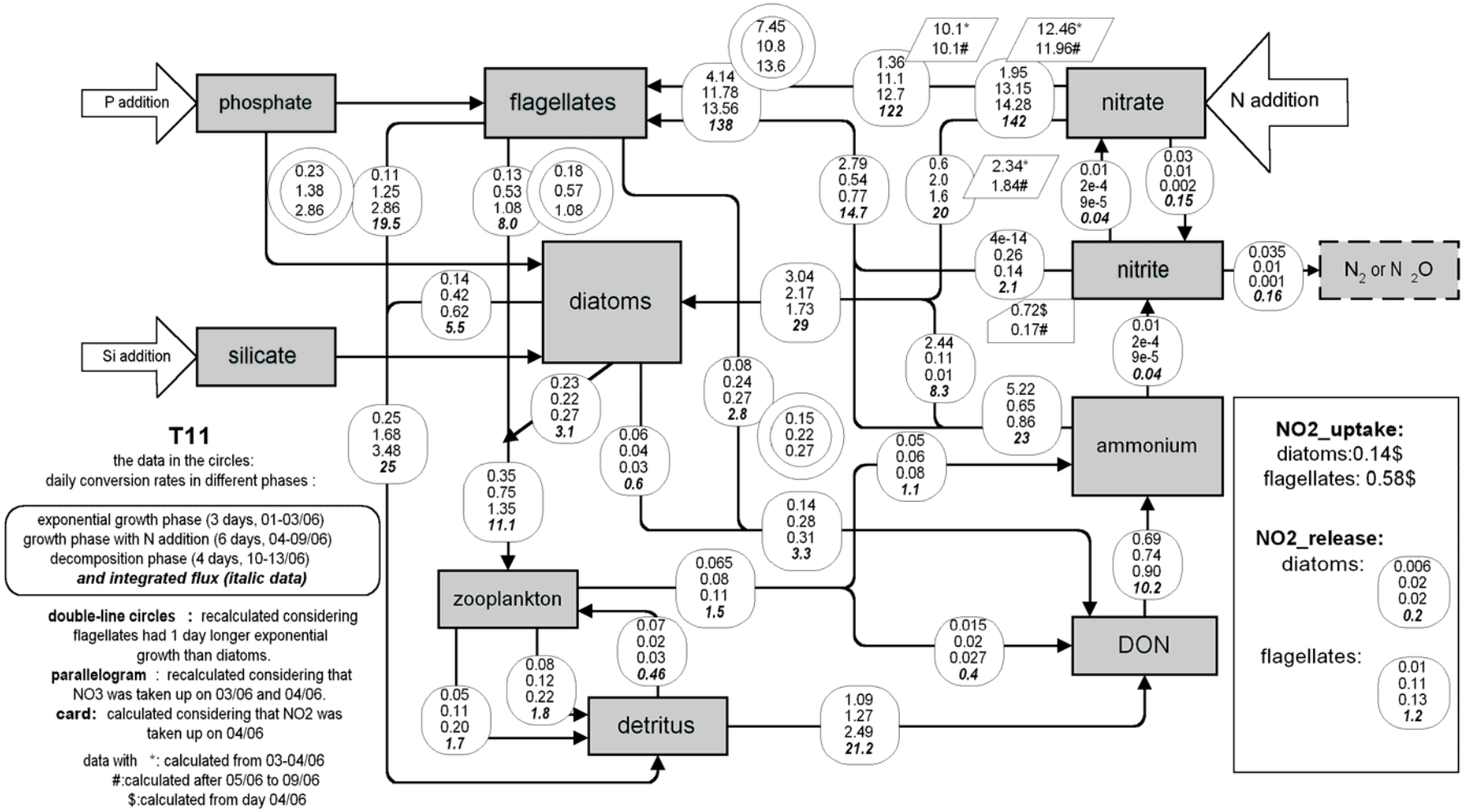

Fig. 4-8 Simulated daily conversion rates (in μM/d) between the main compartments during the different growth phases of the summer experimental system (T11) and integrated N-fluxes (in μM, integrated over the whole duration of 13 days, data in italic style). (data in the double-line circles: the daily conversion rates re-calculated considering that flagellates had 1 day longer exponential growth than diatoms; data in the parallelogram: the daily conversion rates re-calculated considering that NO3 was taken up intensively on 03/06 and 04/06; data in the card: the daily conversion rates re-calculated considering that NO2 was intensively taken up on 04/06.)

4.2.2.3 DON fluxes

DON simulation reflected well the trend of the real development both in spring and summer (Fig. 3-34J, 3-36J). DON, as a bulk parameter in N cycling, is related to various processes between different trophic compartments as already discussed in section 4.1.3.3. In this section, DON turnover is discussed according to the model simulations.

In the spring control bag, DON remained at steady state between detritus decay, phytoplankton release, zooplankton excretion and remineralisation. From the flux flow analysis (Fig. 4-5), it is shown that the gain terms of phytoplankton release, zooplankton excretion, detritus decay, covered 34%, 3% and 63% respectively. Phytoplankton DON release was minor in relation to DIN uptake (2%) during the whole experiment. The loss term of remineralisation covered 91% of the total DON gains. Slight increase in the last week resulted from the increasing release from phytoplankton cells under nutrient stress, and increasing decay of pelagic detritus with increasing temperature as shown in Fig. 4-9A. DON release from phytoplankton occurred mostly in the exponential phase (Brockmann et al. 1983b, 1992, Bronk et al. 1994, Myklestad 2000), as detected from the net flux of DON in Table 4-3. It also occurred in the stationary phase by leaking and cell breaking under nutrient stresses (Sharp 1977), however, the net flux was lower than that in the exponential phase (Table 4-3).

In summer, detritus decay contributed dominantly (covering 90%) to total DON production. Phytoplankton cell release was a minor process (10% of detritus decomposition, in total) (Fig. 4-7). At the same time, decomposition of DON to NH_4^+ was high and removed 75% of produced DON related to high bacterial activity. These processes kept DON in equilibrium (Fig. 4-9C), as discussed in section 4.1.3.3. Net fluxes show that DON accumulation rates were higher in the exponential growth phase than in the decomposition phase (Table 4-3). Compared to spring, the release of DON during the exponential growth was significant and its net fluxes were higher than spring by 3 times. In the decomposition phase, the net flux was higher than that in the decay phase in spring by one magnitude.

DON in T4 and T11 remained in the same range as control bags (T1, T8). Nutrient addition resulted in higher release both in spring and summer (Fig. 4-9B, D), but it also stimulated the growth of bacteria because the latter utilised DON as N source and DON thus partly converted to NH_4^+. From the model simulation, the contribution of zooplankton excretion to the DON pool is of minor importance as formerly assumed (section 4.1.3.3).

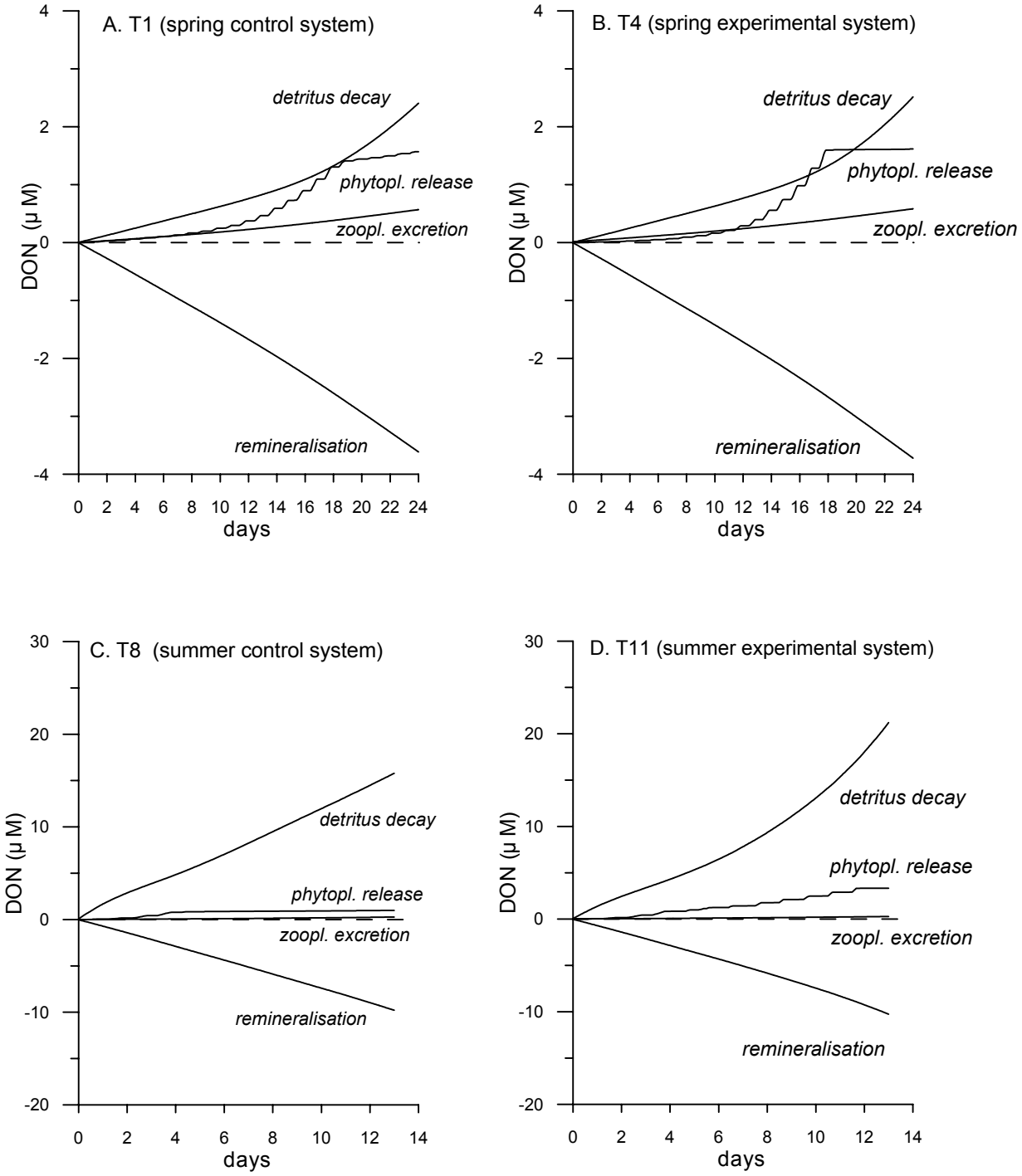

Fig. 4-9 Fluxes of DON from model simulations in the spring and summer experiments (integrated from hourly outputs, dash lines indicate the value of zero.)

4.2.3 Sensitivity analysis

Sensitivity analysis attempts to provide a measure of the sensitivity of parameters, initial condition or forcing functions, or submodels to the state variables of greatest interest in the model. Furthermore, it also reflects the properties of the model, but it may also have implications on the more complex natural systems.

In the current model, the development of diatoms and flagellates was sensitive to the respective initial values both in spring and summer, indicating that the enclosed systems were not biologically steady. The primary production and phytoplankton biomass formation were the dominant processes. The development of main inorganic nutrients corresponding to initial values of diatoms and flagellates reflected the different turnover of nutrients in relation to diatoms and flagellates.

The strong influence of the zooplankton initial value on phytoplankton indicated the top-down control of the pelagic structure and nutrient cycling. Phytoplankton growth was found to be suppressed and the bloom vanished by the fast growth of zooplankton, resulting from high initial values of zooplankton in the model tests. This was different between the enclosed ecosystem and the surrounding water system. Zooplankton might play an important role in controlling the growth of phytoplankton in the harbour water both in spring and summer, as showed by low chlorophyll *a* concentrations (Fig. 3-5, 3-10). In the harbour, large zooplankton, which was not enclosed in the mesocosm, might have provided top-down control of phytoplankon biomass (Glibert 1998).

Meanwhile, higher zooplankton initial values resulted in lower DON concentration (Fig. 3-42, 3-44), which implied that DON was released more by phytoplankton (Brockmann 1992).

As showed from the parameter sensitivity analysis, higher *Sp* values of diatom maximum growth rate than that of flagellates indicated that the diatom uptake and growth were the dominated processes in spring systems (Table A). During summer flagellate growth and uptake was more dominant (Table B). The effect on the nutrients was, in both cases, pointing to a faster uptake of those nutrients, which were more specific of the phytoplankton components: silicate and ammonium for diatoms and phosphate and nitrate for flagellates.

The half-saturation constants (*Ksa, Ksn*) as well as the ammonium and nitrate preference parameters ($\varphi 1$, $\varphi 2$) had only small effects on the model outputs, indicating that nutrients did not limit the growth rates during most of the period, except for a short time when diatoms and flagellates were blooming and nutrient concentrations decreased to the respective threshold. The ammonium concentrations both in the spring and summer bags could not upset the competition between diatoms and flagellates in favor of ammonium and were not controlled by the ammonium preference parameter or by the ammonium uptake formulation.

Because P and Si uptake were calculated according to nitrogen uptake, N/P and N/Si uptake ratios (*Rpn_uptk, Rsn_uptk*) were very essential to phosphorus and Si outputs in the model. On the other hand, low N/P and N/Si ratios would cause PO_4^{3-} and Si in the water to be exhausted earlier and thus

limit phytoplankton nitrogen uptake. For these reasons, these two uptake ratios were very sensitive parameters in the current model.

Zooplankton growth rate (*Rgmax*) had effects mostly on phytoplankton growth especially the higher growth rate suppressed phytoplankton growth. Its effect on DON and ammonium was not so strong, indicating that the influence of zooplankton on DON production was weakened due to the high concentration of refractory DON and low biomass of zooplankton assemblages in our mesocosms.

4.3 Comparison of model simulations and measurements

The results from modelling showed that the current model not only reproduced the main characters of the development of aimed state variables, but also had strong ability to hindcast the systems under nutrient enrichments both in spring and summer situations. The detailed comparison is made in this section, combining all simulations, not only to determine the strengths and weakness of the current model for further improving, but also to apply the model as a tool to provide some hints of evaluating the potential importance of some processes.

4.3.1 Comparison of nutrient simulations

4.3.1.1 Nitrogen nutrients

The model was successful in simulating the patterns of ammonium and nitrate uptake in spring experiments and the patterns of ammonium, nitrate and nitrite in summer experiments, indicating that the related parameters set in the model were acceptable.

The divergence in ammonium simulations in comparison to the measurement both in the spring control and experimental bags (T1 and T4, Fig. 3-34A, Fig. 3-38A) reflected some deficiency concerning the regeneration processes of ammonium in the current model. Significant development of bacteria (Dürselen 2002) could have changed DON remineralisation, due to different activities of different dominant species. This complicated process was simplified to one parameter related to transient DON concentration in the current model (eq. 35). Thus it can be derived that the remineralisation was overestimated, because the bacteria biomass was quite low at the beginning of the spring experiment. However, it was underestimated when the biomass increased quickly in the middle of the experiment. During the last 4 days, when the free bacteria decreased fast, the attached bacteria still had hold high biomass (Dürselen 2002). This high biomass of attached bacteria with simultaneous high activity (Hoppe 1976) together with high detritus contents would definitely fasten ammonium turnover. This constellation was omitted in the current model.

In the summer experiments, the over-estimation at the beginning was also significantly resulted in the time delay of ammonium exhaustion (Fig. 3-36A), which furthermore led to the time delay of nitrate and nitrite uptake (Fig. 3-36B, 3-36C). It again indicates that the fixed constant of DON remineralisation in the model might not be sufficient over the whole experiment in consideration of the different bacteria forms and their activities in the different periods of the experiments. The deviation could be more obvious in summer due to high bacterial activity in relation to high

temperature. Sight improvement in NH_4^+ simulations would reach by increasing the maximum growth rate of phytoplankton, but it will then totally miss the slight increase of ammonium at the end of experiment, because then NH_4^+ uptake rates by phytoplankton would exceed its replenishment from DON remineralisation.

The simulated nitrate both in spring and summer was higher than the measurements at the end, resulting from the earlier stop of uptake due to phosphate exhaustion in the water column. Phosphate exhaustion resulted in very strict P limitation to phytoplankton uptake. This directly resulted from the Michaelis-Menten-Monod equation, which connects the phytoplankton growth only with transient nutrient concentrations. Further discussion is given together with phosphate simulation in section 4.3.1.2.

NO_2^-, as a median product between nitrification and denitrification, is a very sensitive parameter related to variable microbial activities, also because of its low concentrations in the water column. The sensitivity was significantly reflected by the different development in the bags of the same sequence in spring. The main process of NO_2^- is the cell release during the phytoplankton surplus NO_3^- uptake. The accumulation of NO_2^- due to cell release was significantly reflected both in the control and experimental bags (Fig. 3-34C, Fig. 3-38C). However, the model did not strongly reproduce the fast decrease of NO_2^- at night-time, which was supposed due to nitrification/denitrification processes as discussed in section 4.1.3.2 and section 4.1.4. The variation of nitrite is tightly related to nitrification/denitrification, especially with the increase of bacteria and detritus. The deficit to simulate NO_2^- decrease was likely attributed to the simplification of these processes in the current model. In the current model, nitrification and denitrification were only related to the concentrations of nitrate, nitrite and ammonium in the water column.

In summer, turnover nitrification/denitrification was supposed to be faster than spring due to higher temperature and higher bacterial biomass in the water. However, low concentrations of inorganic nitrogen resulted in low fluxes of these processes (Fig. 4-8). And NO_2^- release and uptake were dominant processes and were significantly reflected from the model simulations, especially during the nutrient additions in the experimental bag. Though previous experiments showed that nitrite release and utilisation are related to temperature, light and preconditioning of algae (Raimbault 1986, Sciandra and Amara 1994), which were not considered in the model. However, very fast turnover within one day corresponding to large amount of phytoplankton made it neglectable.

4.3.1.2 Phosphate

The similar curves of PO_4^{3-} development from simulations and measurements indicated that the applied equation (eq. 16) in the current model can basically reflect phosphate uptake by natural phytoplankton assemblage (Fig. 3-34D, 3-36D, 3-38D, 3-40D).

However, both in the spring and summer experiments, there was time delay in PO_4^{3-} simulation. In summer, the time delay (half to one day) was shorter than that in spring (Fig. 3-36D), indicating that for N and P also conversion by other organisms will contribute to the total net turnover especially at

the higher summer temperatures. Anyhow, the time delay was supposed to result from luxury uptake by phytoplankton cells under sufficiently available PO_4^{3-} in the water.

Algae luxury uptake of phosphate was observed from several experiments (Sakamoto and Tanaka 1989, Vargo and Howard-Shamblott 1990, Chrzanowski and Kyle 1996). In this case, the nutrient uptake will be independent of the phytoplankton growth for a short time because the absorbed nutrients cannot be converted into biomass immediately. Therefore, the uptake and growth processes are separated. In the current model, the Michaelis-Menten-Monod equation used for phytoplankton growth could not distinguish the two separate metabolic steps. The simulated decrease of PO_4^{3-} concentrations could reflect the demanded phosphorus related to growth, while the measured PO_4^{3-} reflects the total uptake of phosphorus involving the replenishment of intracellular pools. Accordingly, stored phosphorus could be estimated by comparing the simulated results and real data sets. Furthermore, storage capacity of cells can be calculated in terms of phytoplankton cell number or biomass. The calculated P storage per cell by this way from the spring experimental system was variable from about 2.0×10^{-4} pM P/cell to 3.0×10^{-3} pM P/cell. No available experimental data concerning P storage were found. Measurements from Tarutani and Yamamoto (1994) showed the maximum uptake rate of starved *Skeletonema costatum,* which was about 38.4 fmol/cell per hour, while the minimum cell quota for phosphorus from semi-continuous culture was 2.8×10^{-3} pM P /cell per hour. Rough estimation showed that storage could be 35×10^{-3} pM P/cell. This is 1 or 2 magnitude higher than our estimation. This could be resulted from the fact that the cells in the experimental bags were not under phosphorus starvation.

In addition, the uptake of phosphate by algae was found to exhibit first-order kinetics with respect to the intracellular P-deficit. This deficit is the difference between the maximum and the actual intracellular P-concentration (Portielje and Lijklema 1994). The depletion of transient PO_4^{3-} will no doubt result in enhanced utilisation of intracellularly stored P and increase P uptake capacity (Jansson 1988). In this case, P enrichments will significantly stimulate phytoplankton PO_4^{3-} uptake and lead to luxury P uptake (Istvanovics et al. 1994). It was found also by Portielje and Lijklema (1994) that the maximum storage capacity of P per unit of dry weight of benthic algae was positively correlated to the level of external nutrient loading. Thus, phosphate uptake could have been under-estimated during nutrient enrichments in the summer experimental bag (Fig. 3-40D), when only one constant uptake rate was used for the whole experiments in the current model.

As nitrate simulations were consistent with the measurements, it can be derived that the simulation of nitrogen uptake in the model was acceptable. Because P uptake was simulated according to nitrogen uptake via N/P ratio in the model, it is sure that luxury uptake of P would have changed the instant N/P uptake ratios ($\Delta N/\Delta P$). For this reason, different N/P ($\Delta NO3/\Delta P$) uptake ratios were used to test the outputs of phosphate (Fig. 4-10). Better fits of simulations and measurements were reached when N/P ratios were raised. In the summer experimental system, the simulation was much better when the $\Delta N/\Delta P$ ratio was 10. This higher $\Delta N/\Delta P$ ratio was close to the measurements, which showed that $\Delta N/\Delta P$ was in the range from 10 to 22 (by atom) (table 3-1, section 4.1.3.1.2).

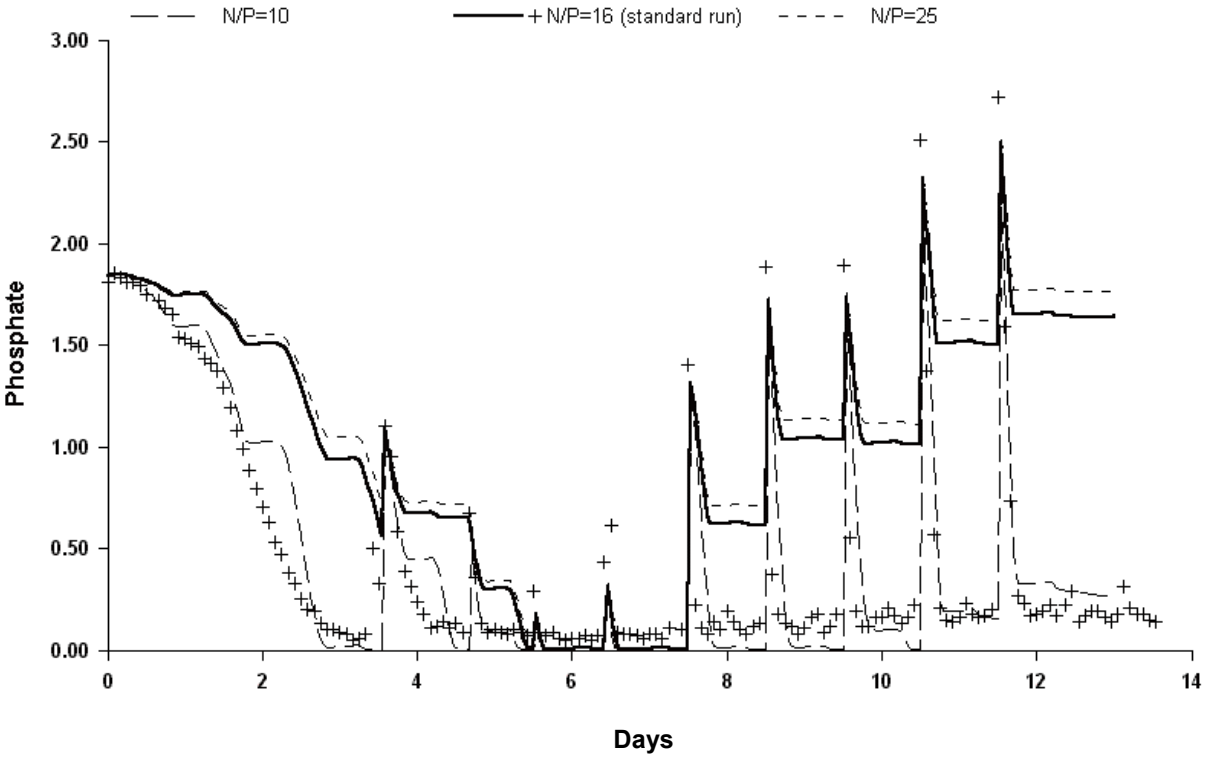

Fig. 4-10 Outputs of phosphate simulations in the summer experimental system (T11), considering different N/P ratios used in the model (Y-axis: phosphate in μM: Crosses: measurements).

4.3.1.3 Silicate

The simulated development of silicate was generally consistent with the measurements (Fig. 3-34E, 3-36E, 3-38E, 3-40E) in both spring control and experimental bags. However, the slight difference between the simulations and measurements might be caused by some simplification in the current model. The model treated the diatoms as a homogenous community at all times and used the same equation and parameters for silicate uptake during the whole spring experiment. This was a very simplified treatment of the real system, where succession of diatom species in the slower exponential phase and exponential phase was significant, resulting in different Si uptake behaviour. Higher concentrations of Si at last (Fig.3-34E) resulted from the P limitation, which caused the earlier stop in the exponential uptake of silicate by phytoplankton, the same as for nitrate.

In summer, the simulated Si fitted better to the measurements compared to spring (Fig. 3-36E). This could be attributed to the short exponential growth period in summer and the diatom species succession being not as variable as in spring. Thus, the diatom community did not change so much over the time and as a consequence the constants concerning to Si uptake in the model were more representative.

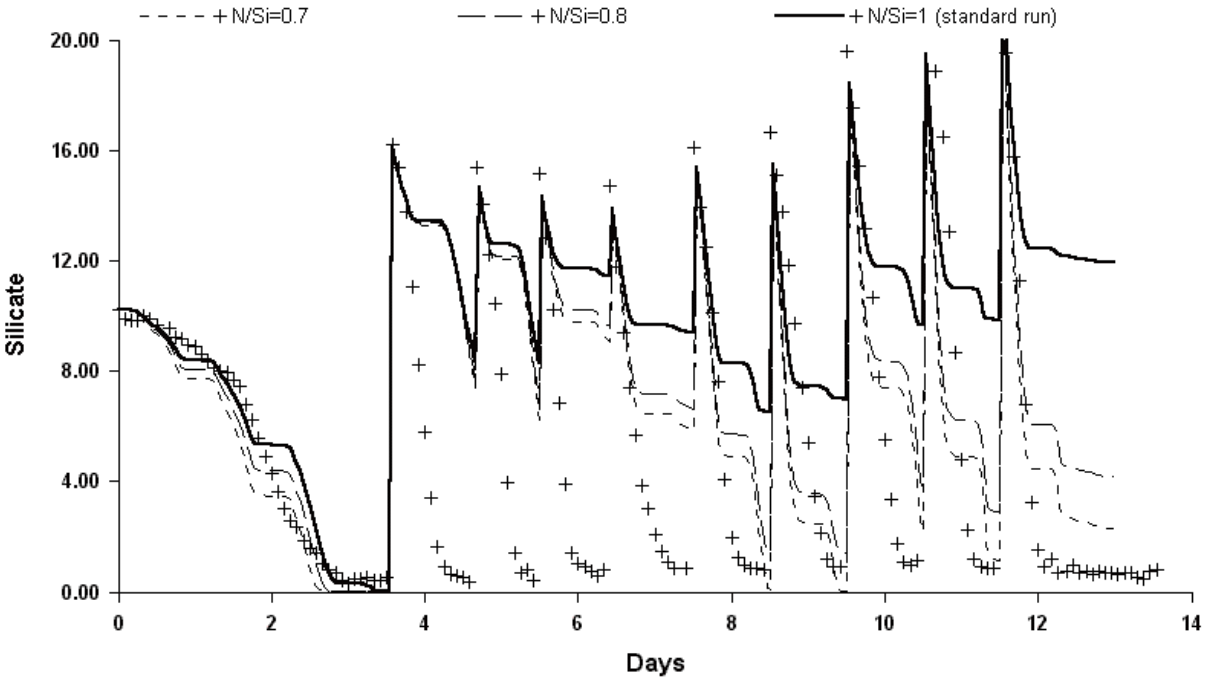

Fig. 4-11 Outputs of silicate simulations in the summer experimental system (T11), considering different Si/N ratios used in the model (Y-axis: silicate in μM: Crosses: measurements)

However, Si uptake during the nutrient additions in the summer experimental bag was of a little insufficiency (Fig. 3-40E). Two reasons might cause the differences between model simulations and the reality. First, diatoms might uptake Si excessively under the sudden addition of Si, which is mostly used for silification of the cell wall instead of growth (Paasche 1973, 1980). On the other hand, diatoms will generally continue to uptake Si also in the descending mode (Rey and Skjoldal 1987, Wassmann et al. 1997). These two processes were not included in the current model. In fact, these processes would finally change the instant N/Si uptake ratio. Considering this, different N/Si uptake ratios were tested to the outputs of silicate in T11 (Fig. 4-11). As expected, decreasing N/Si ratios resulted in better simulations compared to the standard run. However, at the same time, the simulated Si during the first three days was a little lower than the measurement.

Another possibility is related to changes of phytoplankton uptake after sudden nutrient enrichments similar to phosphate. The nutrient uptake rates changed when the cells were fertilised by nutrient addition after starvation, as proven by our measurements (Section 3.1.3.2) and lab experiments (Parslow et al. 1984a, 1984b). Schlüter (1998) observed from their mesocosm experiments that, with nutrient enrichments, the growth rates of diatoms and dinoflagellates could occasionally even reach up to 2.8 d^{-1}. In the model, diatoms were kept the same maximum growth rates as in spring, and flagellates maximum growth rate (*Rfmax*) was increased for the purpose of fitting the measurements. This modification might not be the most adequate change in the case of the current model and thus resulted in unsatisfactory Si simulation. This concerned point will be further discussed together with the simulation of phytoplankton composition in the summer experiments in section 4.3.1.2.

4.3.2 Comparison of DON

The measured DON showed very large scattering. Very frequent variation of DON within short times was not significantly reflected in the current model. DON variation was mostly controlled by detritus decomposition and remineralisation. The integrated changes of these two processes could reach much higher than instant DON concentrations by 3 to 4 times in spring and 20 to 10 times in summer (Fig. 4-9). However, phytoplankton DON release under nutrient pressure and possible phytoplankton utilising DON (Ietswaart et al. 1994) were not included in the model.

4.3.3 Comparison of particulate matter

4.3.3.1 Particulate nitrogen (PN)

The amount of measured PN includes nitrogen contents in phytoplankton, zooplankton, detritus as well as attached bacteria and those were retained on the filters. In the model, bacteria were only implicitly included. The role of bacteria in N turnover was reflected in related parameters and its biomass was mostly in relation to detritus.

The model reproduced the main features of PN development both in the control and experimental bags of the spring experiment (Fig. 3-34F, 4-38F). Significant diurnal variations especially occurred in the exponential phase indicated the dominance of light-dependence of photosynthesis.

As also indicated by the measurements, diatoms dominated the spring phytoplankton community. Phosphate addition to the experimental bag mostly fertilised diatoms, which was consistent with the field observations (Dürselen et al. 2002a). The growth of flagellates was inhibited because flagellates could not compete with faster growing diatoms on N and P uptake when silicate was above the threshold concentration of 2 μM for diatoms (Peperzak et al. 1998). A slight decrease of about 2 to 3 μM of diatom and flagellates biomass in nitrogen during the stationary phase were attributed to slow growth and higher mortality, N release of phytoplankton under P limitation, and increasing grazing pressure as well (Fig. 3-34G).

Both in the control and experimental bags, the overall PN development was well simulated. Considering the earlier stop of nitrate uptake compared to the measurements at the end of the experiments (Fig. 3-34B, 3-34 F), it can be derived that there was some under-estimation in the turnover of particulate N pool to dissolved N pool, which led to some accumulation of PN. Considering the lower ammonium in simulation at the same time (Fig. 3-34A), it implies that detritus decomposition and regeneration of ammonium from organic nitrogen related to different activities in bacteria succession was under-estimated in the model.

In summer, the simulations showed that diatoms dominated phytoplankton during the first 3 days and reached the maximum on day 3. During this period, high Si concentrations prevented flagellates development and ensured diatom dominance as formulated by Officer and Ryther (1980). Afterwards, Si quickly dropped to lower than 1 μM and the diatom bloom started to decay due to silicate limitation. The flagellates then utilised the remaining N and P and dominated the

phytoplankton N pool (Fig. 3-36G). The simulated succession of diatom and flagellates groups are in accordance with the results from other mesocosm experiments (Jacobsen et al. 1995). However, there is of disputation from the observation of our experiments, which showed that diatoms dominated phytoplankton assemblage (Dürselen et al. 2002b). From the experiment view, phytoplankton coexistence and competition are not only controlled by various conditions, such as light climate, nutrients and temperature so on. Temperature could be one of the major factors for the differences. Diatoms were found to have lower temperature optimum than flagellates, according to Harrison and Turpin (1982). The optimum temperature for maximum growth rates of most diatoms lies below 25 °C, while, for most flagellates it may be higher than 25°C. During the whole summer experiment, temperatures varied below 20 °C. Such low temperature might have severely halted the growth of flagellates in the summer enclosures. However, this factor was missed in the current model, in which, same Q_{10} was used both for diatoms and flagellates.

In the experimental bag, nutrient enrichments mostly fertilised flagellates. This was not the case from the observations (Dürselen et al. 2002b), which showed that diatoms again dominated the phytoplankton community in summer enclosures.

Besides the possibility of the different temperature effects on the diatoms and flagellates in the above discussion. There is another possible explanation from modelling view. As discussed in section (4.2.1), the maximum growth rate of flagellates was modified to be higher than that of diatoms for the purpose of fitting the simulation. This can happen when silicate became limiting nutrient from diatoms in the summer water column (with DIN/Si about 4) and flagellates have a higher potential ability to use surplus nitrogen and phosphorus for growth than diatoms as can been seen in the summer control bag.

However, in the experimental bag, a large amount of silicate (with DIN/Si about 1) added to the water could have stimulated the growth of diatoms (Schlüter 1998). Meanwhile, the growth of flagellates could have been suppressed because of the strong ability of diatoms to utilise nitrogen and phosphorus when offered sufficient silicate (Officer and Ryther 1980). This could have resulted in higher abilities of diatoms for silicate uptake (affinity). So in the current model, the assigned maximum growth rates for the respective diatom and flagellate assemblages have not been able to cover the short-term variations of different phytoplankton groups during the sudden additions, and led to the dominance of flagellates and under-estimation of silicate uptake. For this, a test was done by increasing *Rdmax* to 2.8 d^{-1} and keeping *Rfmax* the same as spring (2.4 d^{-1}). The results showed that diatoms dominated over flagellates in the experimental bag without changing total PN development (Fig. 3-40G, simulation2).

In combination with N, P simulation, the simulation of the short-term N uptake would need to consider intracellular nutrient pools. However, by just simply increasing the *Rdmax* may not be the best solution because Si uptake in the first three day then would be over-estimated as shown in Fig. 3-40E (simulation2). As diatom growth is exclusively related to Si availability (Werner 1977). Thus, it is derived from the simulations of Si both in spring and summer that the set *Rdmax* most probably

should be right.

On the other hand, the purpose of increasing *Rfmax* in summer simulations was in consideration to nitrogen and phosphate simulations. But, in the enclosed water column, inorganic N and PO_4^{3-} might have been utilised by bacteria for growth or transferred to DON due to high activity in summer (Wheeler and Kirchman 1986, Fuhrman et al. 1988, Horrigan et al. 1988, Lebo 1991, Groenlund et al. 1996). These processes were not considered in the current model, which have partly caused the under-estimation of DIN and P.

Both in the spring and summer experiments, no zooplankton data were available for the comparisons. The simulated zooplankton biomass increased exponentially both in spring and summer because of little grazing pressure from higher predators, which were excluded by initial filtration through a 1 mm net (Figs. 3-28H). Sufficient food source from phytoplankton biomass, higher temperature and higher initial concentrations made zooplankton develop faster than in spring. In summer experimental bag, nutrient addition caused increase of zooplankton growth, as shown also in flux calculations (Fig. 4-8).

Detritus N occupied majority of total PN at the beginning of the spring experiment. It increased mostly in the stagnation, resulting from phytoplankton mortality under nutrient depression.

In summer, simulated detritus N decreased very fast during the first two days, indicating higher decomposition rates related to higher temperature (Fig. 3-31I). Afterwards, contributions from phytoplankton mortality, zooplankton faecal pellets and mortality led to an increase at the end. However, the detritus contents did not reach spring values because the high loads of attached bacteria biomass (Dürselen 2002) quickly decomposed the detritus to dissolved organic matter under higher temperature, resulting in a simultaneous DON increase (Fig. 3-31J).

4.3.3.2 Particulate phosphorus (PP)

Both in spring, simulations of PP showed some time delay compared to the measurements. As for the PO_4^{3-} simulation, the question of luxury P uptake, which was excluded in the current model, was again a possible reason for this variance. The increase of the differences over the time likely indicated that the excessive P uptake increased with the increase of phytoplankton biomass (cell number) (Vargo and Howard-Shamblott 1990, Chrzanowski and Kyle 1996). This P-storage will cause higher cell quota of P and separates the processes of PO_4^{3-} uptake and its assimilation by cells, which could not be included in the applied Michaelis-Menten-Monod equation.

However, in summer control bag, there was some over-estimation in the decomposition phase. Combined with overestimation of PN during the same period, it likely indicates the insufficient estimation in summer simulations compared to the real situations remineralisation processes e.g. detritus decomposition, phytoplankton release or zooplankton excretion. Different to the control bag, simulated PP was under-estimated, which resulted from the under-estimation of phosphate uptake during the nutrient enrichments.

4.3.4 Summary of the model simulations

The model reproduced the main features of the development of the main N compartments both in spring and summer. The patterns and the interactions of the three forms of nitrogen nutrient uptake, the development of phytoplankton N, as well as the DON development were simulated very well in comparison to the measurements. It is concluded that the nitrogen dynamics in the pelagic system was mostly determined by the biologically mediated transformations of nutrient uptake and regeneration. The higher trophic levels played a minor role in nutrient dynamics. From the nitrogen specific aspect, the model showed strong capability to reasonably detect the development of the pelagic system under nutrient enrichment. Fitness analysis of the model showed that the model is able to explain 90% of the variation in spring and 65% of the variation in summer.

The deficits of the current model to simulate the short-term variations of P and Si uptake after sudden addition were attributed to the applied equation of nutrient uptake: the Michaelis-Menten-Monod equation, relating the phytoplankton reproductive growth rate to the ambient nutrient concentration only (Monod 1950). This equation was used frequently in ecological models and offers numerical stability. Especially on simulating monthly or annual variations in natural ecosystems or enclosed natural systems, the Monod equation should be sufficient for the current model and many other models as well (Fasham et al. 1990, Aksnes et al. 1995, Bissett et al. 1999, Oguz et al. 1996, 1999). However, at the shorter time scale (hourly to daily), especially concerning the short-term uptake and growth under bio-disturbance, the Droop equation with consideration of cell-quota in phytoplankton species could be used to describe the growth of phytoplankton. Under these conditions, the growth was found to be determined more by intracellular nutrient contents (Droop 1968, 1970, 1973). The success of the Droop equation has been shown in some models mostly of results from laboratory experiments and dynamic settings (Flynn et al. 1997, Davidson and Gurney 1999). This is due to the fact that the processes of transportation and assimilation related to different species would be more essential and should be carefully considered (Davison and Gurney 1999, Roelke et al. 1999) on those time scales. It is generally accepted that under the steady-state and not nutrient-limited situation, or equally limited by several nutrients, the Monod and Droop equations are coincident because uptake rates are equal to phytoplankton growth rates and to the ratio of subsistence quotas (Legovic and Cruzado 1997).

However, what should be more carefully considered when using the Droop equation is that some parameters, such as intracellular nutrient status which are not well documented due to the varieties with the species and transient nutrient status, have to be added to the model. This will result in an increase in uncertainty of the model (Jϕrgensen 1992). More experiments and measurements on physiology should be carried out.

Although the microbial loop has been realised to be more and more important to element cycling in various marine ecosystems (Billen et al. 1990, Fuhrman 1992, Capone 1997), our knowledge of it is still very limited and a quantification of the relative processes is yet impossible. The roles of bacteria

were specifically correlated to ammonium and phosphorus remineralisation, DON turnover, nitrification and denitrification in the current model. However, bacteria were only implicitly included, and processes related to bacteria were mainly considered and reflected by some parameters such as detritus decay (*Rddecay0*), DON remineralisation (*Rremin0*), nitrification (*Rni0*) and denitrification (*den0*, *den02*). These parameters were not sensitive according to the sensitivity analysis, indicating that bacteria related processes were not dominant in the development of aimed state variables in the current model. Nevertheless, bacteria might play a more important role in the nitrogen turnover in the summer experiment than suggested by the model, by increasing the values of related parameters as in the current model. The missing implementation of these compartments in the model was maybe an additional reason for the discrepancy between modelled and measured phosphate, beside the luxury uptake, because bacteria compete with the phytoplankton for inorganic phosphate when DOP is not available in sufficient amount in the marine environment (Harrison et al. 1977, Thingstad et al. 1993). Moreover, marine bacteria could also compete for inorganic nitrogen (esp. ammonium) with phytoplankton when there is insufficient nitrogen in organic substance (Wheeler and Kirchman 1986, Fuhrman et al. 1988, Suttle et al. 1990). This could be another reason for higher NH_4^+ concentrations in the simulation of the summer experiments at the beginning of the experiments (Fig. 3-36A, Fig. 3-40A). Bacteria and related processes will be carefully included and considered in the next step of the model improvement.

5 CONCLUSIONS

Though large-scale monitoring studies have provided valuable insights into plankton ecology, they have their limitations in respect to process understanding, caused by the different spatial and temporal scales of planktonic processes, superimposed by hydrodynamic processes as well as by anthropogenic effects especially in coastal areas. Mesocosm experiments have been proven to be an essential tool to study intensively purposive processes in enclosed natural water masses under natural conditions of light climate and temperature, eliminating advective interference.

Meanwhile, model simulation, tested with mesocosm data has proven to be a supplementary tool to qualify the linked processes and supply interdisciplinary understanding of the aimed ecosystem.

Nutrient gradients in the German Bight are strongly influenced by the river Elbe. In spring, high concentrations of nutrients, especially nitrate, resulted from high discharges of the river Elbe in this season can not be utilised in the turbid coastal water due to light limitation. In stratified areas, simulated by the enclosure in mesocosms, nutrients will be converted completely. The surplus of nitrogen is finally causing phosphate and silicate limitation. In the open water, no significant phytoplankton bloom was detected during both spring and summer experiments. Although, similar transmission with the enclosures was measured, the photosynthesis rate decreased below 1% of that in surface underneath 2 meters. Vertical mixing and circulation including deep tidal channels in the coastal water prevented the formation of a phytoplankton bloom over the whole water body. The variations of nutrients in open water over the whole experimental duration were more affected by tidal action, advective exchange, interaction with sediment and local processes such as bacterial utilisation.

The spring experiment started in middle March, which was earlier than the normally detected start of the spring bloom in the open German Bight, during April/May. However, the light climate played the most important role in the turbid water by triggering the phytoplankton blooms in spring and summer as well when the compensation depth was reduced to the upper 2 to 3 m by keeping the enclosures at the surface (2 or 3 m), which enabled a net primary production in comparison to the open system.

The applied mesocosms made it possible to trace the significant patterns of N nutrient utilisations. NH_4^+ is always the preferential N source in comparison to NO_3^- despite of different transient NO_3^- /NH_4^+ ratios from spring to summer. The correlations between chlorophyll and NO3/NH4 indicated co-uptake of NH_4^+ and NO_3^- while NH_4^+ was in the range of 1.0 to 3.0 µM. Nitrite release was tightly coupled to nitrate uptake, reaching about 0.8% to 1% of NO3 uptake. It increased to 1.1% to 2.6% of NO3 uptake during nutrient enrichments. In spite of low concentration (< 0.7 µM), nitrite was a substituent N source, as indicated by its correlation with chlorophyll *a*, when NO_3^- was depleted below 1.0 µM.

Phytoplankton growth was very much dependent on available nutrient concentrations, shown by significant correlations between chlorophyll *a* and nutrients, indicating bottom-up controlled

ecosystem in river plume water.

Si <1.0 µM strictly limited diatom growth. This state was reached even in the shallow mesocosm, indicating the strong fixation of silicate in the cell walls of the diatoms, whereas other nutrients will be remobilised faster. For this reason flagellates covered high proportion in the phytoplankton community in summer compared to spring, showing strong ability to utilise low concentration of N and P in the water under Si depletion.

Different treatments of nutrient addition to the enclosed water in spring and summer were carried out to test the production potential of the ecosystems simulating mixing of nutrient-rich water at river plume fronts. Primary productivity and phytoplankton biomass were significantly enhanced due to nutrient enrichments, in agreement with the field investigations.

Diurnal variations of photosynthesis and nutrient uptake were detected by frequent sampling, allowing the calculation of diurnal turnover rates such as photosynthesis rates and nitrate uptake. Together with chlorophyll *a* increase starting at noon, significant net photosynthesis occurred mostly in the afternoon, reaching 5 to 8 µg POC (µg chl*a*)$^{-1}$ h^{-1} in spring. A shift of maximum photosynthesis to late morning in summer was observed due to photoinhibition. Respiration, cell exudation and cell division resulted in net C decomposition at night, showing the rates of 1 to –2 µg POC (µg chl*a*)$^{-1}$ h^{-1}. Ammonium uptake was characterised by high frequent fluctuation but no significant diurnal changes were observed, resulting from its fast turnover between uptake and regeneration from microzooplankton and bacteria. Significant diurnal changes of nitrate are owed to strong light-dependent uptake by cells related to nitrate reductase activity (NRA). The estimated net NO_3^- uptake reached upto three to four times higher value than that at night.

The similar identical initial concentrations of DON in spring and summer indicate that the major part of DON in the German Bight either was only slowly converted as suggested by the field investigations or was kept at a steady state between the processes of production, such as detritus decomposition, phytoplankton release, zooplankton excretion and losses during partial decomposition by bacteria. From the data analyses, together with model simulations, it is shown that in spring, slight accumulation of DON is more a result of phytoplankton cell release during bloom, whereas in summer, net DON gain is mostly related to bacterial activity.

Both in spring and summer, N losses of 8% (1.5 mmol m^{-2} d^{-1}) and 15% of total nitrogen (2.5 mmol m^{-2} d^{-1}) from the water column are assumed to be caused by denitrification within anoxic microzones enclosed in detritus particles and plankton aggregates.

By the box model, the development of N compartments both in spring and summer experiments was successfully reproduced, with deviations of less than 10%. Phytoplankton biomass formation was the dominant process both in spring and summer enclosures. In spring, it accounted for 74% of DIN consumption. 13% of primary production were transfered to detritus pool. In summer, phytoplankton biomass formation accounted for 60% of DIN uptake. Higher microzooplankton grazing during summer increased remineralisation proecess. Bacteria played a more important role

in N turnover in summer than spring. Phytoplankton biomass decomposition was at 1.2 µM N d^{-1} enhanced due to high temperature during summer and significantly dominated after nutrient depletion.

By comparing the simulations with measurements, it is shown that the Monod equation has high stability to describe the main features of nutrient uptake and phytoplankton growth in our enclosed ecosystems both under spring and summer conditions, especially concerning nitrogen transformation. Differences between model calculations and measurements are related to simulation of phosphate and uptake under nutrient additions. The Droop equation has the advantage in simulating phytoplankton growth under the non-steady state and external perturbation when intracellular nutrient status have to be considered. However, the Monod equations have the advantage to simulate nutrient uptake and phytoplankton growth under the natural conditions within the mesocosm time scales.

Deviations between model and measurements especially during summer require the consideration of bacterial turnover, including also competition with the phytoplankton for nutrients. The bacteria related processes and microbial loop should be more carefully considered and included for further improvement of the model.

The combination of mesocosm experiments with the box model allowed a detailed analysis of the biogeochemical fluxes as shown by nitrogen compounds. The results from the mesocosms and modelling studies could be applied for interpretation of processes within the dynamic nutrient-rich coastal waters. The knowledge of the reaction potential of river plume water is of importance for future mangement measures.

REFERENCES

Aksnes D.L., K.B. Ulvestad, B.M. Balino, J. Berntsen, J.K. Egge and E. Svendsen, 1995. Ecological modelling in coastal waters: Towards predictive physical-chemical-biological simulation models. *Ophelia* 41: 5-36.

Alcaraz M., 1988. Summer zooplankton metabolism and its relation to primary production in the western Mediterranean. Pelagic mediterranean oceanography. In Minas H.J. and P. Nival (Eds): Oceanographie pelagique mediterraneene: Aspects interdisciplinaires-De-L' oceanographie mediterraneene Dans Le domaine pelagique. 9: 185-191.

Alcaraz M., E. Saiz, M. Estrada, 1994. Excretion of ammonia by zooplankton and its potential contribution to nitrogen requirements for primary production in the Catalan Sea (NW Mediterranean). *Mar.-Biol.* 119(1): 69-76.

Anderson S.M. and O.A. Roels, 1981. Effects of light intensity on nitrate and nitrite uptake and excretion by *Chaetoceros curvisetus*. *Mar. Biol.* 62: 257-261.

Andersen V. and P. Nival, 1987. Modelling of a planktonic ecosystem in an enclosed water column. *J. Mar. Biol. Ass. U. K.* 67: 407-433.

Andersen V. and P. Nival, 1989. Modelling of phytoplankton population dynamics in an enclosed water column. *J. Mar. Biol. Ass. U. K.* 69: 625-646.

ARGE Elbe 1999. Wassergütedaten der Elbe, Zahlentafel 1999, 207 pp.

Ayres R.U., W.H. Schlesinger and R.H. Socolow, 1994. Human impacts on the carbon and nitrogen cycles. In: R.H. Socolow, C. Andrews, R. Berkhout and V. Thomas (Eds): Industrial ecology and global change. Cambridge University Press, Cambridge Mass, 121-155.

Banse K., 1976. Determining the carbon to chlorophyll ratio of phytoplankton. In: Book of abstracts of papers presented at Joint Oceanographic Assembly. Edinburgh, UK.

Banse K., 1982. Experimental marine ecosystem enclosures in a historical perspective. In: G.D. Grice and M.R. Reeve (Eds): Marine mesocosms, biological and chemical research in experimental ecosystems. Springer-Verlag, Berlin Heidelberg, 10-24.

Baraniok B., 1994 (Diplomarbeit). Verteilung von Aminosäuren in Küstengewässern der Deutschen Bucht. FBR Chemistry, University Hamburg. 130 pp.

Barnes J., N.J.P. Owens, 1998. Denitrification and nitrous oxide concentrations in the Humber Estuary, UK, and adjacent coastal zones. Mar. Pollut. Bull., 37(3-7): 247-260.

Beddig S., U.H. Brockmann, W. Dannecker, D. Körner, T. Pohlmann, W. Puls, G. Radach, A. Rebers, H-J Rick, M. Schatzmann, H. Schlünzen and M. Schulz, 1977. Nitrogen fluxes in the German Bight. *Marine Pollution Bulletin*, 34 (6): 382-394.

Benitez-Nelson C.R. and K.O. Buesseler, 1999. Variability of inorganic and organic phosphorus turnover rates in the coastal ocean. *Nature* 398(6727): 502-505.

Berges J.A., W.P. Cochlan and P.J. Harrison, 1995. Laboratory and field responses of algal nitrate reductase to diel periodicity in irradiance, nitrate exhaustion, and the presence of ammonium. *Mar. Ecol. Prog. Ser.* 124 (1-3): 259-269.

Bidigare R.R., 1983. Nitrogen excretion by marine zooplankton. In: E.J. Carpenter and D.G. Capone (Eds): Nitrogen in the marine environment. Academic Press, 385-409.

Billen G., C. Joiris, L. Meyer-Reil and H. Lindeboom, 1990. Role of bacteria in the North Sea ecosystem. *Neth. J. of Sea Res.* 26(2-4): 265-293.

Bissett W.P., J.J. Walsh, D.A. Dieterle and K.L. Carder, 1999. Carbon cycling in the upper waters of the Sargasso Sea: I. Numerical simulation of differential carbon and nitrogen fluxes. *Deep-Sea Res. I,* 46: 205-269.

Blackburn T.H. and Sϕrensen J. (Eds) 1988. Nitrogen cycling in coastal marine environments, SCOPE, Wiley and Sons Ltd, New York, 451 pp.

Brockmann U.H., K. Eberlein, H.D. Junge, H. Trageser and K.J. Trahms, 1974. Einfache Folientanks zur Planktonuntersuchung in situ. *Mar. Biol.* 24: 163-166.

Brockmann U.H., K. Eberlein, G. Hentzschel, H.K. Schöne, D. Siebers, K. Wandschneider and A. Weber, 1977. Parallel plastic tank experiments with cultures of marine diatoms. *Helgoländer Wiss. Meeresunters.* 30: 201-216.

Brockmann U.H., K. Eberlein, H.D. Junge, E. Maier-Reimer and D. Siebers, 1979. The development of a natural plankton population in an outdoor tank with nutrient-poor sea water. 2. Changes in dissolved carbohydrates and amino acids. *Mar. Ecol. Prog. Ser.* 1: 283-291.

Brockmann U.H., E. Dahl, J. Kuiper and G. Kattner, 1983a. The concept of POSER (Plankton Observation with Simultaneous Enclosures in Rosfjorden). *Mar. Ecol. Prog. Ser.* 14: 1-8.

Brockmann U.H., V. Ittekkot, G. Kattner, K. Eberlein and K.D. Hammer, 1983b. Release of dissolved organic substances in the course of phytoplankton blooms. In: J. Sündermann and W. Lenz (Eds): North Sea dynamics. Springer-Verlag, Berlin, Heidelberg, New York, 530-548.

Brockmann U.H., and K. Eberlein, 1986. River input of nutrients into the German Bight. In S. Skreslet (Ed): The freshwater outflow in coastal marine ecosystem, 231-240.

Brockmann U.H., 1990, Pelagic mesocosms: 2. Process studies. In: C.M. Lalli (Ed): Enclosed experimental marine ecosystems: a review and recommendations. Springer-Verlag, 81-108.

Brockmann U.H., 1992. Enclosed plankton ecosystems in harbours, Fjords and the North Sea - release and uptake of dissolved organic substances. In: C.S. Wong and P.J. Harrison (Eds): Marine ecosystem enclosed experiments, IDRC, Ottawa, CA, 66-86.

Brockmann U.H., T. Pohlmann, G. Becker, P. König, L Aletsee, H.J. Rick, M. Krause, P. Martens, R. Knickmeyer and K. Heyer, 1994. Ecological situation in the North Sea during spring and winter 1986/1987. In: J. Suendermann (Ed): Circulation and contaminant fluxes in the North Sea. Springer-Verlag, Berlin, 56-89.

Brockmann U.H. and G. Kattner, 1997. Winter-to-summer changes of nutrients, dissolved and particulate organic material in the North Sea. *Dt. hydrogr. Z.* 49: 229-242.

Brockmann U H, T. Raabe, K.-J Hesse, K. Viehweger, T. Pohlmann, H.-J. Rick, A. Starke, B. Fabiszisky, R. Heller, 1998. Phase transfer, turnover and transport of nutrients in the German Bight during spring, summer and winter (1994-1996). In: KUSTOS and TRANSWATT Abschlussbericht, Band 2, ZMK, University Hamburg, 279-348

Brockmann U., T. Raabe, K. Hesse, K. Viehweger, S. Rick, A. Starke, B. Fabiszisky, D. Topcu and R. Heller, 1999a. Seasonal budgets of the nutrient elements N and P at the surface of the German Bight during winter 1996, spring 1995, and summer 1994. *Dt. hydrogr. Z.* 51(1): 1-24.

Brockmann U.H., K. Viehweger, T. Raabe, S. Rick, H.-J. Rick, R. Heller and D. Topcu., 1999b. Conversion of nutrients in the Elbe River plume during drift experiments in the German Bight during spring 1995 and summer 1994. *Dt. hydrogr. Z.* 51(2/3): 293-312.

Brockmann U.H. and D. Topcu , 2001. Nutrient atlas of the North Sea, UBA, Berlin (ca. 300 pp., in print).

Brockmann U.H., M. Zhang, S. Qian, C. Dürselen, K. Hesse, T. Raabe and A. Starke, 2002. Mesocosm studies at Büsum, German Bight in 1999. Frame, reproduceability and representativity. (ca. 21 pp., in prep.).

Bronk D.A. and P.M. Glibert, 1993. Application of a ^{15}N tracer method to the study of dissolved organic nitrogen uptake during spring and summer in Chesapeake Bay. *Mar. Biol.* 115(3): 501-508.

Bronk D.A., P.M. Glibert and B.B. Ward, 1994. Nitrogen uptake, dissolved organic nitrogen release, and new production. *Science* 265: 1843-1846.

Bronk D.A. and B.B. Ward, 1999. Gross and net nitrogen uptake and DON release in the euphotic zone of Monterey Bay, California. *Limnol. Oceanogr.* 44(3): 573-585.

Brzezinski M. A., 1985. The Si:C:N ratio in marine diatoms: Interspecific variability and the effect of some environmental variables. *J. Phycol.* 21: 347-357.

Burckhardt R. and R. Heerkloss, 1999. Consumption and faecal pellet production for *Eurytemora affinis* (Poppe) (*Calainoida, Copepoda)*. Rostock. Meeresbiol. Beitr., No.7: 91-110.

Butler E.I., E.D.S. Corner and S.M. Marshall, 1970. On the nutrition and metabolism of zooplankton. VII. Seasonal survey on nitrogen and phosphorus excretion by *Calanus* in the Clyde sea area. *J. Mar. Biol. Ass. U.K.* 50: 525-560.

Butler E.I., S. Knox and M.I. Liddicoat, 1979. The relationship between inroganic and organic nutrients in sea water. *J. Mar. Biol. Ass. U. K.* 59: 239-250.

Cabrita, M. T., F. Catarino, G. Slawyk, 1999. Interaction of light, temperature and inorganic nitrogen in controlling planktonic nitrogen utilization in Tagus Estuary. *Aquatic Ecology* 33(3): 251-261

Cadèe G.C. and J. Hegemann, 1993. Persisting high levels of primary production at declining phosphate concentrations in the Dutch coastal area (Marsdiep). *Neth. J. Sea Res.* 31: 147-152.

Capone D.G., 1997. Microbial nitrogen cycling. In: C.J. Hurst, G.R. Knudsen, M.J. McInerney, L.D. Stetzenbach and M.V. Walter (Eds): Manual of environmental microbiology. ASM Press, Washington, D.C., 334-342.

Carpenter E.J., Remsen C.C. and Watson S.W., 1972. Utilization of urea by some marine phytoplankters. *Limnol. Oceanogr.* 17, 265.

Carpenter E.J. and D.G. Capone (Eds), 1983. Nitrogen in the marine environment. Academic Press. Kluwer Academic Publishers, Dordrecht/Boston/London, 900 pp.

Carter R.A., P. D. Bartlett, V.P. Swart, 1986. Estimates of the nitrogen flux required for the maintenance of subsurface chlorophyll maxima of the Agulhas Bank. *Marine interfaces ecohydrodynamics.* Nihoul J.C.J. (Ed) 42: 331-340.

Chapelle A, P. Lazure and A. Menesguen, 1994. Modelling eutrophication events in a coastal ecosystem. Sensitivity analysis. *Estuarine, Coastal and Shelf Science* 39: 529-548.

Chrzanowski T.H. and M. Kyle, 1996. Ratios of carbon, nitrogen and phosphorus in Pseudomonas fluorescens as a model for bacterial element ratios and nutrient regeneration. *Aquat. Microb. Ecol.* 10 (2): 115-122.

Cochlan W.P., P.J. Harrison and K.L. Denman, 1991. Diel periodicity of nitrogen uptake by marine phytoplankton nitrate rich environments. *Limnol. Oceanogr.* 36 (8): 1689-1700.

Collos Y., 1982. Transient situations in nitrate assimilation by marine diatoms II: Changes in nitrate and nitrite following a nitrate perturbation. *Limnol. Oceanogr.* 27 (3): 528-535.

Collos Y., 1998. Nitrate uptake, nitrite release and uptake, and new production estimates. *Mar. Ecol. Prog. Ser.* 171: 293-301.

Dagg M.J., 1976. Complete carbon and nitrogen budgets for the carnivorous amphipod, Calliopius laeviusculus (Krϕyer). *Int. Rev. Gesamten Hydrobiol.* 61: 297-357.

Danovaro R., 1998. Do bacteria compete with phytoplankton for inorganic nutrients? Possible ecological implications. *Chem. Ecol.,* 14(2): 83-96.

Davidson K. and W.S.C. Gurney, 1999. An investigation of non-steady-state algal growth II. Mathematical modelling of co-nutrient limitated algal growth. *J. Plankton Res.* 21(5): 839-858.

De Groot W.T., 1983. Modelling the multiple nutrient limitation of algal growth. *Ecol. Modelling* 18: 99-119.

De Jonge V.N., J.F. Bakker and M. van Stralen, 1996. Recent changes in the contributions of the river Rhine and North Sea to the eutophication of the western Dutch Wadden Sea. *Neth. J. Aquat Ecol* 30: 27-39.

De Wilde P.A.W.J., 1990. Benthic Mesocosms: I Basic research in soft-bottom benthic mesocosms. In: C.M. Lalli (Ed): Enclosed experimental marine ecosystems: a review and Recommendations, Springer-Verlag, Berlin Heidelberg, 109-121.

Dick S., U.H. Brockmann, J.E.E. van Beusekom, B. Fabiszisky, M. George, K.-J. Hesse, B. Mayer, T. Nitz, T. Pohlmann, K. Poremba, K. Schaumann, W. Schoenfeld, A. Starke, U. Tillmann and G. Weide, 1999. Exchange of matter and energy between the Wadden Sea and the coastal waters of the German Bight – estimations based on numerical simulations and field measurements. *Dt. hydrogr. Z.* 51: 181-219.

Dortch Q., 1982. Effect of growth conditions on accumulation of internal nitrate, ammonium, amino acids and protein in three marine diatoms. *J. Exp. Mar. Biol. Ecol.* 61: 242-264.

Dortch Q., 1990. The interaction between ammonium and nitrate uptake in phytoplankton. *Mar. Ecol. Prog. Ser.* 61:183-20.

Dortch Q., P. A. Thompson and P. J. Harrison, 1991. Short-term interaction between nitrate and ammonium uptake in *Thalassiosira pseudonana*: effect of preconditioning nitrogen source and growth rate. *Mar. Biol.* 110: 183-193.

Droop M.R., 1968. Vitamin B_{12} and marine ecology. IV. The kinetics of uptake, growth and inhibition in Monochrysis lutheri. *J. Mar. Biol. Ass. U. K.* 48: 689-733.

Droop M.R., 1970. Vitamin B_{12} and marine ecology. V. Continuous culture as an approach to nutritional kinetics. *Helgoländer wiss. Meeresunters* 20: 629-636.

Droop M.R., 1973. Some thoughts on nutrient limitation in algae. *J. Phycol.* 9: 264-272.

Dugdale R.C. and J.J. Georing, 1967. Uptake of new and regenerated forms of nitrogen in primary productivity. *Limnol. Oceanogr.* 12: 196-206.

Dugdale R.C., 1972. Chemical oceanography and primary productivity in upwelling regions. *Geoforum* 7: 47-61.

Dugdale R.C. and F.P. Wilkerson, 1998. Silicate regulation of new production in the eastern equatorial Pacific Ocean. *Nature* 391: 270-273.

Dunne J.P., J.W. Murray and A.K. Aufdenkampe, 1999. Silicon-nitrogen coupling in the equatorial Pacific upwelling. *Global Biogeochemical cycling* 13(3): 715-726.

Dunstan W. M. and K.R. Tenore, 1974. Control of species composition in enriched mass cultures of natural phytoplankton populations. *J. Appl. Ecol.*, 11(2): 529-536.

Dürselen C.D., 2002. Significance of heterotrophic pelagic bacteria for the fluxes of matter in coastal water mesocosms during spring and summer. (ca. 52 pp., in prep.).

Dürselen C.D., T. Raabe, U.H. Brockmann, J. Sun and S. Qian, 2002a. Development of the phytoplankton spring bloom during a 25 day mesocosm experiment in 1999. (ca. 41 pp., in prep.).

Dürselen C.D., T. Raabe, U.H. Brockmann, J. Sun and S. Qian, 2002b. Succession of the phytoplankton community during two summer mesocosm experiments in 1999. (ca. 56 pp., in prep.).

Dzierzbicka-Glowacka L. and A. Zielinski, 1997. Numerical studies of the influence of the nutrient regeneration mechanism on the chlorophyll a concentration in a stratified sea. *Oceanologia* 39 (1): 55-82.

Eberlein K. and G. Kattner, 1987. Automatic method for the determination of ortho-phosphate and total dissolved phosphorus in the marine environment. *Fresenius Z Anal Chem* 326: 354-357.

Egge J. K. and A. Jacobsen, 1997. Influence of silicate on particulate carbon production in phytoplankton. *Mar. Ecol. Prog. Ser.* 147: 219-230.

Eppley R.W., J.L. Coatsworth and L. Solorzano, 1969. Studies of nitrate reductase in marine phytoplankton. *Limnol Oceanogr.* 14: 194-205.

Eppley R.W., T.T. Packard and J.J. MacIsaa, 1970a. Nitrate reductase in Peru Current phytoplankton in the deep ocean. *Nature* 282: 677-680.

Eppley, R.W., Reid, F.M.H. and Strickland, J.D.H., 1970b. Estimates of phytoplankton crop size, growth rate, and primary production. Bull. Scripps Inst. Oceanogr. 17, 33-42.

Eppley R.W., A.F. Carlucci, O. Holm-Hansen, D. Kiefer, J.J. McCarthy, E. Venrick and P.M. Williams, 1971. Phytoplankton growth and composition in shipboard cultures supplied with nitrate, ammonium or ureas as the nitrogen source. *Limnol. Oceanogr.* 16: 741.

Eppley R.W., 1972. Temperature and phytoplankton growth in the sea. *Fish. Bull. U. S.* 70: 1063-1085.

Eppley R.W., P. Koeller and G.T. Wallace, 1978. Stirring influences the phytoplankton species composition within enclosed columns of coastal sea water. *J. Exp. Mar. Biol. Ecol.* 2: 219-239.

Escaravage V.E., T.C. Prins, A.J. Pouwer, H.A. Haas and J.C.H. Peeters, 1994. Phytoplankton dynamics along a phosphorus gradient. In: Smaal, A.C., J.C.H. Peeters and C.H.R. Heip (Eds): The impact of marine eutrophication on phytoplankton and benthic suspension feeders. Progress report 1: results of mesocosm experiments with reduced P-load and increased grazing pressure. Report RIKZ-94.035, NIOO-CEMO 1994-2, Middelburg, The Netherlands, 41-68.

Escaravage V.E., T.C. Prins, A.C. Smaal and J.C.H. Peeters, 1996. The response of phytoplankton communities to phosphorus input reduction in mesocosm experiments. *J. Exp. Mar. Biol. Ecol.* 198: 55-79.

Fasham M.J.R., 1985. Flow analysis of materials in the marine euphotic zone. In Ulanowicz R.E. and T. Platt

(Eds): Ecosystem theory for biological oceanography. Kromar printing Ltd., Winnipeg, Manitoba. 139-162.

Fasham M.J.R., H.W. Duklow and S.M. McKelvie, 1990. A nitrogen-based model of plankton dynamics in the oceanic mixed layer. *J. Mar. Res.* 48: 591-639.

Flynn K.J., M.J.R. Fasham and C.R. Hipkin, 1997. Modelling the interactions between ammonium and nitrate uptake in marine phytoplankton. *Phil. Trans. R. Soc. Lond. B* 352: 1625-1645.

Fogg G.E., 1983a. The ecological responses of phytoplankton to natural light regimes. *J. Plankton Res.* 6: 295-307.

Fogg G.E., 1983b. The ecological significance of extracellular products of phytoplankton photosynthesis. *Bot. Mar.* 26: 3-14.

Frangoulis C., S. Belkhiria, A. Goffart and J.H. Hecq, 2001. Dynamics of copepod faecal pellets in relation to a *Phaeocystis* dominated phytoplankton bloom: characteristics, production and flux. *J. Plankton Res.* 23 (1): 75-88.

Fransz H.G., J.P. Mommaerts and G. Radach, 1991. Ecological modelling of the North Sea. *Neth. J. Sea Res.* 28 (1/2): 67-140.

French D.P., M.J. Furnas, and T.J. Smayda, 1983. Diel changes in nitrite concentration in the chlorophyll maximum in the Gulf of Mexico. *Deep-Sea Res.* 30 (7A): 707-722.

Fuhrman J.A., S.G. Horrigan and D.G. Capone, 1988. The use of ^{13}N as tracer for bacterial and algal uptake of ammonium from seawater. *Mar. Ecol. Prog. Ser.* 45: 271-278.

Fuhrman J., 1992. Bacterioplankton roles in cycling of organic matter: the microbial food web. In: Falkowski P.G. and A.D. Woodhead (Eds): Primary productivity and biogeochemical cycles in the sea. Plenum Press, New York, 361-383.

Gaarder T. and H.H. Gran, 1927. Investigation of the production of plankton in the Oslo Fjord. Rapp. P. V. Reun. Cons. Perm. Int. Explor. Mer 42.

Galloway J.N., W.H. Schlesinger, H. Levy, A. Michaels and J.L. Schnoor, 1995. Nitrogen-fixation: anthropogenic enhancement-environmental response. *Global Biogeochemical Cycling* 9: 235-252.

Galloway J.N., R.W. Howarth, A.F. Michaels, S.W. Nixon, J.M. Prospero and F.J. Dentener, 1996. Nitrogen and phosphorus budgets of the North Atlantic Ocean and its watershed. *Biogeochemistry* 35: 3-25.

Gerlach S.A., 1990. Nitrogen, phosphorus, plankton and oxygen deficiency in the German Bight and in Kiel Bay. Kieler Meeresforschungen, Sonderheft Nr. 7; Institut für Meereskunde, Kiel.

Glibert P.M. and J.C. Goldman, 1981. Rapid ammonium uptake by marine phytoplankton. mar. Biol. Lett. 2: 5-31.

Glibert P.M., 1998, Interactions of top-down and bottom-up control in planktonic nitrogen cycling. *Hydrologia* 363: 1-12.

Goes J.I., S. Caeiro and H. Gomes, 1999. Phytoplankton – zooplankton inter-relationships in tropical waters – grazing and gut pigment dynamics. *Indian J. Mar. Sci.* 28 (2): 116-124.

Goldman J.C., J.J. McCarthy and D.G. Peavey, 1979. Growth rate influence on the chemical composition of phytoplankton in oceanic waters. *Nature*, 279: 210-215.

Goldman J.C., 1980. Physiological processes, nutrient availability, and the concept of relative growth rate in marine phytoplankton ecology. In: P.G. Falkowski (Ed.): Primary productivity in the Sea Plenum Press, New York, 179-194.

Goldman J.C. and P.M. Glibert, 1982. Comparative rapid ammonium uptake by four species of marine phytoplankton. *Limnol. Oceanogr.* 27: 814-827.

Goldman J.C. and M.R. Dennett, 2000. Growth of marine bacteria in batch and continuous culture under carbon and nitrogen limitation. *Limnol. Oceanogr.* 45(4): 789-800.

Goldman J.C. and M.R. Dennett, 2001. Rapid nitrogen uptake by marine bacteria. *Limnol. Oceanogr.* 46(5): 1195-1198.

Gotschalk C.C. and A.L. Alldredge, 1989. Enhanced primary production and nutrient regeneration within aggregated marine diatoms. *Mar. Biol.* 103: 119-129.

Grasshoff K.M., Ehrhardt and K. Kremling (Eds), 1983. Methods of seawater analysis, Verlag Chemie.

Grice G.D. and M.R. Reeve, 1982. Introduction and description of experimental ecosystems. In: G.D. Grice and M.R. Reeve (Eds): Marine mesocosms, biological and chemical research in experimental ecosystems. Springer-Verlag, Berlin, 2-9.

Groenlund L., K. Kononen, E. Lahdes, K. Mäkelä, 1996. Community development and modes of phosphorus utilization in a late summer ecosystem in the Central Gulf of Finland, the Baltic Sea. *Hydrobiologia* 331(1-3): 97-108.

Grossart H.P. and M. Simon, 1993. Limnetic macroscopic organic aggregates (lake snow): Occurrence, characteristics, and microbial dynamics in Lake Constance. *Limnol. Oceanogr.* 38: 532-546.

Grossart H.P. and H. Ploug, 2001. Microbial degradation of organic carbon and nitrogen on diatom aggregates. *Limnol. Oceanogr.* 46(2): 267-277.

Hammer K.D., U.H.Brockmann and G. Kattner, 1981. Release of dissolved free amino acids during a bloom of *Thalassiosira ritual*. *Kieler Meeresforsch*, Sonderh 5: 101-109.

Hammer K.D., K. Eberlein, G. Kattner and U.H. Brockmann, 1983. Fluctuations of dissolved amino acids: A comparison of natural and enclosed phytoplankton populations in the North Sea. In: J. Sündermann and W. Lenz (Eds): North Sea dynamics. Springer-Verlag, Berlin, 559-572.

Hammer K. D. and S. Luck, 1987. An automated fluorescence assay for dissolved total amino acids from marine waters in the presence of interfering material. *Fresenius Z. Anal. Chem.* 327: 513-520.

Harris R.P., 1973. Feeding, growth, reproduction and nitrogen utilization by the harpacticoid copepod, *Trigriopus brevicornis. J. Mar. Biol. Ass. U. K.* 53: 785-800.

Harrison W.G., F. Azam, E.H. Renger and R.W. Eppley, 1977. Some experiments on phosphate assimilation by coastal marine phytoplankton. *Mar. Biol.* 40: 9.

Harrison P.J., D.H. Turpin, 1982. The manipulation of physical, chemical and biological factors to select species from natural phytoplankton communities. In G.D. Grice and M.R. Reeve (eds): Marine mesocosms, biological and chemical research in experimental ecosystems. Springer-Verlag, Heidelberg, 275-303 (430pp)

Hasegawa T.I. Koike and H. Mukai, 2000. Release of dissolved organic nitrogen by a phytoplanktonic community in Akkeshi Bay. *Aquat. Microb. Ecol.* 24(1): 99-107.

Hattori A., 1983. Denitrification and dissimilatory nitrate reduction. In: E.J. Carpenter and D.G. Capone (Eds): Nitrogen in the marine environment. Academic Press, New York, 191-232.

Hein M. and B. Riemann, 1995. Nutrient limitation of phytoplankton biomass or growth rate: An experimental approach using marine enclosures. *J. Exp. Mar. Biol. Ecol.* 188 (2): 167-180.

Helder W., de Vries R.T.P., Rutgers van der Loeff M.M., 1981. Behavior of nitrogen nutrients and silica in the Ems-Dollard Estuary. Proceedings of the symposium on the dynamics of tubid coastal environments 1983, pp. 188-200, *Can. J. Fish. Aquat. Sci.,* 40 (suppl.1).

Hickel W., M. Eickhoff and H. Spindler, 1994. Changes in the German Bight pelagic environment during three decades. Copenhagen Denmark, ICES, 8 pp.

Hickel W., M. Eickhoff and H. Spindler. 1995. Langzeit-Untersuchungen von Nährstoffen und Phytoplankton in der Deutschen Bucht. *Dt. hydrogr. Z., Suppl.* 5: 197-211.

Hillebrand H., C.D. Dürselen, D. Kirschtel, U. Pollingher and T. Zohary, 1999. Biovolume calculation for pelagic and benthic microalgae. *Journal of Phycology* 35, 403 - 424.

Holz J.C., K.D. Hoagland, A. Joern, D.F. Millie and P. Kurgens, 2000. Experimental study of phytoplankton species composition, alternate states, and community breakpoint along a phosphorus gradient. *J. Phycol.* 36(3): 31.

Hoppe H.G., 1976. Determination and properties of activity metabolising heterotrophic bacteria in the sea investigate by means of micro-autoradiography. *Mar. Biol.* 36: 291-302.

Horrigan S.G., A. Hagström, I. Koike and F. Azam, 1988. Inorganic nitrogen utilization by assemblages of marine bacteria in seawater culture. *Mar. Ecol. Prog. Ser.* 50: 147-150.

Howarth R.W. (Ed), 1996. Nitrogen cycling in the North Atlantic Ocean and its watersheds. Report of the

international scope nitrogen project. Kluwer Academic Publishers. Dordrecht, Netherlands, 304 pp.

Hydes D.J., B.A. Kelly-Gerreyn, A.C. Le Gall, R. Proctor, 1999. The balance of supply of nutrients and demands of biological production and denitrification in a temperate latitude shelf sea—a treatment of the sourthern North sea as an extended estuary. *Mar. Chem.,* 68(1-2): 117-131.

Ietswaart T, P.J. Schneider and R.A. Prins, 1994. Utilization of organic nitrogen sources by two phytoplankton species and a bacterial isolate in pure and mixed cultures. *Appl. Environ. Microbiol.,* 60(5): 1554-1560.

Istvanovics V., J. Padisak, K. Pettersson and D.C. Pierson, 1994. Growth and phosphorus uptake of summer phytoplankton in Lake Erken (Sweden). *J. Plankton Res.* 16(9): 1167-1196.

Ittekkot V., U.H. Brockmann, W. Michaelis and E.T. Degens, 1981. Dissolved free and combined carbohydrates during a phytoplankton bloom in the Northern North Sea. *Mar. Ecol. Prog. Ser.* 4: 299-305.

Ittekkot V., E.T. Degens, U.H. Brockmann, 1982. Monosaccharide composition of acid-hydrolysable carbohydrates in particulate matter during a plankton bloom. *Limnol Oceanogr,* 27: 770-776.

Jacobsen A., J.K. Egge, B.R. Heimdal, 1995. Effects of increased concentration of nitrate and phosphate during a spring bloom experiments in mesocosm. *J. Exp. Mar. Biol. Ecol.* 187: 239-251.

Jannasch H.W., 1960. Versuche über Denitrifikation und die Verfügbarkeit des Sauerstoffes in Wassern und Schlamm. *Arch. F. Hydrobiol.* 56: 355-369.

Jansson M., 1988. Phosphate uptake and utilization by bacteria and algae. *Hydrobiologia*. 170:177-189.

Jeffrey S.W. and G.F. Humphrey (1975): New spectrophotrometric equations for determining chlorophylls a, b, c1 and c2 in higher plants, algae and natural phytoplankton. *Biochem. Physiol. Pflanz*. 167, 191-194.

Jφrgensen S.E., S.N. Nielsen and L.A. Jφrgensen, 1991. Handbook of ecological parameters and ecotoxicology. Elsevier, Amsterdam, London, New York, 1227 pp.

Jφrgensen S.E., 1992. Recent and future development in environment modelling. In: P. Melli and P. Zannetti (Eds): Environmental Modelling. Elsevier Applied Science, London, New York, 351-372.

Jφrgensen S.E., 1994. Fundamental of Ecological Modelling (2nd Edition) Elsevier Science B. V. Netherlands. 623 pp.

Kanda J., D.A. Zieman, L.D. Conquest and P.K. Bienfang, 1990. Nitrate and ammonium uptake by phytoplankton populations during the spring bloom in Suke Bay, Alaska. *Estuar. Coast. Shelf. Sci.,* 30(5): 509-524.

Kaplan W.A., 1983. Nitrification. In: E.J. Carpenter and D.G. Capone (Eds): Nitrogen in the marine environment. Academic Press, 139-190.

Kattner G. and U.H. Brockmann, 1980. Semi-automated method for the determination of particulate phosphorus in marine environment. *Z.Anal. Chem.* 301: 14-16.

Ketchum B.H., 1939. The absorption of phosphate and nitrate by illuminated cultures of *Nitzschia closterium*. *Am. J. Bot*. 26: 399-407.

Kerner M., 1996. Sink and source reactions of N_2O within the sediment-water interface formed by settling seston from the Elbe Estuary. *Estuar. Coast. Shelf Sci.*, 43(4): 419-432.

King F.D., T.L. Cucci, D.W. Townsend, 1987. Microzooplankton and macrozooplankton glutamate dehydrogenase as indices of the relative contribution of these fractions to ammonium regeneration in the Gulf of Maine. *J. Plankton Res*. 9 (2): 277-289.

Kirk J.T.O., 1992. The nature and measurement of the light environment in the ocean. In: P.G. Falkowski and A.D. Woodhead (Eds): Primary productivity and biogeochemical cycles in the sea. Plenum Press, New York, 9-29.

Koike I., A. Hattori, M. Takahashi and J. J. Goering, 1982. The use of enclosed experimental ecosystems to study nitrogen dynamics in coastal waters. In: G.D. Grice and M.R. Reeve (Eds): Marine Mesocosms. Biological and chemical research in experimental ecosystems. Springer-Verlag, New York, Heidelberg, Berlin, 291-332.

Kremer J.N. and S.W. Nixon (Eds), 1978. A Coastal Marine Ecosystem. Springer-Verlag, Berlin, New York. 217 pp.

Kuiper J., 1977. Development of North Sea coastal plankton communities in separate plastic bags under identical conditions. *Mar. Biol.* 44: 97-107.

Kuiper J., 1981. Fates and effects of mercury in marine plankton communities in experimental enclosures. *Ecotoxicol. Environ. Saf.* 5: 106-134.

Laake M., A.B. Dahle, K. Eberlein and K. Rein, 1983. A modelling approach to the interplay of carbohydrates, bacteria and non-pigmented flagellates in a controlled ecosystem experiment with *Skeletonema costatum*, *Mar. Ecol. Prog. Ser.* 14: 71-79.

Lalli C.M. (Ed), 1990. Enclosed experimental marine ecosystems: a review and recommendations. Springer-Verlag, Berlin Heidelberg, 218 pp.

Lalli C. M. and T.R. Parsons, 1997. Biological oceanography, an introduction, 2rd edition. Thomson Litho Ltd, Scotland.

Lebo M.E., 1991. Biogeochemical phosphorus cycling in the Delaware, an urbanized coastal plain estuary. *Diss. Abst, Int. Pt. B- Sci. & Eng.* 51(11), 272 pp.

Legovic T. and A. Cruzado, 1997. A model of phytoplankton growth on multiple nutrients based on the Michaelis-Menten-Monod uptake, Droop's growth and Liebig's law. *Ecological Modelling* 99: 19-31.

Lehman J.T. and C.D. Sandgren. 1982. Phosphorus dynamics of the procaryotic nanoplankton in a Michigan lake. *Limnol. Oceanogr.* 27: 828-838.

Lenhart H.J., J. Paetsch and G. Radach, 1996. Daily nutrients loads of the European continental rivers for the years 1977-1993. Ber. Zentr. Meeres-Klimaforsch. Univ. Hamb. 159 pp.

Lohse L., J.F.P. Malschaert, C.P. Slomp, W. Helder, W. van Raaphorst, 1993. Nitrogen cycling in North Sea sediments: interaction of denitrification and nitrification in offshore and coastal areas. *Mar. Ecol. Prog. Ser.*, 101(3): 283-296.

Lohse L., H.T. Kloosterhuis, W. van Raaphorst, W. Helder, 1996. Denitrification rates as measured by the isotope pairing method and by the acetylene inhibition technique in continental shelf sediments of the North Sea. *Mar. Ecol. Prog. Ser.*, 132: 169-179.

Lomas M.W. and P.M. Glibert, 1999. Interactions between NH_4^+ and NO_3^- uptake and assimilation of diatoms and dinoflagellates at several temperatures. *Mar. Biol.* 133: 541-551.

Lomas M.W., C.J. Rumbley and P.M. Glibert, 2000. Ammonium release by nitrogen sufficient diatoms in response to rapid increases in irradiance. *J. Plankton Res*. 22(12): 2351-2366.

Lopes P.F., M.C. Oliveira and P. Colepicolo, 1997. Diurnal fluctuation of nitrate reductase activity in the marine red alga *Gracilaria tenuistipitata* (Rhodophyta). *J. Phycol.* 33(2): 225-231.

Mackenzie F.T., L.M. Ver, C. Sabine, M. Lane and A. Lerman, 1993. C N P S global biogeochemical cycles and modeling of global change NATO ASI Series Vol. 14. In: R. Wallast, F.T. Mackenzie and L. Chou (Eds): Interactions of C N P and S Biogeochemical cycles and global changes. Springer-Verlag, Berlin, 1-61.

Madhupratap M., P. Haridas, N. Ramaiah and C.T. Achuthankutty, 1992. Zooplankton of the southwest coast of India: Abundance, composition, temporal and spatial variability in 1987. In Desai B.N. (Ed): Oceanography of the Indian Ocean. New Delhi India Oxford and Ibh. pp. 99-112.

Maestrini S.Y., M. Balode, C. Bechemin and I. Purina, 1999. Nitrogenous organic substances as potential nitrogen sources, for summer phytoplankton in the Gulf of Riga, eastern Baltic Sea. Plankton Biol. Ecol. 46(1): 8-17.

Mague T.H., H. Friberg, D.J. Hughes and I. Morris, 1980. Extracellular release of carbon by marine phytoplankton: A physiological approach. *Limnol. Oceanogr.* 25: 262-279.

Malone T. C., C. Garside, K.C. Haines and O.A. Roels. 1975. Nitrate uptake and growth of *Chaetoceos sp.* in large outdoor continuous cultures. *Limnol. Oceanogr.* 20 (1): 9-19.

McCarthy J.J., 1981. The kinetics of nutrient utilization. In: Physiological ecological bases of phytoplankton ecology. *Can. Bull. Fish. Aquat. Sci.* 210: 211-233.

McCarthy J.J. and J.C. Goldman, 1979. Nitrogenous nutrition of marine plankton in nutrient depleted waters. *Science* 203: 670-672.

Meng F., S. Qian, D. Liu, J. Sun and J. Yang, 2002. The mesozooplankton of mesocosm around coast of Buesum (ca. 17pp, in prep.).

Menzel D.W. and J.J. Goering, 1966. The distribution of organic detritus in the ocean. *Limnol. Oceanogr.* 11: 333-337.

Middelburg J.J. and J. Nieuwenhuize, 2000. Nitrogen uptake by heterotrophic bacteria and phytoplankton in the nitrate-rich Thames estuary. *Mar. Ecol. Prog. Ser.* 203: 13-21.

Moldaenke C., K.H. Vanselow and U.-P. Hansen, 1995. The 1Hz fluorometer: a new approach to fast and sensitive long-term studies of active chlorophyll and environmental influences. *Helgoländer Meeresunters*. 49, 785-796.

Monod J., 1950. La technique de la culture continue: Theorie et applications. *Annales d'Institut Pasteur, Lille* 79: 390-410.

Mozetic P., V. Turk, A. Malej, S. Terzic, M. Ahel and G. Cauwet, 1997. Coastal plankton response to nutrient enrichment: An experimental system. Water Pollution IV. Modelling, measuring and prediction. Computational Mechanics Publications, 151-160.

Myklestad S.M., 2000. Dissolved organic carbon from phytoplankton. In: P.J. Wangersky (Ed): The handbook of Environmental Chemistry Vol. 5 Part D: Marine Chemistry. 111-148.

Nehring S., Hesse K.J. and U. Tillmann, 1995. The German Wadden Sea: A problem area for nuisance blooms? In: Lassus, P. Et al. (Eds.): Harmful Marine Algal Blooms. Lavoisier, intersep. Limited. 199-204.

NSTF 1993. North Sea Quality Status Report 1993. Oslo and Paris Commissions, Fredensborg, Denmark, Olsen & Olsen, 132 pp.

Nixon S.W., J.W. Ammerman, L.P. Atkinson, V.M. Berounsky, G. Billen, W.C. Boicourt, W.R. Boynton, T.M. Church, D.M. Ditoro, R. Elmgren, J.H. Garber, A.E. Giblin, R.A. Jahnke, N.J.P. Owens, M.E.Q. Pilson, 1996. The fate of nitrogen and phosphorus at the land-sea margin of the North Atlantic Ocean. Nitrogen cycling in the North Atlantic Ocean and its watersheds., Kluwer academic publishers, Dordrecht (The Netherlands), 141-180.

Officer C.B. and J.H. Ryther, 1980. The possible importance of silicon in marine eutrophication. *Mar. Ecol. Prog. Ser.* 3: 83-91.

Oguz, T., H. Ducklow, P. Malanotte-Rizzoli, S. Tugrul, N. Nezlin and U. Unluata, 1996. Simulation of annual plankton productivity cycle in the Black Sea by one dimensional physical – biological model. *J. of Geophysical Research.* 101 (C7): 16585-16599.

Oguz, T., H. Ducklow, P. Malanotte-Rizzoli, J.M. Murray, E.A. Shushkina, V.I. Vedernikov and U. Unluata, 1999. A physical-biochemical model of plankton productivity and nitrogen cycling in the Black Sea. *Deep-Sea Res.* I 46: 597-636.

Oviatt C.A., 1984. Introduction: Ecology as an experimental science and management tool. In: H.H. White (Ed.): Concepts in marine pollution measurements. Tech. Rep. MD. Univ., Sea Grant Program, 539-548.

Oviatt C., P. Doering, B. Nowicki, L. Reed, J. Cole, J. Frithsen, 1995. An ecosystem level experiment on nutrient limitation in temperate coastal marine environment. *Mar. Ecol. Prog. Ser.* 116: 171-179.

Paasche E., 1973. Silicon and ecology of marine plankton diatoms. I. *Thalassiosira pseudonana* (Cyclotella nana) grown in a chemostat with silicate as limiting nutrient. *Mar. Biol*. 19: 117-126.

Paasche E., 1980. Silicon content of five marine plankton diatom species measured with a rapid fiter method. *Limnol. Oceanogr.* 25: 474-480.

Parslow J.S., P.J. Harrison and P.A. Thompson, 1984a. Development of rapid ammonium uptake during starvation of batch and chemostat cultures of the marine diatom *Thalassiosira pseudonana*. *Mar. Biol.* 83: 43-50.

Parslow J.S., P.J. Harrison and P.A. Thompson, 1984b. Saturated uptake kinetics: transient response of the marine diatom *Thalassiosira pseudonana* to ammonium, nitrate, silicate or phosphate starvation.

Mar. Biol. 83: 51-59.

Parslow J.S., P.J. Harrison and P.A. Thompson 1985. Ammonium uptake by phytoplankton cells on a filter: A new high-resolution technique. *Mar. Ecol. Prog. Ser.* 25: 121-129.

Parsons T. R. and P. J. Harrison, 1983. Nutrient cycling in Marine Ecosystems. In: O.L. Lange, P.S. Nobel, C.B. Osmond and H. Ziegler (Eds.): Encyclopedia of Plant Physiology, New Series, Volume, 12D, Physiological Plant Ecology 4, 85-115.

Parsons T.R., M. Takahashi and B. Hargrave, 1984. Biological Oceanographic Processes. 3rd Edition, Pergamon Press. Oxford, New York, 330 pp.

Parsons T.R., 1990. The use of mathematical models in conjunction with mesocosm ecosystem research. In: C.M. Lalli (Ed.) Enclosed experimental marine ecosystem: A review and recommendations. Springer-Verlag, New York, 197-210.

Parsons T., 1991. Manual on marine experimental ecosystems. *Unesco technical papers in marine science.* 61, 175 pp.

Paul J.H., 1983. Uptake of organic nitrogen. In: E.J. Carpenter and D.G. Capone (Eds). Nitrogen in the marine environment. Academic Press, 275-308.

Peperzak, L., F. Colinjn, W.W.C. Gieskes and J.C.H. Peeters, 1998. Development of the diatom-*Phaeocystis* spring bloom in the Dutch coastal zone of the North Sea: the silicon depletion versus the daily irradiance threshold hypothesis. *J. Plankton Res*. 20 (3): 517-537.

Perez-Martinez C., P. Sanchez-Castillo, L. Cruz-Pizarro, 1994. Effect of nutrient fertilization and of zooplankton predation on the biomass and production of phytoplankton in a mesotrophic reservoir. In: Straskrabova V. and J.F. Talling (Eds): Proceedings of the second international conference on reservoir limnology and water quality. Stuttgart frg schweizerbart' sche verlagsbuchhandl. 40: 185-195.

Perez-Martinez C., L. Cruz-Pizarro, 1995. Species-specific phytoplankton responses to nutrients and zooplankton manipulations in enclosure experiments. *Freshwat. Biol.* 33(2): 193-203.

Petipa T.S., 1966. Relationship between growth, energy metabolism, and ration in A. Clausi. Physiology of Marine Animals, Akad. Nauk, USSR, Oceanographical Commision, 82-91.

Philippart C.J.M. and G.C.Cadèe, 2000. Was total primary production in the western Wadden Sea stimulated by nitrogen loading? *Helgol. Mar. Res.* 54: 55-62.

Pohlmann T., S. Beddig, U. Brockmann, S. Dick, R. Doefffer, M. Engel, K.-J Hesse, P. Koenig, B. Mayer, A. Moll, D. Murphy W. Puls, T. Raabe, H.-J. Rick, R. Schmidt-Nia, W. Schoenfeld and J. Sündermann, 1998. Combined analysis of field and model data: A field study of the phosphate dynamics in the German Bight in summer 1994. In: Abschlussbericht KUSTOS (BMBF-Project 03F0111) und TRANSWATT (BMBF-Project 03F0130), Band 2, Mai 1998, 471-512.

Pomeroy L., R., H.M. Matthews and H.S. Min, 1963. Excretion of phosphate and soluble organic phosphorus compounds by zooplankton. *Limnol. Oceanogr.* 8: 50-55.

Portielje R. and L. Lijklema, 1994. Kinetics of luxury uptake of phosphate by algae-dominated benthic communities. Nutrient dynamics and biological structure in shallow freshwater and brackish lakes. *Hydrobiologia* 275/276: 349-358.

Postma H., 1984. Introduction to the symposium on organic matter in the Wadden Sea. In: R.W. Laane and W.J. Wolff (Eds): Proceedings of the fourth international Wadden Sea symposium: The role of organic matter in the Wadden Sea. 1-3 Nov. 1983. Texel, The Netherlands. Netherlands Institute for Marine Research, 15-22.

Quality Status Report 2000. Published by OSPAR Commission, London 2000, ISBN 0 946956529.

Raabe T., U.H. Brockmann, C.D. Dürselen, M. Krause and H.-J. Rick, 1997. Nutrient and plankton dynamics during a spring drift experiment in the German Bight. *Mar. Ecol. Prog. Ser.* 156: 275-288.

Radach G. and M. Bohle-Carbonell., 1990. Strukturuntersuchungen der meteorologischen, hydrographischen, Nährstoff- und Phytoplankton-Langzeitreihen in der Deutschen Bucht bei Helgoland. *Ber. Biol. Anst. Helgoland* 7: 1-425. ISSN 0930-8148.

Radach G. and A. Moll, 1993. Estimation of the variability of production by simulating annual cycles of

phytoplankton in the central North Sea. *Prog. Oceanogr.* 31: 339-419.

Raimbault P., 1986. Effect of temperature on nitrite excretion by three marine diatoms during nitrate uptake. *Mar. Biol.* 92: 149-155.

Raimbault, R., G. Slwyk and N. Garcia, 2000. Comparison between chemical and isotopic measurements of biological nitrate utilization: further evidence of low new-production levels in the equatorial Pacific. *Mar. Biol.* 136: 1147-1155.

Raymont J.E.G., 1980. Plankton and productivity in the oceans. Volume 1. Phytoplankton. Pergamon Press. Oxford, New York, Toronto, 489 pp.

Reay D.S., D.B. Nedwell, J. Priddle and J.C. Ellis-Evans, 1999. Temperature dependence of inorganic nitrogen uptake: Reduced affinity for nitrate at suboptimal temperatures in both algae and bacteria. Appl. Environ. Microbiol. 65(6): 2577-2584.

Redfield A.C., 1958. The biological control of chemical factors in the environment. *Amer. Sci.* 46: 205-221.

Reeve M.R., G.D. Grice and R.P. Harris, 1982. The CEPEX approach and its implications for future studies in plankton ecology. In: G.D. Grice and M.R. Reeve (Eds.): Marine Mesocosms. Biological and chemical research in experimental ecosystems. Springer-Verlag, New York, 389-398.

Ren L., U.H. Brockmann, M.P. Zhang, 2002a. Pelagic nitrogen cycling in Jiaozhou Bay, a model study I: phytoplankton dynamic and primary production. (in prep.).

Ren L., U.H. Brockmann, T. Raabe, M.P. Zhang. 2002b. Nitrogen conversion in enclosed ecosystem during spring 1999, in the German Bight. (ca. 34 pp., in prep.).

Rey F. and H.R. Skjoldal, 1987. Consumption of silic acid below the euphotic zone by sedimenting diatom blooms in the Barents Sea. *Mar. Ecol. Prog. Ser.* 36: 307-312.

Rick S. 1999. (dissertation) The spring bloom in the German Bight: Effects of high inorganic N:P ratios on the phytoplankton development. Institut fuer Meereskunde an der Christian-Albrechts-University Kiel. 142 pp.

Riegman R. and L.R. Mur, 1984. Regulation of phosphate uptake kinetics in *Oscillatoria agardhii*. *Archives of Microbiology* 139: 28-32.

Riegman R., A.M. Noordeloos and G.C. Cadee, 1992. *Phaeocystis* blooms and eutrophication of the continental coastal zones of the North Sea. *Mar. Biol.* 112: 479-484.

Riley G.A., 1957. Phytoplankton in the North Central Sargasso Sea, 1950-52. *Limnol. Oceanogr*. 2: 252-270.

Rivkin R.B., M.R. Anderson and C. Lajzerowicz, 1996. Microbial processes in cold oceans. 1. Relationship between temperature and bacterial growth rate. *Aquat. Microb. Ecol.* 10 (3): 243-254

Roelke D.L., P.M. Eldridge and L.A. Cifuentes, 1999. A model of phytoplankton competition for limiting and nonlimiting nutrients: implications for development of estuarine and near shore management schemes. *Estuaries* 22(1): 92-104.

Roth M., 1971. Fluorescence reaction for amino acids. *Anal. Chem.* 43: 880-882.

Sakamoto M. and T. Tanaka, 1989. Phosphorus dynamics associated with phytoplankton blooms in eutrophic Mikawa Bay. *Mar. Biol.* 101(2): 265-271.

Schlüter L., 1998. The influence of nutrient addition on growth rates of phytoplankton groups, and microzooplankton grazing rates in a mesocosm experiment. *J. Exp. Mar. Biol. Ecol.* 228: 53-71.

Schöllhorn E. and E. Graneli, 1993. Is the increase of flagellates in coastal waters caused by changes in ratios of N, P, and Si. In: T.J. Smayda, and Y. Shimizu (Eds): Toxic phytoplankton blooms in the sea. Elsevier Science Publishing Co. Inc., Amsterdam, 811-817.

Sciandra A. and R. Amara, 1994. Effects of nitrogen limitation on growth and nitrite excretion rates of the dinoflagellate *Prorocentrum minimum*. *Mar. Ecol. Prog. Ser.* 105: 301-309.

Seki H., 1982. Organic materials in aquatic ecosystems. CRC press. USA. 201 pp.

Shankes A.L. and J.D. Trent, 1980. Marine snow: Sinking rates and potential role in vertical flux. *Deep-Sea Res*. 27: 137-144.

Sharp P.H., 1977. Excretion of organic matter by marine phytoplankton: Do healthy cells do it? *Limnol. Oceanogr.* 22: 381-399.

Shiomoto A., and S. Hashimoto, 1999. Relationship between chlorophyll a and nutrients in Suruga Bay, central Japan, May, 1996. *Bull. Jap. Soc. Fish. Oceanogr.* 63 (1): 1-7.

Smayda T.J., 1990. Novel and nuisance phytoplankton blooms in the sea: evidence for a global epidemic. In: E. Graneli, B. Sundstroem, L. Edler and D.M. Anerson (Eds): Toxic marine phytoplankton. Elsevier Science Publishing Co., Amsterdam, 29-41.

Smith R.C. and K.S. Baker, 1981. Optical properties of the clearest natural waters. *Appl. Opt.,* 20: 177-184.

Smith W., V.R. Gobson and J.F. Grassle, 1982. Replication in controlled marine systems: Presenting the evidence. In: G.D. Grice and M.R. Reeve (Eds.): Marine mesocosms. Biological and chemical research in experimental ecosystems. Springer-Verlag, New York, 217-225.

Sommaruga R. and D. Conde, 1997. Seasonal variability of metabolically active bacterioplankton in the euphotic zone of a hypertrophic lake. *Aquat. Microb. Ecol.*13(3): 241-248.

Sϕndergaard M., P.J.L. Williams, G. Cauwet, B. Riemann, C. Robinson, S. Terzic, E.M.S. Woodward and J. Worm, 2000. Net accumulation and flux of dissolved organic carbon and dissolved organic nitrogen in marine plankton communities. *Limnol. Oceanogr.* 45(5): 1097-1111.

Sournia A., 1969. Cycle annuel du phytoplancton et de la production primaire dans les mers tropicales. *Mar. Biol.* 3: 287-303.

Sournia A., 1974. Circadian periodicities in natural populations of marine phytoplankton. *Adv. Mar. Biol.* 12: 325-389.

Starke A., T. Raabe and U. Brockmann, 2002. Development of dissolved organic matter during mesocosm experiment in summer of 1999. (ca. 29 pp., in prep.).

Steele J.H., 1962. Environmental control of photosynthesis in the sea. *Limnol. Oceanogr.* 7: 137-150.

Steele J.H., 1974. The structure of marine ecosystems. Harvard University Press, Cambridge, Massachusetts. 128pp.

Sterman, N.T. (1988): Spectrophotometric and fluorometric chlorophyll analysis. In: C.S. Lobba, D.J. Chapman and P. Kremer, P. (Eds.): Experimental phycology. Cambridge University Press.

Strauss E.A., W.K. Dodds, C.C. Edler, 1994. The impact of nutrient pulses on trophic interactions in a farm pond. *J. Freshwat.-Ecol.* 9(3): 217-228.

Strickland J.D.H. and L.D.B. Terhune, 1961. The study of in situ marine photosynthesis using a large plastic bag. *Limnol. Oceanogr.* 6: 93-96.

Strickland J.D.H., 1967. Between beakers and bays. *New Scientist* 2: 276-278.

Strickland J.D.H. and T.R. Parsons, 1972. A practical handbook of seawater analysis. *Fisheries Research Board of Canada* 167.

Suttle C.A., J.A. Fuhrman and D.G. Capone, 1990. Rapid ammonium cycling and concentration-dependent partitioning of ammonium and phosphate: implications for carbon transfer in planktonic communities. *Limnol. Oceanogr.* 36: 424.

Suzuki M., M. Sagehashi and A. Sakoda, 2000. Modelling the structural dynamics of a shallow and eutrophic water ecosystem based on mesocosm observations. *Ecol. Model.* 128(2/3): 221-243.

Syrett P. J., 1981. Nitrogen metabolism in microalgae. In: T. Platt (Ed): Physiological bases of phytoplankton ecology. *Can. Bull. Fish. Aquatic. Sciences* 210: 182-210.

Takahashi M., W.H. Thomas, D.L.R. Seibert, J. Beers, P. Koeller and T.R. Parsons, 1975. The replication of biological events in enclosed water columns. *Arch. Hydrobiol.* 76 (1): 5-23.

Tarutani K. and T. Yamoto, 1994. Phosphate uptake and growth kinetics of *Skeletonema costatum* isolated from Hiroshima Bay. *Appl. Biol. Sci. Seibutsu Seisangaku Kenkyu* 33(1): 59-64.

Taylor D., S. Nixon, S. Granger and B. Buckley, 1995. Comparative impacts of nutrient enrichment of shallow and deep coastal marine systems. Second annual marine and estuarine shallow water science and management conference, U. S. EPA, Philadelphia, PA (USA), 34 pp.

Tett P., A. Edwards and K. Jones, 1986. A model for the growth of shelf-sea phytoplankton in summer. *Estuarine, Coastal and Shelf Science* 23: 641-672.

Thingstad T.F., E.F. Skjoldal and R.A. Bohne, 1993. Phosphorus cycling and algal-bacterial competition in Sandsfjord, western Norway. *Mar. Ecol. Prog. Ser.* 99: 239-259.

Utermöhl, H. (1958): Zur Vervollkommnung der quantitativen Phytoplankton-Methodik. - Mitteilungen der Internationalen Vereinigung für Theoretische und Angewandte Limnologie 9: 1-38.

Valiela I., 1995. Marine ecological processes. Springer-Verlag, New York, 686 pp.

Tupas I.M., I. Koike, D.M. Karl and O. Holm-Hansen, 1994. Nitrogen metabolism by heterotrophic bacterial assemblages in Antarctic coastal waters. *Polar Biol.* 14(3): 195-204.

Van Beusekom J.E.E. and S. Diel-Christiansen, 1994. A synthesis of phyto and zooplankton dynamics in the North Sea environment. WWF, Godalming (UK), 148 pp.

Van Beusekom J.E.E., U.H. Brockmann, K.-J. Hesse, W. Hickel, K. Poremba and U. Tilmann, 1998. Sediment – water interaction in the German Wadden sea and adjacent coastal zone. In: Abschlussbericht KUSTOS (BMBF-Project 03F0111) und TRANSWATT (BMBF-Project 03F0130), Band 1, 255-278.

Van Haren H., D.K. Mills and P.M.J. Wetsteyn, 1998. Detailed observations of the phytoplankton spring bloom in the stratifying central North Sea. *J. Mar. Res.*, 56(3): 655-680.

Van der Rol M.W.M. and J.C.A. Joordens, 1993. Modelling of a phytoplankton community in a pelagic mesocosm. In: J.C.H. Peeters, J.C.A. Joordens, A.C. Smaal and P.H. Nienhuis (Eds): The impact of marine eutrophication on phytoplankton and benthic suspension feeders: results of a mesocosm pilot study. Royal Netherlands Academy of Arts and Science.

Varela D.E. and Harrison P.J., 1999. Effect of ammonium on nitrate utilization by *Emiliania huxleyi,* a coccolithophore from the oceanic northeastern Pacific. *Mar. Ecol. Prog. Ser.*: 186: 67-74.

Vargo G.A. and D. Howard-Shamblott, 1990. Phosphorus dynamics in Ptychodiscus brevis: Cell phosphorus, uptake, and growth requirements. *Toxic Marine Phytoplankton* 324-329.

Veldhuis M.J.W., F. Colijn and L.A.H. Venekamp, 1986. The spring bloom of *Phaeocystis pouchetii* (Haptophyceae) in Dutch coastal waters. *Neth. J. Sea Res.* 20(11): 37-48.

Vergara J.J., J.A. Berges and P.G. Falkowski, 1998. Diel periodicity of nitrate reductase activity and protein levels in the marine diatom *Thalassiosira weissflogii* (Bacillariophyceae). *Journal of Neurocytology* 27(4): 952-961.

Viitasalo M., M. Rosenberg, A.S. Heiskanen and M. Kosi, 1999. Sedimentation of copepod faecal material in the coastal northern Baltic Sea: Where did all the pellets go? *Limnol. Oceanogr.* 44 (6): 1388-1399.

Vitousek P.M. and R.W. Howarth, 1991. Nitrogen limitation on land and in the sea: how can it happen? *Biogeochemistry* 13: 87-115.

Von Westernhagen H., E. Bauernfeind, W. Hickel and U. Niermann, 1986. New findings about the eutrophication in the German Bight. In: V. Dethlefsen and K. Tiews (Eds): New aspects of the possible utilization of coastal waters of the North Sea, 43: 49-63.

Wada E. and A. Hattori (Eds), 1991. Nitrogen in the sea: Forms, Abundances, and Rate Processes. CRC press, Boca Raton, 208 pp.

Wassmann P., J.K. Egge, M. Reigstad and D.L. Aksnes, 1997. Influence of dissolved silicate on vertical flux of particulate biogenic matter. *Mar. Poll. Bull.* 33: 10-21.

Wen Y.H. and R.H. Peters, 1994. Empirical models of phosphorus and nitrogen excretion rates by zooplankton. *Limnol. Oceanogr.* 39(7): 1669-1679.

Werner D., 1977. Silicate metabolism. *Bot. Monogr.* 13: 110-149.

Wheeler P.A. and D.L. Kirchman, 1986. Utilization of inorganic and organic nitrogen by bacteria in marine systems. *Limnol. Oceanogr*. 31(5): 998-1009.

Wheeler P.A., 1983. Phytoplankton nitrogen metabolism. In: E.J. Carpenter and D.G. Capone (Eds): Nitrogen in the marine environment. Academic Press, London, 309-346.

Wheeler P.A. and S.A. Kokkinakis, 1990. Ammonium recycling limits nitrate use in the oceanic subarctic Pacific. *Limnol. Oceanogr.* 35 (6): 1267-1278.

Winkler L.W. (1988): Die Bestimmung des im Wasser gelösten Sauerstoffes. *Chem. Ber.* 21: 2843-2855.

Yin K., P.J. Harrison and Q. Dorth, 1998. Lack of ammonium inhibition of nitrate uptake for a diatom grown under low light conditions. *J. Exp. Mar. Biol. Ecol.* 228 (1): 151-165.

Zehr J.P., P.G. Falkowski, J. Fowler and D.G. Capone, 1988. Coupling between ammonium uptake and incorporation in a marine diatom: Experiments with the short-lived radioisotope 13N. *Limnol. Oceanogr.* 33: 518-527.

Zevenboom W. and L.R. Mur, 1979. Influence of growth rate on short term and steady state nitrate uptake by nitrate limited *Oscillatoria agardhii*. *Federation of European Microbiological Societies Microbiology Letter* 6: 209-212.

Zevenboom W., 1994. Assessment of eutrophication and its effects in marine waters. *German J. of Hydrography.* Supplement 1: 141-170.

APPENDIX

Table A: Results of the sensitivity analysis of some selected parameters to the outputs of the main compartments in spring

Parameters		standard run		diatom N	flagellatesN	nitrate	ammonium	nitrite	DON (sum)	zoopt_N	detritus N	phosphate	silicate
Rdmax	1.2	2.4	3.6	**1.6312**	**-1.5951**	-0.2894	**-1.8969**	0.0208	0.0511	0.2900	**0.6199**	**-1.5912**	**-0.8639**
				0.6101	**-0.6587**	-0.1212	**-0.7019**	0.0060	0.0285	0.1498	0.4335	**-0.6530**	**-0.3547**
Rfmax	1.2	2.4	3.6	0.0136	**-1.0833**	0.0006	0.0183	0.0000	-0.0003	-0.0035	-0.0041	0.0058	-0.0072
				0.0068	**-0.5417**	0.0003	0.0092	0.0000	-0.0001	-0.0017	-0.0020	0.0029	-0.0036
Iopt	35	70	105	-0.0909	-0.0370	0.0191	0.0661	-0.0011	-0.0036	-0.0081	-0.0555	0.0958	0.0508
				-0.2319	-0.1310	0.0452	0.2836	-0.0026	-0.0094	-0.0527	-0.1410	0.2467	0.1303
K0	0.4	0.8	1.2	-0.1512	-0.0780	0.0307	0.1591	-0.0017	-0.0065	-0.0302	-0.0986	0.1624	0.0859
				-0.2185	-0.1218	0.0429	0.2566	-0.0025	-0.0088	-0.0486	-0.1329	0.2323	0.1228
Ksa	0.25	0.5	0.75	-0.0148	0.0188	0.0028	0.0166	-0.0002	-0.0006	-0.0012	-0.0087	0.0152	0.0083
				-0.0336	0.0421	0.0065	0.0346	-0.0004	-0.0013	-0.0046	-0.0202	0.0345	0.0188
Ksn	0.25	0.5	0.75	0.0000	0.0000	0.0000	0.0000	0.0000	0.0000	0.0000	0.0000	0.0000	0.0000
				0.0000	0.0000	0.0000	0.0000	0.0000	0.0000	0.0000	0.0000	0.0000	0.0000
thi1	1	1.5	2	-0.0129	0.0165	0.0030	-0.0026	-0.0002	-0.0005	-0.0009	-0.0075	0.0132	0.0072
				-0.0097	0.0126	0.0023	-0.0020	-0.0001	-0.0004	-0.0006	-0.0055	0.0098	0.0054
Rpexud	0.01	0.02	0.03	-0.0337	-0.0153	0.0027	0.0144	-0.0002	0.0235	-0.0043	-0.0157	0.0137	0.0073
				-0.0336	-0.0155	0.0028	0.0144	-0.0002	0.0232	-0.0044	-0.0156	0.0138	0.0074
Rpmort0	0.005	0.01	0.02	-0.1293	-0.1928	0.0057	0.0299	-0.0003	0.0059	-0.0131	0.3354	0.0303	0.0156
				-0.1138	-0.1644	0.0060	0.0301	-0.0003	0.0046	-0.0131	0.2767	0.0315	0.0162
b1	0.7	0.85	1	-0.0310	-0.0294	0.0024	0.0111	-0.0002	-0.0007	**0.8921**	-0.0970	0.0074	0.0038
				-0.0366	-0.0333	0.0027	0.0127	-0.0002	-0.0009	**1.1274**	-0.1255	0.0080	0.0041
b2	0.4	0.6	0.8	-0.0113	-0.0148	0.0011	0.0065	-0.0001	-0.0003	0.2262	-0.0230	0.0052	0.0022
				-0.0122	-0.0158	0.0012	0.0069	-0.0001	-0.0003	0.2448	-0.0249	0.0055	0.0024
c1	0.5	0.7	0.9	-0.0387	0.1088	0.0049	0.0344	-0.0003	-0.0002	0.1318	-0.0035	0.0261	0.0147
				-0.0314	0.0857	0.0041	0.0293	-0.0002	-0.0002	0.0986	-0.0044	0.0220	0.0124
Rgmax	0.06	0.12	0.24	-0.0868	-0.1235	0.0089	0.0569	-0.0005	0.0001	**0.8641**	-0.0383	0.0441	0.0225
				-0.2407	**-0.2512**	0.0192	0.1018	-0.0011	0.0019	**2.8253**	-0.0558	0.0905	0.0459
Kg	0.25	0.5	0.75	0.0170	0.0278	-0.0022	-0.0149	0.0001	0.0002	-0.1368	0.0107	-0.0112	-0.0057
				0.0132	0.0214	-0.0016	-0.0113	0.0001	0.0001	-0.1073	0.0081	-0.0085	-0.0043
Rzmort0	0.005	0.01	0.02	0.0009	0.0009	-0.0001	-0.0004	0.0000	0.0000	-0.0234	0.0026	-0.0003	-0.0001
				0.0009	0.0009	-0.0001	-0.0004	0.0000	0.0000	-0.0229	0.0025	-0.0003	-0.0001

Table A: Results of the sensitivity analysis of some selected parameters to outputs of the main compartments in spring

Parameters		standard run		diatom N	flagellatesN	nitrate	ammonium	nitrite	DON (sum)	zoopt_N	detritus N	phosphate	silicate
Rexcr0	0.01	0.02	0.04	0.0001	-0.0001	0.0016	0.0122	-0.0001	0.0036	0.0000	0.0001	-0.0001	-0.0001
				0.0001	-0.0001	0.0016	0.0124	-0.0001	0.0036	0.0000	0.0001	-0.0001	-0.0001
Rddecay0	0.025	0.05	0.1	-0.0010	-0.0015	0.0004	0.0022	0.0000	0.0361	0.0019	-0.1260	0.0006	0.0003
				-0.0009	-0.0014	0.0003	0.0021	0.0000	0.0312	0.0017	-0.1091	0.0005	0.0003
Rni0	0.0005	0.001	0.002	0.0007	-0.0008	-0.0016	0.0399	-0.0003	0.0000	0.0001	0.0004	-0.0007	-0.0004
				-0.0015	0.0017	0.0035	-0.0889	0.0007	-0.0001	-0.0003	-0.0010	0.0016	0.0008
Rden0	0.00005	0.0001	0.0002	0.0015	-0.0017	-0.0044	0.0879	0.0400	0.0001	0.0002	0.0010	-0.0015	-0.0008
				-0.0008	0.0008	0.0008	-0.0439	0.0409	0.0000	-0.0001	-0.0005	0.0008	0.0004
Rden02	0.003	0.005	0.007	0.0019	-0.0021	-0.0043	0.1099	-0.0355	0.0001	0.0003	0.0012	-0.0019	-0.0010
				-0.0019	0.0021	0.0043	-0.1099	-0.0332	-0.0001	-0.0003	-0.0012	0.0019	0.0010
Rremin(0)	0.0025	0.005	0.0075	0.0015	-0.0017	-0.0034	0.0879	0.0266	0.0001	0.0002	0.0010	-0.0015	-0.0008
				-0.0003	0.0004	0.0128	-0.0003	0.0001	-0.0710	0.0000	-0.0002	0.0003	0.0002
Rpn_uptk	0.03	0.055	0.07	**-0.7207**	**-0.2417**	0.1437	**0.2780**	-0.0138	-0.0187	-0.0036	-0.1754	**-0.2723**	**0.3629**
				-0.5171	**-0.2033**	0.1130	-0.0454	-0.0077	-0.0141	-0.0068	-0.1451	**-0.2221**	**0.2631**
Rsn_uptk	0.8	1	1.2	0.0028	-0.0031	-0.0063	0.1611	-0.0012	0.0001	0.0004	0.0017	-0.0028	**-0.5282**
				-0.0144	0.0066	0.0080	-0.1447	0.0011	-0.0004	-0.0005	-0.0023	0.0131	**-0.5181**
r1	0.03	0.06	0.09	0.3677	0.1863	-0.0777	-0.2471	0.0037	0.0141	0.0690	0.2096	-0.3860	-0.2042
				0.2737	0.1498	-0.0533	-0.3703	0.0036	0.0122	0.0614	0.1853	-0.2966	-0.1568
r8	0.02	0.04	0.06	0.0479	0.0167	-0.0107	0.1023	-0.0001	-0.0160	0.0007	0.0122	0.0271	-0.0242
				0.0514	0.0223	-0.0049	-0.0717	0.0013	-0.0182	0.0002	0.0117	0.0339	-0.0258

Table B: Results of the sensitivity analysis of some selected parameters to outputs of the main compartments in summer. (to be continued)

parameters		Standard run		diatom N	flagellatesN	nitate	ammonium	nitrite	DON	zoopt_N	detritus N	phosphate	silicate
Rdmax	1.2	2.4	3.6	**1.0520**	-0.2960	-0.1615	**-0.3910**	0.0003	0.0160	0.0262	0.0419	-0.1956	**-5.6171**
				0.0837	-0.0052	0.0078	**-0.4440**	0.0179	0.0085	0.0186	0.0196	-0.0889	**-0.5952**
Rfmax	2	2.8	4.0	0.1211	**0.6774**	**-2.5789**	**-1.1089**	**-2.1131**	0.1075	0.0491	0.3933	**-2.0822**	0.0113
				0.0110	**0.2161**	**-0.7729**	**-0.6177**	**-0.9024**	0.0518	0.0273	0.1381	**-0.7028**	0.1812
Iopt	35	70	105	0.0779	0.0726	-0.2986	**-0.5667**	-0.0343	0.0252	0.0298	0.0681	**-0.3289**	**-0.4238**
				0.0039	-0.0179	0.0844	-0.0737	0.0918	-0.0023	0.0032	-0.0083	0.0460	-0.0374
K0	0.4	0.8	1.2	0.0130	-0.0016	0.0115	-0.1220	0.0751	0.0020	0.0064	0.0039	-0.0153	-0.0814
				-0.0165	-0.0385	0.1761	0.0504	0.0988	-0.0092	-0.0032	-0.0266	0.1363	0.0704
Ksa	0.25	0.5	0.75	-0.0003	-0.0052	0.0188	0.0118	0.0122	-0.0010	-0.0002	-0.0031	0.0160	-0.0014
				-0.0042	-0.0108	0.0461	0.0238	0.0188	-0.0026	-0.0009	-0.0073	0.0377	0.0158
Ksn	0.25	0.5	0.75	0.0001	-0.0001	0.0004	-0.0002	-0.0020	0.0000	0.0000	0.0000	0.0002	-0.0007
				0.0000	0.0000	0.0003	-0.0002	-0.0021	0.0000	0.0000	0.0000	0.0001	0.0000
thi1	1	1.5	2	-0.0008	-0.0042	0.0197	-0.0017	0.0110	-0.0009	-0.0002	-0.0027	0.0137	0.0015
				-0.0012	-0.0033	0.0164	-0.0004	0.0072	-0.0008	-0.0002	-0.0023	0.0115	0.0045
Rpexud	0.01	0.02	0.03	-0.0214	-0.0224	0.0188	0.0122	0.0144	0.0212	-0.0014	-0.0132	0.0069	0.0094
				-0.0214	-0.0225	0.0192	0.0123	0.0109	0.0212	-0.0015	-0.0132	0.0072	0.0095
Rpmort0	0.005	0.01	0.02	-0.1748	-0.1402	0.0235	0.0212	0.0171	0.0949	-0.0081	0.4915	0.0115	0.0207
				-0.1473	-0.1211	0.0246	0.0215	0.0111	0.0820	-0.0082	0.4085	0.0133	0.0215
b1	0.7	0.85	1	-0.0747	-0.0602	0.0049	0.0054	0.0031	-0.0305	**0.9893**	-0.1327	-0.0104	0.0039
				-0.0889	-0.0741	0.0051	0.0062	0.0032	-0.0398	**1.2754**	-0.2023	-0.0133	0.0040
b2	0.4	0.6	0.8	-0.0074	-0.0048	0.0013	0.0012	0.0007	-0.0018	0.0677	-0.0042	-0.0001	0.0013
				-0.0075	-0.0049	0.0013	0.0012	0.0007	-0.0019	0.0691	-0.0044	-0.0001	0.0013
c1	0.5	0.7	0.9	-0.0976	0.0257	-0.0188	0.0052	-0.0145	0.0037	0.0436	0.0119	-0.0144	0.0334
				-0.0797	0.0212	-0.0138	0.0041	-0.0133	0.0028	0.0336	0.0091	-0.0107	0.0268
c2	0.4	0.6	0.8	0.0741	-0.0424	0.0320	0.0139	0.0274	0.0003	0.0354	0.0055	0.0250	-0.0101
				0.0504	-0.0310	0.0293	0.0126	0.0172	-0.0001	0.0250	0.0026	0.0228	-0.0085
Rgmax	0.15	0.2	0.25	**-0.2006**	-0.1259	0.0444	0.0480	0.0270	0.0160	**0.9885**	0.0978	0.0171	0.0531
				-0.2604	-0.1849	0.0499	0.0536	0.0220	0.0222	**1.4263**	0.1444	0.0140	0.0588

Table B: Results of the sensitivity analysis of some selected parameters to outputs of the main compartments in summer.

parameters		Standard run		diatom N	flagellatesN	nitate	ammonium	nitrite	DON	zoopt_N	detritus N	phosphate	silicate
Kg	0.25	0.5	0.75	0.0151	0.0074	-0.0065	-0.0075	-0.0028	-0.0006	-0.0586	-0.0044	-0.0045	-0.0087
				0.0132	0.0065	-0.0055	-0.0063	-0.0026	-0.0006	-0.0517	-0.0039	-0.0037	-0.0073
Rzmort0	0.005	0.01	0.02	0.0433	0.0349	-0.0033	-0.0037	-0.0020	0.0177	-0.5769	0.0818	0.0079	-0.0028
				0.0352	0.0271	-0.0031	-0.0031	-0.0019	0.0128	-0.4264	0.0489	0.0059	-0.0026
Rexcr0	0.01	0.02	0.01	0.0005	0.0130	0.0031	0.0085	0.0029	0.0048	0.0001	0.0042	-0.0333	-0.0001
				0.0005	0.0116	0.0031	0.0251	0.0030	0.0048	0.0001	0.0040	-0.0298	-0.0001
Rddecay0	0.1	0.15	0.2	-0.0058	0.0142	0.0055	0.0103	0.0045	0.1211	0.0102	**-0.9870**	-0.0437	0.0023
				-0.0046	0.0090	0.0046	0.0086	0.0034	0.0741	0.0072	**-0.6080**	-0.0279	0.0021
Rni0	0.0005	0.001	0.002	0.0000	0.0000	0.0006	-0.0017	0.0002	0.0000	0.0000	0.0000	0.0000	0.0000
				0.0000	0.0000	0.0006	-0.0017	0.0002	0.0000	0.0000	0.0000	0.0000	0.0000
Rden0	0.00005	0.0001	0.0002	0.0000	-0.0003	-0.0029	0.0000	0.0699	0.0000	0.0000	-0.0001	0.0010	0.0000
				0.0000	-0.0003	-0.0029	0.0000	0.0696	0.0000	0.0000	-0.0001	0.0010	0.0000
Rden02	0.003	0.005	0.007	-0.0002	-0.0046	0.0000	-0.0002	-0.1210	-0.0003	-0.0001	-0.0017	0.0119	0.0000
				-0.0002	-0.0041	0.0000	-0.0001	-0.1130	-0.0003	-0.0001	-0.0016	0.0108	0.0000
Rremin(0)	0.01	0.015	0.02	0.0069	0.1525	0.0449	0.1086	0.0461	-0.1599	0.0019	0.0511	-0.3917	-0.0011
				0.0033	0.0564	0.0456	**1.1057**	0.0598	-0.1523	0.0008	0.0230	-0.1504	-0.0009
Rpn_uptk	0.03	0.065	0.06	-0.0013	-0.0143	0.0524	0.0034	0.1868	-0.0028	-0.0004	-0.0085	**-3.6200**	0.0000
				-0.0514	**-0.8864**	**2.6882**	**1.6796**	**5.1609**	-0.0697	-0.0152	-0.3386	**-0.5033**	0.0000
Rsn_uptk	0.8	1	1.2	**-0.9921**	0.3087	0.0960	0.0017	0.1229	-0.0048	-0.0019	-0.0142	0.0716	**-0.5653**
				-0.6804	0.2063	0.0930	0.0075	0.0227	-0.0047	-0.0021	-0.0133	0.0669	**-0.4131**
r1	0.03	0.05	0.07	0.2039	0.3063	**-1.2634**	**-1.2157**	**-0.9814**	0.0770	0.0584	0.2318	**-1.1672**	**-0.9939**
				0.1013	0.1499	**-0.6165**	**-0.6910**	**-0.5873**	0.0455	0.0312	0.1184	**-0.5980**	**-0.5021**
r8	0.02	0.04	0.06	0.0041	0.0881	0.0213	0.0626	0.0099	-0.0911	0.0011	0.0302	0.0516	-0.0007
				0.0050	0.1139	0.0294	0.0862	0.0092	-0.1185	0.0014	0.0394	0.0817	-0.0008

Table C: Specific uptake rates of NH4 and NO3 during the spring experiment. (Calculated from daily NH4 and NO3 disappearance divided by daily mean PN concentrations.

date	specific NH_4 uptake rate ($\mu M\ \mu M^{-1}PN\ d^{-1}$)		specific NO_3 uptake rate ($\mu M\ \mu M^{-1}PN\ d^{-1}$)	
	T1	T4	T1	T4
16/03/99	0.0570	0.0431		
17/03/99	0.0673	0.0494		
18/03/99	0.0581	0.0331		
19/03/99	0.0057	-0.0028		
20/03/99	0.1423	0.0888		
21/03/99	0.1636	0.1399		
22/03/99	0.1149	0.0744		
23/03/99	0.1449	0.1240		
24/03/99	0.1386	0.1112		
25/03/99	0.2202	0.1701		
26/03/99	0.1737	0.1756	0.0335	0.0329
27/03/99			0.1288	0.0744
28/03/99			0.3825	0.5110
29/03/99			0.3871	0.4022
30/03/99			0.2141	0.3526
31/03/99			0.1607	0.3201
01/04/99			0.1073	0.2613
02/04/99			0.0877	0.1437
03/04/99			0.0223	0.0595

Table D: Specific uptake rates of N nutrients during the summer experiment. (Calculated from N nutrient disappearance within 2 hours divided by mean PN concentrations and converted from h^{-1} to d^{-1} by multiplying 24. 0:00 indicates average from 0:00 to 04:00; 6:00 indicates average from 06:00 to 10:00; 12:00 indicates average from 12:00 to 16:00; 18:00 indicates average from 18:00 to 22:00.)

		specific NH4 uptake rate ($\mu M\ \mu M^{-1}PN\ d^{-1}$)		specific NO3 uptake rate ($\mu M\ \mu M^{-1}PN\ d^{-1}$)		specific NO2 uptake rate ($\mu M\ \mu M^{-1}PN\ d^{-1}$)	
date	time	T8	T11	T8	T11	T8	T11
01/06/99	0:00	0.2809	0.4550	-0.0666	-0.0853	0.0043	-0.0018
	6:00	0.3902	0.3711	-0.0291	0.0010	-0.0005	-0.0012
	12:00	0.5754	0.3871	0.0982	0.0597	0.0005	0.0011
	18:00	0.4757	0.3417	0.0502	0.0166	0.0013	-0.0002
02/06/99	0:00	0.4753	0.3986	-0.0040	-0.0159	-0.0014	-0.0023
	6:00	0.8457	0.7421	0.0548	0.0472	-0.0017	-0.0006
	12:00	0.8138	0.8136	0.1997	0.1197	-0.0005	0.0005
	18:00	0.2676	0.3377	0.2697	0.2365	0.0024	0.0012
03/06/99	0:00	0.0310	0.0180	0.5046	0.4841	-0.0027	-0.0067
	6:00	0.0120	0.0223	0.9279	0.8582	-0.0056	-0.0085
	12:00	-0.0101	-0.0082	0.9209	0.9190	0.0009	0.0010
	18:00			0.3464	0.3359	0.0015	0.0051
04/06/99	0:00			0.1919	0.2060	0.0047	0.0048
	6:00			0.3054	0.3406	0.0197	0.0257
	12:00			0.1352	0.1218	0.0216	0.0356
	18:00			0.0202	0.0014	0.0102	0.0085
05/06/99	0:00			-0.0024	0.0032	0.0071	0.0008
	6:00					0.0073	-0.0027
	12:00					0.0031	-0.0025
	18:00					0.0012	0.0047

Table E: Photosynthesis rates (unit: µg POC µg chl*a*)$^{-1}$ h^{-1}) during the spring and summer mesocosm experiments, 1999. (Calculated from POC change within 2 hours divided by mean chlorophyll *a*. 0:00 indicates average from 0:00 to 04:00; 6:00 indicates average from 06:00 to 10:00; 12:00 indicates average from 12:00 to 16:00; 18:00 indicates average from 18:00 to 22:00.)

spring				summer			
date	time	T1	T4	date	time	T8	T11
26/03/99	0:00	5.8457	-3.0313	01/06/99	0:00	2.9977	0.1973
	6:00	-2.7438	6.6499		6:00	-3.9231	2.3150
	12:00	1.0311	-0.4841		12:00	1.4159	2.9474
	18:00	-0.7653	1.0394		18:00	0.3555	1.3563
27/03/99	0:00	-0.3459	-2.5842	02/06/99	0:00	-0.7518	-1.0884
	6:00	4.8073	7.0766		6:00	4.6551	2.8357
	12:00	6.8540	4.5999		12:00	3.0537	5.3743
	18:00	-1.7604	-3.7683		18:00	0.1277	-0.7254
28/03/99	0:00	-1.6495	3.6777	03/06/99	0:00	-1.0078	-0.3397
	6:00	2.2629	1.3144		6:00	1.7251	1.5568
	12:00	8.0830	5.3715		12:00	2.4895	2.9215
	18:00	-1.4061	-2.0014		18:00	-0.5006	-0.4475
29/03/99	0:00	-1.7004	0.5199	04/06/99	0:00	-0.4877	-0.2210
	6:00	3.1012	3.7760		6:00	2.4145	1.2327
	12:00	6.6825	3.4557		12:00	2.4972	2.3304
	18:00	-0.8886	-0.9191		18:00	-0.7329	0.0093
30/03/99	0:00	-0.3605	-0.9496	05/06/99	0:00	-0.4844	-0.5365
	6:00	2.8783	2.9670		6:00	0.6467	0.9945
	12:00	5.4499	4.5179		12:00	3.9775	1.2775
	18:00	-1.8527	-1.9491		18:00	-0.9778	-0.7787
31/03/99	0:00	-1.6664	1.4245	06/06/99	0:00	-0.4979	-0.2389
	6:00	2.4091	1.7682		6:00	3.3732	1.9148
	12:00	5.9949	5.2981		12:00	1.7911	1.0470
	18:00	-2.6449	-2.0750		18:00	-0.1718	-0.2784
01/04/99	0:00	2.1312	-0.6473	07/06/99	0:00		0.3882
	6:00	4.0380	3.7803		6:00		1.1790
	12:00	-2.5206	3.9148		12:00		1.3403
	18:00	2.2672	-0.4639		18:00		-0.8661
02/04/99	0:00		-0.7450	08/06/99	0:00		0.0959
	6:00		2.5014		6:00		0.0174
	12:00		5.1883		12:00		0.2215
	18:00		-1.0017		18:00		-0.1317
03/04/99	0:00		-1.7706	09/06/99	0:00		0.0170
	6:00		3.0670		6:00		0.1233
	12:00		1.7142		12:00		0.0886
	18:00		-1.4210		18:00		-1.1350
04/04/99	0:00		-0.5757	10/06/99	0:00		0.4721
	6:00		1.5295		6:00		0.2923
	12:00		3.6023		12:00		0.1477
	18:00		-2.1612		18:00		-0.9689

Table F: Nitrate uptake rates (µmol NO3 (µg chla)$^{-1}$ h^{-1}) during the spring experiment. (Calculated from NO3 disappearance within 2 hours, divided by the mean chlorophyll *a* concentrations. Night-time: 20:00-08:00; daytime: 10:00-18:00.)

	T1		T4	
date	daytime	night-time	daytime	night-time
25/03/99	-0.0236	0.0308	0.0000	0.0161
26/03/99	0.0100	0.0045	-0.0286	0.0167
27/03/99	0.0187	0.0107	0.0043	0.0046
28/03/99	0.0480	0.0249	0.0431	0.0167
29/03/99	0.0459	0.0193	0.0515	0.0128
30/03/99	0.0275	0.0081	0.0484	0.0176
31/03/99	0.0168	-0.0005	0.0475	0.0104
01/04/99	0.0103	0.0061	0.0360	0.0103
02/04/99	0.0107	0.0018	0.0218	0.0044
03/04/99	0.0049	-0.0009	0.0090	0.0011
04/04/99	-0.0048	0.0049	-0.0027	0.0001
05/04/99	0.0008	-0.0031	0.0004	0.0022

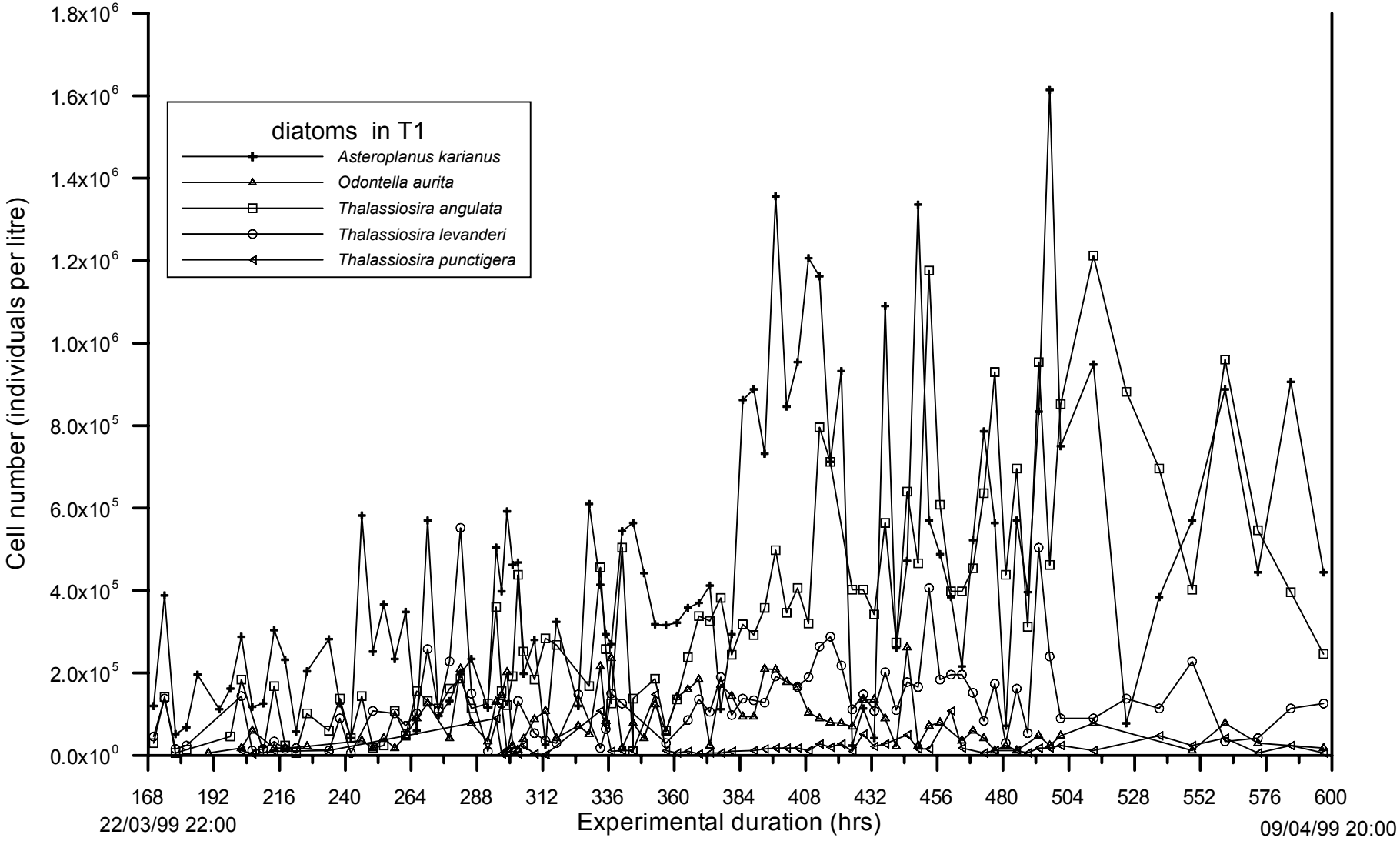

Fig. A: Development of dominant phytoplankton species in T1 (series 1, Buesum, Mar./Apr., 1999)

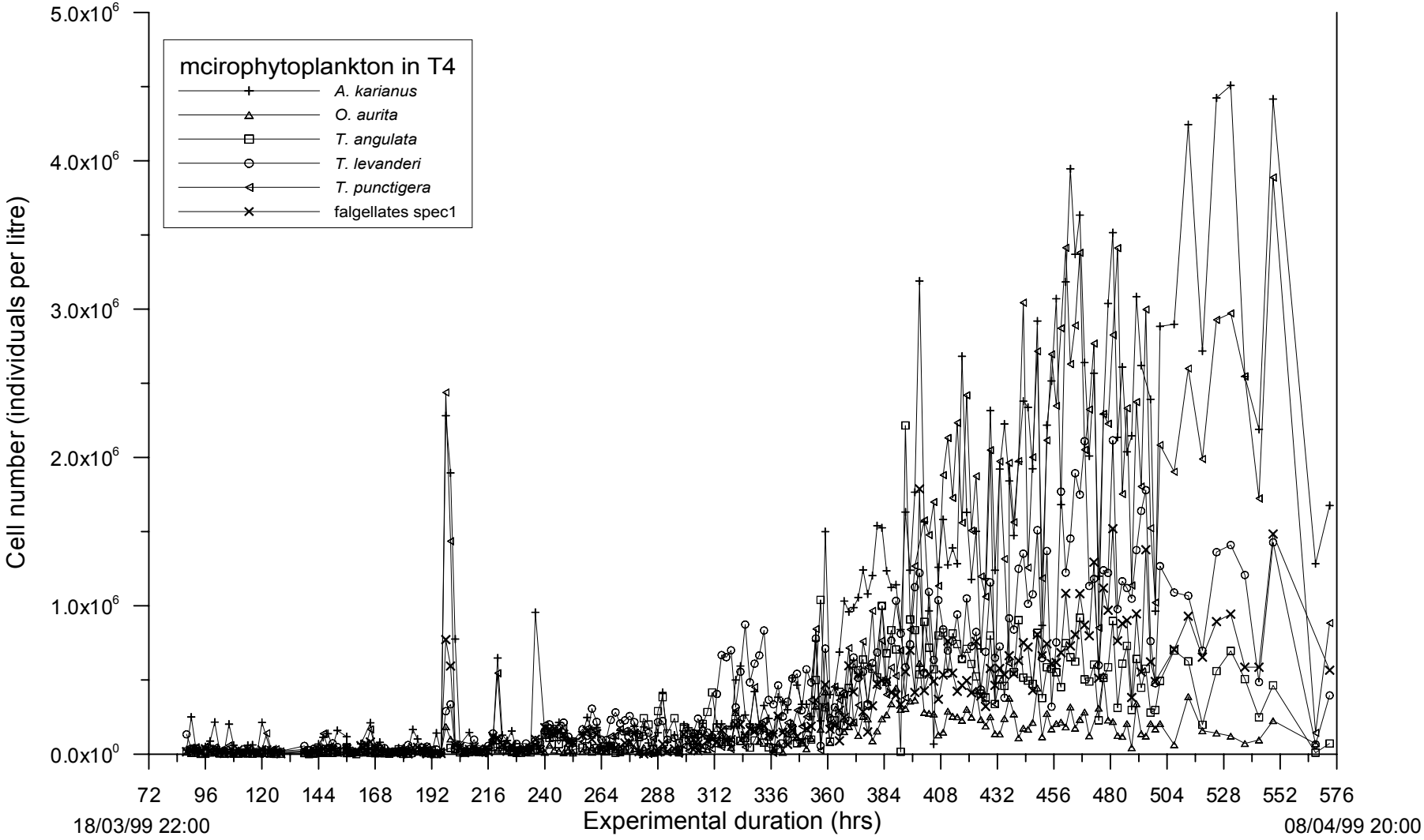

Fig. B: Development of dominant phytoplankton species in T4 (series 1, Büsum, Mar./Apr., 1999)

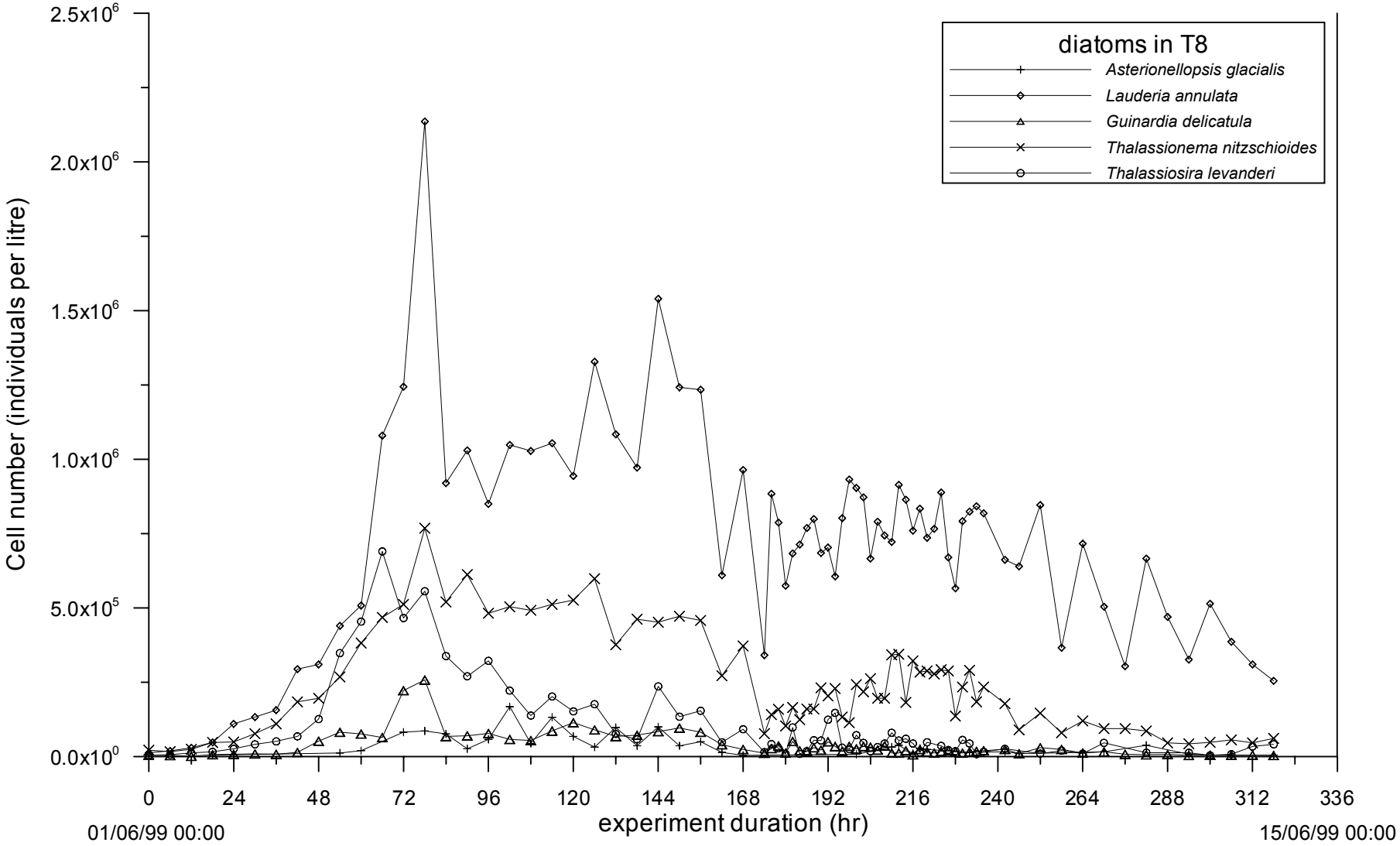

Fig. C: Development of dominant diatom species in T8 (series 2, Büsum, Jun., 1999)

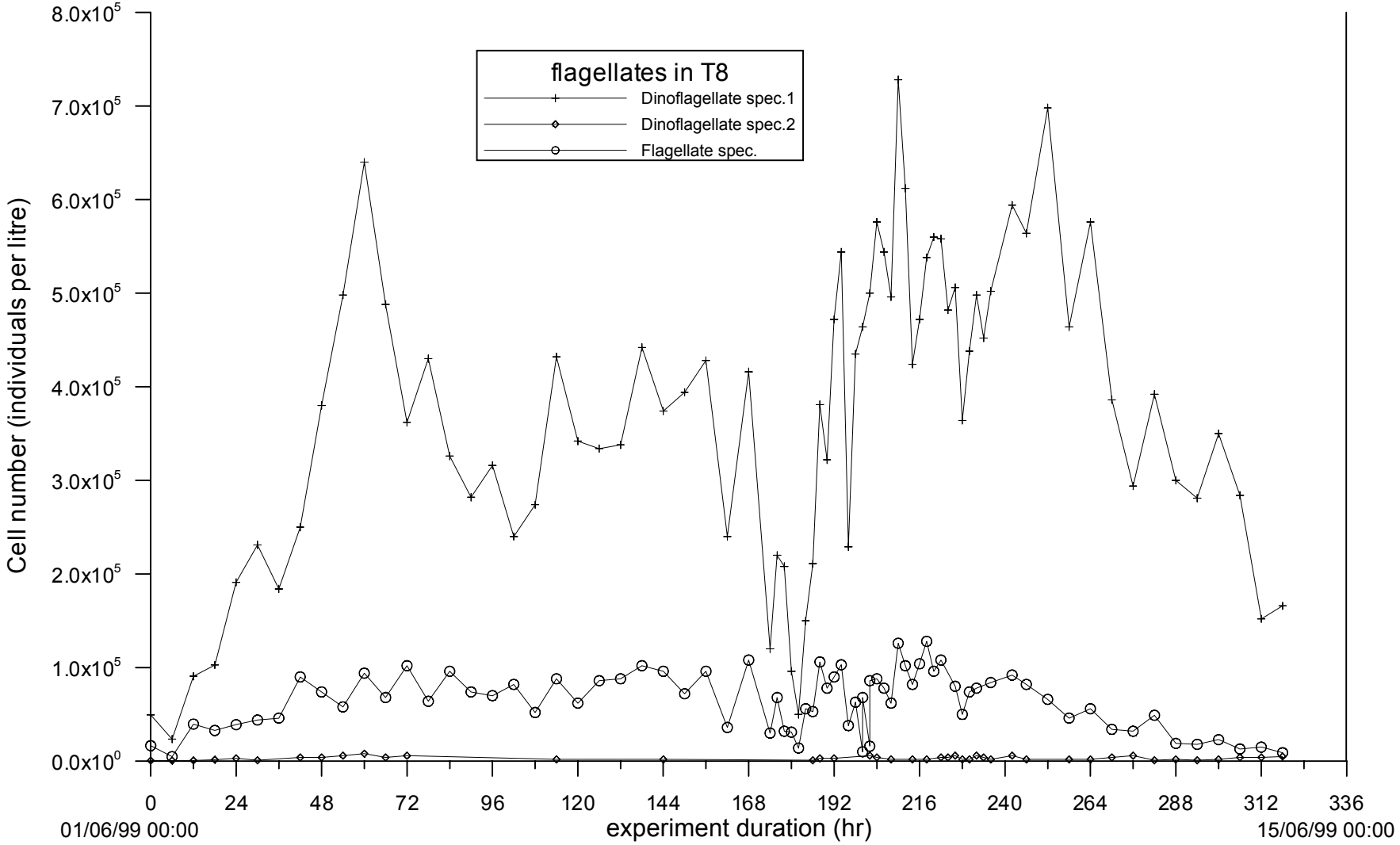

Fig. D: Development of flagellates in T8 (series 2, Büsum, Jun., 1999)

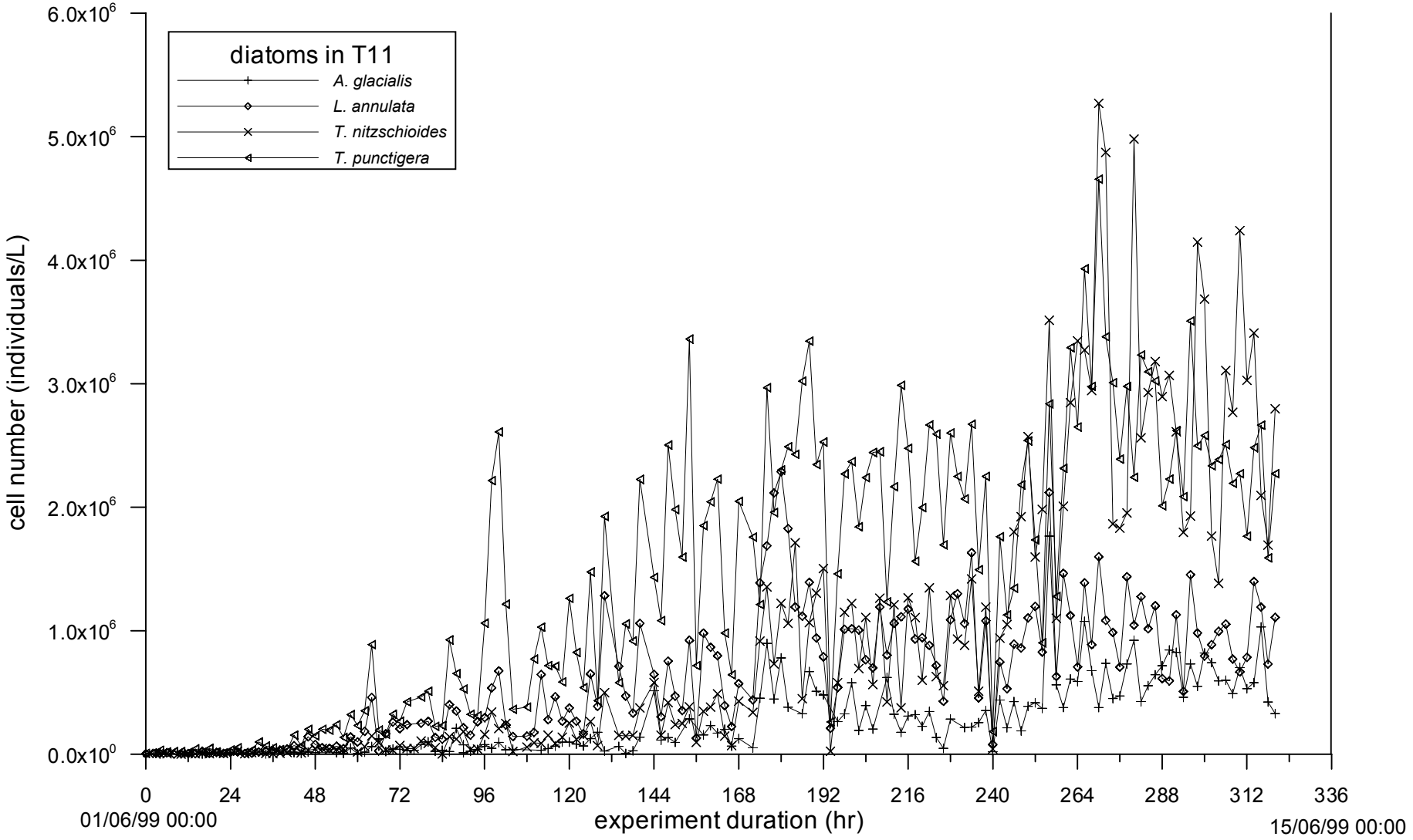

Fig. E: Development of dominant diatom species in T11 (series 2, Büsum, Jun., 1999)

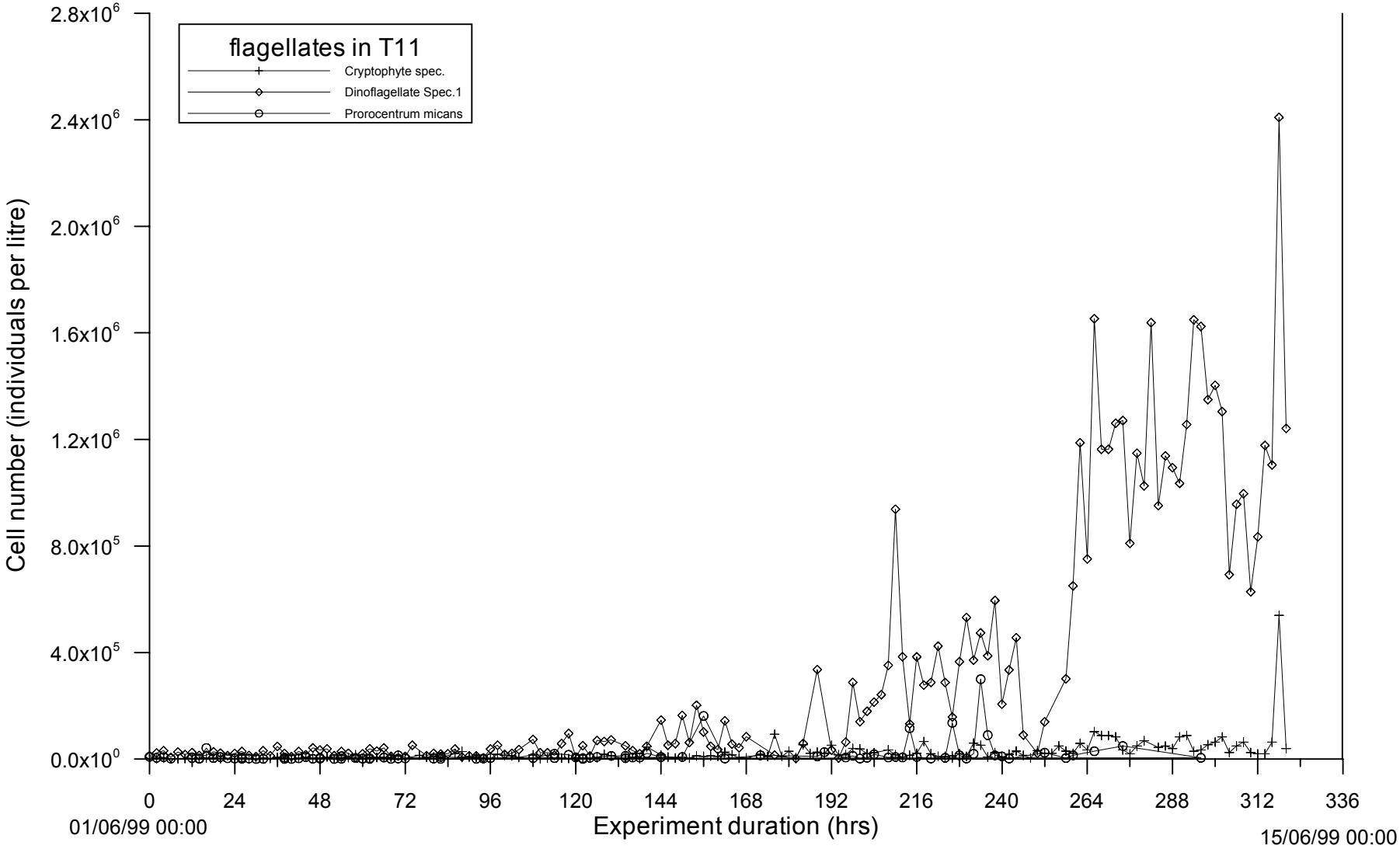

Fig. F: Development of flagellates in T11 (series 2, Büsum, Jun., 1999)

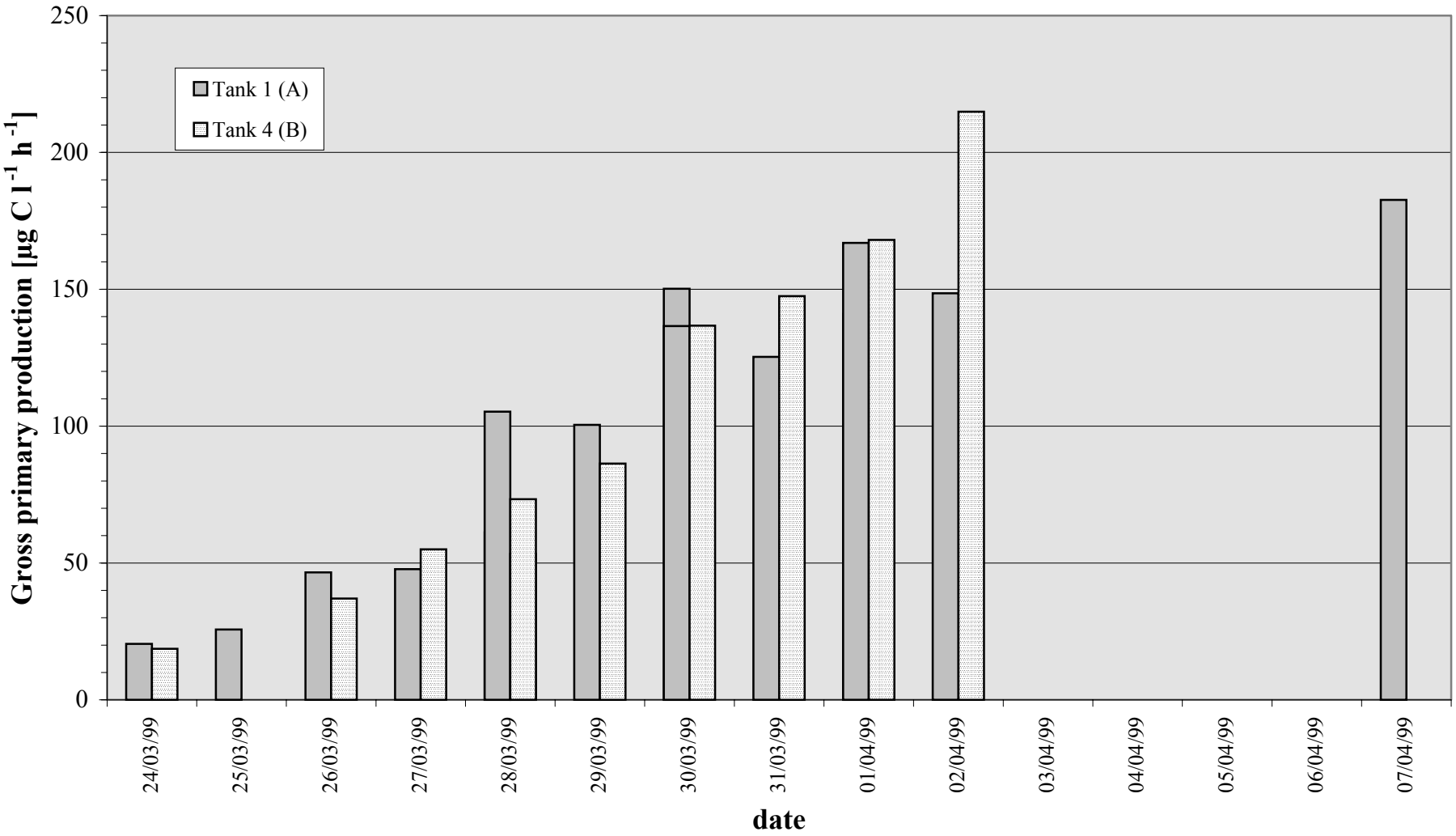

Fig. G: Development of gross primary production

Mesocosm experiments Büsum spring 1999

kindly supplied by C.D. Dürselen

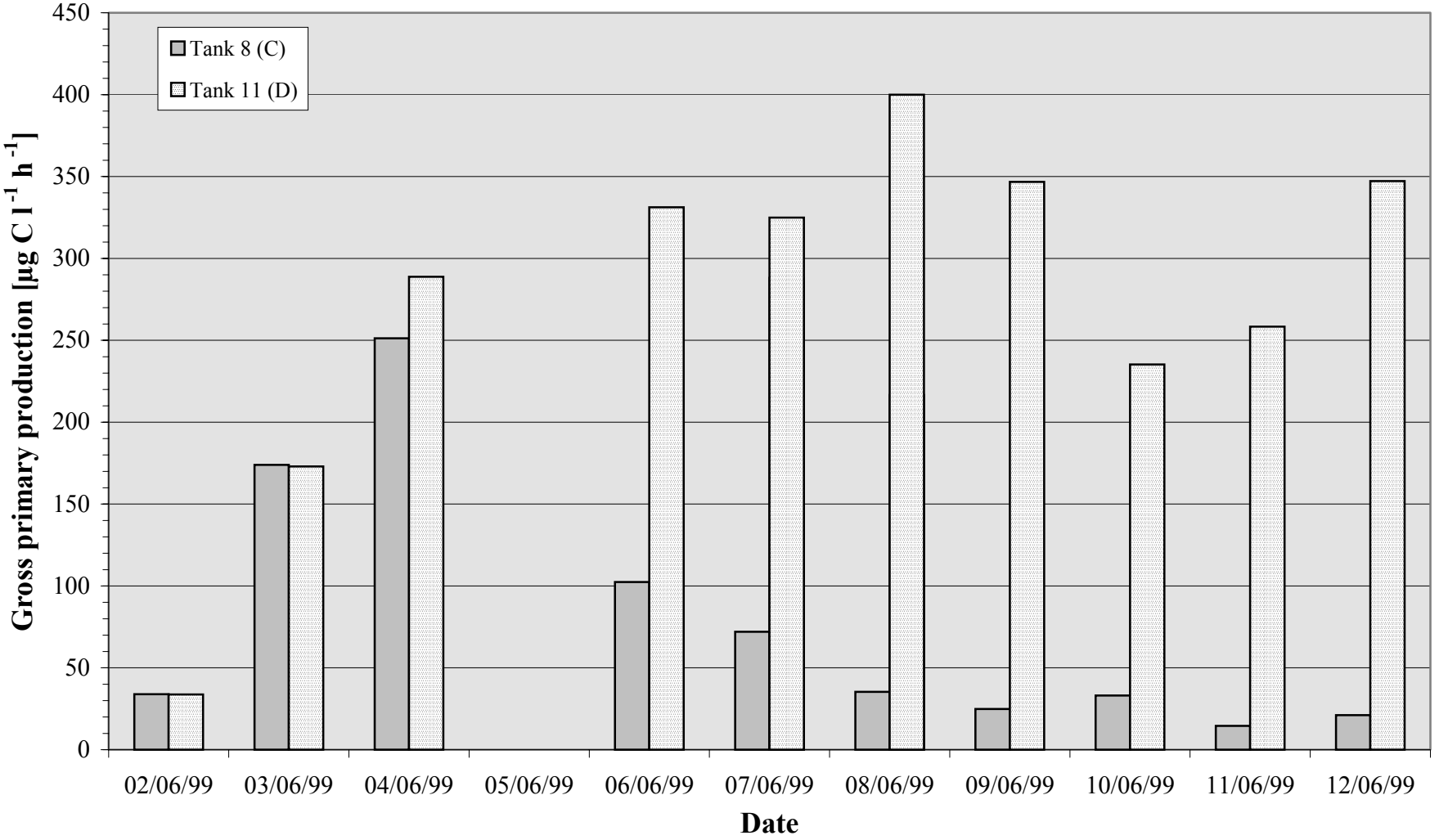

Fig. H: Development of gross primary production

Mesocosm experiments Büsum summer 1999

kindly supplied by C.D. Dürselen

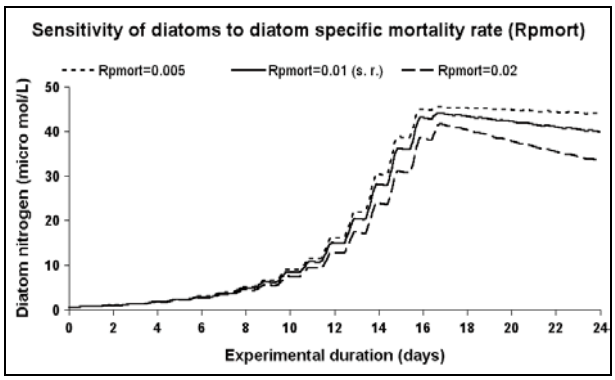

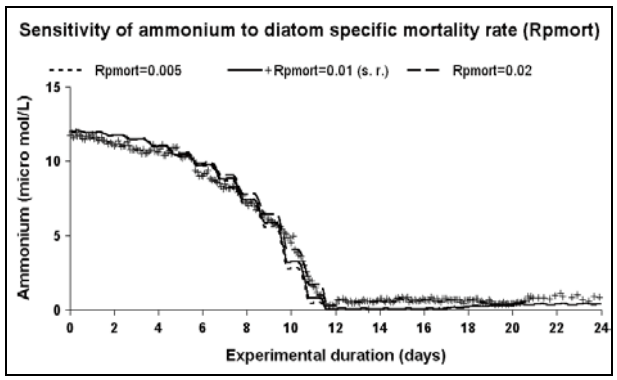

S*p:* 0.13, 0.11 S*p:* 0.02, 0.03

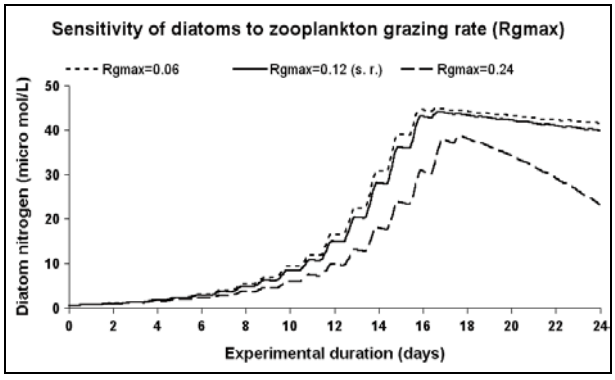

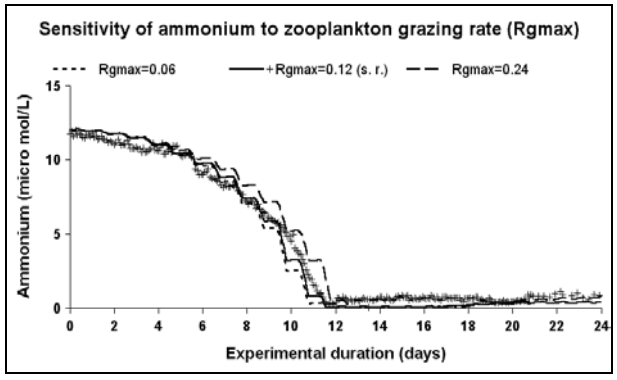

S*p:* -0.08, -0.24 S*p:* 0.06, 0.10

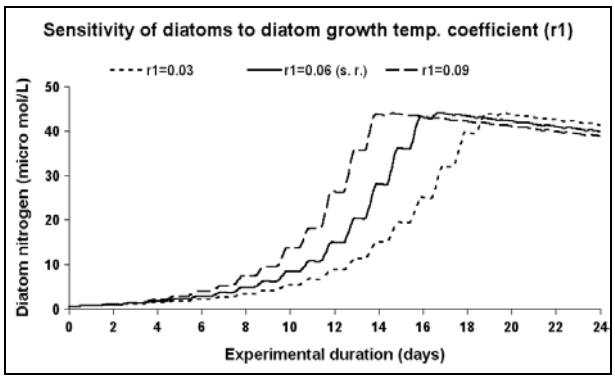

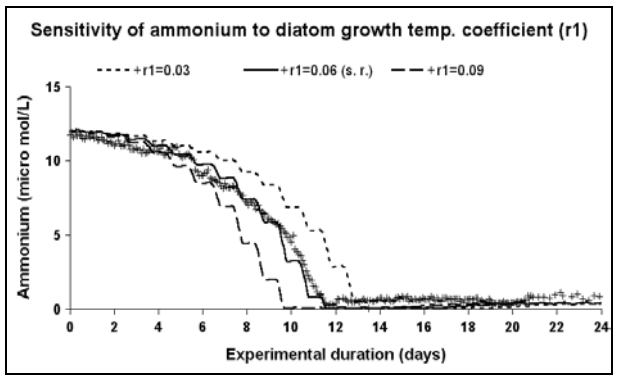

S*p:* 0.36, 0.27 S*p:* -0.24, -0.37

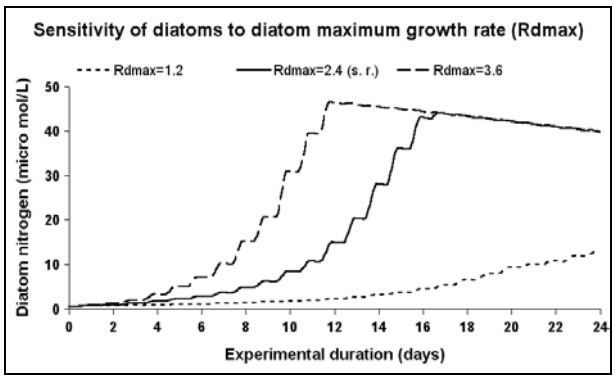

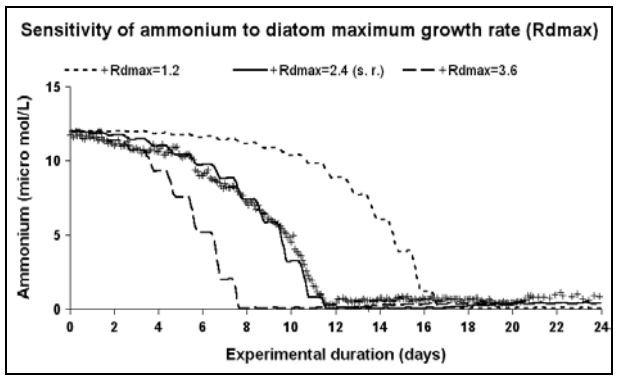

S*p:* 1.63, 0.61 S*p:* -1.89, -0.70

Fig. I: Some outputs of parameter sensitivity analyses with different *Sp* values (***Sp*:** sensitivity of parameter P, see Table 3-4; **s. r.**: standard run.)

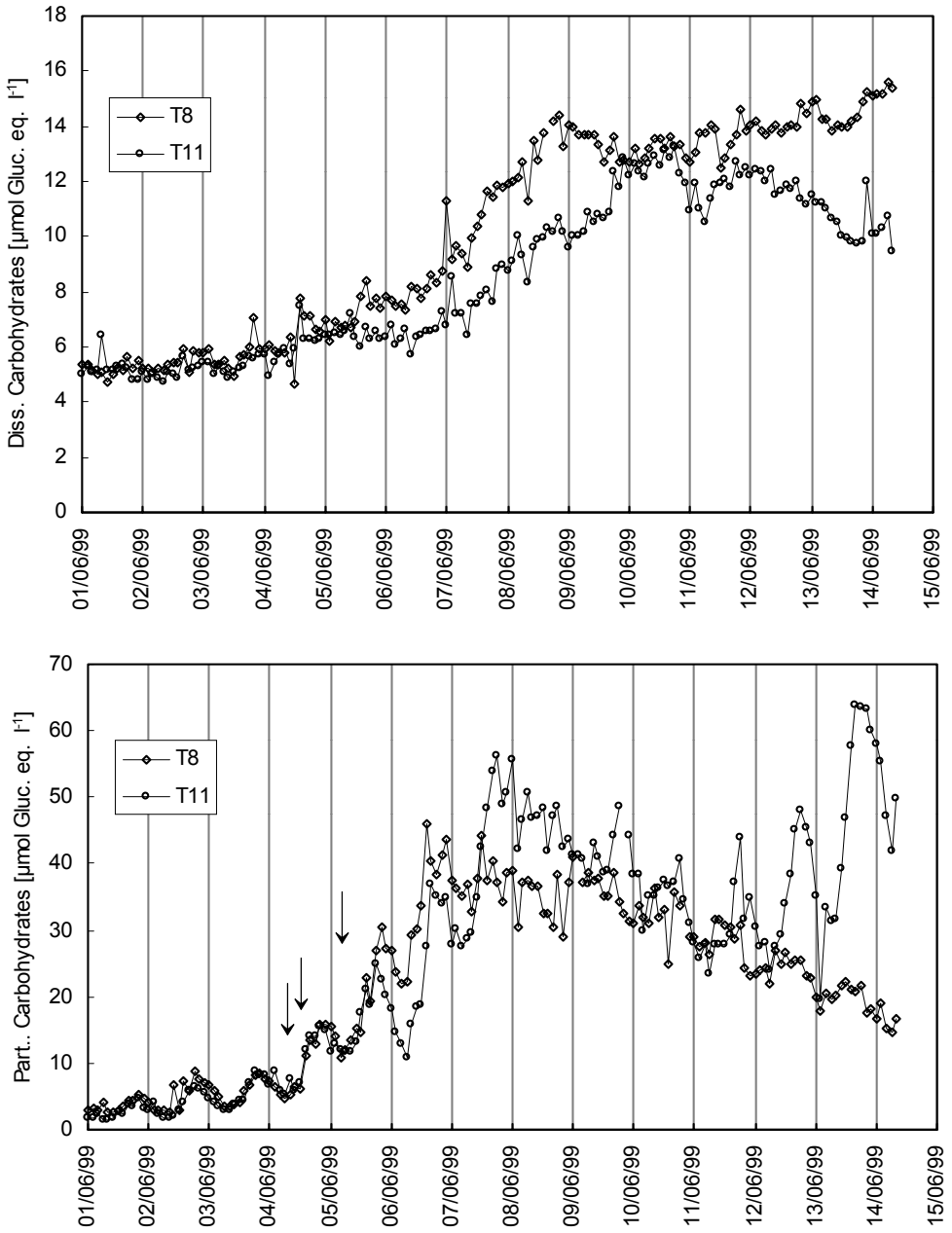

Fig. J: Dissolved and particulate carbohydrates in summer experiment (T8, T11, Jun. 1999 Büsum, arrows marked nutrient addition, kindly supplied by A. Starke)

ACKNOWLEDGEMENTS

I am grateful for the support from Prof. Dr. V. Ittekkot and his kind offer to supervise this thesis. I would like to express my sincere thanks to Dr. U. H. Brockmann for his supervision throughout the years with his great patience to me and enthusiasm for marine research as well as for giving me the great chance to participate in the project UJEK and finish the study.

The mesocosm experiments have been an achievements contributed by every member in the project. Most of all I would thank all dedicated German and Chinese scientists. Without them, this work would no be possible. Thanks to all my colleagues for their continuous supports after the mesocosms experiments and following work. I appreciate the friendly atmosphere created by them.

Many thanks to Dr. C.D. Dürselen for all his fruitful discussions and supports of biological data as well as revising the manuscripts.

Thanks to Thomas Raabe for supplying DOC data with helpful discussions and his tolerance to be disturbed time to time for instant questions. Thanks also to Andreas Starke for the carbohydrates data and related discussions. Many thanks to Monica Schütt and Ilse Büns, not only for their excellent work in the lab for nutrients, DON, DOP, PP, but also for their friendship and encouragement in depressive moments. Thanks to Gitta Hemken for her POC, PN measurements. Thanks also to Delik Topcu for her supporting for literatures and unforgettable warmth.

Sincere thanks to Waltraud Walenius, Monica Schütt and Thomas Raabe for their kindness to review my manuscript and braveness to struggle with my Chinese-English.

Thanks to my family for their love. They have been waiting for me for so long time. Thanks all my friends around for sharing the joys and troubles during the period.

Last but not least, I appreciated the financial support from DLR (Deutsches Zentrum für Luft und Raumfarhrt), BMBF. This study is in the frame of the project UJEK, funded by the German Ministry for Education and Research under contract No. 03F0189B.